Glaciers of Asia—

GLACIERS OF THE FORMER SOVIET UNION

By V.M. KOTLYAKOV, *senior author, with contributions from* A.M. DYAKOVA (Siberia), V.S. KORYAKIN (Russian Arctic Islands), V.I. KRAVTSOVA (Caucasus, Altay), G.B. OSIPOVA (Tien Shan), G.M. VARNAKOVA (Pamirs and Alai Range), V.N. VINOGRADOV (Kamchatka), O.N. VINOGRADOV (Caucasus), *and* N.M. ZVERKOVA (Ural Mountains and Taymyr Peninsula)

SATELLITE IMAGE ATLAS OF GLACIERS OF THE WORLD

Edited by RICHARD S. WILLIAMS, JR., *and* JANE G. FERRIGNO

U.S. GEOLOGICAL SURVEY PROFESSIONAL PAPER 1386–F–1

CONTENTS

Glaciers of the Former Soviet Union — by V.M. Kotlyakov, senior author, with contributions from A.M. Dyakova (Siberia), V.S. Koryakin (Russian Arctic Islands), V.I. Kravtsova (Caucasus, Altay), G.B.Osipova (Tien Shan), G.M. Varnakova (Pamirs and Alai Range), V.N. Vinogradov (Kamchatka), O.N. Vinogradov (Caucasus), and N.M. Zverkova (Ural Mountains and Taymyr Peninsula) ---------- **1**

Abstract ---------- **1**

Introduction ---------- **1**

Discussion of Glaciers by Region ---------- **2**

FIGURE 1. Glacierized regions of the Former Soviet Union according to the Glacier Inventory of the USSR ---------- **3**

TABLE 1. Data on the glaciers of the Former Soviet Union ---------- **3**

FIGURE 2. Morphological types of mountain glaciers adopted for the Glacier Inventory of the USSR ---------- **4**

Caucasus (in Russia and the Republic of Georgia) ---------- **4**

FIGURE 3. Map of the glacierization of a large portion of the Caucasus region, compiled for the World Atlas of Snow and Ice Resources ---------- **5**

TABLE 2. Distribution of glaciers in the main regions of the Caucasus ---------- **5**

TABLE 3. Glacier complexes and large glaciers of the Caucasus ---------- **6**

TABLE 4. The distribution of glaciers and glacier complexes in the Caucasus based on their area ---------- **6**

TABLE 5. The distribution of glaciers of the Caucasus according to morphological types ---------- **7**

FIGURE 4. Part of an enlarged Landsat 2 MSS image taken on 9 July 1976, and map of the morphologial types of glaciers of the same part of the Western Caucasus, including Gora El'brus ---------- **7**

FIGURE 5. Aerial photograph of the Lednik Marukhskiy taken on 15 September 1955, and a series of glaciological maps of this glacier based on detailed studies done during the IHD ---------- **8–9**

FIGURE 6. Enlargement of part of a Landsat 2 MSS image taken on 9 July 1976, depicting the El'brus massif ---------- **10**

FIGURE 7. Panoramic photographic mosaic of the northern and southern slopes of Gora El'brus ---------- **10**

FIGURE 8. Part of an enlargement of a Landsat 2 MSS image of the Central Caucasus, taken on 13 September 1977, and map of the morphological types of glaciers of the Central Caucasus ---------- **11**

FIGURE 9. Two enlargements of the part of the Central Caucasus around Lednik Bezengi depicted on Landsat 2 MSS images taken on 9 July 1976 and 13 September 1977 ---------- **12**

FIGURE 10. Illustrations of the surging *Lednik Kolka*, Gora Kazbek: Aerial photograph, sketch map of the advance, and morphology of the glacier basin ---------- **13**

FIGURE 11. Part of the Eastern Caucasus with the *Djul'tydag* range depicted on a Landsat 2 MSS image taken on 28 August 1976 ---------- **14**

Pamirs, Alai (Alayskiy), and Gissar (Hisor) Ranges (in the Republics of Tajikistan, Kyrgyzstan, and Uzbekistan) ---------- **14**

TABLE 6. Largest glaciers of the Pamirs and the Gissar (Hisor) and Alai (Alayskiy) Ranges ---------- **15**

TABLE 7. Distribution of glaciers based on their area ---------- **15**

FIGURE 12. Landsat 2 MSS image of the Central Pamirs acquired on 28 September 1977, and the distribution pattern of the area and number of glaciers related to glacier orientation in the Hisor and Alayskiy Ranges and the Pamirs ---------- **16**

FIGURE 13. The Lednik Bivachnyy surging glacier, tributary of Lednik Fedchenko with loops of medial moraines ---------- **17**

Figure 14. Enlargement of part of the Landsat image, showing the Lednik Fedchenko basin, and sketch map showing the distribution pattern of morphological types of glaciers in this area ---- 18
Figure 15. Enlargement of part of the Landsat image of 28 September 1977, showing the eastern part of Zaalayskiy Khrebet (Qatorkŭhi Pasi Oloy) and part of the Eastern Pamirs, and sketch map showing the pattern of morphological types of glaciers in this region ---- 19
Figure 16. Debris-free slope glaciers of the Eastern Pamirs ---- 20
Figure 17. Enlargement of part of the Landsat image, showing the upper reaches of the Saukdara river, and sketch map of surges of the Saukdara group of glaciers from 1973 to 1977 ---- 20
Figure 18. Photograph taken August 1976 of the rapid advance of ice of *Lednik Valy* caused by its surge ---- 21
Figure 19. Photograph showing the western part of the Khrebet Alayskiy on 18 September 1976 ---- 22
Tien Shan (in the Republics of Kyrgyzstan and Kazakhstan) ---- 22
Figure 20. Morphological types of glaciers in the western part of Khrebet Alayskiy delineated from space photographs and images ---- 23
Table 8. Distribution of Tien Shan glaciers in various river or lake basins ---- 23
Piks Pobedy and *Khan-Tengri* in Central Tien Shan ---- 24
Figure 21. Part of a Landsat 2 MSS image of the Pobedy and *Khan Tägiri/ Kan-Too* peak region taken on 16 October 1976 ---- 24
Table 9. Largest glaciers in the Tien Shan ---- 25
Table 10. Distribution of glaciers in two regions of the Central Tien Shan based on their area ---- 25
Figure 22. Enlargement of part of a Landsat 1 MSS image taken on 18 September 1973, and aerial photograph and map of the same area ---- 26
Khrebet Ak-Shyyrak in Central Tien Shan ---- 27
Figure 23. Enlargement of part of a Landsat 1 MSS image of Khrebet Ak-Shyyrak taken on 18 September 1973, map of the morphological types of glaciers, and distribution pattern of the area and number of glaciers ---- 28
Figure 24. Aerial photograph of *Lednik Severniy Karasay* in Khrebet Ak-Shyyrak ---- 28
Altay (Russia and Kazakhstan) ---- 29
Figure 25. Glaciers in the main mountain-glacier areas of the Altay — on the Katunskiy, Severo-Chuyskiy, and Yuzhno-Chuyskiy Khrebet, and the distribution pattern of the area and number of glaciers ---- 29
Table 11. Largest glaciers in the Russian Altay ---- 30
Figure 26. Image of the central Altay with the Gora Belukha glacier group taken from the Salyut–1 space station on 14 June 1971; and comparison of the delineation of the glacier boundaries shown on topographic maps and derived from the space image ---- 31
Figure 27. Part of a Landsat 2 MSS image of Katunskiy Khrebet taken on 11 July 1977, map of surface morphology, and morphological types of glaciers in this region ---- 32
Figure 28. Part of the Landsat 2 MSS image taken on 11 July 1977 of the *Bish-Irdu* glacier complex in the Severo-Chuyskiy Khrebet, enlarged portion of the image, and depiction of this region on a map ---- 33
Ural Mountains (Ural'skiye Gory) ---- 34
Figure 29. Enlargement of a Landsat 1 MSS image of the Northern Urals acquired on 25 June 1973 ---- 34
Figure 30. Distribution pattern of glaciers in the Polar Urals, and by area and number related to orientation ---- 35
Figure 31. Part of an enlargement of a Landsat 1 MSS image of part of the Polar Urals acquired on 6 March 1973: *Bol'shoy Khadyta* river-valley, and location of the *Lednik Obrucheva* ---- 36

Figure 32. Aerial photograph taken on 30 July 1953 of *Lednik Obrucheva*; morphology of the surface; and changes of the surface elevation of the *Lednik Obrucheva* in the Polar Urals ---- **36**

The Byrranga Mountains (Gory Byrranga) in Northern Russia ---- **37**

Figure 33. Landsat 1 MSS image acquired 26 July 1973 showing the distribution of glaciers in the Gory Byrranga in the region near lat. 76°N., long. 108°E.; sketch of glacier location; and distribution pattern of glacier orientation in the Gory Byrranga ---- **37**

Northeastern Siberia ---- **38**

Figure 34. Distribution of glaciers over Khrebet Suntar-Khayata; distribution patterns of the number and area of glaciers relating to the orientation in Khrebet Suntar-Khayata; and Khrebet Cherskogo ---- **38**

Table 12. Distribution of glaciers in the Khrebet Suntar-Khayata based on their size ---- **39**

Figure 35. Enlargements of two Landsat 2 MSS images of the Koryakskoye highland, northeastern Siberia, taken on 2 July 1975 and 26 August 1975; and distribution of glaciers in the highest part of the Koryakskoye highland ---- **39**

Figure 36. Distribution of aufeis areas in northeastern Siberia ---- **40**

Kamchatka ---- **40**

Figure 37. Morphological types of present-day glaciers in the volcanic regions of Kamchatka ---- **41**

Figure 38. Aerial photograph of glaciers in the crater and on the slopes of Vulkan Mutnovskaya Sopka ---- **41**

Russian Arctic ---- **42**

Franz Josef Land (Zemlya Frantsa-Iosifa) ---- **42**

Figure 39. Glacierized regions of Franz Josef Land: western region; central region; and eastern region ---- **43**

Table 13. The area of glaciers in Franz Josef Land ---- **43**

Figure 40. Landsat 3 MSS image of the western part of Franz Josef Land acquired on 24 March 1978 ---- **44**

Severnaya Zemlya ---- **44**

Figure 41. Glacierization of Severnaya Zemlya ---- **45**

Table 14. The area of glaciers on Severnaya Zemlya ---- **45**

Figure 42. Landsat 1 MSS image of the northern part of Severnaya Zemlya taken on 28 July 1973 ---- **46**

Novaya Zemlya ---- **47**

Conclusions ---- **47**

Figure 43. Glacierization of Novaya Zemlya ---- **48**

Acknowledgments ---- **48**

Table 15. The glaciers on Novaya Zemlya ---- **49**

Figure 44. Landsat 1 MSS image of the central part of *Novozemel'skiy ice cap* taken on 23 July 1973 ---- **49**

Table 16. Optimum Landsat 1, 2, and 3 MSS images of glaciers of the Former Soviet Union ---- **50–55**

Figure 45. Index map of the optimum Landsat 1, 2, and 3 MSS images of the Former Soviet Union ---- **56–58**

Fluctuations of Glaciers of the Central Caucasus and Gora El'brus, with a Section on the Glaciological Disaster in North Osetiya — by V.M. Kotlyakov, O.V. Rototaeva, and G.A. Nosenko ---- **59**

Introduction ---- **59**

Figure 46. Image of Gora El'brus and its glaciers on 25 August 2002 ---- **60**

Figure 47. ASTER image of the glaciers on the southern slope of Gora El'brus taken on 15 September 2001 ---- **60**

Figure 48. Map of the glaciers of Gora El'brus ---- **61**

Table 17. Changes in the position of the termini of El'brus glaciers during different periods of observation ---- 61
Figure 49. Part of the 25 August 2002 International Space Station image enlarged to show the lake-moraine complex near the terminus of the retreating *Lednik Birdzhalytchiran*, Gora El'brus ---- 63
Figure 50. Aerial and space photographs of *Lednik Bol'shoy Azau*, Gora El'brus, showing changes in the terminus shape and position ---- 64
Figure 51. Aerial photograph (1987) of the terminus of *Lednik Ullumalienderku*, Gora El'brus, during a surge event ---- 65
Glaciological Disaster in North Osetiya ---- 66
Figure 52. Photographs (1981 and 2004) of the Lednik Kukurtli, Gora El'brus ---- 67
Figure 53. ASTER image taken on 15 September 2001, showing glaciers of the central Caucasus ---- 68
Table 18. Changes in the position of glacier termini from 1987 to 2001/04 in the Tcherek River basin ---- 68
Figure 54. Image taken from the International Space Station in 2002, showing the retreating Lednik Karaugom ---- 69
Figure 55. Aerial photograph taken in July 2004 of the terminus of *Lednik Ailama* and the stagnant terminus of *Lednik Dykh-su* covered with debris ---- 69
Figure 56. Photograph taken in August 2003 of the advancing front of *Lednik Mizhirgitchiran* ---- 70
Figure 57. Oblique aerial photograph of avalanche debris in the Karmadon basin caused by the 20 September 2002 catastrophic collapse of the *Lednik Kolka* ---- 70
Figure 58. Two ASTER images of the Genaldon river valley, scene of the *Lednik Kolka* disaster ---- 71
Figure 59. Oblique aerial photograph taken on 21 September 2002, looking southwest at the avalanche debris saturated with water ---- 72
Figure 60. Oblique aerial photograph taken on 24 September 2002, looking south at the mountain crest in the source region of *Lednik Kolka* ---- 73
Figure 61. International Space Station image taken on 13 August 2002 of Lednik Maili and *Lednik Kolka* ---- 74
Figure 62. Oblique aerial photograph taken September 2002, looking south at the empty cirque of *Lednik Kolka* after the disaster ---- 74
Figure 63. International Space Station image taken on 19 October 2002, looking south at Gora Kasbek volcanic massif and the cirques of Ledniki Maili and *Kolka* ---- 75
Figure 64. Enlarged section of 27 September 2002 ASTER image ---- 75
Figure 65. Terrestrial photograph taken on 28 June 2003 of one of the lakes in the *Kolka* bed dammed by a combination of ice and debris ---- 76
Figure 66. Oblique aerial photograph taken on September 2003, looking southeast at the collapsing avalanche debris in Karmadon basin and the dammed lake near Saniba settlement one year after the disaster ---- 76
Investigations of the Fluctuations of Surge-Type Glaciers in the Pamirs based on Observations from Space — by V.M. Kotlyakov, G.B. Osipova, and D.G. Tsvetkov ---- 77
Introduction ---- 77
Compilation of an Inventory of Surging Glaciers of the Pamirs ---- 77
Table 19. The number of surge-type glaciers in the large river basins of the Pamirs ---- 78
Table 20. The largest observed surges of the glaciers of the Pamirs from 1960 to 2003 ---- 78
Figure 67. KFA-1000 photograph taken in 1973 from a Resurs-F1 satellite showing surge-type glaciers in the Central Pamirs ---- 79

Figure 68. KFA-1000 photograph taken in 1985 from a Resurs-F1 satellite showing surge-type glaciers in the central part of Zaalayskiy Khrebet (Qatorkŭhi Pasi Oloy in Tajikistan, Chong Alay Kyrka Toosu in Kyrgyzstan) ---- 80
Investigation of the Fluctuation Regime of Compound Glaciers ---- 80
Figure 69. Morphology of the lower part of Lednik Oktyabr'skiye from 1946 to 1990 ---- 81
Figure 70. Photographs from space of Lednik Oktyabr'skiye ---- 82
Figure 71. Graph of the velocity of the ice movement along longitudinal profile of Lednik Oktyabr'skiye, showing the stage of recovery (1972–1985) and the surge (1985–1990) ---- 82
Figure 72. Photographs of *Lednik Bivachniy* and Lednik Moscow State University: 1973, pre-surge; 1980, post-surge; and 2001 soon after the successive surge ---- 83
Figure 73. Images from space of the Gando-*Dorofeeva* glacier system before, during, and after the 1989–1990 surge ---- 84
The State of Surging Glaciers — Ledniki Medvezhiy and Geograficheskogo Obshchestva ---- 85
Figure 74. Aerial photographs showing the tongue of Lednik Medvezhiy during the surge of 1988 to 1989, and in 2001 ---- 86
Figure 75. Sketch map of the Lednik Geograficheskogo Obschestva (RGO Glacier) basin showing glaciers, the reconstructed outline of the glacier's terminus in 1916, a reconstructed dammed lake in 1916, locations of velocity profiles, and a mudflow on the surface of the glacier in September 2002 ---- 88
Figure 76. Aerial photograph taken on 13 October 2002 of the terminus of Lednik RGO, looking northeast ---- 89
Figure 77. International Space Station images of Lednik RGO taken on 25 June 2001 and 30 September 2002 ---- 90
Investigations of the Fluctuations of "Normal" Non-Surging Glaciers in the Eastern Pamirs ---- 90
Figure 78. Landsat image of the Eastern Pamirs where glacier-retreat measurements listed in table 21 were made ---- 91
Table 21. Retreat velocity of the termini of glaciers of the Eastern Pamirs from 1972 to 2001 ---- 92
Figure 79. Sketch map showing the retreat of the terminus of *Lednik Severniy Zulumart* (Eastern Pamirs) based on interpretation of a 1946 aerial photograph and 1972, 1978, 1990, and 2001 space images and photographs ---- 92
Table 22. Retreat of the terminus and decrease in the area of the tongue of *Lednik Severniy Zulumart* from 1946 to 2001 ---- 93
The Glaciology of the Russian High Arctic from Landsat Imagery — by J.A. Dowdeswell, E.K. Dowdeswell, M. Williams, and A.F. Glazovskii ---- 94
Abstract ---- 94
Introduction ---- 95
Glaciological Background ---- 95
Figure 80. Map of the Russian High Arctic showing the major ice-covered archipelagos of Franz Josef Land, Novaya Zemlya, and Severnaya Zemlya, together with the smaller glacierized islands further east ---- 96
Figure 81. Diagrams showing the effects of cloud cover on Landsat image quality for selected Path–Rows in the Russian High Arctic, including Franz Josef Land, Novaya Zemlya, and Severnaya Zemlya: April to September, May, July, and September ---- 97
Franz Josef Land ---- 98
Severnaya Zemlya ---- 98
Figure 82. Map of the Franz Josef Land archipelago showing the distribution of ice masses ---- 99

Figure 83. Map of the islands of Severnaya Zemlya showing the distribution of ice masses ---- 100
Figure 84. Landsat false-color Multispectral Scanner image of the ice caps in northern Severnaya Zemlya ---- 101
Novaya Zemlya ---- 102
Other Glacierized Islands in the Russian High Arctic ---- 102
Figure 85. Map of Novaya Zemlya showing the distribution of ice masses ---- 103
Glaciological Investigation of Russian High Arctic Ice Masses from Landsat Imagery ---- 104
Ice-Surface Topography ---- 104
Figure 86. Map of the ice divides on the ice caps of Franz Josef Land, shown on a georeferenced mosaic of Landsat TM images acquired on 25 July 1986 ---- 105
Ice Dynamics ---- 105
Outlet Glaciers and Icebergs ---- 105
Figure 87. Landsat TM image sub-scene showing an example of the major ice divides on the Ostrov Gallya ice cap in Franz Josef Land ---- 106
Figure 88. Digitally enhanced Landsat TM image sub-scene of the major ice divide running along the northeast-southwest trending spine of Novaya Zemlya ---- 107
Figure 89. Landsat TM images of iceberg-producing outlet glaciers draining ice caps in the Russian High Arctic ---- 108
Figure 90. Four georeferenced and edge-enhanced sub-scenes of Landsat images of the Lednik Znamenityy on Zemlya Vil'cheka, Franz Josef Land, showing large numbers of tabular icebergs ---- 109
Floating Ice Shelves or Ice Tongues ---- 110
Figure 91. Annotated Landsat TM band 3 image sub-scene of the *Lednik Matusevicha* on Ostrov Oktyabr'skoy Revolyutsii, Severnaya Zemlya ---- 110
Figure 92. Graph showing ice-surface profiles from two ice shelves and their parent drainage basins on Severnaya Zemlya, derived from analysis of Russian aerial photographs from the 1950s ---- 111
Figure 93. Landsat TM image of three flat ice-marginal glacier termini on the ice cap on Ostrov Zemlya Georga, western Franz Josef Land ---- 112
Figure 94. Map of the ice caps on Franz Josef Land, with marginal areas of low surface gradient ---- 113
Surge-Type Glaciers ---- 114
Figure 95. Digitally enhanced Landsat TM image of the outlet glaciers entering Zaliv Nordenshel'da, Novaya Zemlya ---- 115
Snow-and-Ice Facies and Glacier Mass Balance ---- 115
Figure 96. Digitally enhanced Landsat TM sub-scene showing the snow-and-ice facies on a summer image of the Lednik Kropotkina on Ostrov Zemlya Aleksandry, Franz Josef Land ---- 116
Figure 97. Landsat TM sub-scene of Ostrov Ketlitsa, Franz Josef Land ---- 117
Conclusions ---- 118
Acknowledgments ---- 119
References Cited ---- 119

GLACIERS OF ASIA—

GLACIERS OF THE FORMER SOVIET UNION[1]

By V.M. KOTLYAKOV[2], senior author, with contributions from A.M. DYAKOVA (Siberia), V.S. KORYAKIN (Russian Arctic Islands), V.I. KRAVTSOVA (Caucasus, Altay), G.B. OSIPOVA (Tien Shan), G.M. VARNAKOVA (Pamirs and Alai Range), V.N. VINOGRADOV(Kamchatka), O.N. VINOGRADOV (Caucasus), *and* N.M. ZVERKOVA (Ural Mountains and Taymyr Peninsula)

Abstract

Glaciers in the Former Soviet Union cover a total area of 78,938 km^2; 72 percent (56,894 km^2) are in the Russian Arctic (Franz Josef Land, Severnaya Zemlya, Novaya Zemlya, and Wrangel Island) and 28 percent (22,044 km^2) in various mountain ranges (mainly the Caucasus, Pamirs, Alai Range (Alayskiy Khrebet), Tien Shan, Altay, Ural Mountains, and those of Northeastern Siberia) in Russia and in the Republics of Georgia, Kazakhstan, Kyrgyzstan, Tajikistan, and Uzbekistan. The Glacier Inventory of the USSR and the World Atlas of Snow and Ice Resources records a total of 26,881 glaciers, 1,983 in the Russian Arctic, and 24,898 in Russia and in the four independent republics. Information from the Glacier Inventory, World Atlas, Landsat 1, 2, and 3 MSS images from the 10-year Landsat Baseline Period (1972–1981), Soviet space imagery, aerial photographs, and maps were used to provide information on the glacierized areas. Russian glaciologists recognize 20 morphological types of mountain glaciers and 7 types of ice caps, ice fields, and ice sheets from a global perspective (World Atlas). Glaciers in the Former Soviet Union represent 11 of the 20 types of mountain glaciers and all of the types of ice caps and ice fields. The early (1972–1981) Landsat MSS images were found to be useful in delineating the margins and ice divides on ice caps and the termini and some margins of larger mountain glaciers, if the images were acquired under conditions of minimum cloud cover and late season, residual snow pack, but before new snowfall. Analysis of changes in smaller glaciers was not possible with the limitations of pixel resolution (80 m) of MSS images. Later Landsat TM and more recent Landsat ETM+ and ASTER images have overcome the spatial resolution problem. The Resurs-F1 KFA-1000 photographs and Landsat MSS images were especially useful for identifying surge-type glaciers and for determining the position of termini of glaciers.

Introduction

The information presented in this part of the chapter is the result of interpretation of Landsat images, Soviet space images, and aerial photographs. The data presented in the Soviet Glacier Inventory (USSR Academy of Sciences, 1965–1983) are also widely used in this chapter, as are some of the sketches and sections of maps compiled for the World Atlas of Snow and Ice Resources (Kotlyakov, 1997).

---

[1]Editors' Note: This manuscript was originally written in 1981 to describe the glaciers of the Former Soviet Union in the late 1970s and early 1980s, the "benchmark" time period for the Satellite Image Atlas of Glaciers of the World, U.S. Geological Survey Professional Paper 1386-A–K. Because there were delays in publishing, the authors and editors updated this manuscript by adding references to more recent work while still retaining the original benchmark information. In addition, three supplemental sections were added to give a fuller description of more recent glaciological work — "Fluctuations of Glaciers of the Central Caucasus and Gora (Mount) El'brus with a section on the Glaciological Disaster in North Osetiya," "Investigations of the Fluctuations of Surge-type Glaciers in the Pamirs Based on Observations from Space," and "The Glaciology of the Russian High Arctic from Landsat Imagery."

[2]Institute of Geography, Russian Academy of Sciences, Staromonetny 29, Moscow, Russia.

The Glacier Inventory of the USSR was published between 1965 and 1983 as a series of publications that comprise 108 issues. The Inventory provides quantitative information on all of the main characteristics of glaciers — dimensions, shape, position, and regime. These data were obtained from interpretation of aerial photographs and cartographic materials, sometimes supplemented by field and aerial studies of the glaciers. In some cases, the Inventory has made it possible to correctly interpret space images; and in some areas such as the Altay, interpretations using the Soviet space images have provided additional data to the Glacier Inventory.

According to the Glacier Inventory of the USSR, glaciers are situated in 26 regions of the Former Soviet Union (fig. 1). In addition to the glacierized regions shown on the index map (fig. 1), isolated glaciers and perennial snow patches are situated in the Kharaulakhskiy[3] Khrebet (Mountains) to the north of the Khrebet Orulgan, and on the Khrebet Pekul'ney (Range) on the Chukotka peninsula north of the Koryakskoye Nagor'ye (Highland). [Recent work includes Sedov (1997a, b) and Dolgushin and Osipova (1989).]

Based on the data in the Glacier Inventory of the Former Soviet Union, glaciers had an area of 78,938 km^2, of which 56,894 km^2 is in the Arctic and 22,044 km^2 is in mountain regions. The total number of individual glaciers is 28,881, of which 1,983 are in the Arctic and 24,898 are in the mountains. Table 1 lists the number of glaciers and the total glacierized area for each of the 26 glacierized regions of the Former Soviet Union.

The Former Soviet Union had previously established its own morphological classification of glaciers, which was standardized with due regard to the inventorying of glaciers. The Guide for the Compilation of the Glacier Inventory of the USSR (USSR Academy of Sciences, 1966) distinguishes 20 morphological types of mountain glaciers and 7 types of ice caps/ice fields/ice sheets. Figure 2 shows examples of the 11 major morphological types of mountain glaciers described in the Former Soviet Union. They are shown on the maps of glacier morphology contained in this chapter. The colors assigned to each glacier type are consistent on all of the maps.

Discussion of Glaciers by Region

Glaciers within seven of the major regions of the Former Soviet Union are discussed in this section. These regions include the Caucasus, the Pamirs and surrounding ranges, Tien Shan, Altay, the Ural Mountains, Kamchatka, and the Russian Arctic. Within the Tien Shan, the Piks Pobedy, *Khan-Tengri*, and Khrebet Ak-Shyyrak areas are discussed in more detail. After the Ural Mountain region, the Byrranga Mountains and Northeast Siberia are discussed. And within the Russian Arctic, Franz Josef Land, Severnaya Zemlya, and Novaya Zemlya are described in more detail.

[3]Official geographic place-names for foreign countries are required to be used in U.S. Government publications to the greatest extent possible. In this section, the use of geographic place-names is based on the U.S. Board on Geographic Names (BGN) as listed on the GEOnet Names Server (GNS) website: *http://earth-info.nga.mil/gns/html/index.html*. The website lists some conventional names and those will be used when available, for example Caucasus, Franz Josef Land, and Kara Sea. All other names will be the Russian names introduced by or with the English equivalent in parenthesis if needed for understanding. Names not listed in the BGN website will be shown in italics. Commonly used Russian generic terms are lednik, ledniki (glacier, glaciers); khrebet (mountain range); Gora, Gory (mount, mountains); pik, piks (peak, peaks); ozera (lake); poluostrov (peninsula); proliv (strait); and ostrov (island).

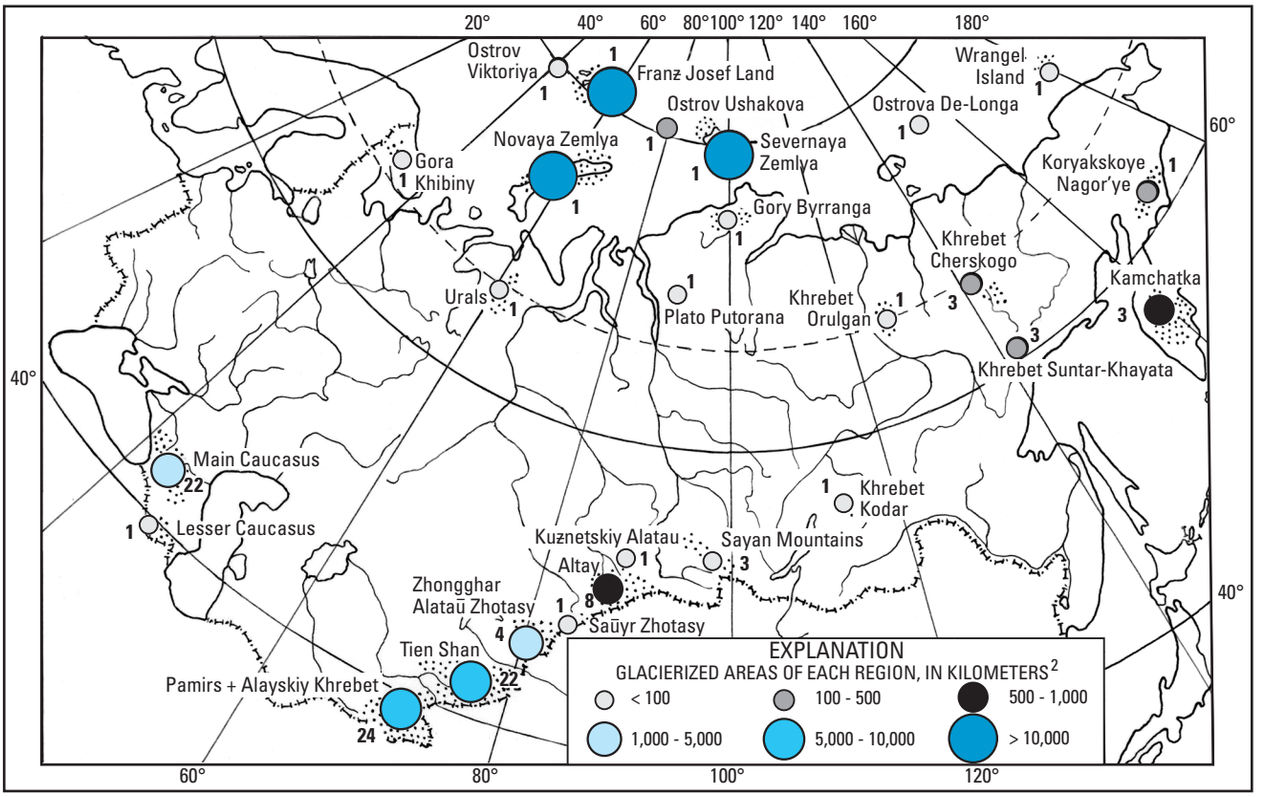


***Figure 1.**—Glacierized regions of the Former Soviet Union according to the Glacier Inventory of the USSR. The number near the symbol for each region denotes the section of the Glacier Inventory that describes that region.*

TABLE 1.—*Data on the glaciers of the Former Soviet Union*

[Data source: USSR Academy of Sciences (1965–1983). Unit: km^2, square kilometer]

Glacierized area	Number of glaciers	Total area of glacierization (km^2)	Date of area calculation
ICE CAPS AND ASSOCIATED OUTLET GLACIERS			
Novaya Zemlya	685	24,413	1960–80
Severnaya Zemlya	285	18,325	1960–80
Franz Josef Land (Zemlya Frantsa-Iosifa)	995	13,738.8	1960–80
Ostrov Ushakova (Ushakov Island)	2	325.4	1960–80
Ostrova De-longa (De Long Islands)	15	80.6	1960–80
Ostrov Viktoriya (Victoria Island)	1	10.7	1960–80
Total	1,983	56,893.5	1960–80
MOUNTAIN GLACIERS			
Qatorkŭhi Hisor/Hisor Tizmasi and Alayskiy Khrebet	3,893	2,335.8	1960–80
Pamirs	6,730	7,493.4	1960–80
Subtotal	10,623	9,829.2	1960–80
Tien Shan	6,347	7,251.7	1960–80
Main Caucasus	2,047	1,424.4	1960–80
Zhongghar Alatau-Zhostasy	1,369	1,000	1960–80
Altay	1,499	906.5	1960–80
MOUNTAIN GLACIERS (Continued)			
Kamchatka	405	874.1	1960–80
Koryakskoye Nagor'ye (upland)	1,302	240.6	1960–80
Khrebet Suntar-Khayata	208	201.6	1960–80
Khrebet Cherskogo	372	156.2	1960–80
Gory Byrranga	96	30.5	1960–80
Sayany	105	30.3	1960–80
Ural Mountains	143	28.7	1960–80
Kodar	30	18.8	1960–80
Orulgan	74	18.4	1960–80
Saūyr	18	16.6	1960–80
Kuznetskiy Alatau	91	6.8	1960–80
Lesser Caucasus	42	3.8	1960–80
Wrangel Island (Ostrov Vrangelya)	101	3.5	1960–80
Plato Putorana	22	2.5	1960–80
Khibiny	4	0.1	1960–80
Grand Total	24,898	22,044.3	1960–80

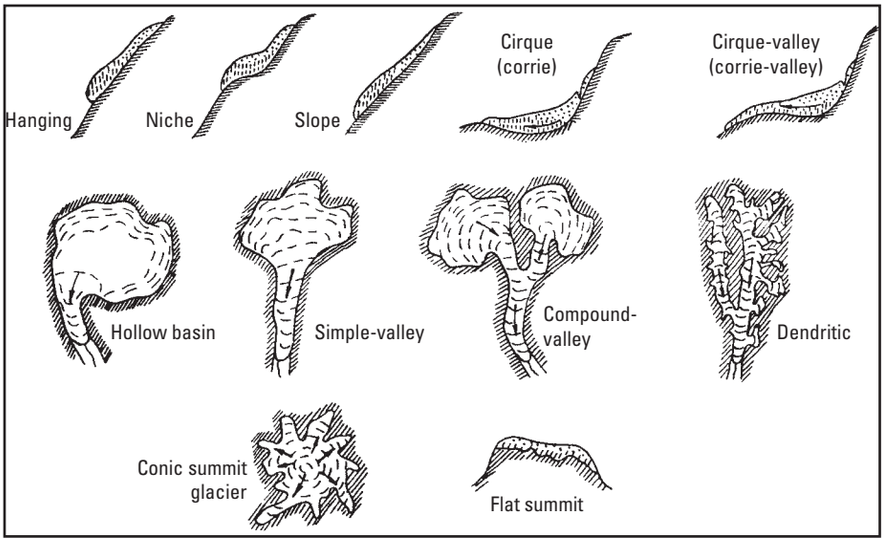


***Figure 2.**—Morphological types of mountain glaciers adopted for the Glacier Inventory of the USSR and used in this chapter.*

Caucasus (in Russia and the Republic of Georgia)

The Caucasus mountain system consists of two major mountain ranges: the southern Lesser Caucasus, and the northern Greater, or Main, Caucasus. Precipitation in the Lesser Caucasus is much lower, and glaciers are concentrated in the Main Caucasus, which is the subject of this section and referred to herein as the Caucasus. The study of glaciers in the Caucasus began in the first quarter of the 18th century. The first data on glaciers can be found in the works of Vakhushti Bagrationes (1997). In the middle and the second half of the 19th century, studies of glaciers were carried out together with geological investigations, geographical travels, mountaineering, and topographic studies. At the beginning of the 20th century, active glaciological investigations of the Caucasus were undertaken by the Russian Geographical Society.

The compilation of the first reliable map of the Caucasus, at a scale of 1:420,000 and depicting the largest glaciers, was completed by 1862. Topographic surveys of the Caucasus at a scale of 1:42,000 were accomplished 30 years later. Having analyzed these maps, K.I. Podozerskiy (1911) published the first inventory of Caucasus glaciers, compiling data on the lengths and areas of all of the glaciers.

In 1911, the German explorer H. Burmester (1913) performed the first phototheodolite surveys of the *Bol'shoy Azau* and *Shkelda* Glaciers. Tachymetric surveys of the termini of many glaciers were undertaken in 1932 during the Second International Polar Year (IPY, 1932-1933) (Russia, Committee of the Second International Polar Year, 1936b). Aerial photographs acquired during the 1940s and topographic maps compiled and published during the 1950s provided the basis for more modern studies and inventories of glaciers.

During the International Geophysical Year (IGY) (1957–1959) and for the next ten years, the glaciers of the Caucasus were studied during expeditions by Kharkov University (Kharkov University, 1960–1961), Moscow University (Tushinskiy, 1968), Institutes of Geography of the USSR Academy of Sciences (Various authors, 1964) and Georgian Academy of Sciences. Repeated aerial photography and phototheodolite surveys of some glacier areas were also undertaken. The comprehensive surveys performed by Moscow University in the El'brus area resulted in the compilation of the Atlas of El'brus Glaciers (Various authors, 1967).

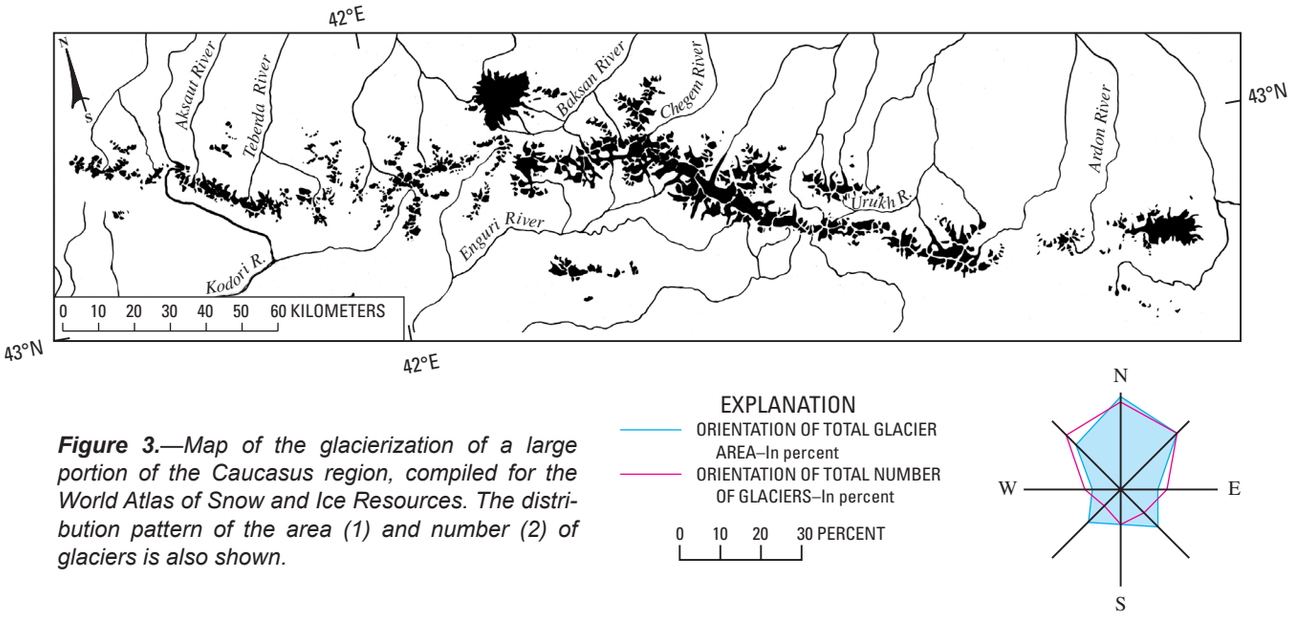


Figure 3.—*Map of the glacierization of a large portion of the Caucasus region, compiled for the World Atlas of Snow and Ice Resources. The distribution pattern of the area (1) and number (2) of glaciers is also shown.*

Comprehensive Caucasus studies used to compile the Glacier Inventory of the USSR, as well as water, ice, and heat-balance studies, were carried out in the representative Marukhskiy, Dzhankuat, and Gergetskiy glacier basins under the International Hydrological Decade (IHD) program from 1965 to 1974 (Golubev and others, 1978; Krenke and others, 1988; Panov, 1993). Results of these studies provided the basis for the Caucasus maps in the World Atlas of Snow and Ice Resources (Kotlyakov, 1997). Cartographic sources, aerial photographs, and space images were used to compile later maps of the glaciers of the Caucasus (Dolgushin and Osipova (1989)). Figure 3 is an example.

The glacierized area of the Caucasus extends for about 1,000 km from the northwest to the southeast. It is traditionally subdivided into three main regions: Western, Central, and Eastern Caucasus. The Western Caucasus region lies generally between the Black Sea and Mount El'brus, the Central Caucasus region, between Mount El'brus and Mount Kazbek, and the Eastern Caucasus region, between Mount Kazbek and the Caspian Sea. The northern and southern slopes are also considered separately. The distribution of glaciers in these areas is shown in table 2.

The Caucasus contains two large glacier complexes — one includes 23 glaciers on Gora (Mount) El'brus, at the west end of the Central Caucasus region, and the other includes 14 glaciers on Gora Kazbek, at the eastern end of the Central Caucasus region. Additionally, there are 11 valley and compound valley glaciers, each with an area of more than 10 km^2 (table 3). However, small glaciers with areas less than or equal to 1 km^2 prevail in the Caucasus (table 4). The number of these small glaciers is 85 percent of the total number of glaciers, but the area covered by them is 29 percent of the total area of glacierization. More than 60 percent of glaciers (57 percent of the glacierized area) have a northern exposure: northwest, north, or northeast (see fig. 3). However, the glaciers facing south are, in general, 1.5 times larger than the glaciers that have a northern exposure (Vinogradov and others, 1976).

Most of the morphological types of glaciers can be found in the Caucasus. Compound-valley glaciers and two glacier complexes on conic summits spread along the main ridge of the Central Caucasus, and the extent of glacierization in that area is more than 50 percent. Valley glaciers are situated at the edges of compound-valley glaciers. Cirque glaciers occur most frequently on the

TABLE 2.—*Distribution of glaciers in the main regions of the Caucasus*

[Unit: km^2, square kilometer]

Region of glacierization	Number of glaciers	Total area (km^2)
Western Caucasus	565	277.7
Central Caucasus	1,110	1,033.3
Eastern Caucasus	372	113.4
Total	2,047	1,424.4
Northern Slope	1,471	992.4
Southern Slope	576	432.0
Total	2,047	1,424.4

TABLE 3.—*Glacier complexes and large glaciers of the Caucasus*

[Abbreviations: km, kilometer; m, meter; AP, aerial photography; SI, surface investigation]

Glacier name	Name of the river basin	Area (km^2)	Length (km)	Elevation of the tongues (m)	Elevation of the firn line (m)	Firn line observations	
						Methodology	Dates
Gora El'brus glacier complex	Kuban' Malka, Baksan	122.6	—	2,480–3,697	3,550–4,000	AP	22 Aug 1957
The glacier complex of Gora Kazbek	Terek, Gizel'don	64.8	—	2,260–3,450	3,260–3,720	AP	1960–1965
Bezengi	Cherek	36.2	17.6	2,080	3,400–3,750	AP	15 Aug 1957
Dykh-Su	Cherek	34.0	13.3	2,070	2,900–3.750	AP	16 Sep 1957
Lekziry	Enguri	33.7	11.8	2,020	3,090	SI	3 Sep 1959
Tsaneri	Enguri	28.8	10.1	2,390	3,190	SI	25 Aug 1960
Karaugom	Urukh	26.6	13.3	1,830	3,440	AP	15 Sep 1957
Tviberi	Enguri	20.1	5.8	2,200	3,150	SI	15 Aug 1960
Agashtan	Cherek	15.9	9.8	2,250	3,140–3,380	AP	10 Sep 1957
Kvitlodi	Enguri	11.9	7.8	2,320	3,160	SI	30 Aug 1960
Chalaati	Enguri	11.3	7.3	1,850	2,980	SI	5 Sep 1959
Khalde	Enguri	11.0	8.4	2,450	3,440	SI	2 Sep 1962
Shaurtu	Chegem	10.1	9.1	2,220	3,220	AP	15 Aug 1957

TABLE 4.—*The distribution of glaciers and glacier complexes in the Caucasus based on their area*

[Unit: km^2, square kilometer]

Dimensions of glaciers and glacier complexes	Number of glaciers	Total area (km^2)
Largest (>100 km^2)	1 complex (El'brus)	122.6
Large (10.1–100 km^2)	1 complex (Kazbek); 11 other glaciers listed in table 3	304.4
Middle-sized (1.1–10.0 km^2)	250	581.9
Small (≤1 km^2)	1,749	415.5

Western Caucasus and on the northern slope of the Central Caucasus. Hanging glaciers are found everywhere, but they are most numerous in the Central Caucasus. Table 5 summarizes data on the distribution of the main morphological types of glaciers in the Caucasus. In the table, the category of valley glaciers also includes cirque-valley glaciers; the category of cirque glaciers incorporates hanging cirque glaciers, and the category of hanging glaciers also includes spill-over glaciers, glaciers lying near the crest, and niche glaciers. Table 5 only contains data on glaciers whose area is ≥0.1 km^2; the number of glaciers included in glacier complexes is shown in parenthesis.

Morphological characteristics of certain glacierized areas of the Caucasus are well depicted on Landsat images. The image of the Western Caucasus and Mount El'brus (fig. 4*A*) shows the spectacularly scattered and dispersed nature of the glacierization, with prevailing cirque and cirque-valley glaciers extending along and abutting the mountain crests. The relationship between morphological types of glaciers of this area is well represented on the map of the same area compiled for the World Atlas of Snow and Ice Resources (fig. 4*B*).

TABLE 5.—*The distribution of glaciers of the Caucasus according to morphological types*

[Values in parenthesis indicate number of individual glaciers. Abbreviations: N, number of glaciers; A, glacierized area, in square kilometers]

Glacierized area	Glacier complexes on conic summits		Compound-valley		Valley (includes cirque-valley)		Cirque (Corrie) (includes hanging cirque)		Hanging (includes spill-over and niche)		Flat summits' glaciers		Total	
	N	A	N	A	N	A	N	A	N	A	N	A	N	A
Western Caucasus	—	—	—	—	61	121.6	338	135.6	53	13.7	—	—	452	270.9
Central Caucasus	2 (37)	187.4	14	230.1	188	416.8	413	155.0	129	26.3	—	—	781	1,015.6
Eastern Caucasus	—	—	—	—	33	39.5	182	55.1	64	12.4	2	1.8	281	108.8
Northern Slope	2 (37)	187.4	11	165.0	143	306.0	668	267.7	212	43.5	2	1.8	1,073	971.4
Southern Slope	—	—	3	65.1	139	271.9	265	78.0	34	8.9	—	—	441	423.9
Total Caucasus	2 (37)	187.4	14	230.1	282	577.9	933	345.7	246	52.4	2	1.8	1,514	1,395.3

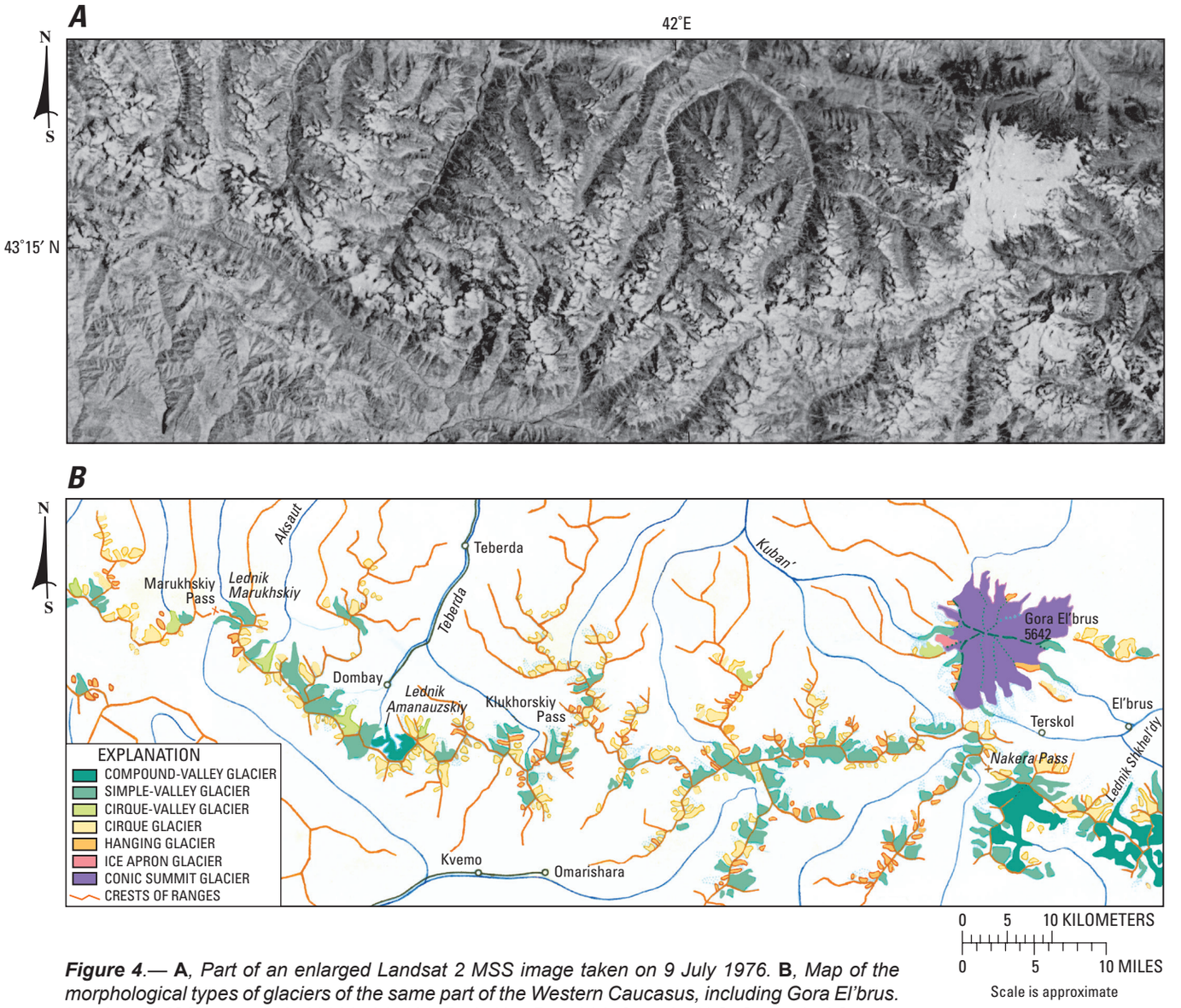


Figure 4.— **A**, *Part of an enlarged Landsat 2 MSS image taken on 9 July 1976.* **B**, *Map of the morphological types of glaciers of the same part of the Western Caucasus, including Gora El'brus. Landsat 2 MSS image 2185030007619190, Path 185–Row 30 is from the U.S. Geological Survey, EROS Data Center, Sioux Falls, S. Dak. 57198.*

During the IHD, detailed studies were undertaken in the Western Caucasus, in the representative Marukh mountain-glacier basin (fig. 4). These studies resulted in a series of regime maps of the Marukh Glacier (Lednik Marukhskiy) (fig. 5), which served as a model for similar maps in the World Atlas of Snow and Ice Resources.

The Landsat image makes it possible to distinguish the star-like shape of the Gora El'brus glacierization (fig. 6) with its complex of conic summit glaciers. Despite the small scale of this image, the termini of 14 large glaciers can be recognized. The glaciers can be seen in detail on the phototheodolite panoramas (photographic mosaic) of the northern (fig. 7*A*) and southern (fig. 7*B*) slopes of Gora El'brus.

Glacierization of the Central Caucasus has a fairly continuous nature, as can be seen on part of the Landsat image shown in figure 8*A*. It is well represented by the map of morphological types of glaciers, compiled for the World Atlas of Snow and Ice Resources (fig. 8*B*). Unlike the mostly debris-free glaciers of Western Caucasus, the Central Caucasus glaciers are characterized by well-developed moraines, which can be seen in space images on the surface of large valley glaciers.

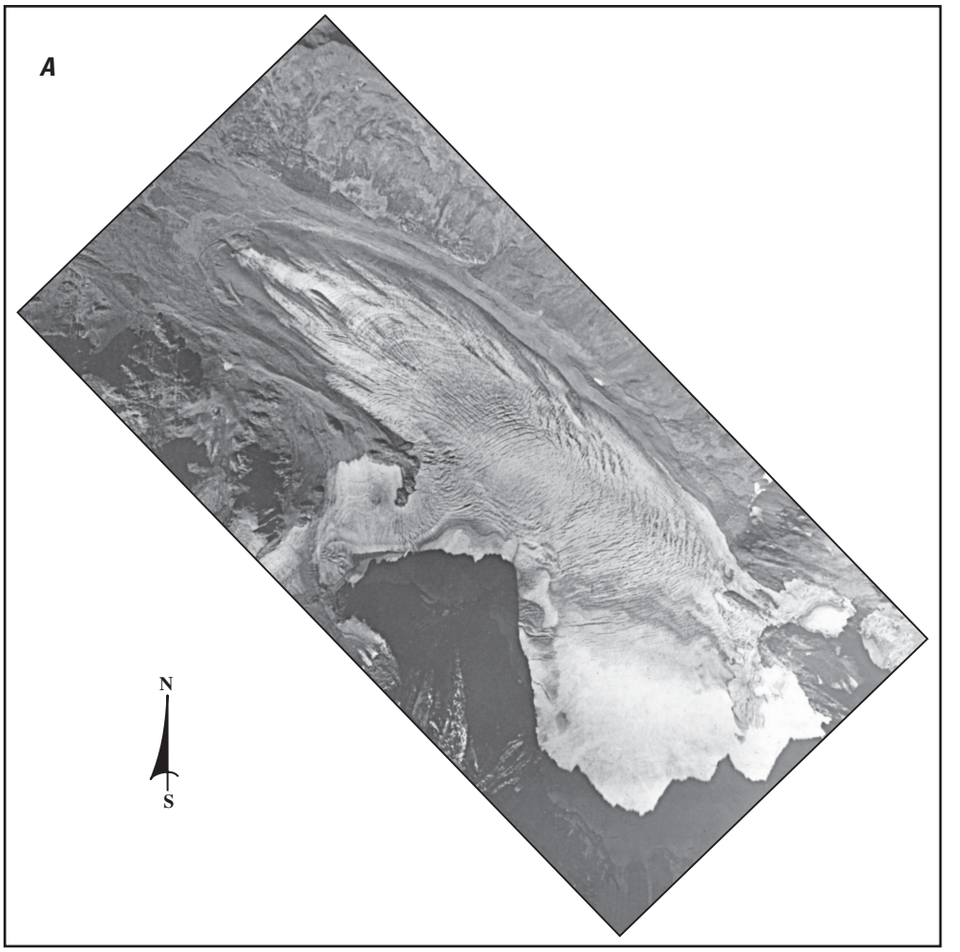
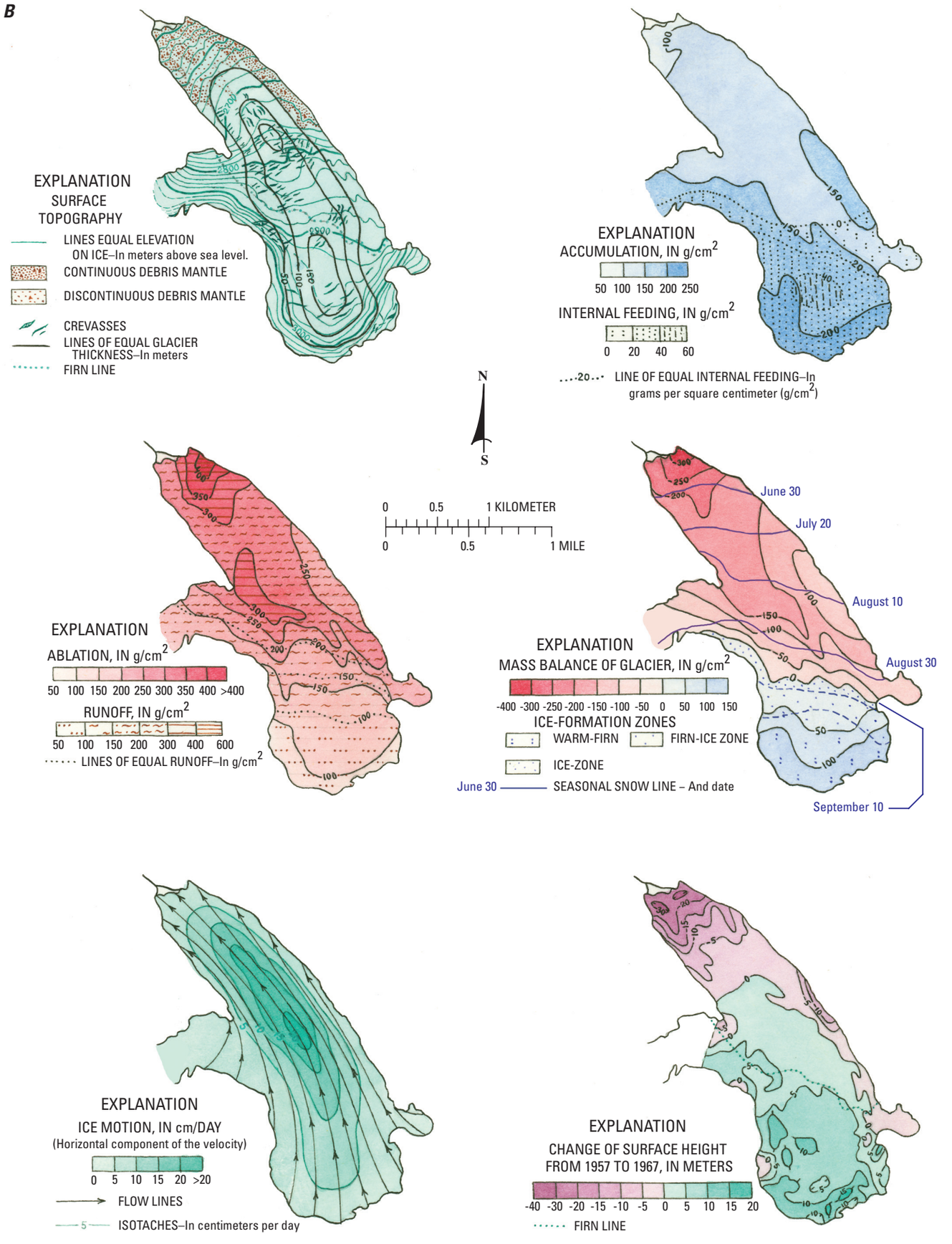
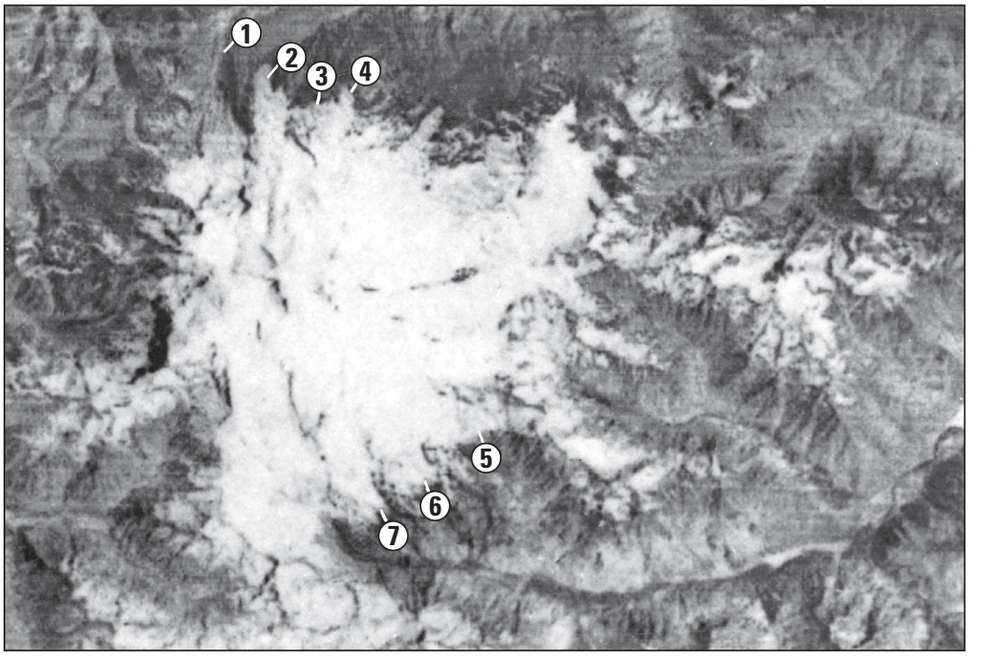


***Figure 5.**—(above and continued at right)* **A**, *Aerial photograph of the Lednik Marukhskiy (see fig. 4 for location) taken on 15 September 1955, and* **B**, *a series of glaciological maps of this glacier based on detailed studies done during the IHD.*


B
EXPLANATION
SURFACE TOPOGRAPHY
LINES EQUAL ELEVATION ON ICE–In meters above sea level.
CONTINUOUS DEBRIS MANTLE
DISCONTINUOUS DEBRIS MANTLE
CREVASSES
LINES OF EQUAL GLACIER THICKNESS–In meters
FIRN LINE
EXPLANATION
ACCUMULATION, IN g/cm2
50 100 150 200 250
INTERNAL FEEDING, IN g/cm2
0 20 40 60
-20- LINE OF EQUAL INTERNAL FEEDING–In grams per square centimeter (g/cm2)
N
S
0 0.5 1 KILOMETER
0 0.5 1 MILE
EXPLANATION
ABLATION, IN g/cm2
50 100 150 200 250 300 350 400 >400
RUNOFF, IN g/cm2
50 100 150 200 300 400 600
LINES OF EQUAL RUNOFF–In g/cm2
June 30
July 20
August 10
August 30
September 10
EXPLANATION
MASS BALANCE OF GLACIER, IN g/cm2
-400 -300 -250 -200 -150 -100 -50 0 50 100 150
ICE-FORMATION ZONES
WARM-FIRN
FIRN-ICE ZONE
ICE-ZONE
June 30 SEASONAL SNOW LINE – And date
EXPLANATION
ICE MOTION, IN cm/DAY
(Horizontal component of the velocity)
0 5 10 15 20 >20
FLOW LINES
5 ISOTACHES–In centimeters per day
EXPLANATION
CHANGE OF SURFACE HEIGHT FROM 1957 TO 1967, IN METERS
-40 -30 -20 -15 -10 -5 0 5 10 15 20
FIRN LINE

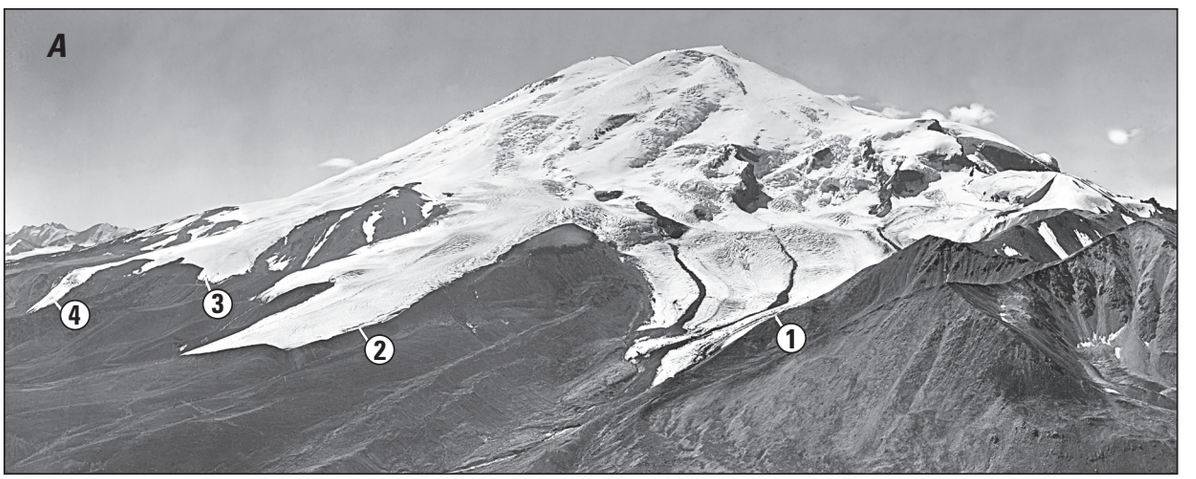


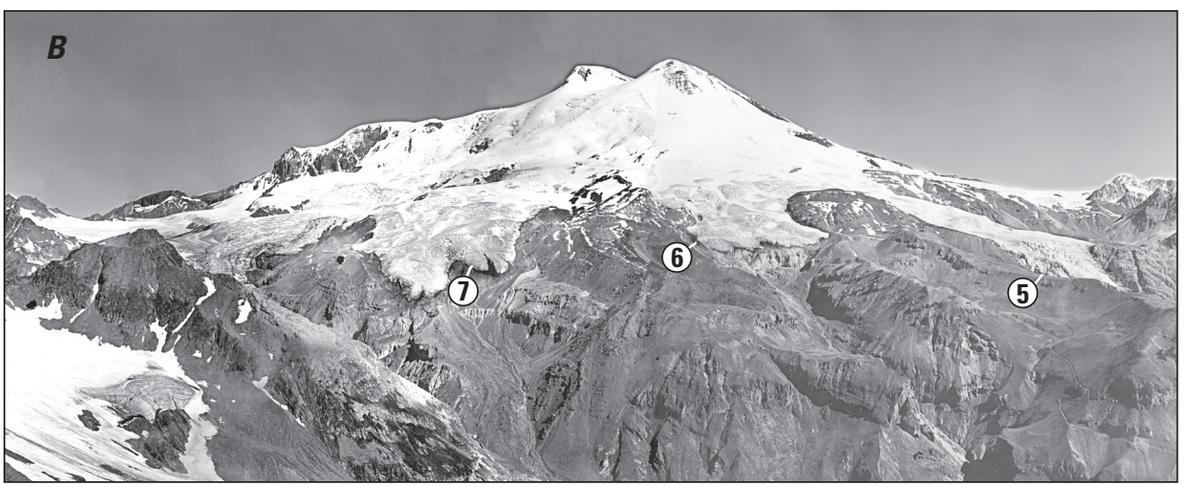
0 5 KILOMETERS
0 5 MILES
Scale is approximate

EXPLANATION

1 *Lednik Ulluchiran*
2 *Lednik Karachaul*
3 *Lednik Ullukol*
4 *Lednik Ullumalienderku*
5 *Lednik Terskol*
6 *Lednik Garabashi*
7 *Lednik Maliy Azau*

N
S





EXPLANATION

1 *Lednik Ulluchiran*
2 *Lednik Karachaul*
3 *Lednik Ullukol*
4 *Lednik Ullumalienderku*
5 *Lednik Terskol*
6 *Lednik Garabashi*
7 *Lednik Maliy Azau*

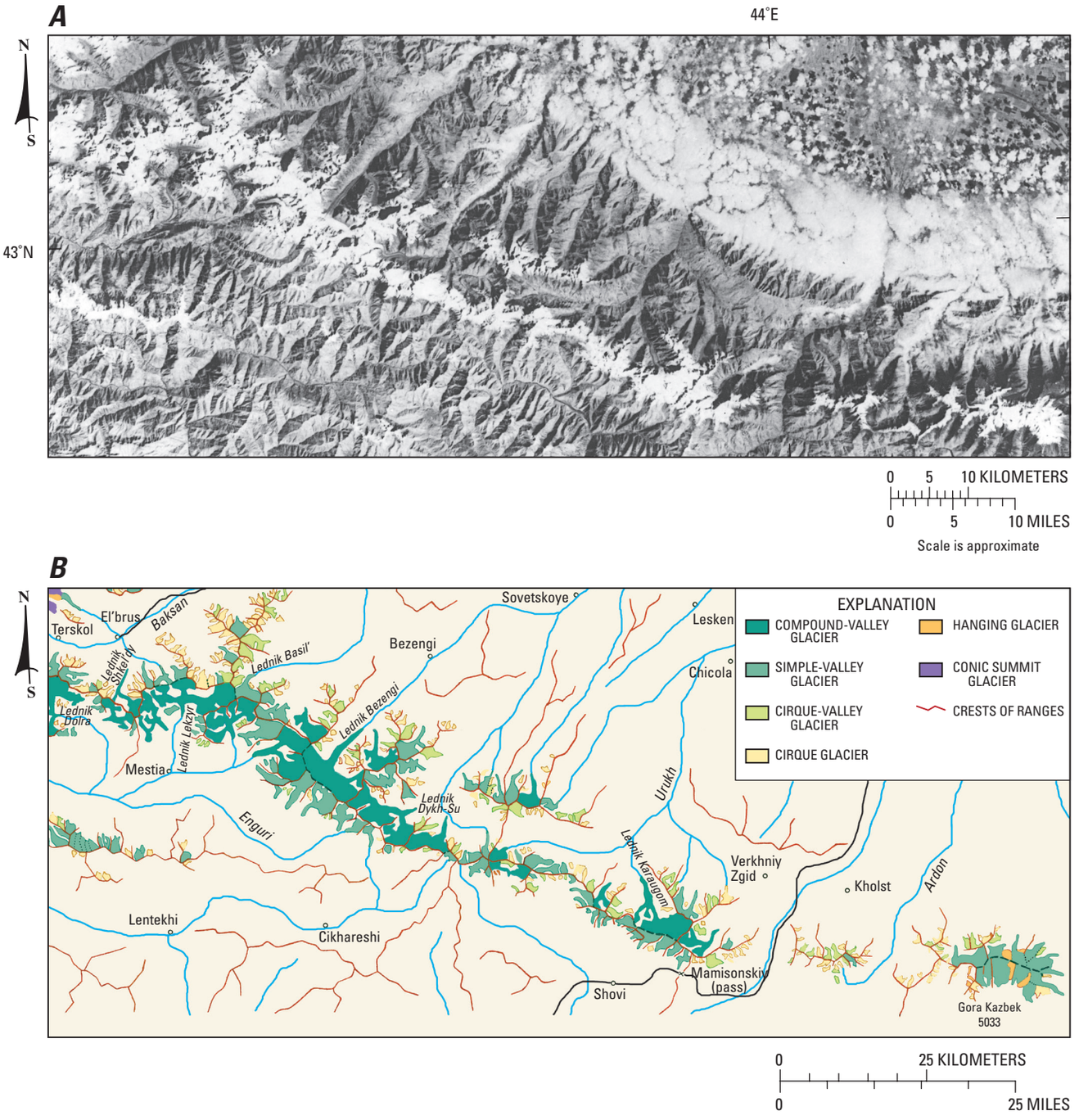


Figure 6.— *(at left, top) Enlargement of part of a Landsat 2 MSS image taken on 9 July 1976, depicting the El'brus massif (lat 43°21'N., long 42°26'E.). Landsat 2 MSS 2185030007619190, Path 185–Row 30, is from the U.S. Geological Survey, EROS Data Center, Sioux Falls, S. Dak. 57198.*

Figure 7.— *(at left, bottom) Panoramic photographic mosaic of the northern (***A***) and southern (***B***) slopes of Gora El'brus. Phototheodolite surveys were done by F.N. Nikulin in 1957 and A.V. Brukhanov in 1958, respectively.*

Figure 8.— *(this page)* **A**, *Part of an enlargement of a Landsat 2 MSS image of the Central Caucasus, taken on 13 September 1977.* **B**, *Map of the morphological types of glaciers of the Central Caucasus. Landsat 2 MSS image 2184030007725690, Path 184–Row 30, is from the U.S. Geological Survey, EROS Data Center, Sioux Falls, S. Dak. 57198.*

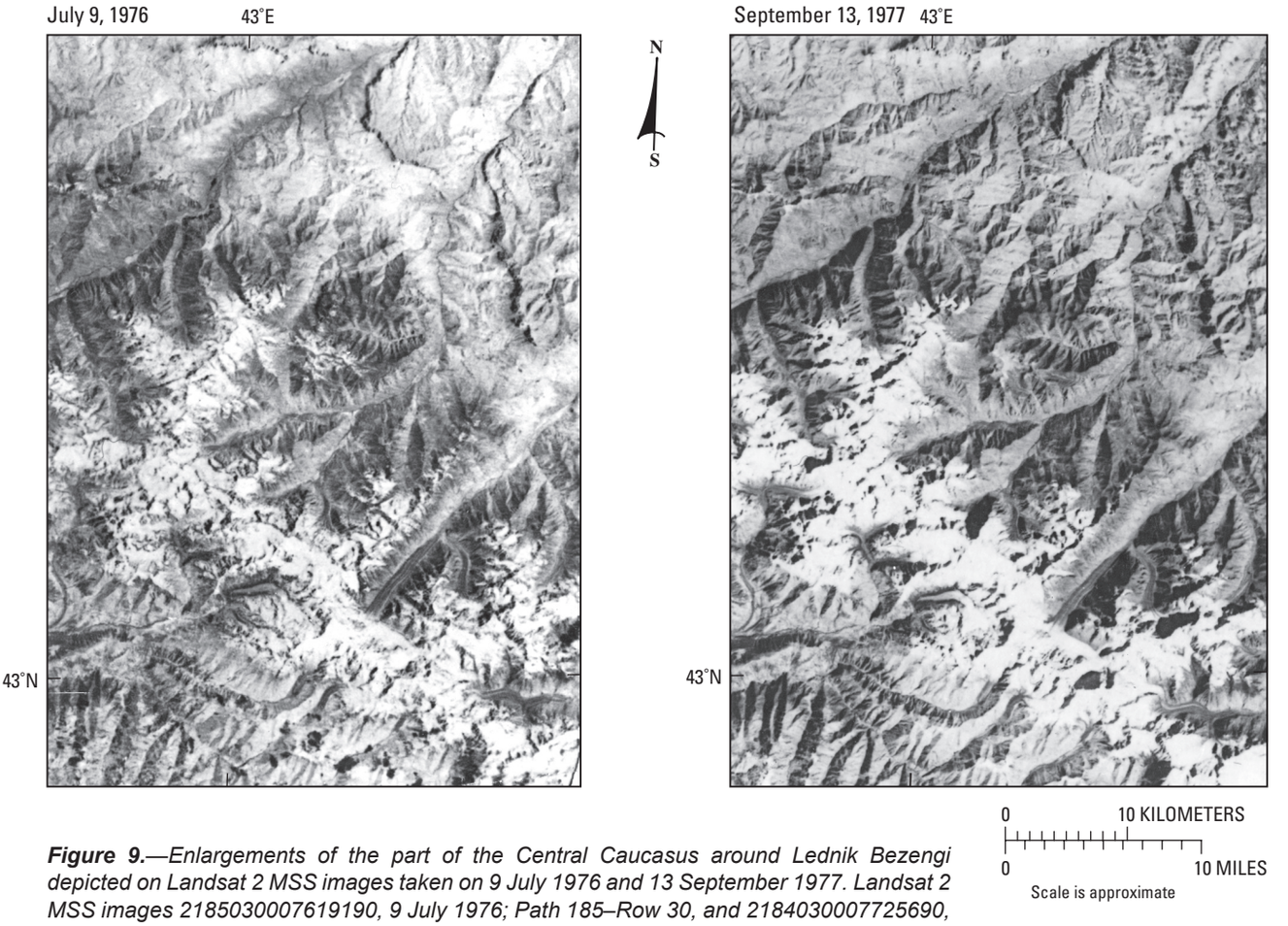


***Figure 9.**—Enlargements of the part of the Central Caucasus around Lednik Bezengi depicted on Landsat 2 MSS images taken on 9 July 1976 and 13 September 1977. Landsat 2 MSS images 2185030007619190, 9 July 1976; Path 185–Row 30, and 2184030007725690, 13 September 1977; Path 184–Row 30, are from the U.S. Geological Survey, EROS Data Center, Sioux Falls, S. Dak. 57198.*

The ability to identify glaciers on space images depends naturally on the season, residual snow pack, or new snow cover at the time of the surveys. For example, a comparison of two images of the same area of the Caucasus taken on 9 July 1976 and on 13 September 1977 (fig. 9), suggests that the latter image is not as useful for observing the glaciers because the upper parts of the ranges already had been covered with early autumn snowfalls.

The Kazbek massif in the eastern part of the Central Caucasus can be seen very well in figure 8. The surging *Lednik Kolka* is situated here, and a surge was observed in the winter of 1969/70. Continued investigations undertaken in this area by the Institute of Geography, the USSR Academy of Sciences, made it possible to compile the sketches shown in figures 10*B* and *C*. They indicated that the overloading of this glacier by debris was one of the main causes of its surge, which is clearly seen in the aerial photograph (fig. 10*A*) (see also companion section in this part of the chapter which provides a discussion of the 2002 surge of the *Lednik Kolka*).

Glacierization of the Eastern Caucasus has a disparate nature. Separate groups of glaciers are confined to the high parts of crests that have cirques. On the northern slopes of these ranges, small cirque glaciers are situated in the near-crest zone. One such area of glacierization situated on the *Djul'tydag* range in the upper reaches of the Karakoysu river is seen in the part of the Landsat image shown in figure 11. This image, together with two other parts of Landsat images of the Western and Central Caucasus, testifies to the differences in the general nature of the mountain glaciers depicted on space images.

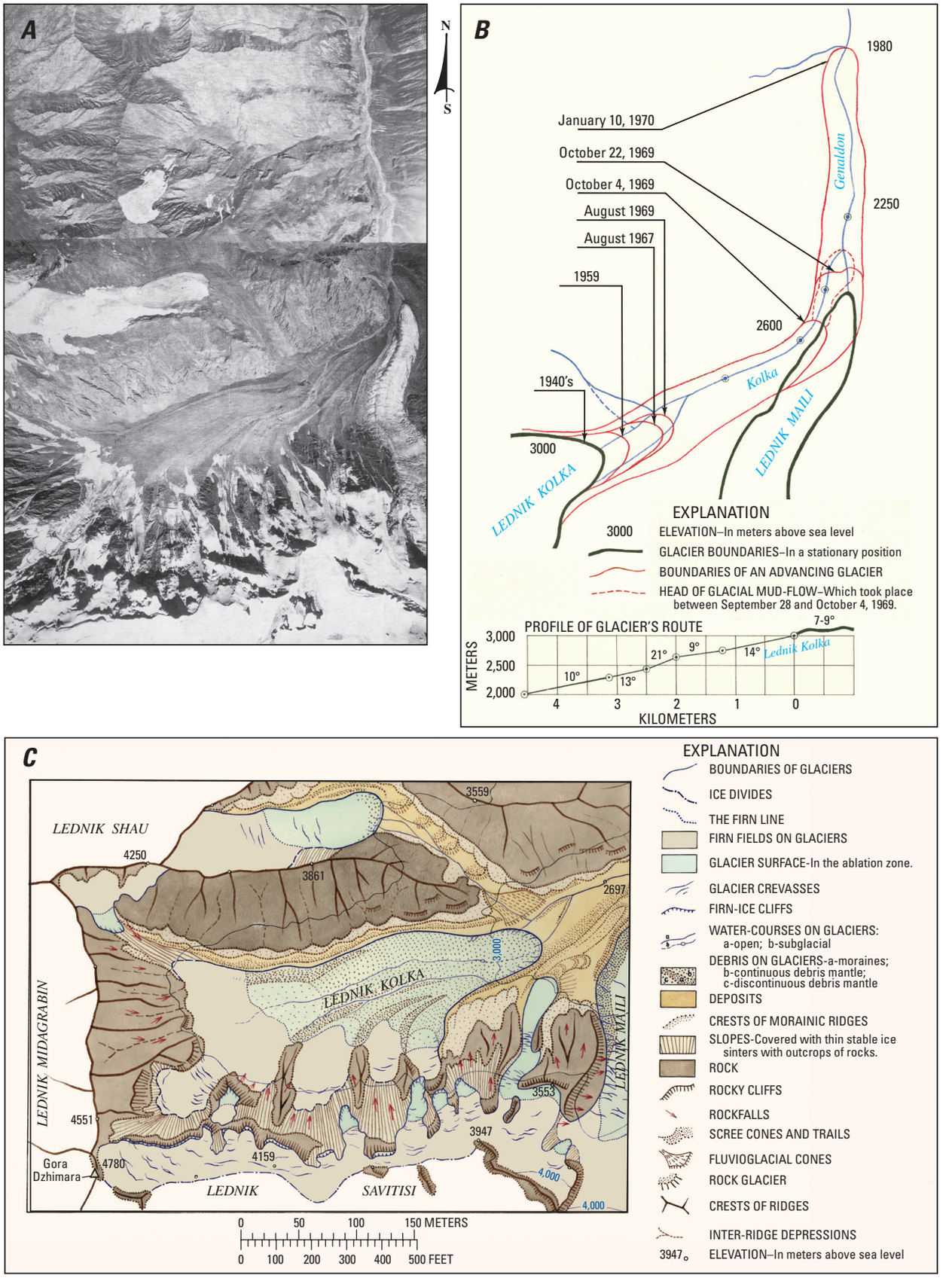


Figure 10.— *Illustrations of the surging* Lednik Kolka *(approximate lat 42°50'N., long 44°30'E.), Gora Kazbek:* **A**, *Aerial photograph,* **B**, *sketch map of the advance, and* **C**, *morphology of the glacier basin.*

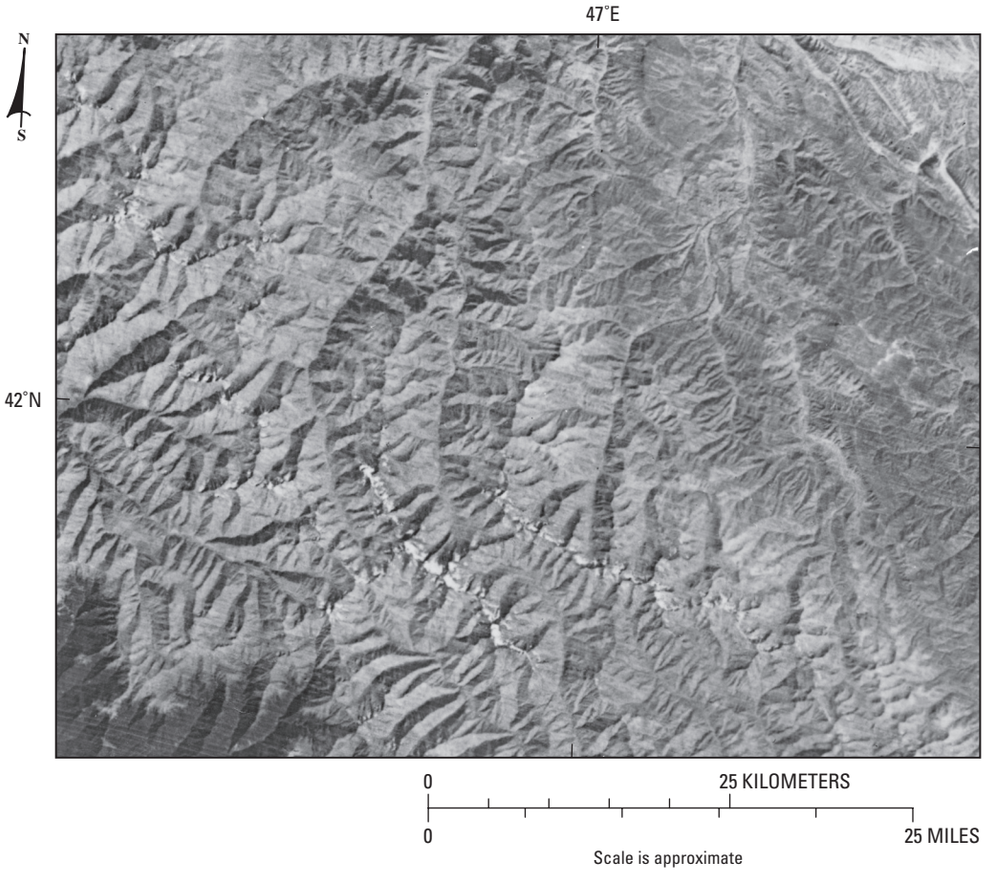


Figure 11.—*Part of the Eastern Caucasus with the* Djul'tydag *range depicted on a Landsat 2 MSS image taken on 28 August 1976. The Landsat 2 MSS image 2181031007624190, Path 181–Row 31, is from the U.S. Geological Survey, EROS Data Center, Sioux Falls, S. Dak. 57198.*

Pamirs, Alai (Alayskiy), and Gissar (Hisor) Ranges (in the Republics of Tajikistan, Kyrgyzstan, and Uzbekistan)

Studies of the glaciers of the Pamirs, located in eastern Tajikistan (fig. 1), were begun during the second half of the 19th century and were initially connected with the names of well-known geographers, geologists, and botanists: A.P. and B.A. Fedchenko, I.V. Mushketov, V.F. Oshanin, G.E. Grum-Grzhimailo, and V.I. Lipskiy. The first systematic data on the glaciers of the Pamirs were obtained by N.L. Korzhenevskii, who began studying these glaciers in 1903, and in 1930, published the first inventory of Central Asian glaciers (Korzhenevskii, 1930).

Field studies conducted during the Soviet-German expedition of 1928 and later during the Tajik-Pamirian expedition of the USSR Academy of Sciences (1929-1932) resulted in the compilation of a topographic map of the alpine area of the Central Pamirs, a region previously unknown. The expeditions also resulted in the discovery of the highest peak (7,495 m) in the USSR — Communism Peak (Pik Kommunizma, now named Pik Imeni Ismail Samani) and the describing of numerous glaciers on many Pamirian ranges.

During the Second International Polar Year (1932–1933), the primary glaciological studies were concentrated around the area of Fedchenko Glacier (Lednik Fedchenko). Here, at an elevation of 4,200 m a.s.l., an observatory was constructed and repeated phototheodolite surveys of the Tanymas group of glaciers and Lednik Fedchenko were carried out (Russia, Committee of the Second International Polar Year, 1936a).

During the post-World War II years, complete aerial photography of the area was acquired, and compilation of a large-scale topographic map was completed. Using these data, R.D. Zabirov compiled an inventory of glaciers of the Pamirs and published it as a monograph (Zabirov, 1955). This inventory lists 1,085 glaciers that were each more than 1.5 km in length, covering a total area of about 8,041 km^2.

Since 1962, the Institute of Geography, the USSR Academy of Sciences (now the Russian Academy of Sciences) has been responsible for investigations of Pamirian glaciers. From 1968 to 1978, the Institute carried out a series of comprehensive field studies connected to the inventorying of glaciers. The new glacier inventory of the Pamirs and the Alai Range (Alayskiy Khrebet) was compiled on the basis of interpretation of aerial photographs complemented by analysis of space images.

Glaciers are located on nearly all of the Pamirian ranges and occupy more than 10 percent of the total surface area at higher elevations. Their sizes are varied — from scattered small glaciers to large glacier complexes. Table 6 contains a list of the largest glaciers of the Pamirs and the Alayskiy Khrebet; table 7 presents their distribution based on size. Medium-sized glaciers (more than 1 km^2 but less than 10 km^2) are most common, but large glaciers (more than 10 km^2 but less than 100 km^2) are also numerous, a fact that differentiates this area from the glacierization of the Caucasus.

TABLE 6.—*Largest glaciers of the Pamirs and the Gissar (Hisor) and Alai (Alayskiy Khrebet) Ranges*

[Units: km, kilometer; m, meter]

Glacier name	River basin	Area (km^2)	Length (km)	Elevation of the tongue (m)	Elevation of the firn line (m)
Fedchenko	Muksu	651.7	77.0	2,910	4,700
Grumm-Grzhemaylo	Bartang	142.9	37.0	3,610	5,080
Zeravshanskiy	Zeravshan	132.6	27.8	2,810	4,000
Garmo	Obikhingob	114.6	30.4	2,970	4,900
Oktyabr'skiye	Karakul'	88.2	19.0	4,440	5,200
Korzhenevskogo	Kyzylsu	73.0	21.5	3,890	5,100
Geograficheskogo Obshchestva	Vanj	64.4	24.2	2,580	4,200
Fortambek	Muksu	57.3	27.2	2,850	4,170
Lenina	Kyzylsu	55.3	13.5	3,760	4,500
Severniy Tanymas	Bartang	55.0	18.0	3,790	4,900
Nura	Kyzylsu Vostochnaya	54.2	13.8	3,520	4,550
Preobrazhenskogo-Rama	Zeravshan	54.0	12.8	2,960	4,080
Bol'shoya Sauk-Dara	Muksu	53.0	20.6	4,240	5,470
Uisu	Markansu	49.9	13.8	4,390	5,200

TABLE 7.—*Distribution of glaciers based on their area*

[Abbreviations: km^2, square kilometer; N, number of glaciers; A, area of glaciers, in square kilometers]

Glaciers	Small ≤1 km^2		Medium ≤10 km^2		Large ≤100 km^2		Largest >100 km^2		Totals	
	N	A	N	A	N	A	N	A	N	A
Pamirs	5,488	1,559.6	1,151	2,988.5	88	2,036.1	3	909.2	6,730	7,493.4
Qatorkŭhi Hisor/ Hisor Tizmasi and Alayskiy Khrebet	3,449	945.6	431	1,008.5	12	249.1	1	132.6	3,893	2,335.8
Total	8,937	2,505.2	1,582	3,997.0	100	2,285.2	4	1,041.8	10,623	9,829.2

The nature of the Pamirian glacierization changes from west to east and is also affected by elevation. Scattered cirque and small valley glaciers prevail in the western part of the mountains. They are gradually replaced eastward by larger valley, compound-valley, and lastly, dendritic glaciers. A Landsat image (fig. 12) demonstrates well the narrow valleys, surrounded by sharp crests, where valley glaciers occur. Compound-valley glaciers are situated in the upper heads of the valleys, and many of the glaciers' tongues have thick mantles of debris (fig. 13).

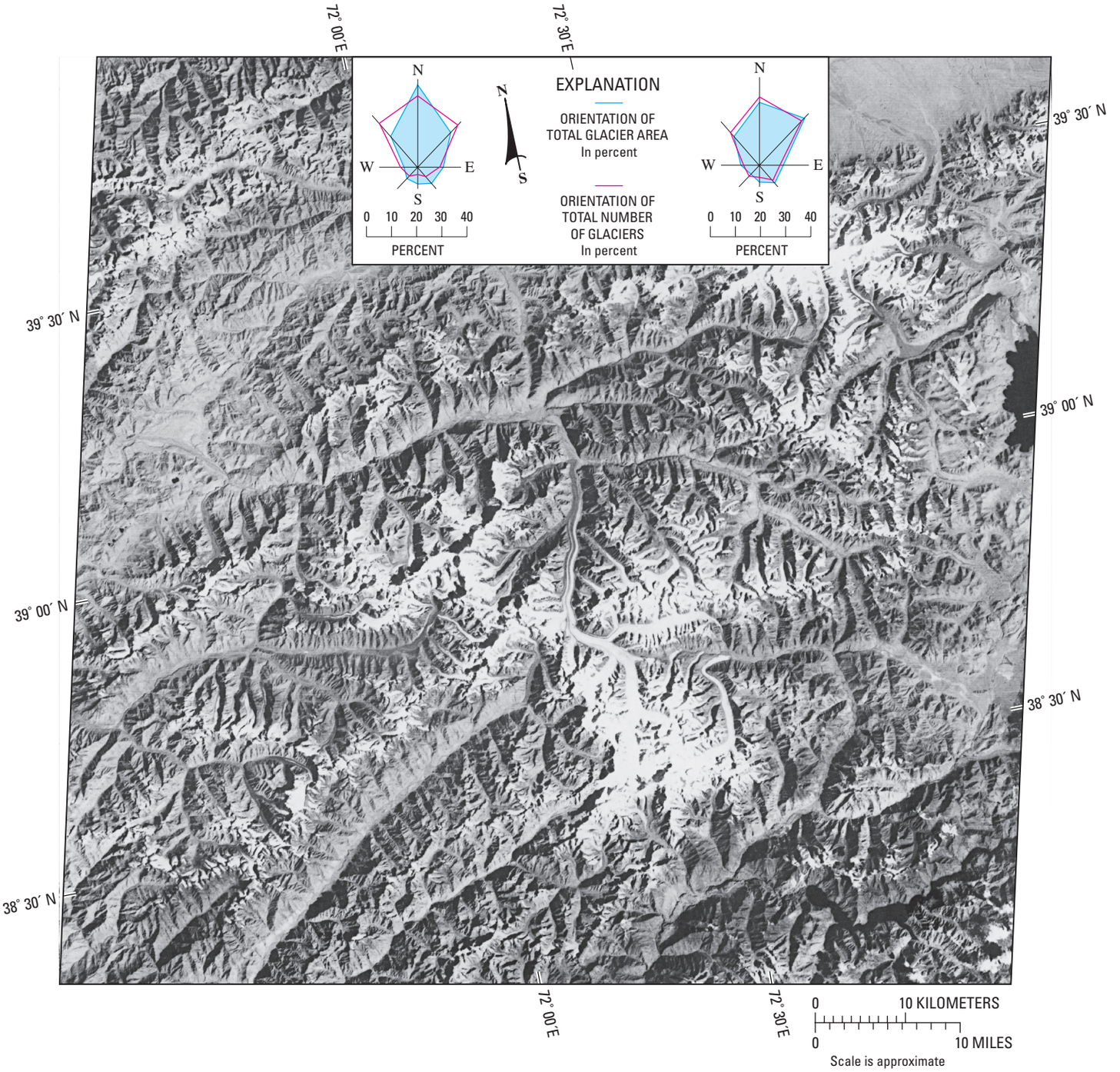


***Figure 12.**—Landsat 2 MSS image of the Central Pamirs acquired on 28 September 1977 and the distribution pattern of the area (in blue) and number (in red) of glaciers related to glacier orientation in the Hisor and Alayskiy Ranges (left) and the Pamirs. Landsat 2 MSS image 2980-04445 (band 6), Path 163–Row 33, is from the U.S. Geological Survey, EROS Data Center, Sioux Falls, S. Dak. 57198.*

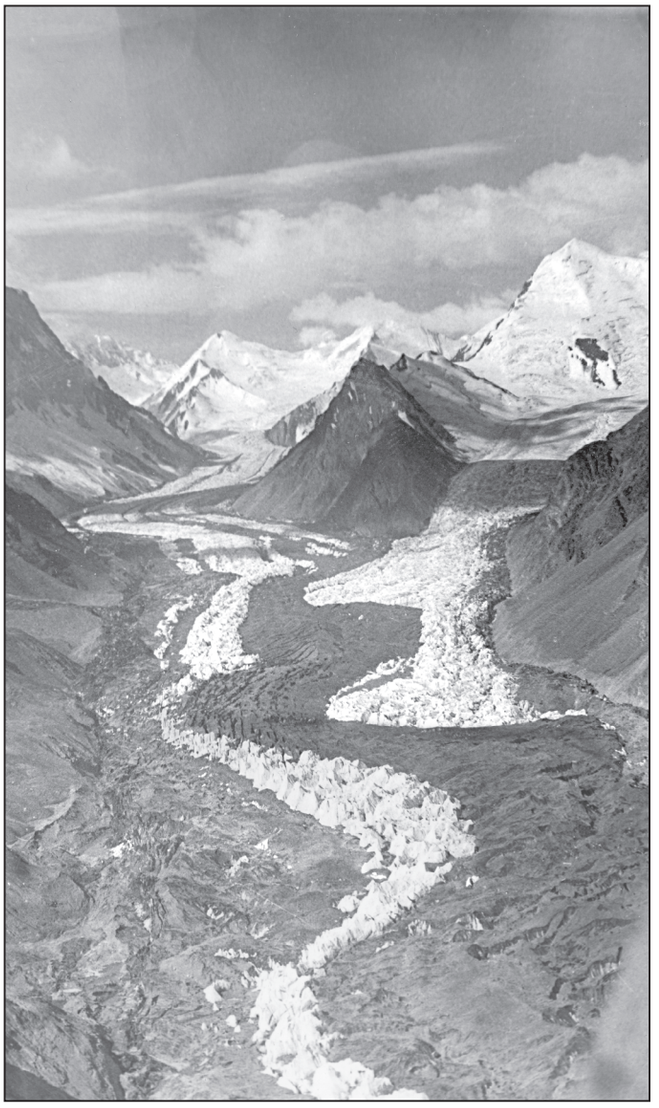


***Figure 13.**—The Lednik Bivachnyy surging glacier, tributary of Lednik Fedchenko with loops of medial moraines.*

In the Central Pamirs, compound glacier complexes consisting of adjoining compound-valley and dendritic glaciers are present. The largest is the Lednik Fedchenko complex. It has 26 tributaries and is illustrated in the enlarged part of a Landsat image (fig. 14*A*) and on the map prepared for the World Atlas of Snow and Ice Resources (fig. 14*B*). Within the area of the satellite image presented in figure 14*A*, the extent of glacierization in different areas is very large — from 60 to 85 percent.

The *Zaalayskiy Khrebet* lies in northeastern Tajikistan on the border with Kyrgyzstan, in the northern portion of the Pamirs. Glacierization of the central part of the *Zaalayskiy Khrebet* (Qatorkŭhi Pasi Oloy (in Tajikistan)) or Chong Alay Kyrka Toosu (in Kyrgyzstan), is similar in nature. The similarity in glacierization can be seen in figure 15, where large compound-valley glaciers flow from the second highest summit of the Pamirs, Lenin Peak (Pik Lenina).

However, in some areas, the typical glacierization of the Eastern Pamirs is quite different from that of the Central Pamirs. Eighty percent of the Eastern Pamirs (both numerically and in area) is occupied by small valley glaciers, and especially niche glaciers, which were first identified here. They cover the wide and gently sloping mountains with a relatively thin layer (some tens of meters) of glacier ice (fig. 15); the ice surface is debris free (fig. 16). In general, East Pamirian glacierization has a scattered nature; individual groups of glaciers are separated by dozens of kilometers.

The good quality early Landsat 1, 2, and 3 MSS images of the Pamirs that are cloud-free in glacier areas, have minimal snow cover, and have a pixel resolution of 80 m, make it possible to easily interpret the boundaries of Pamirian glaciers that have an area >1 km^2. Big valley, compound-valley, and dendritic glaciers depicted on space images convey a great deal of information. Upper boundaries of such glaciers can be well delineated when they are surrounded by rock. Debris mantle of varying compactness is clearly seen on the surface of glacier tongues, and the linear outlines of medial moraines are highly visible, making it possible to determine the tributaries of compound-valley glaciers and their relative importance. The most informative images are those taken at the beginning of September for the Western and Central Pamirs and those taken at the end of August for the Eastern Pamirs.

The Pamirs is a classic area of surge-type glaciers, similar to Alaska (Post, 1969). About 100 surge-type glaciers are known in the Pamirs, and many of them are easily identified on space images. This work was pioneered by R. Krimmel of the U.S. Geological Survey on the basis of Landsat imagery (Krimmel and others, 1976; Krimmel, 1978), and, soon thereafter, interpretation of Soviet space images made it possible to detect a number of glaciers at different stages of a surge cycle (Desinov and others, 1978). The diagnostic features of surge-type glaciers — looped medial moraines (fig. 13), active crevassing of the surface, the reduction of surface albedo, and rapid advance of

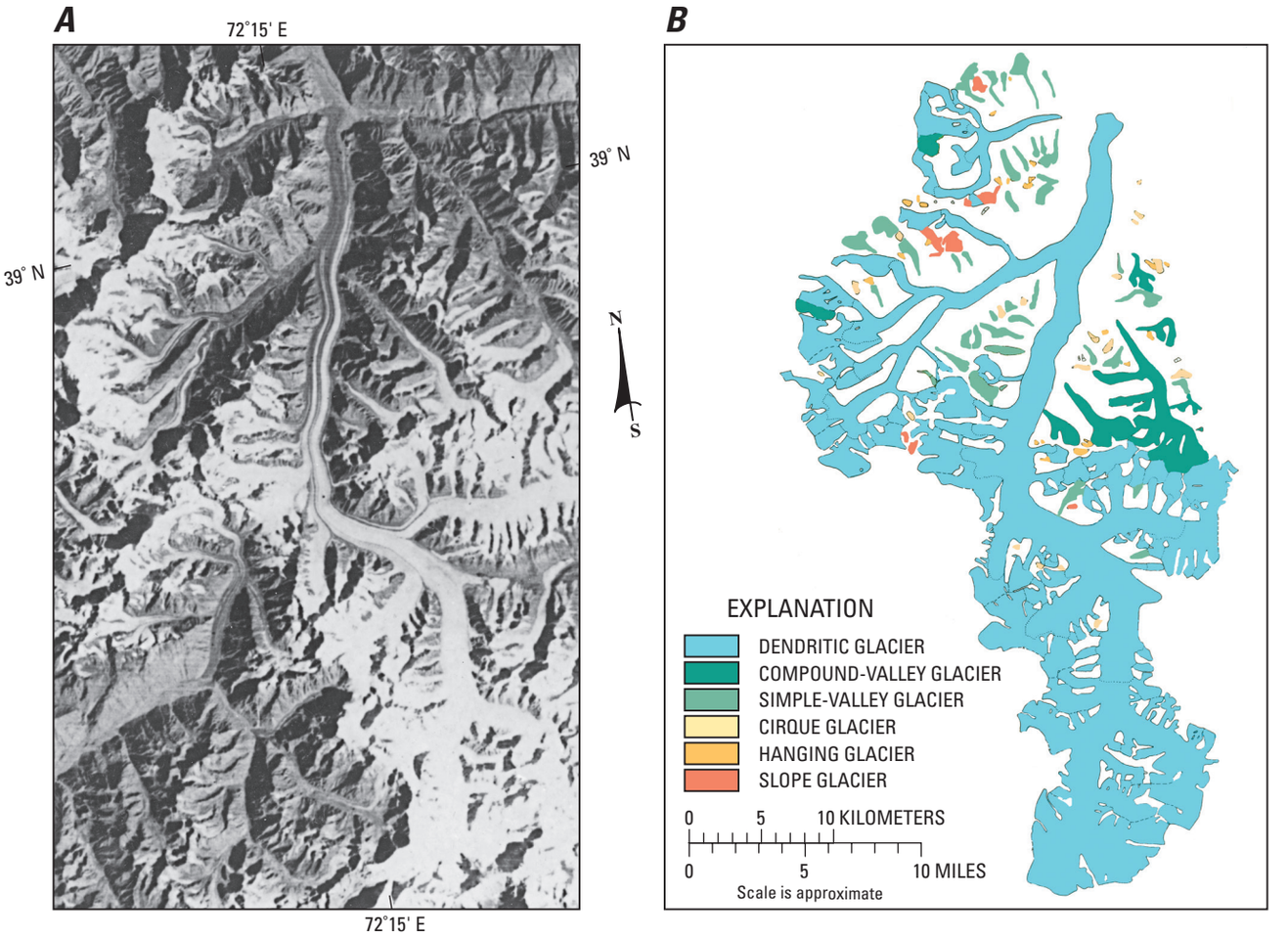


Figure 14.—**A**, *Enlargement of part of the Landsat image (fig. 12), showing the Lednik Fedchenko basin; and* **B**, *the sketch map showing the distribution pattern of morphological types of glaciers in this area.*

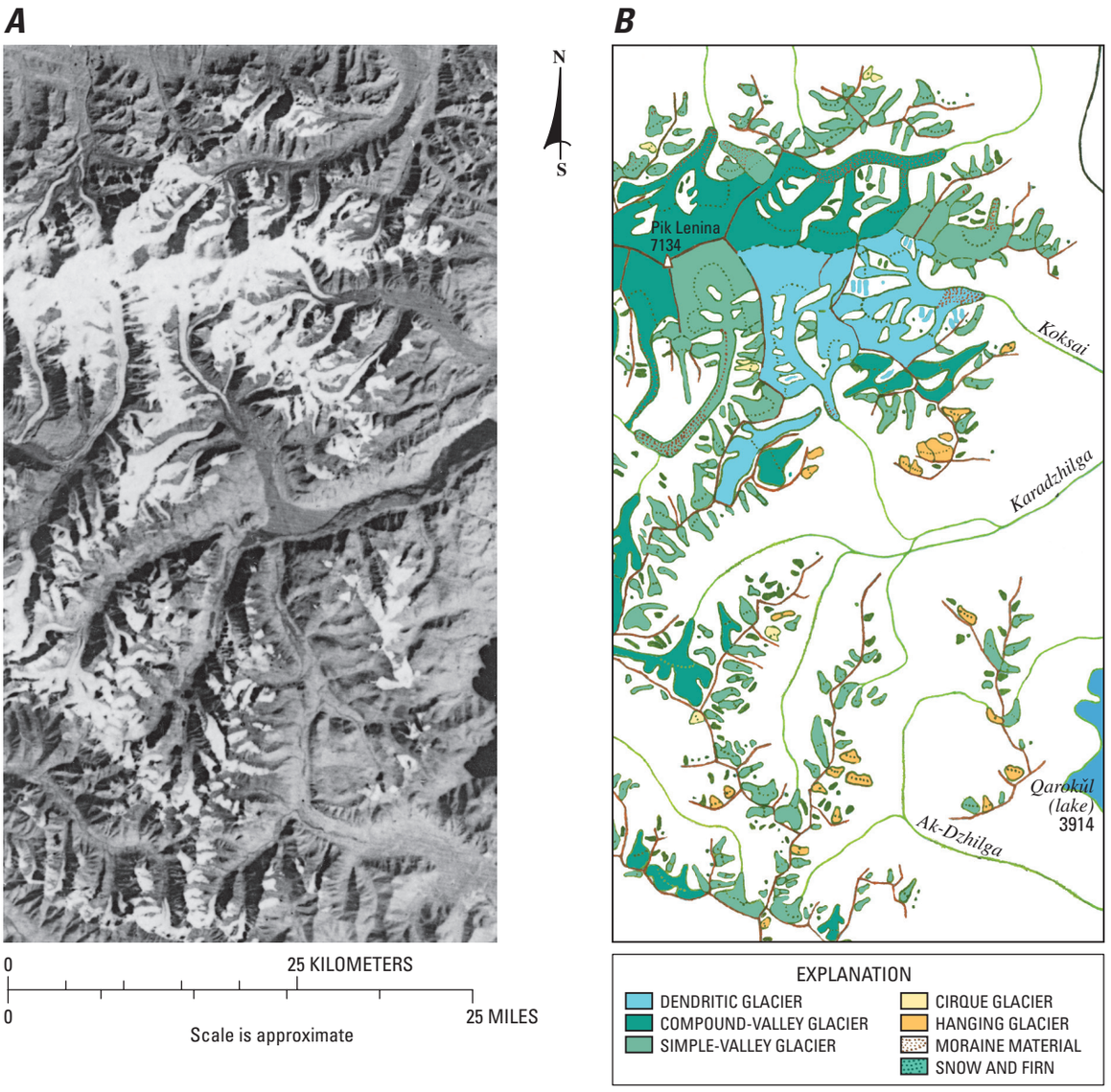


***Figure 15.*—A**, *Enlargement of part of the Landsat image of 28 September 1977 (fig. 12) showing the eastern part of Zaalayskiy Khrebet (at the top) (Qatorkŭhi Pasi Oloy) and part of the Eastern Pamirs (at the bottom).* **B**, *Sketch map showing the pattern of morphological types of glaciers in this region.*

a large volume of ice beyond the previous position of the terminus (figs. 17 and 18) — permit one to reliably detect surge-type glaciers on space images and to survey them from space. The Salyut–6 astronauts made such observations, which permitted them not only to identify a number of new surge-type glaciers in the Pamirs, but also to predict the beginning of their next surge.

Very interesting results were obtained by observing a group of glaciers in the upper reaches of the Saukdara river on the southern slope of Qatorkŭhi Pasi Oloy (fig. 17*A*), where three large glaciers — *Valy*, *Dzerzhinskogo*, and *Maliy Saukdara* — advanced abruptly from 1973 to 1977 (fig. 17*B*). The advance was first seen in 1973 on *Ledniki Dzerzhinskogo* and *Maliy Saukdara*. Their surges stopped in 1976 and 1975, respectively. *Lednik Valy* started advancing in 1975 and continued into 1977. Changes in the positions of these glaciers were clearly visible on Landsat images taken in July 1973 and in September 1977, and on some Soviet space images taken annually of this area.



Figure 16.—*Debris-free slope glaciers of the Eastern Pamirs.*

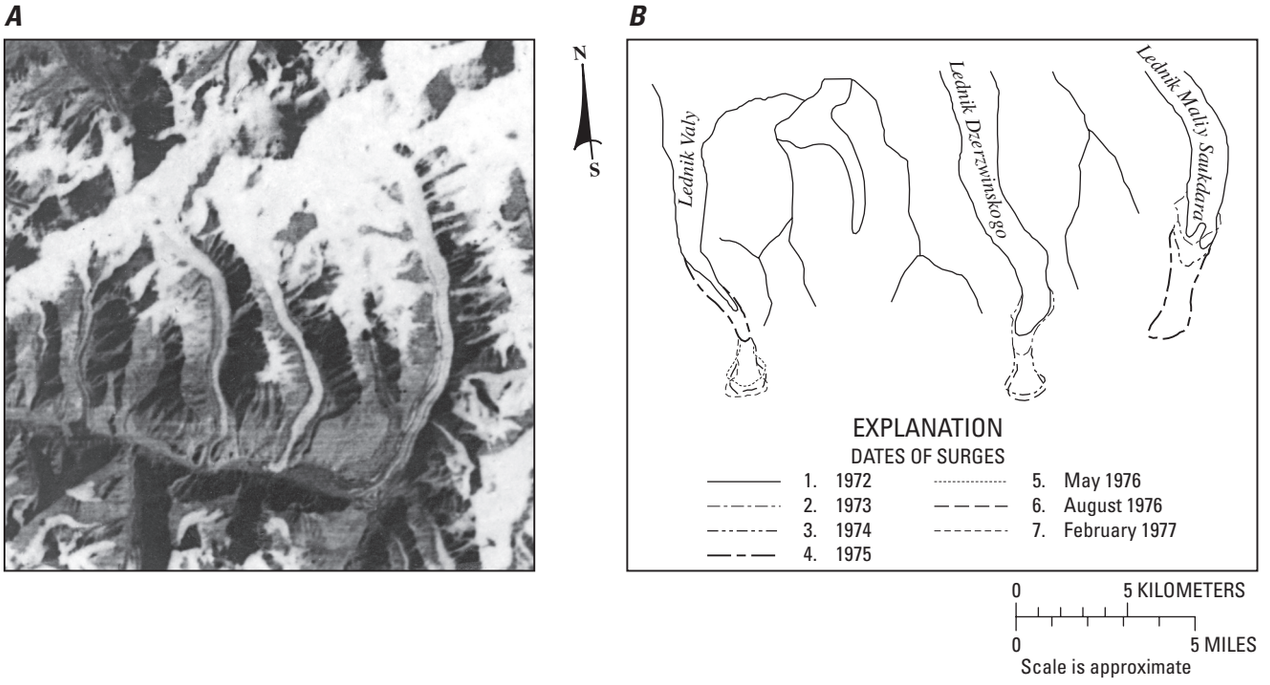


Figure 17.—**A**, *Enlargement of part of the Landsat image (fig. 12), showing the upper reaches of the Saukdara river (lat ~39°20'N., long 72°50'E.); and* **B**, *A sketch map of surges of the Saukdara group of glaciers from 1973 to 1977.*

The Gissar Range lies northwest of the Pamirs, in the northwest portion of Tajikistan (there called Qatorkŭhi Hisor) and in southeastern Uzbekistan (there called Hisor Tizmasi). This mountain range has very few glaciers, and will not be discussed further in this chapter.



***Figure 18.**—Photograph taken August 1976 of the rapid advance of ice of* Lednik Valy *caused by its surge.*

The Alai Range (Alayskiy Khrebet) lies to the north of the Pamirs, mainly in southern Kyrgyzstan. On the Alayskiy Khrebet, cirque and cirque-valley glaciers with areas of 1 to 3 km^2 prevail in the mountains; and the upper reaches of big valleys contain valley and compound-valley glaciers 5 to 10 km in length with areas of 10 to 15 km^2. Among them is the *Abramov Glacier*, situated in a representative mountain glacier basin, where detailed glaciological observations were initiated during the IHD. Glacier tongues are debris-mantled for one third of their area, which hampers the delineation of their boundaries.

For the interpretation of glaciers in the Alayskiy Khrebet, high resolution (20–30 m) multispectral photographs were taken from the Soyuz-22 spacecraft on 18 September 1976 and analyzed (Kravtsova and Chaikina, 1980). Figure 19 is one of these photographs, showing the western part of the Alayskiy Khrebet. For comparison, Landsat images of the same region, obtained on 10 September 1972 and on 12 July 1973, were also studied. By analyzing these images in several spectral bands, it was possible to draw the boundaries of glacier tongues and firn basins, distinguish snow-and-firn covered areas of glaciers from the bare ice surface, map medial moraines on the glaciers and terminal and lateral moraines in the glacier valleys, and to see the largest icefalls. Morphological types of glaciers were determined, and a map was compiled for the World Atlas of Snow and Ice Resources. Figure 20 shows the map of the same area photographed in figure 19. From the space photograph taken from the Soyuz-22 spacecraft, it became possible to detect and map approximately four times more glaciers than are shown on conventional topographic maps of this region (fig. 20*A*, *B*).

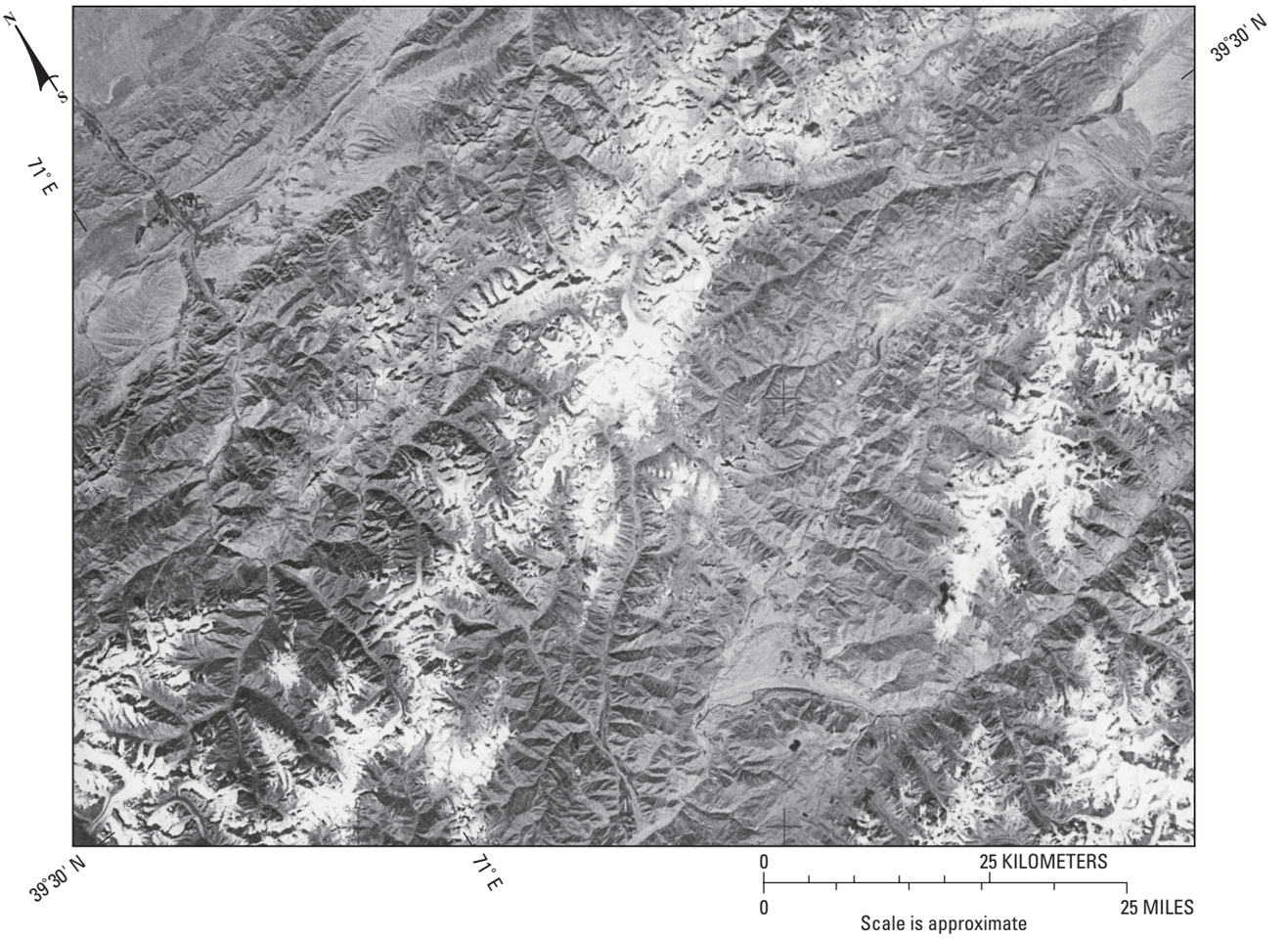


Figure 19.—*Part of the photograph taken by a cosmonaut on the Soyuz-22 spacecraft, showing the western part of the Khrebet Alayskiy on 18 September 1976.*

Based on these studies in regions of wide-spread glacierization, space images can serve as a reliable source of information for (1) identification of glaciers that have an area larger than 1 km^2, and for (2) detection of surge-type glaciers. Multispectral images may also reveal morphological features of certain types of glaciers.

Tien Shan (in the Republics of Kyrgyzstan and Kazakhstan)

The Tien Shan trends west to east for nearly 2,500 km, 1,200 km of which lies in the Republics of Kyrgyzstan and Kazakhstan (both Soviet Socialist Republics within the Former Soviet Union). The orographic features of the Tien Shan make it possible to subdivide the range into 4 parts: Northern, Western, Central, and Eastern. The Eastern part is within China (see the Glaciers of China portion of this chapter). Distribution of glaciers within the Former Soviet Tien Shan is shown in table 8; it was compiled from data in the Glacier Inventory of the USSR and used in the World Atlas of Snow and Ice Resources. Glacierization of the Central Tien Shan is discussed here with special reference to the two glacier groups, Piks Pobedy and *Khan-Tengri* (Khan Tägiri in Kazakhstan, Kan-Too in Kyrgystan), and also Khrebet Ak-shyyrak, because these regions are covered by good Landsat images.

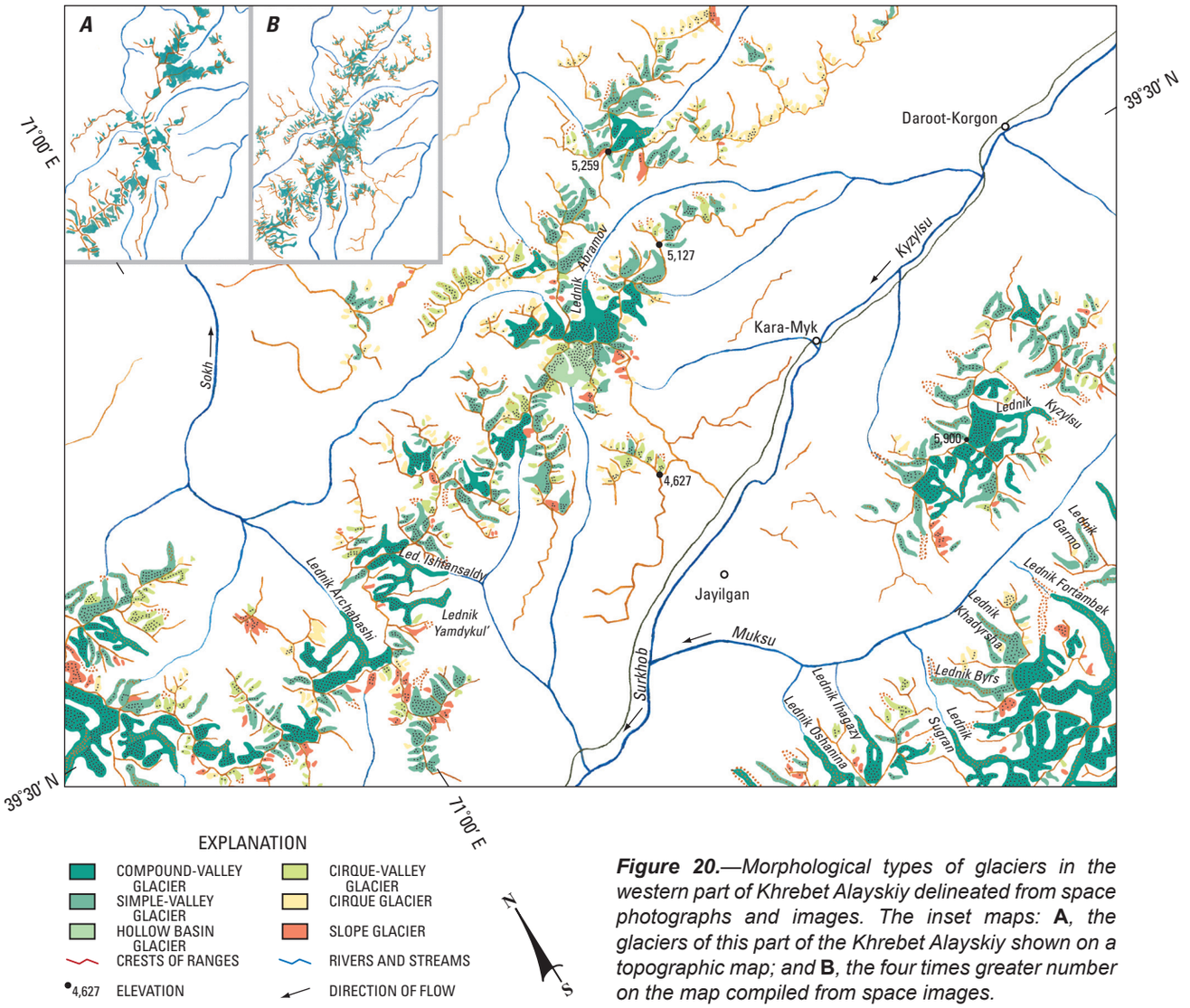


***Figure 20.**—Morphological types of glaciers in the western part of Khrebet Alayskiy delineated from space photographs and images. The inset maps: **A**, the glaciers of this part of the Khrebet Alayskiy shown on a topographic map; and **B**, the four times greater number on the map compiled from space images.*

TABLE 8.—*Distribution of Tien Shan glaciers in various river or lake basins*

[Data from Vinogradov and others (1980). Unit: km^2, square kilometer]

Name of river or lake basin	Number of glaciers	Glazierized area (km^2)	Average area of individual glaciers (km^2)
Syr Darya	2,441	1,658.0	0.7
Assa	48	42.0	0.9
Talas	162	117.3	0.7
Chu	790	722.9	0.9
Ili	583	751.6	1.3
Ozero Issyk-Kul' (Lake)	631	636.4	1.0
Ozero Chatyr-Kël' (Lake)	3	2.8	0.9
Taushkan Darya	372	674.7	1.8
Aksu	1,317	2,646.0	2.0
Total Tien Shan	6,347	7,251.7	1.14

[Recent work includes Dyurgerov and others, 1995; Kuzmichenok and Chaohai, 1995; Vilesov and Uvarov, 2001; Solomina and others, 2004; Aizen and others, 2006, 2007; Kotlyakov, 2006; Narama and others, 2006; Aizen and Kuzmichenok, 2007; and Bolch, 2007.]

Piks Pobedy and *Khan-Tengri* in Central Tien Shan

The largest glacier complex in the Tien Shan is situated in the area of Piks Pobedy and *Khan-Tengri*. P.P. Semenov was the first scientist to travel there in 1856 to 1857 (Semenov, 1858), and he discovered the large glaciers. The first glaciological map of this region was compiled by G. Merzbacher (1905) in the 1900s. During the Second International Polar Year, a glaciological expedition headed by S.V. Kalesnik worked in the Central Tien Shan (Kalesnik, 1937). From 1929 to 1934, a topographical survey of this region was undertaken and surveys of the largest Tien Shan glaciers were carried out. During the course of topographical surveys from 1941 to 1943, the highest summit of the Tien Shan, Pik Pobedy was discovered. Subsequent aerial photography of the Tien Shan has revealed the dynamics of its glacierization.

The Landsat image in figure 21 shows the general nature of Tien Shan glacierization: latitudinal extension of ranges and valleys bounded by the high mountain range, *Khrebet Meridional'niy*. The Former Soviet Union part of the Tien Shan region contains 704 glaciers which cover an area of 1,697.5 km^2. Large compound-valley and dendritic glaciers with numerous tributaries are widespread; their termini are often debris-mantled (table 9). As can be seen in table 10, the major part of the area is covered by large valley glaciers, all of which can be easily seen on space images.

Figure 21.—Part of a Landsat 2 MSS image of the Pobedy and Khan Tägiri/Kan-Too *peak region taken on 16 October 1976. The Landsat image, 2158031007629090, Path 158–Row 31, is from the U.S. Geological Survey, EROS Data Center, Sioux Falls, S. Dak. 57198.*

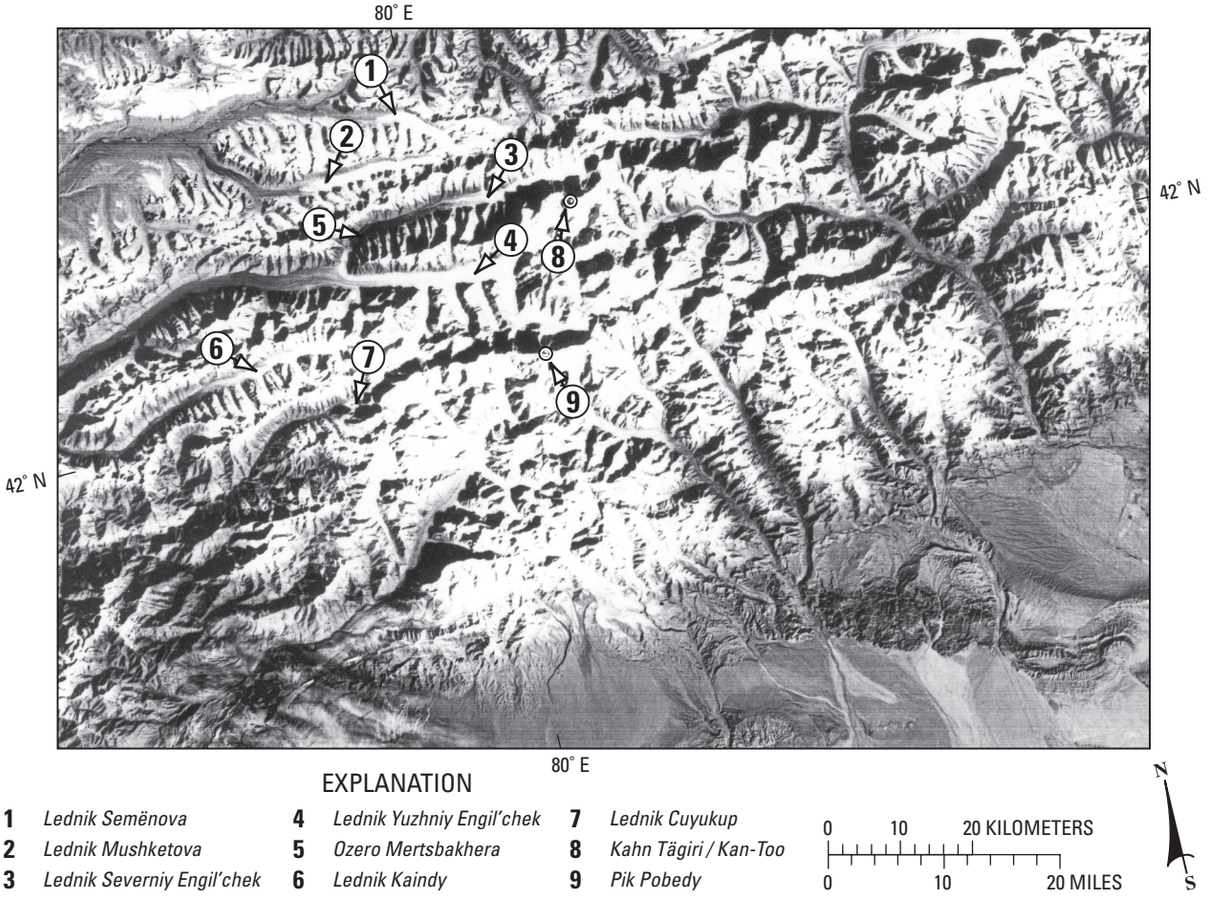


TABLE 9.—*Largest glaciers in the Tien Shan*

[Units: km, kilometer; m, meter]

Glacier name	River Basin	Length (km)	Total area, including tributaries (km^2)	Debris-covered area (km^2)	Elevation of the terminus (m)	Elevation of the firn line (m)
GLACIERIZED AREA OF POBEDY AND KHAN TÄGIRI/KAN-TOO PEAKS						
Yuzhniy Engil'chek	Engil'chek	60.5	567.2	25.2	2,800	4,500
Severniy Engil'chek	Engil'chek	32.8	181.2	37.6	3,400	4,550
Kaindy	Sarydzhaz	19.0	84.1	11.0	3,400	4,440
Mushketova	Adyr Ter	20.5	68.7	—	3,440	4,150
Semënova	Sarydzhaz	20.2	56.6	0.9	3,340	4,200
KHREBET AK-SHYYRAK						
Petrova	*Kumtor*	11.3	69.8	1.9	3,730	4,270
Severniy Karasay	Karasay	12.2	49.2	1.2	3,800	4,160
Kaindy	Kaindy	8.0	24.3	1.1	3,850	4,200

TABLE 10.—*Distribution of glaciers in two regions of the Central Tien Shan based on their area*

[Abbreviations: km^2, square kilometer; N, number of glaciers; A, total area, in square kilometers]

Region	<1 km^2		1.0–4.9 km^2		5.0–9.9 km^2		10.0–49.9 km^2		>50 km^2		Total	
	N	A	N	A	N	A	N	A	N	A	N	A
Pobedy and *Khan Tägiri/Kan-Too* peaks	429	176.5	209	445.6	46	308.0	16	339.2	4	428.2	704	1,697.5
Khrebet Ak-Shyyrak	78	28.1	52	113.2	13	94.2	6	130.1	1	69.8	150	435.4

Similar to the Pamirs, one can easily distinguish on space images the large, primarily linear features on the surface of the large glaciers — medial moraines, zones of large crevasses, and other features. Accuracy in the delineation of glacier boundaries depends on the time of the survey. For example, it is easy to detect the features on the Landsat image of 18 September 1973 (fig. 22), because the image was obtained at the end of the ablation period. However, it is difficult to distinguish these features on the Landsat image of 16 October 1976 (fig. 21), because the upper heads of glaciers and abutting slopes were already covered by a fresh snowfall.

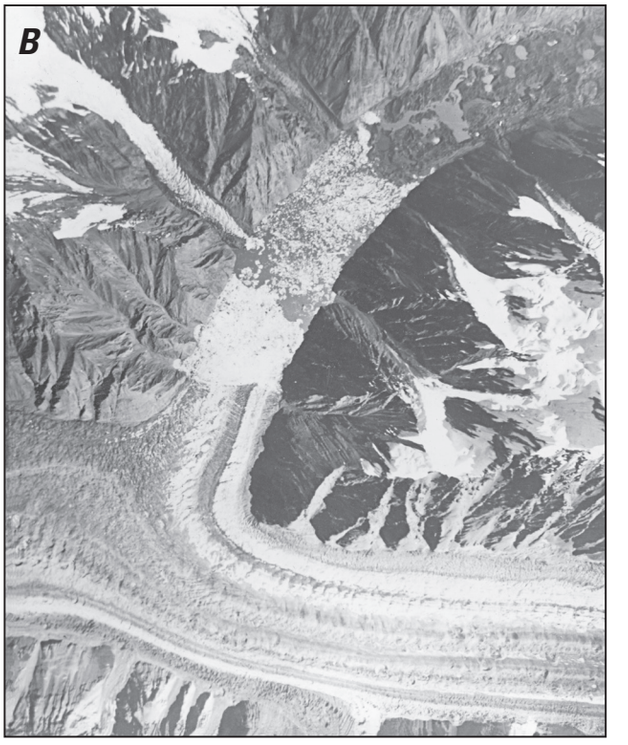
Surging glaciers can be distinguished by the contorted loops of medial moraines. Such loops were visible on the Lednik Mushketova, whose surge was observed in 1956 and 1957. By August 1957, the glacier tongue had advanced nearly 5 km in one year, and its surface became covered by a dense network of crevasses for several kilometers. Since then, the glacier has been retreating. Lednik Kaindy advanced 1,300 m between 1943 and 1960. Variations on this scale for relatively small time intervals can be measured on repeated space images.

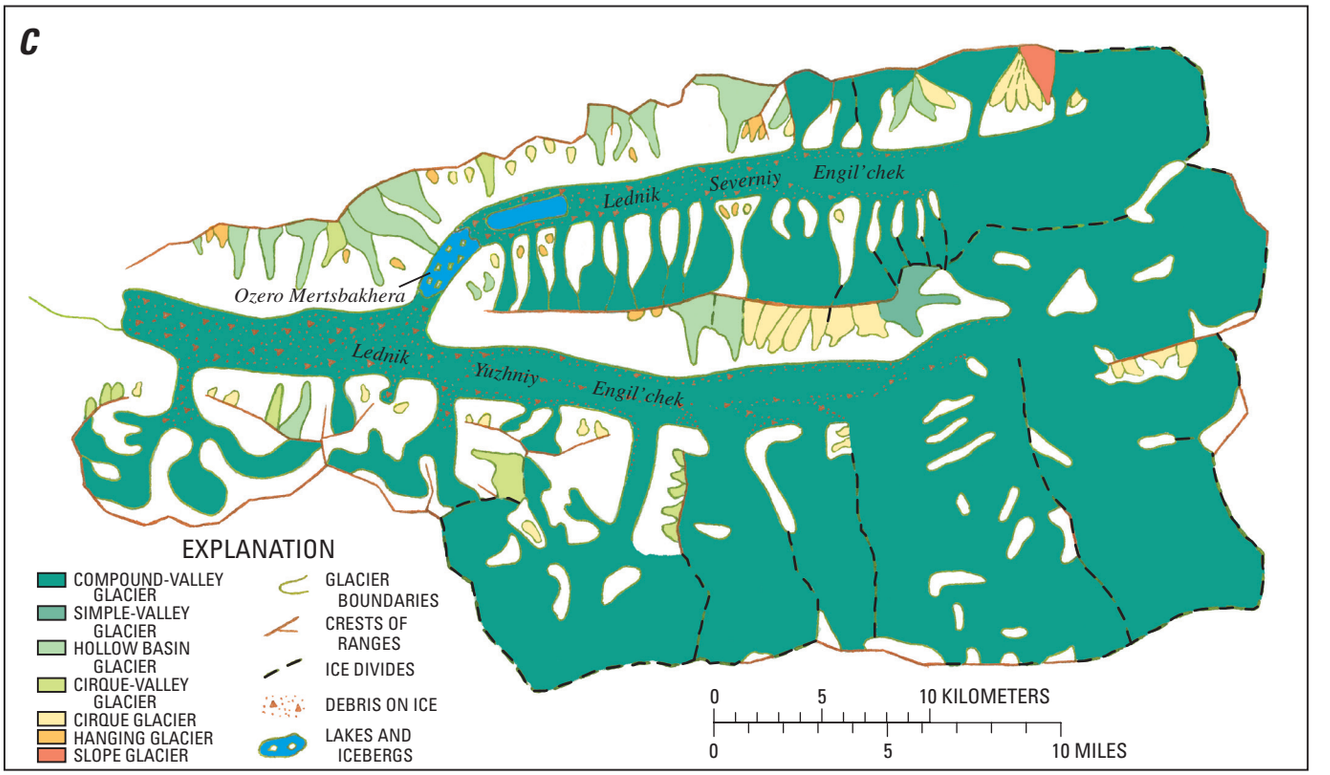
Figure 22 presents part of a Landsat image (fig. 22*A*) an aerial photograph (fig. 22*B*), and a map (fig. 22*C*) compiled from them of *Ledniki Severniy and Yuzhniy Engil'chek,* and Ozero Mertsbakhera (lake). The lake is situated at an elevation of about 3,400 m a.s.l., and at high water level it has an area of 4.5 km^2, a length of about 4 km, an average width of 1 km, and an approximate volume of 200×10^6 m^3. The bottom of the lake is composed of lacustrine sediments. The lake was created by the retreat of *Lednik Severniy Engil'chek* and the filling of the mouth of this glacier valley with melting water and ice

flowing down *Lednik Yuzhniy Engil'chek* (Zabirov and Bakov, 1981). The flow of this ice, with its distinctive medial moraine, can be clearly seen on the Landsat image as it turns into the valley of *Lednik Severniy Engil'chek*. Ozero Mertsbakhera reaches its maximum dimensions by the end of the ablation period. Glacier outburst floods (jökulhlaups) from the lake occur annually, sometimes twice a year, and usually in the summer (Kotlyakov, 1997), similar to Alaska (Post and Mayo, 1971). The Landsat image in figure 22*A* shows the lake after the jökulhlaup.

***Figure 22.*—A**, *Enlargement of part of a Landsat 1 MSS image taken on 18 September 1973. Compare with figure 21 for location.* **B**, *Aerial photograph; and* **C**, *Map of the* Ledniki Severniy *and* Yuzhniy Engil'chek *basin and the Ozero Mertsbakhera. The map was compiled from the Landsat image and the aerial photograph. The Landsat 1 MSS image 1159031007326190, Path 159–Row 31, is from the U.S. Geological Survey, EROS Data Center, Sioux Falls, S. Dak. 57198.*







Khrebet Ak-Shyyrak in Central Tien Shan

Khrebet Ak-Shyyrak consists of three parallel mountain ranges trending northeast-southwest. One hundred and fifty glaciers, covering an area of 435.4 km^2 are situated here. The extent of the glacierization of the massif is very high — 46 percent. [Editors' note: Recent work by Aizen and others (2006) suggests that this massif has 178 glaciers with a total area of 371.6 km^2.]

The first information on this region was obtained by A.V. Kaulbars in 1869 (Kaulbars, 1874). Instrumental topographical surveys were undertaken here from 1911 to 1913. The inventory by N.L. Korzhenevskiy (1930) contains data on 29 glaciers of Khrebet Ak-Shyyrak. During the Second IPY, the entire region encompassed by the massif was explored, and the termini of some glaciers were surveyed by phototheodolite. In the second half of the 1940s, the glaciers of this region were studied by G.A. Avsiuk (1952), and, in the 1950s, a comprehensive investigation of the massif were undertaken by the Tien Shan geographical station. These efforts served as the basis for a monograph on the glaciers of Khrebet Ak-Shyyrak (Bondarev, 1963) and a publication by Zabirov and Knizhnikov (1962). The entire region was covered by aerial photography in 1943 and again in 1977. [Editors' note: also in 1995]

The part of the Landsat 1 MSS image shown in figure 23*A* shows the deep longitudinal valley between the Severniy (northern) and Sredniy (central) mountain ranges, where the largest glacier of the massif exists — Lednik Petrova (table 9). The glaciers of the Karasay system are situated between the Sredniy (central) and Yuzhniy (southern) mountain ranges in the western part of the massif. Glaciers of the Kaindy river basin lie in the eastern part of the massif. The western slopes of Khrebet Ak-Shyyrak are nearly completely buried under ice and firn; 32.5 percent of the glacierized area is confined to the slopes that have northern and western exposures (fig. 23*C*).

Khrebet Ak-Shyyrak contains many types of glaciers (fig. 23*B*), from hanging to compound-valley. Flat summit glaciers occur on plateau-like crests of ranges. One of them is evident on the satellite image (fig. 23*A*). Seven compound-valley glaciers occupy more than 45 percent of the entire glacierized area. Glaciers with an area of more than 5 km^2 cover 67.5 percent of the glacierized area, although their number makes up only 13.4 percent of the total number of glaciers (see table 10). The shapes of these glaciers are evident on space images if they lie on rocky slopes. However, if the upper reaches of large glaciers merge with flat firn areas, it is practically impossible to distinguish between them.

Several surge-type glaciers have been identified in Khrebet Ak-Shyyrak. Among them, *Lednik Severniy Karasay* is of the greatest interest. It advanced at the beginning of the 20th century, creating a push moraine and a dammed lake. At the end of the 1940s, it actively retreated (Avsiuk, 1952), but by 1958 it had advanced 920 to 1,000 m, forming a push moraine up to 45 m high and about 150 m wide. L.G. Bondarev (1963) dates this surge as occurring from 1955 to 1956. Based on aerial photographs (fig. 24), the glacier began to retreat again in 1957. The Landsat 1 MSS image of 18 September 1973 (fig. 23*A*) shows that this retreat has continued. [Recent work includes Khromova and others (2003).]

Analysis of space images of the Tien Shan region testifies to their usefulness in studies of the general nature of glacierization of large mountain massifs and glacier complexes. Landsat MSS images are most useful for mapping glaciers at scales of 1:1,000,000 and less, and are most valuable for poorly studied mountain-glacier areas. Because of the repetitive nature of the Landsat satellite coverages, Landsat images are useful for monitoring potential natural hazards, such as glacier surges and outbursts (jökulhlaups) from dammed lakes. Higher pixel resolution and more recent Landsat spacecraft

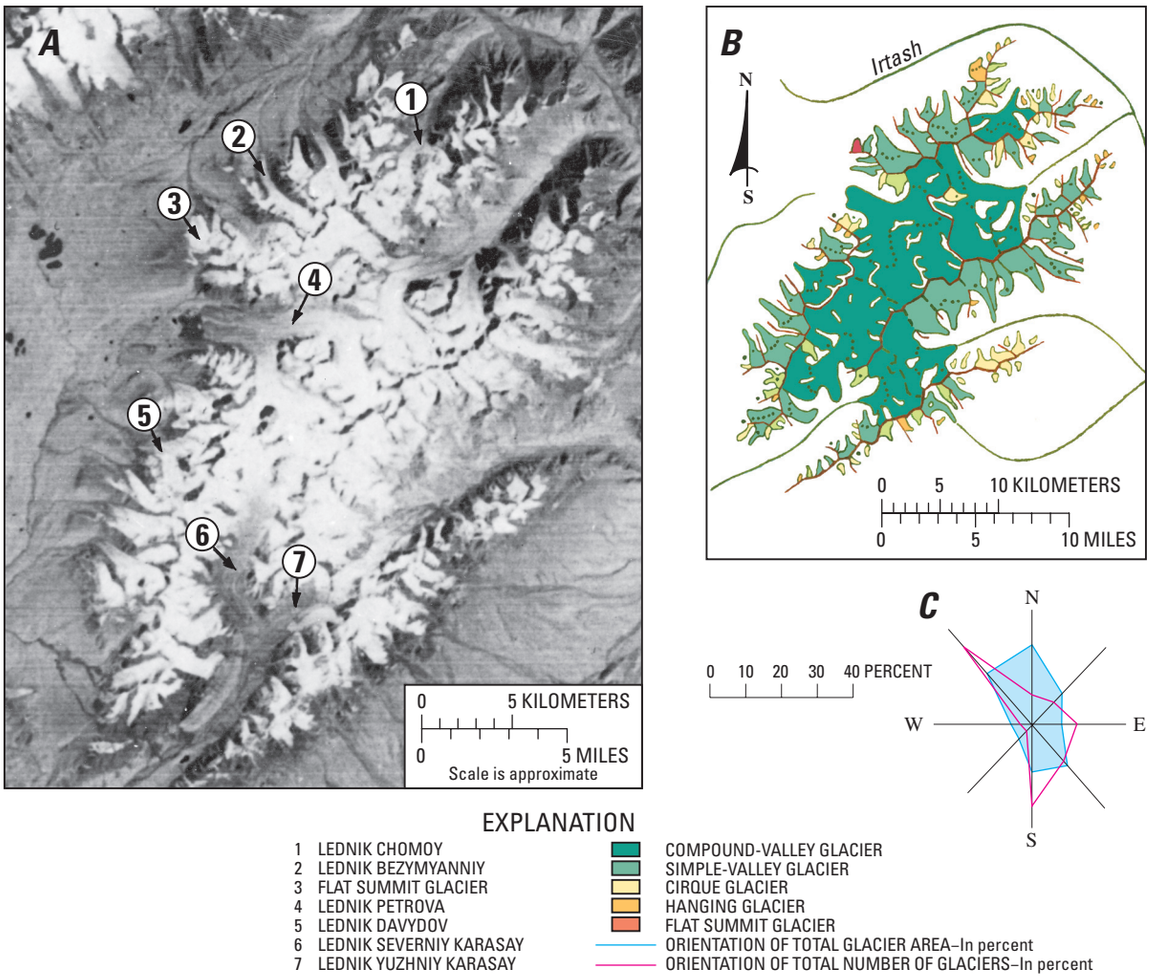


Figure 23.— *(above)* **A**, *Enlargement of part of a Landsat 1 MSS image of Khrebet Ak-Shyyrak (lat 41°50'N., long 78°20'E.) taken on 18 September 1973.* **B**, *Map of the morphological types of glaciers; and* **C**, *Distribution pattern of the area (blue) and the number of glaciers (red) along the Khrebet Ak-Shyyrak.*



Figure 24.—*Aerial photograph of* Lednik Severniy Karasay *in Khrebet Ak-Shyyrak.*

[for example, Landsat 3 return beam vidicon (RBV, 28m), Landsats 4, 5, and 7 thematic mapper (TM, 28 m), and Landsat 7 ETM+ panchromatic (15 m), and other satellite images such as the Advanced Spaceborne Thermal Emission Radiometer (ASTER), which acquires multispectral stereoscopic images (15 m) used for the Global Land Ice Measurements from Space (GLIMS) Program] will, of course, produce data at larger scales. None of that data were available in this earlier phase of study, which was focused on the Landsat baseline period (1972–1981).

Altay (Russia and Kazakhstan)

Studies of the glaciers of Altay were initiated by V.V. Sapozhnikov (1901, 1911), who discovered about 150 glaciers during his several expeditions from 1895 to 1911. Following this, explorers turned their attention to studying the former glacierization of Altay. Aerial photographs of Altay taken in the 1940s and 1950s were important in the study of present-day glaciers, and led to the compilation of new maps that were used as the basis of the Glacier Inventory. The leading role in glaciological studies of the Altay belongs to Tomsk University. A great contribution was made by the pioneer of the Tomsk glaciological school, Professor M.V. Tronov, who wrote monographs on Altay (Tronov, 1949, 1954). A new phase of investigations began in the Altay region in 1971, when the first space surveys were performed from the first Soviet orbital space station, Salyut–1.

There are 1,499 glaciers in the Altay with a total area of more than 900 km^2 and a volume of approximately 57 km^3 of ice. More than 80 percent of the glaciers are concentrated on the highest ranges of Altay, rising 4,400 m a.s.l. — on Katunskiy Khrebet (Qatyn Zhotasy in Kazakhstan), Yuzhno-Chuyskiy Khrebet, and Severo-Chuyskiy Khrebet (fig. 25) — and also on the southern Altay. Glaciers occur mainly on slopes with northern or southern exposures because of latitudinal extension and asymmetry of the ranges, whose southern slopes are steep and northern slopes have flattened areas. In addition, more snow is concentrated on leeward slopes with northern and northeastern exposures due to the dominant transport of air masses from the south and southwest in the Altay.

In Altay, small glaciers prevail. Sixty-three percent of the glaciers are either cirque or hanging glaciers. Cirque-valley and valley glaciers are mainly concentrated in the central parts of glacier clusters, and occupy 57 percent of the total glacierized area of the Altay. There are only 15 glaciers with an area greater than 5 km^2 (table 11). The mean ice thickness of large valley glaciers in the Altay varies from 120 to 150 m.

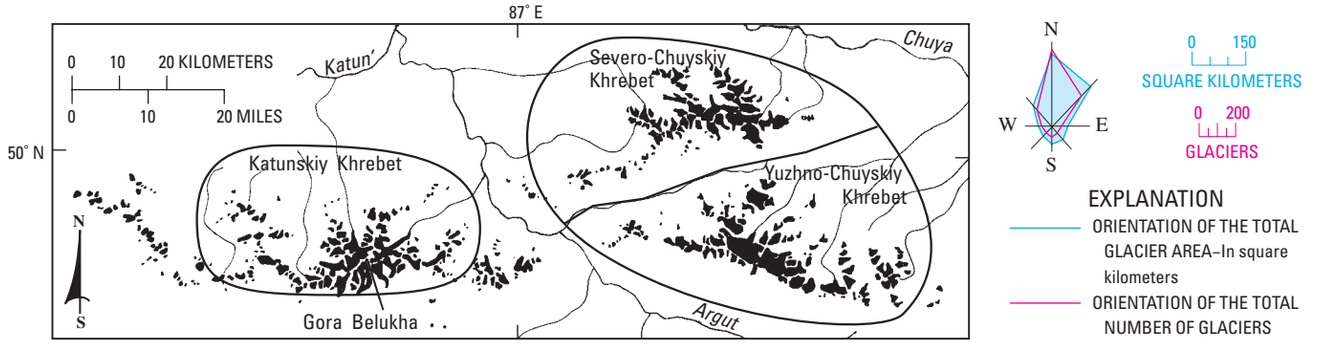


Figure 25.—*Glaciers in the main mountain-glacier areas of the Altay — on the Katunskiy, Severo-Chuyskiy, and Yuzhno-Chuyskiy Khrebet, and the distribution pattern of the area (blue) and the number (red) of glaciers.*

TABLE 11.—*Largest glaciers in the Russian Altay*

[Units: km, kilometer; m, meter]

Name of glacier	Name of river basin	Area (km^2)	Length (km)	Elevation of glacier terminus (m)	Elevation of equilibrium line (m)
Bol'shoy Taldurinskiy	*Taldura*	28.2	7.5	2,450	2,950
Alakhinskiy	Akalakha	19.2	6.0	2,395	3,000
Sofiyskiy	Ak-Kol	17.6	7.9	2,620	2,950
Bol'shoy Maashey	*Maashey*	16.0	8.2	2,200	2,990
Mensu (Sapozhnikova)	*Iedygem*	13.2	10.5	2,120	2,800
Bol'shoy Berel'skiy	Belaya-Berel'	12.2	10.4	1,985	3,120
Maliy Berel'skiy	Belaya-Berel'	8.9	8.3	2,100	2,810
Bratjev Tronovykh	*Kochurla*	8.6	10.5	2,050	2,750
Katunskiy *(Geblera)*	Katun'	8.5	8.5	1,970	2,800
Akkemskiy (Rodzevicha)	Akkem	8.5	7.8	2,200	3,000
Yadrintsev	Karaoyuk	8.0	4.8	2,650	3,080
Ukokskiy	Akalakha	7.1	4.0	2,610	3,050
Leviy Karagem	Karagem	6.6	4.0	2,375	3,760
Leviy Aktru	*Aktru*	5.2	6.5	2,500	3,050
Korumdu	*Eshtykol*	5.0	4.2	2,235	2,950

Space observations of Altay were first undertaken onboard the Salyut–1 space station on 14 June 1971 under conditions of 20 percent cloudiness, when glaciers were still covered by seasonal snow. Despite these problems, images taken from the space station were later successfully used for delineation of glacier boundaries (fig. 26). Comparison of these Salyut–1 images with those from Landsat 2, taken less than one month later in the season, on 11 July 1977 (fig. 27*A*), illustrates convincingly the seasonal changes of glacier landscapes.

Characteristics of the exposure and morphology of the glaciers on Katunskiy Khrebet are evident on the Landsat 2 MSS image taken on 11 July 1977 (fig. 27*A*). This image illustrates the dominant cirque glaciers, curved crests of ranges, and cirques with numerous cirque lakes in the western part of the range, and the Gora Belukha with its cluster of predominant valley glaciers in the central part of the range. Differences in the morphology of Katunskiy Khrebet glaciers are well demonstrated on maps of surface morphology and morphological types of glaciers (fig. 27*B, C*) compiled for the World Atlas of Snow and Ice Resources from cartographic data, and also on images from the Soviet space station, Salyut–1 (fig. 26).

Three glaciers, *Ledniki Bratjev Tronovykh*, *Akkemskiy*, and Mensu, were easily distinguished by white tongues against the dark background of glacier valleys in the images taken from the Salyut–1 space station, but they had a dark tone on the Landsat images and blended in with the appearance of the glacier valleys. This is due to the fact that by the middle of July when the Landsat image was taken, the hot summer weather had caused the snow on the glacier tongues' surfaces to melt, and the dark, debris-covered glacier termini became visible. The ablation area of these glaciers and the snow-covered accumulation area were easily distinguished and, in some places, the firn line was clearly seen. Therefore, although a quick glance at the 11 July 1977 Landsat 2 MSS image produces the impression of a very small area of glaciers because only the white tone of their accumulation areas is visible, this is an erroneous assumption.

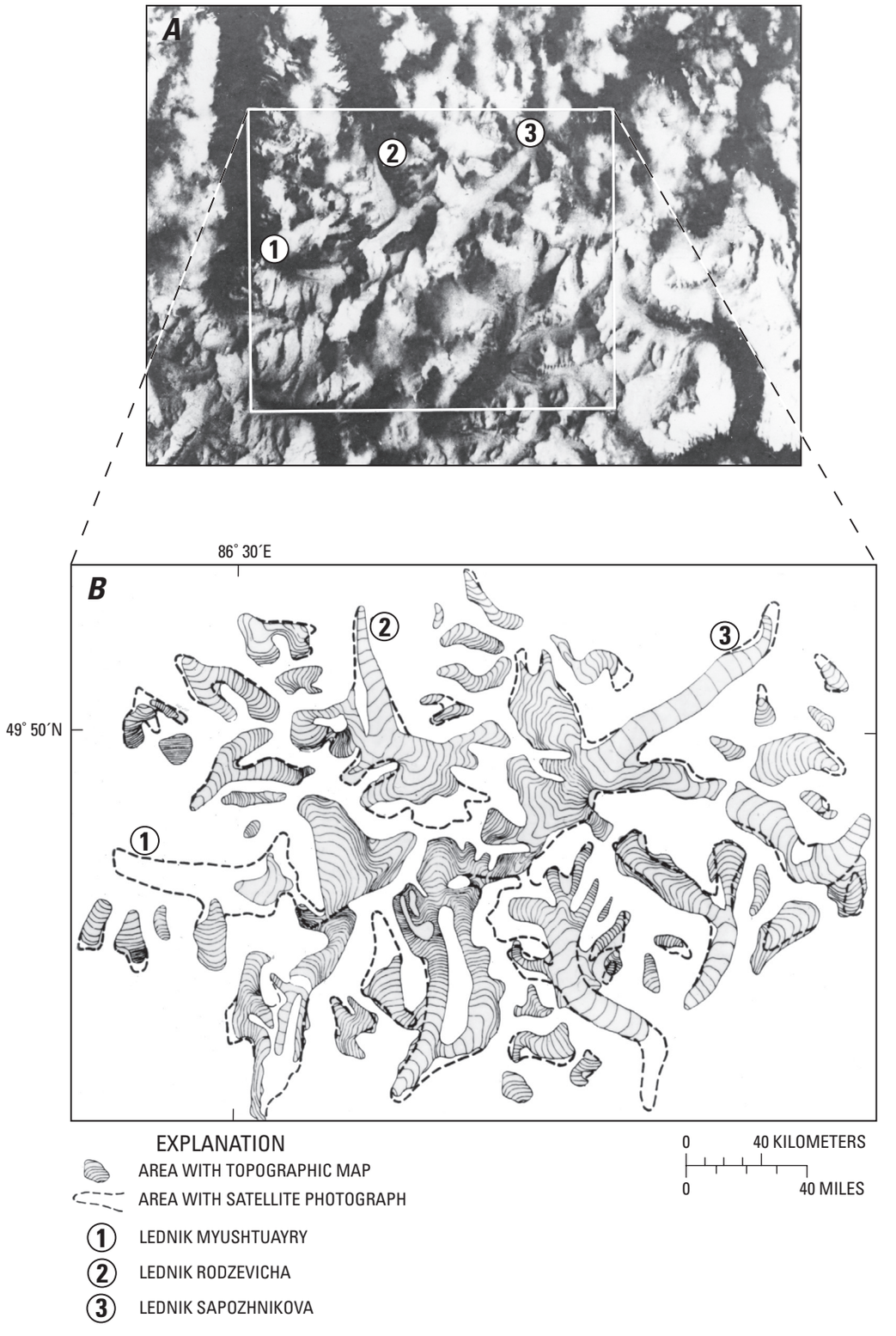


Figure 26.—**A**, *Image of the central Altay with the Gora Belukha glacier group taken from the Salyut–1 space station on 14 June 1971; and* **B**, *Comparison of the delineation of the glacier boundaries shown on topographic maps and derived from the space image.*

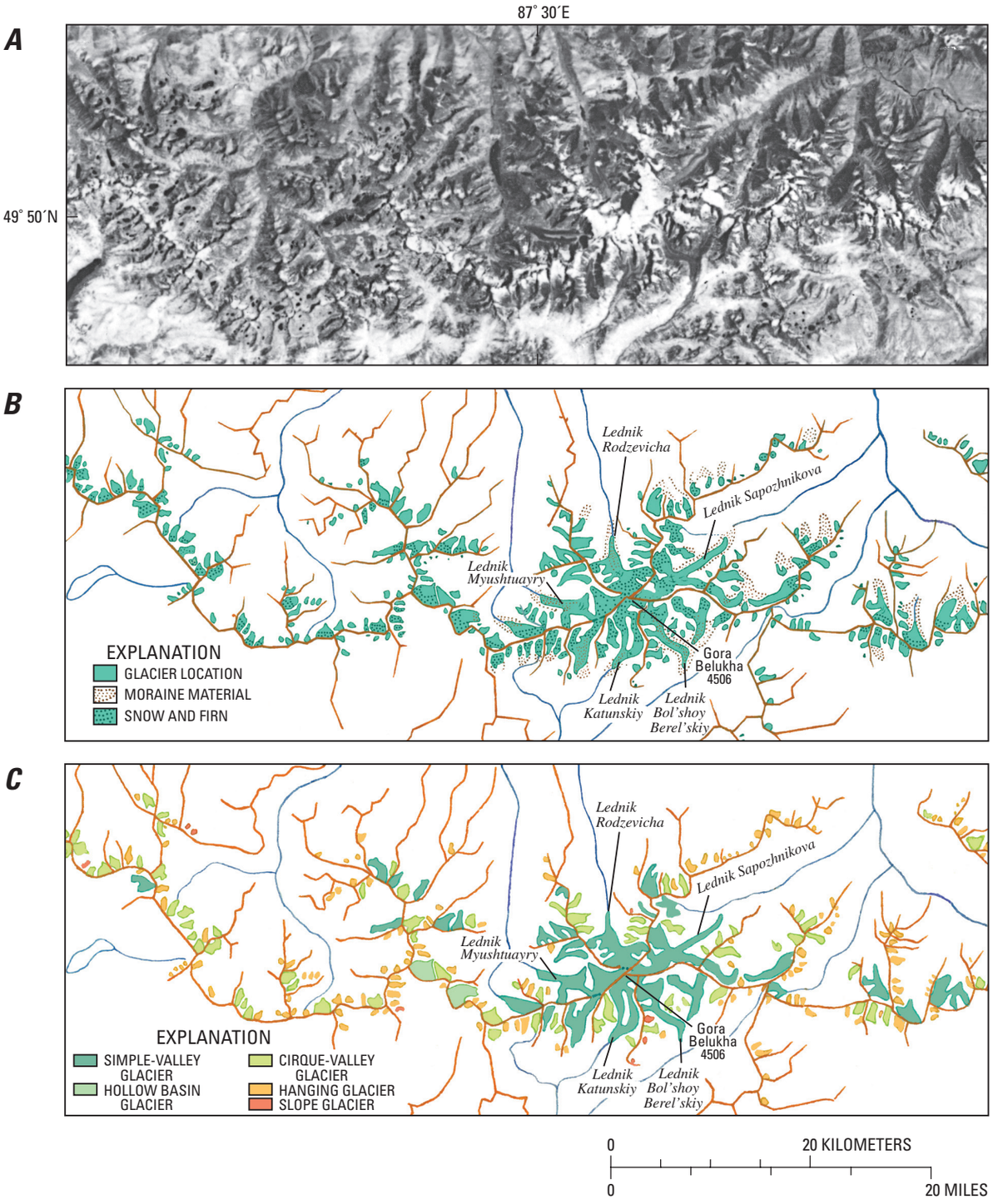


***Figure 27.—A**, Part of a Landsat 2 MSS image of Katunskiy Khrebet taken on 11 July 1977;* **B**, *Map of surface morphology; and* **C**, *Morphological types of glaciers in this region. Landsat image is from the U.S. Geological Survey, EROS Data Center, Sioux Falls, S. Dak. 57198.*

Comparison of the greatly enlarged part of the Landsat image of the *Bish-Irdu* glacier group with the cartographic presentation of these glaciers (fig. 28) furnishes an excellent example of the genuine relationship between the map and the Landsat image depiction of glacierization. This figure also shows the *Aktru* glaciers, well known in glaciology, that have been studied for a long time by glaciologists of Tomsk University (Tronov, 1949, 1954) [More recent work includes Galakhov and others (1987).]

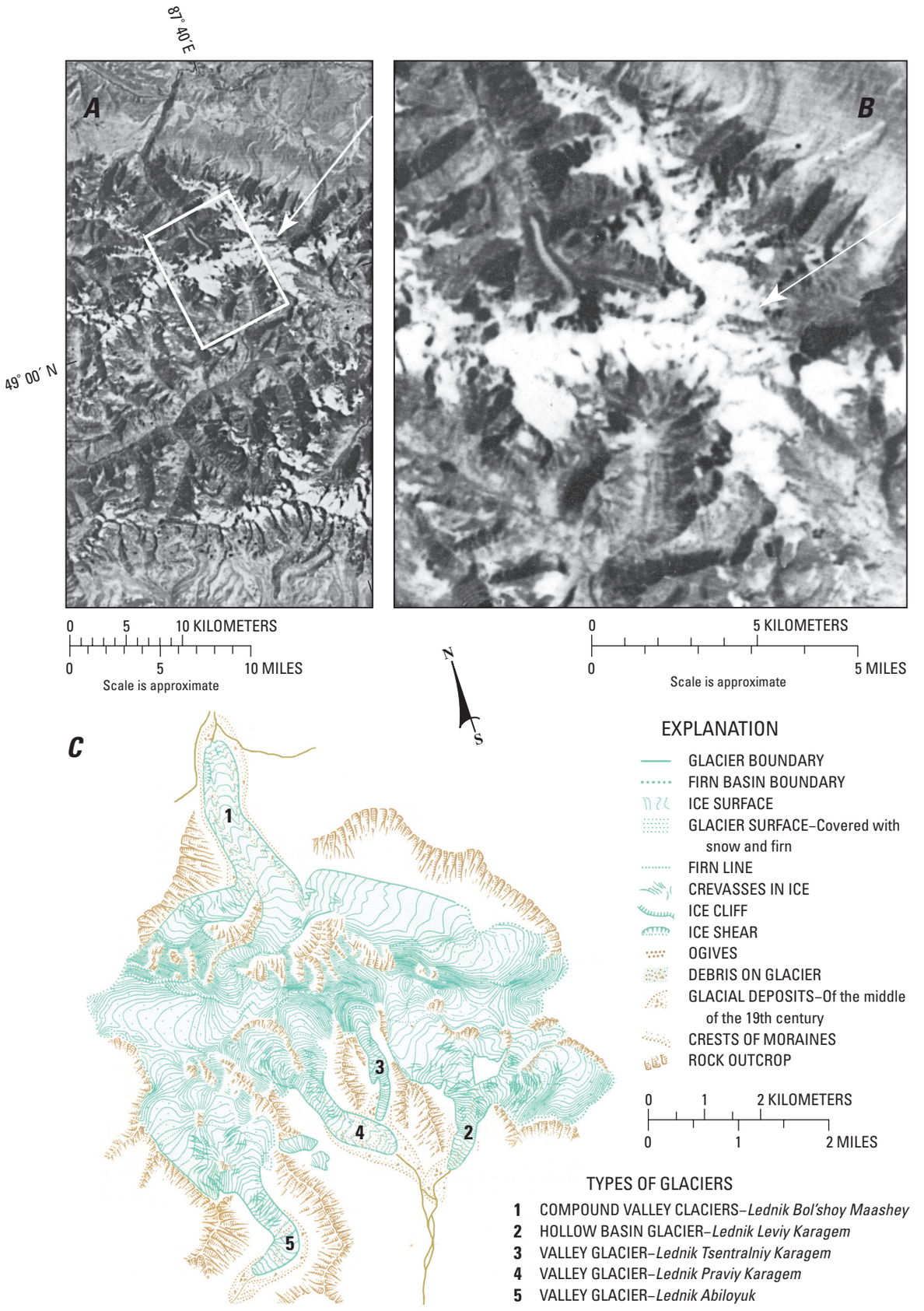


Figure 28.— **A**, *Part of the Landsat 2 MSS image taken on 11 July 1977 of the* Bish-Irdu *glacier complex in the Severo-Chuyskiy Khrebet;* **B**, *enlarged portion of the image; and* **C**, *depiction of this region on a map. The white arrows show* Aktru *glaciers. Landsat image is from the U.S. Geological Survey, EROS Data Center, Sioux Falls, S. Dak. 57198.*

Ural Mountains (Ural'skiye Gory)

The Ural Mountains are a typical region of small glaciers. Glaciers extend over a distance of more than 500 km — from latitude 63°53′N. to latitude 68°40′N. The glaciers are situated in the *Polar*, *Subpolar*, and *Northern Urals* in groups confined to the highest and most dissected parts of the mountains. The *Polar Urals* rise for 1,000 to 1,200 m, with the highest point at 1,499 m; the *Subpolar Urals* have elevations of 1,300 to 1,400 m; with the highest point at 1,894 m; the *Northern Urals* seldom exceed 1,000 m, and the highest summit, Gora Telpoziz, rises to 1,617 m a.s.l.

The first glaciers were discovered in the Ural Mountains in 1929. They were again observed during the Second IPY and the International Geophysical Year; the studies continued during the IHD. Glaciers situated in the Telpoziz mountain range and discovered quite recently (Dolgushin and Osipova, 1979) were identified on the space image of the *Northern Urals* (fig. 29). Now, regular observations are made and aerial and ground stereophoto-surveys have been conducted.

The majority of the glaciers, 91 of the 143, are situated in the *Polar Urals* and cover 20.8 km^2 of the total glacierized area of 28.7 km^2. Nearly all the glaciers lie on the western side of the Ural Mountains, facing the moisture-bearing air masses; however, they are all situated on the eastern slopes of individual ranges (fig. 30*B*), where snow is concentrated by wind transport. The area of present-day glaciers coincides exactly with the zone of maximum snowcover in the mountains (Troitskiy and others, 1966).

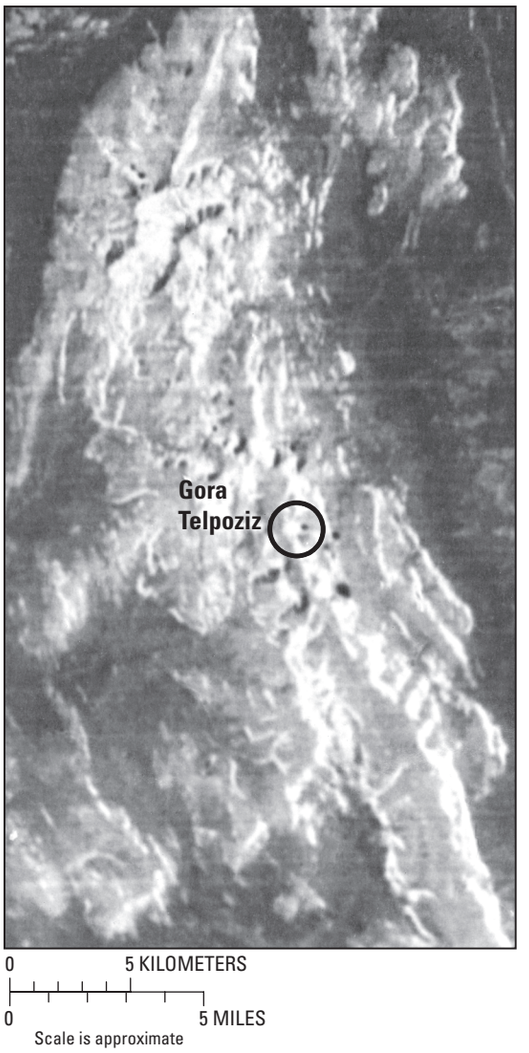


Figure 29.—*Enlargement of a Landsat 1 MSS image of the Northern Urals acquired on 25 June 1973. The Gora Telpoziz glacier (lat 63°55'N., long 59°11'E.) is circled. The Landsat 1 MSS image 1182014007317590, Path 182–Row 14, is from the U.S. Geological Survey, EROS Data Center, Sioux Falls, S. Dak. 57198.*

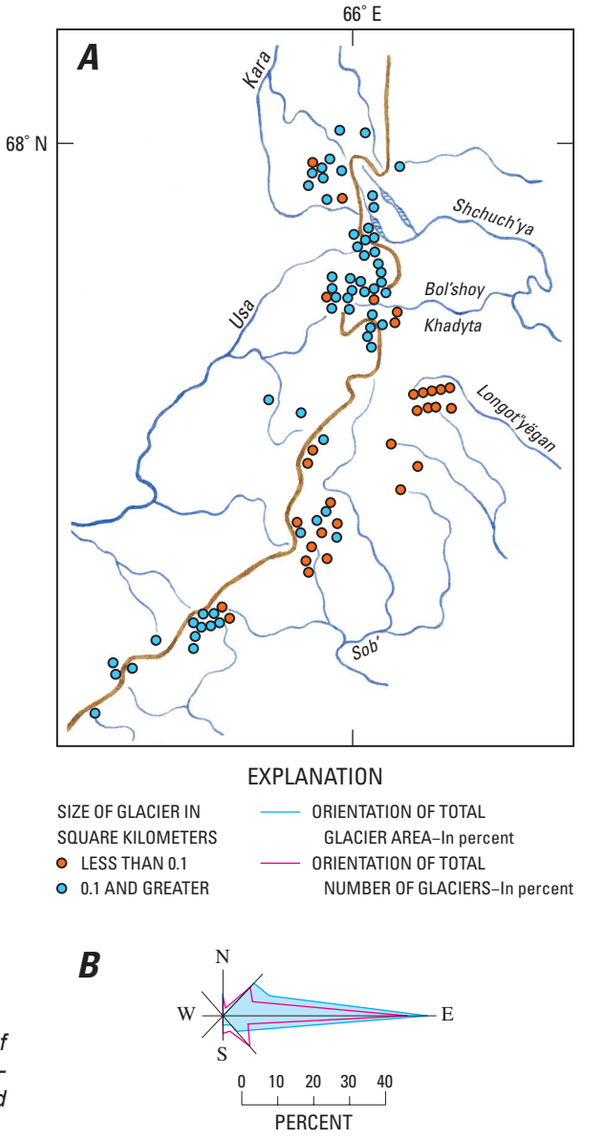


***Figure 30.*—A**, *Distribution pattern of glaciers in the Polar Urals; and* **B**, *Distribution of the glaciers by area (blue) and number (red) related to orientation.*

Recent glacierization in the *Polar Urals* is represented by cirque and niche glaciers. Only two of them — *IGAN* and *MGU* glaciers — have an area more than 1 km^2. More than 60 percent of the glaciers have an area of 0.1 to 0.6 km^2; about one third of them do not exceed 0.1 km^2 (fig. 30*A*).

Understandably, space images that have coarse resolution are not useful for studies of such small glaciers. And the available Landsat 1, 2 and 3 MSS images are not useful because of the unfavorable time of their acquisition — at the beginning of March, when all of the Ural Mountains were covered with snow. It is possible to identify the main mountain ranges and waterbodies on these images, however. The cirques of certain glaciers are visible too, but the glaciers themselves are covered with snow and long shadows from the near-by ranges and summits (fig. 31).

The end of August is the most suitable time for surveys of the glaciers of the Ural Mountains. At this time, it is possible to identify the largest cirque glaciers on images of 1:1,000,000 scale. However, for the correct interpretation of niche glaciers that greatly resemble snow patches, better resolution, larger-scale images are needed. These images would depict the details of the structure of the cirque glaciers, similar to that shown in figure 32 of Lednik Obrucheva.

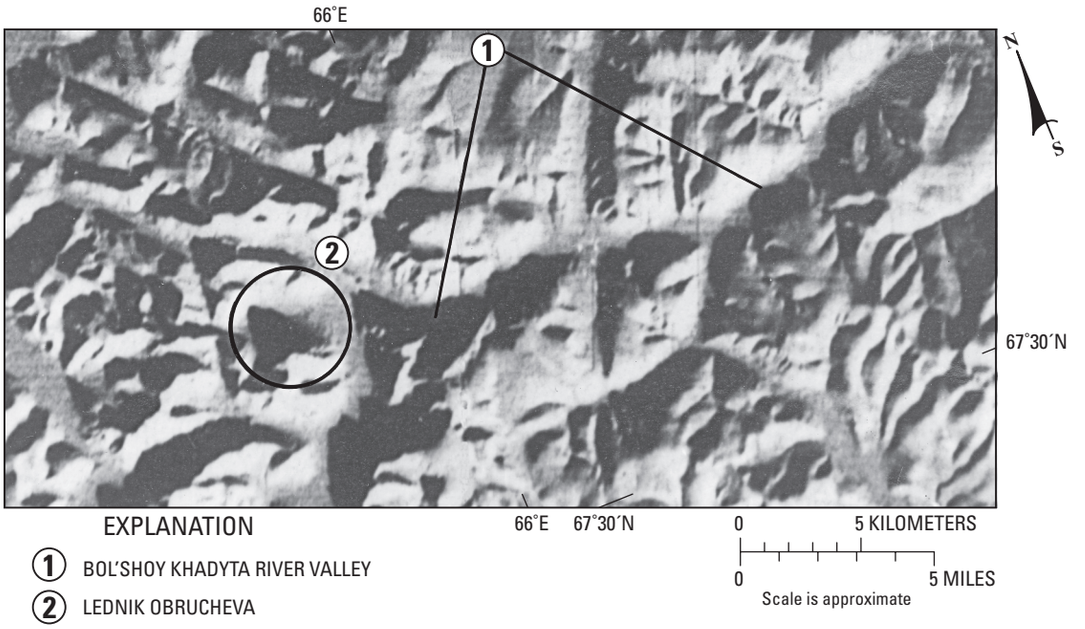


Figure 31.—*Enlargement of a Landsat 1 MSS image of part of the Polar Urals acquired on 6 March 1973. Landsat 1 MSS image 1179012007306590, Path 179–Row 12, is from the U.S. Geological Survey, EROS Data Center, Sioux Falls, S. Dak. 57198.*

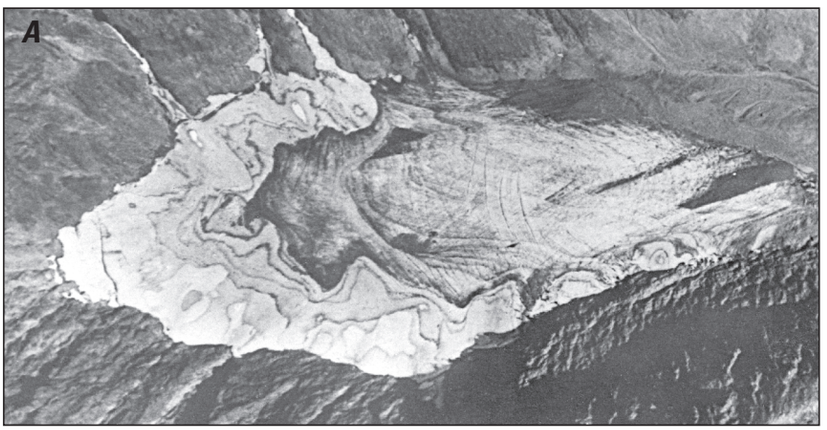
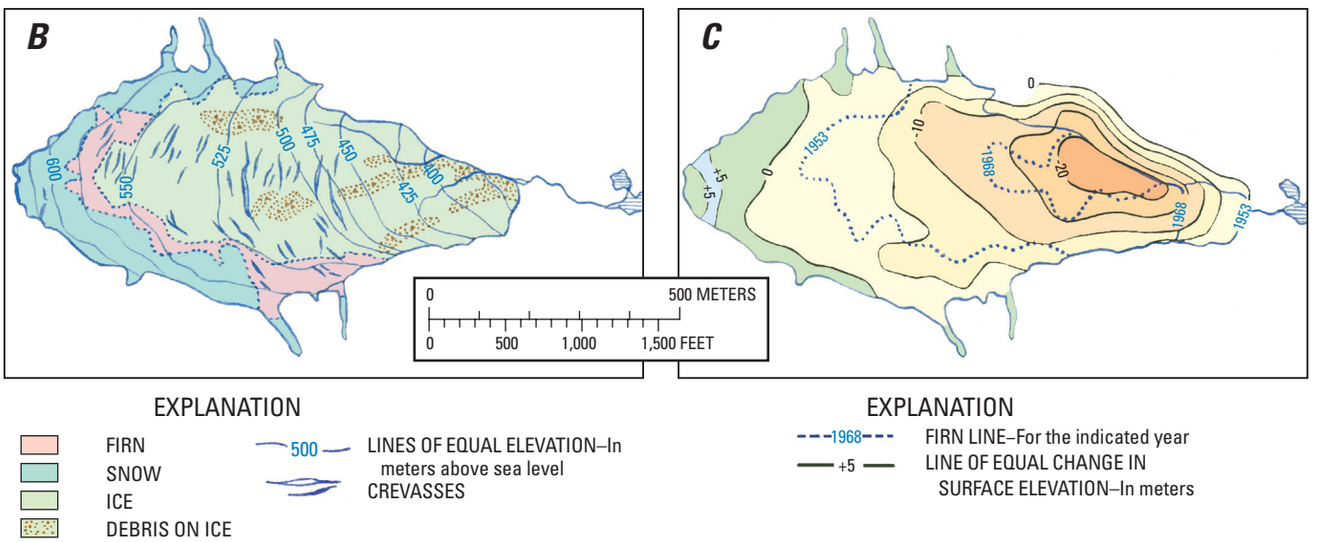


Figure 32.—**A**, *Aerial photograph taken on 30 July 1953 of* Lednik Obrucheva*;* **B**, *Morphology of the surface; and* **C**, *Changes of the surface elevation of the* Lednik Obrucheva *in the Polar Urals.*



The Byrranga Mountains (Gory Byrranga) in Northern Russia

The Gory Byrranga are situated on the Poluostrov Taymyr (peninsula) in central northern Russia. Glaciers extend over the most northern and highest part of the mountains between latitudes 75° and 76°N. and longitudes 106° and 111°E. The largest glaciers are concentrated within an area of 400 km^2. The area of the largest glacier is 4.3 km^2, and its length is approximately 3.8 km.

The first glaciers were discovered in Gory Byrranga in 1949. In the 1950s, the region was covered by aerial photography and soon the first maps of the glaciers were made. According to the glacier inventory of Gory Byrranga, the region has 96 glaciers, which occupy 30.5 km^2 (fig. 33*B*). Among them, there are 29 valley glaciers, 23 cirque, and 15 niche glaciers (USSR Academy of Sciences, 1965-1983). They have various orientations (fig. 33*C*).

There were not many Landsat 1, 2, or 3 MSS images of the Gory Byrranga area acquired. One of the few is shown in figure 33*A*. In this Landsat image, acquired on 26 July 1973 during the ablation period, the glacierized area lies near the edge of the image and is only partially visible. In the mountains there are traces of new snowfall, and because of this it was impossible to identify all of the glaciers in the image, although they could likely be seen under better conditions. A characteristic of the Gory Byrranga glaciers is their small accumulation areas which occupy broadened cirques.

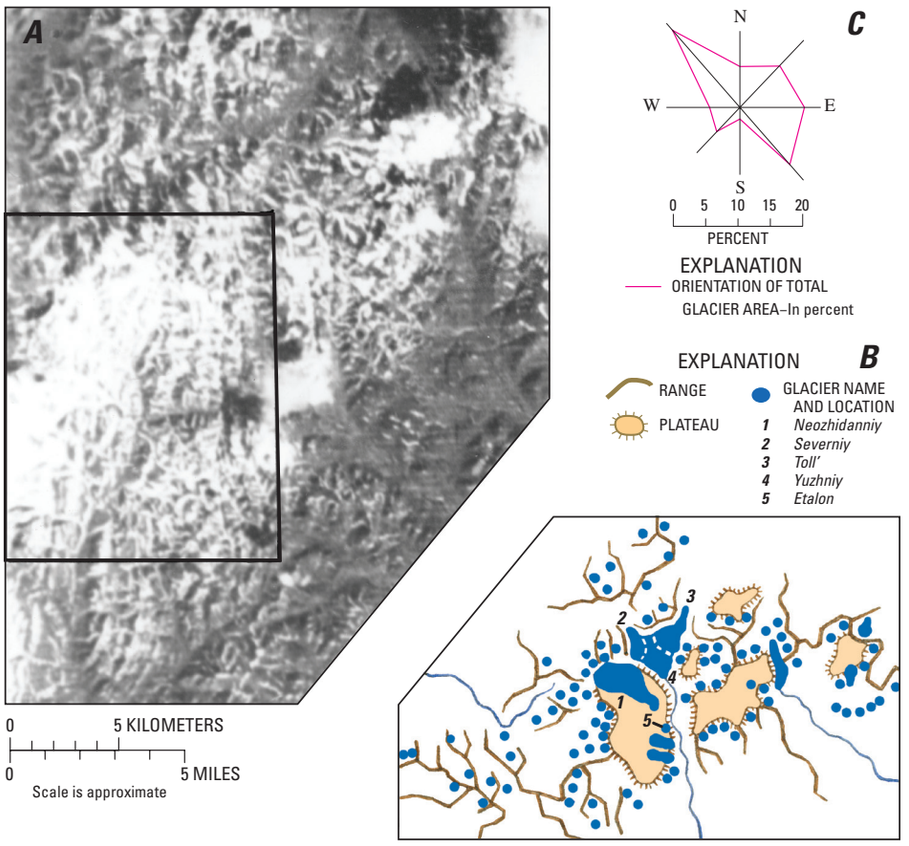


Figure 33.—**A**, *Landsat 1 MSS image acquired 26 July 1973, showing the distribution of glaciers in the Gory Byrranga in the region near lat 76°N., long 108°E.;* **B**, *Sketch of glacier location; and* **C**, *Distribution pattern of glacier orientation in the Gory Byrranga. Landsat 1 MSS image 1159006007320790, Path 159–Row 6, is from the U.S. Geological Survey, EROS Data Center, Sioux Falls, S. Dak. 57198.*

Northeastern Siberia

Over the vast territory of Northeastern Siberia, glaciers are situated in widely separated areas: Khrebet Suntar-Khayata, the Khrebet Cherskogo, and Koryakskoye Nagor'ye (upland). Khrebet Suntar-Khayata is situated near one of the coldest places in the Northern Hemisphere — Oymyakan settlement. The first mention of the permanent snow on the summits of Khrebet Suntar-Khayata was made by I.D. Chersky as early as the late 19th century. However, glaciers were not found in that area until 1939. The scale of glacierization was estimated only after aerial photographic surveys were carried out in the 1940s (USSR Academy of Sciences, 1965–1983). The first comprehensive work on the Suntar-Khayata glaciers was published by L.L. Berman (1947). About 20 glaciers were described during geological surveys at the beginning of the IGY; and during the IGY, one of the eleven Soviet glaciological stations was located here (Koreisha, 1963).

According to the data of the USSR Glacier Inventory, Khrebet Suntar-Khayata has 208 glaciers with a total area of 201.6 km^2 (fig. 34*A*). Similar to the Khrebet Cherskogo, nearly all of the glaciers have a northern exposure (fig. 34*B*, *C*). More than half of the total glacierized area is found in valley glaciers. Small glaciers with an area less than 1 km^2 prevail (table 12). On a Landsat 1 MSS image of 26 July 1973, it was possible to identify only one glacier that had an area of 4.4 km^2; glaciers of smaller dimensions were difficult to distinguish.

The ability to identify the small isolated glaciers that characterize northeastern Siberia depends primarily on the time of the surveys. However, very few Landsat 1, 2, and 3 MSS images were acquired of the glacierized regions of Siberia and, of these, very few were acquired during the optimum time for observing the glaciers, usually in early to mid-August. As a result, the Landsat 1, 2 and 3 MSS images have very limited usefulness in this region. For example, figure 35 shows a comparison of two enlarged Landsat images, one acquired on 2 July 1975 (fig. 35*A*) and the other on 26 August 1975 (fig. 35*B*); they both show the highest point of the Koryakskoye upland, at 2,115 m high. On the 2 July 1975 image, the glaciers are masked by the mantle of seasonal snow that is still present. And on the 26 August 1975 image, the boundaries of the glaciers are difficult to delineate. Unfortunately, there is no ideal Landsat image of this area.

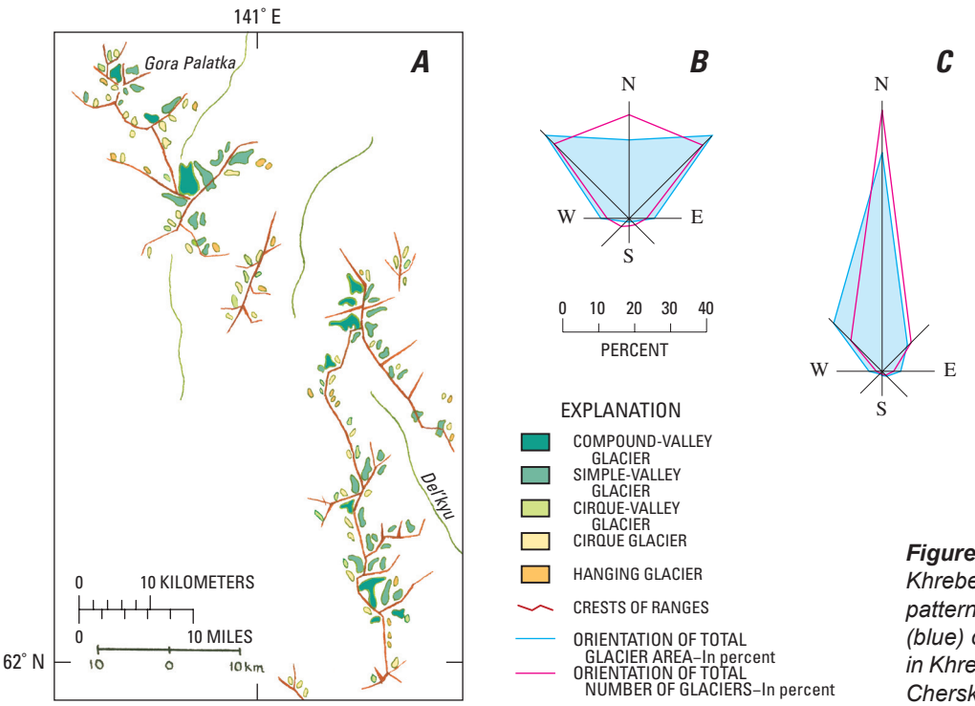


Figure 34.—**A**, *Distribution of glaciers over Khrebet Suntar- Khayata;* **B**, *Distribution patterns of the number (red) and area (blue) of glaciers relating to the orientation in Khrebet Suntar-Khayata; and* **C**, *Khrebet Cherskogo.*

TABLE 12.—*Distribution of glaciers in the Khrebet Suntar-Khayata based on their size*

[Unit: km^2, square kilometer]

Indices	<0.5 (km^2)	0.6–1.0 (km^2)	1.1–2.0 (km^2)	2.1–3.0 (km^2)	>3.0 (km^2)
Number of glaciers	87	68	27	14	12
Percentage	41.8	32.7	13.0	6.7	5.8
Total area of glaciers (km^2)	20.4	50.2	39.8	37.3	53.9
Percentage	10.2	24.9	19.7	18.5	26.7

Space images are very helpful in studies of aufeis (also called naled' or icing). Aufeis is a sheet-like mass of layered ice that forms from successive flows of ground water during freezing temperatures. In addition to showing the geographic location of aufeis, space images can reveal some of their structural elements: large faults, zones of intense crevassing, ring structures, and local depressions. The best time of image acquisition for analyzing aufeis is during the first weeks after the disappearance of snow cover. Using images larger than 1:500,000 scale, it is possible to study the morphology and geological changes in aufeis; images larger than 1:1,000,000-scale can be used to map large aufeis areas (fig. 36) and to study their variability from year to year. [See also Williams (1986, p. 536, fig. 9–24), who delineated four icing remnants on a 1:1,000,000-scale, 4 August 1973, Landsat 1 MSS image (1377-21112-6) of northeastern Alaska in the Sagavanirktok River area and environs.]

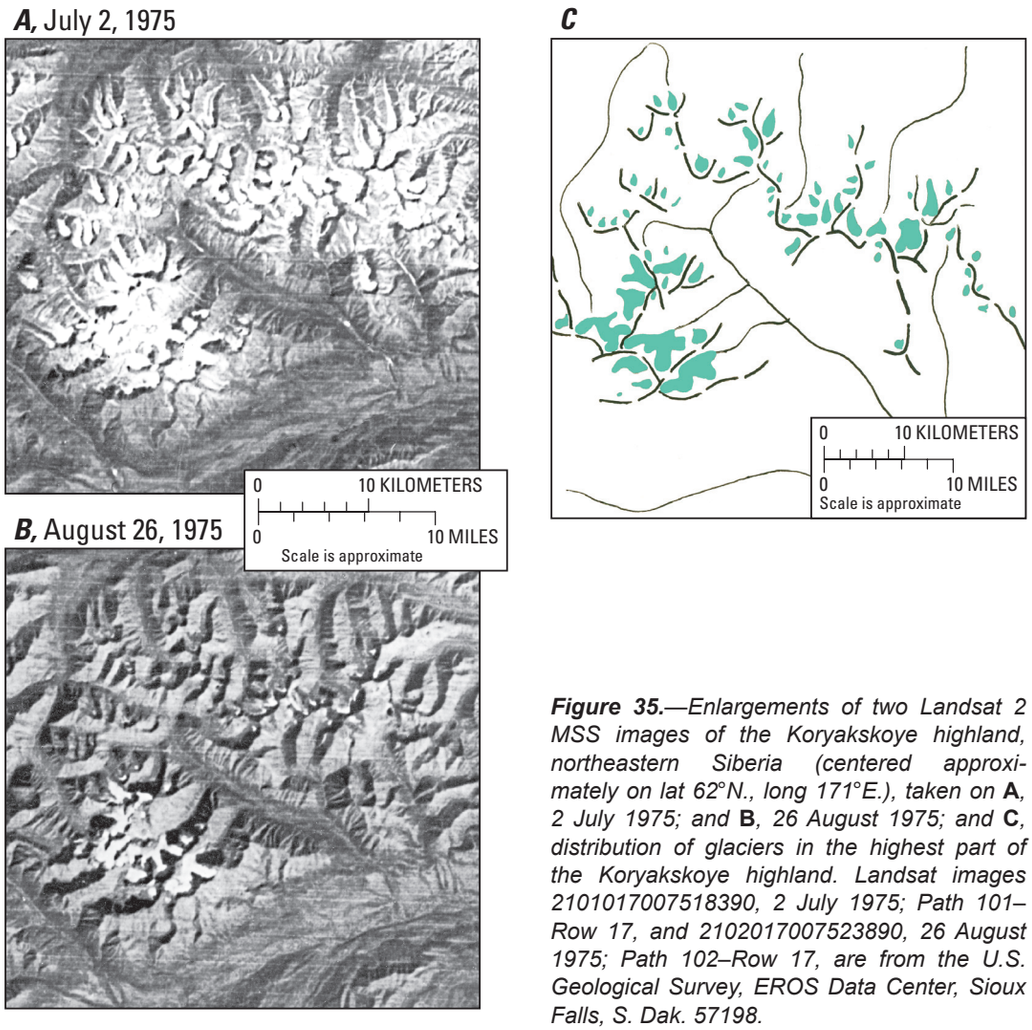


Figure 35.—*Enlargements of two Landsat 2 MSS images of the Koryakskoye highland, northeastern Siberia (centered approximately on lat 62°N., long 171°E.), taken on* **A**, *2 July 1975; and* **B**, *26 August 1975; and* **C**, *distribution of glaciers in the highest part of the Koryakskoye highland. Landsat images 2101017007518390, 2 July 1975; Path 101–Row 17, and 2102017007523890, 26 August 1975; Path 102–Row 17, are from the U.S. Geological Survey, EROS Data Center, Sioux Falls, S. Dak. 57198.*

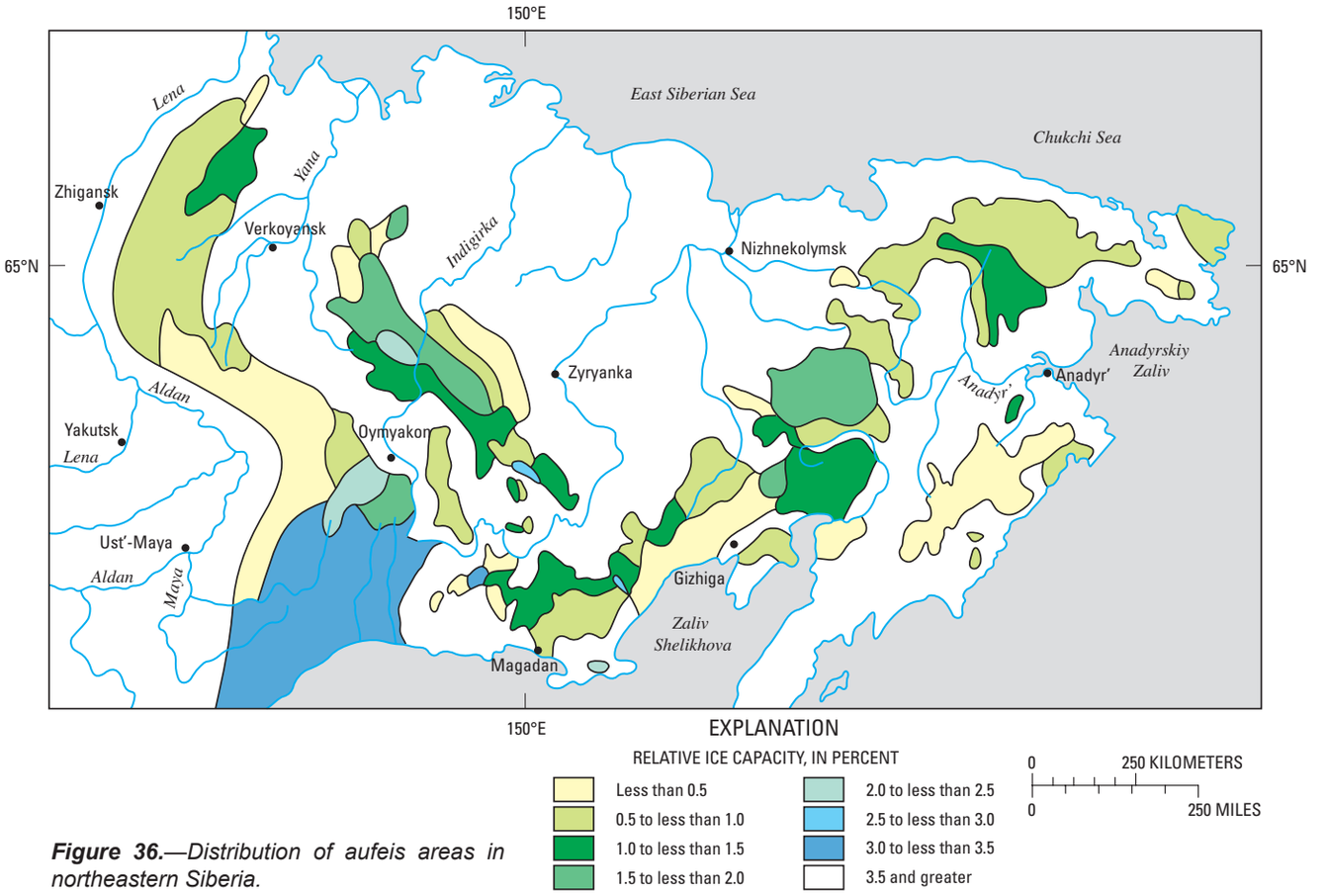


***Figure 36.**—Distribution of aufeis areas in northeastern Siberia.*

Kamchatka

The Kamchatka region is located on the far eastern side of the Former Soviet Union (fig. 1). The presence of ice fields and firn fields on the volcanoes of Kamchatka has been known since the 18th century, and their characteristics had been noted by the end of the 19th century (Bogdanovich, 1899). Studies of the glaciers of Kamchatka began in the 20th century, and in the 1950s a general map of the glacierization of Kamchatka was compiled from available cartographic data (Ivan'kov, 1958). Later, glaciological investigations of Kamchatka were undertaken by the Institute of Volcanology of the USSR Academy of Sciences.

Inventories and interpretation of aerial photographs of the Kamchatka Peninsula revealed 405 glaciers that are greater than 0.1 km^2 in area; these glaciers have a total area of 874 km^2 (Vinogradov, 1968). The majority of glaciers are situated in the craters or calderas of, or on the flanks of, volcanoes, giving rise to the following specific morphological types (fig. 37):

Ice belts (fig. 37*A*) are confined to the highest and most active volcanoes. Snow and ice accumulate on steep (less than 30°), dissected slopes of the volcano, while glacier tongues drain the lower part of the ice belt.

Crater glaciers (fig. 37*B*) are located in the craters of dead, dormant, or active volcanoes (during their quiescent stage). Well-pronounced, ring-like crests of craters contribute to the identification of such glaciers on Vulkan Mutnovskaya Sopka (fig. 38).

Caldera glaciers are situated in calderas of large volcanoes. Usually they do not spill over the caldera rims containing them, and they have short outlet tongues.

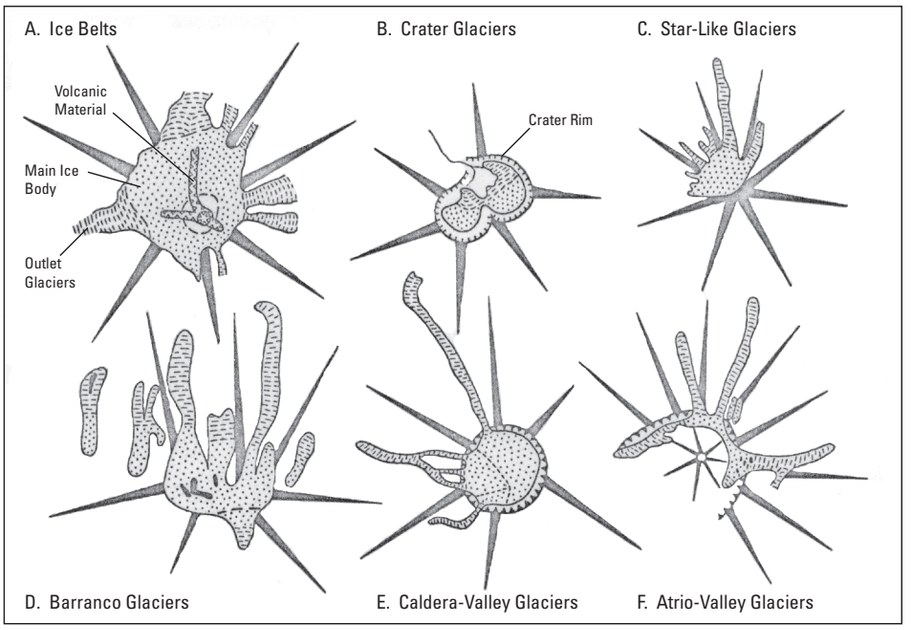


Figure 37.— *Morphological types of present-day glaciers in the volcanic regions of Kamchatka:* **A**, *Ice belt on Vulkan Klyuchevskaya Sopka;* **B**, *Crater glaciers on Vulkan Mutnovskaya Sopka;* **C**, *A star-like glacier on Vulkan Kronotskaya Sopka;* **D**, *Barranco glaciers on Vulkan Zhupanovskaya;* **E**, *Caldera-valley glaciers on* Vulkan Dal'niy Ploskiy*; and* **F**, Atrio-*valley glaciers on Vulkan Avachinskaya Sopka.*

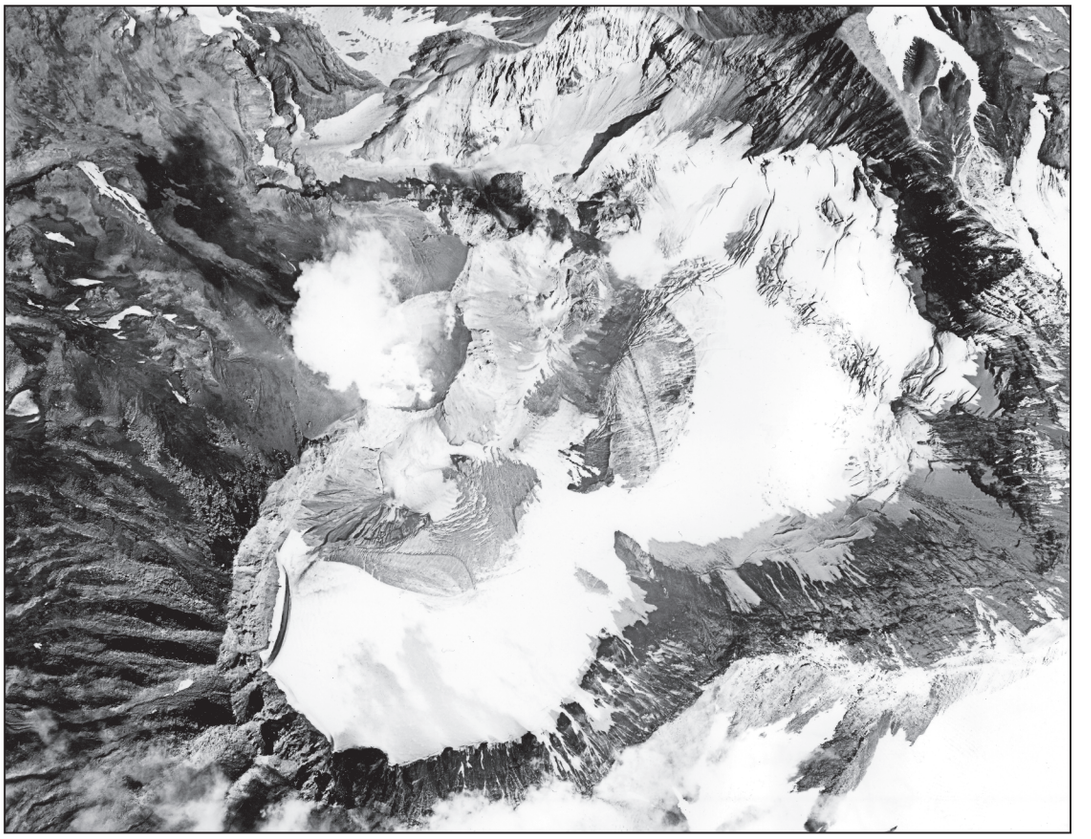


Figure 38.—*Aerial photograph of glaciers in the crater and on the slopes of Vulkan Mutnovskaya Sopka (see fig. 37*B*).*

Star-like glaciers (fig. 37*C*) are situated in the near-summit area of dead or dormant volcanoes and have irregular boundaries and outlet tongues, mainly on slopes that have a northern exposure.

Barranco glaciers (fig. 37*D*) spread over recently active or dormant volcanoes. They are confined to the medial and upper parts of barrancos (steep slopes), and are usually on northern slopes. They are nourished by snow-avalanches.

Caldera-valley glaciers (fig. 37*E*) have their accumulation area in the caldera of volcanoes. They have long tongues. They are confined to the late Holocene calderas of dead, dormant, and active volcanoes; surge-type glaciers may be encountered among them.

Atrio-valley glaciers (fig. 37*F*) have their accumulation areas in large *atrio* (central parts) of calderas and ablation areas on the slopes of a volcanic somma. Glacier tongues drain the *atrio* in the form of ice-falls of several hundred meters.

Unfortunately, it is very difficult to identify Kamchatka glaciers on the available Landsat 1, 2, and 3 MSS images. Not many images have been acquired and most are cloudy or snow-covered. However, interpretation of snow-covered images can be of great interest, as they may reveal the impacts of present volcanism on glaciers. Kamchatka glaciers in the areas of active volcanism — on the Kluchevskaya and Avachinskaya group of volcanoes — differ greatly from glaciers occupying areas of Quarternary volcanism (Khrebet Sredinnyy) or non-volcanic areas (Kronotskiy Poluostrov) (Vinogradov, 1975). The morphology of these glaciers is also very different (Vinogradov and Glazyrin, 1979).

In areas of active volcanism, glaciers are mantled by the products (especially tephra) of volcanic eruptions. The thickness of the pyroclastic mantle increases from the equilibrium line to the glacier termini, and in certain areas it reaches 1 m thick. This mantle favors reduced ablation of ice and is seen more often than bare ice at the termini of glaciers. Because of this, it is difficult to identify glacier boundaries in volcanic areas from space images.

Russian Arctic[4]

The Russian Arctic consists of numerous islands and archipelagos north of mainland Russia, in the Barents and Kara Seas. This section highlights the glacierization on three of the more significant archipelagos — Franz Josef Land, Severnaya Zemlya, and Novaya Zemlya.

Franz Josef Land (Zemlya Frantsa-Iosifa)

This polar archipelago, whose existence was predicted by the Russian geographer N. Schilling (Schilling, 1865), was discovered in 1873 by the Austro-Hungarian Expedition of J. Payer and K. Weyprecht (Payer, 1876). By the time F. Nansen wintered there in 1895–1896 (Nansen, 1897), the general nature of glacierization of the archipelago had been determined. In 1931, the Swedish-Norwegian Expedition of H. Ahlmann (Ahlmann, 1933) undertook a phototheodolite survey of glacierized coasts of George Land (Ostrov Zemlya Georga). The present-day map of Franz Josef Land was compiled from aerial photography taken during 1952–1953. The map served as the basis for compiling the glacier inventory of the archipelago (USSR, Academy of Sciences, 1965 [1965–1983], Katalog lednikov SSSR, vol. 3, part 1), which,

[4]See also companion section in this part of the chapter, The Glaciers of the Russian High Arctic.

together with a monograph based on studies of Franz Josef Land during the IGY-IGC (Grosswald and others, 1973), is the main source of information on the glaciers of the archipelago.

Based on the nature of the glacierization, Franz Josef Land is subdivided into three regions: western, central, and eastern (fig. 39). In all parts of the archipelago, ice-cap complexes prevail (table 13). Present-day glaciers occur on 56 islands of Franz Josef Land. Glaciers cover approximately 85 percent of the archipelago. Their mean thickness is about 180 m, their area is 13,738.8 km^2, and their total ice volume is approximately 2,500 km^3. Glaciers cover 1,570 km, or approximately 60 percent of the total length of the 2,255 km coast line.

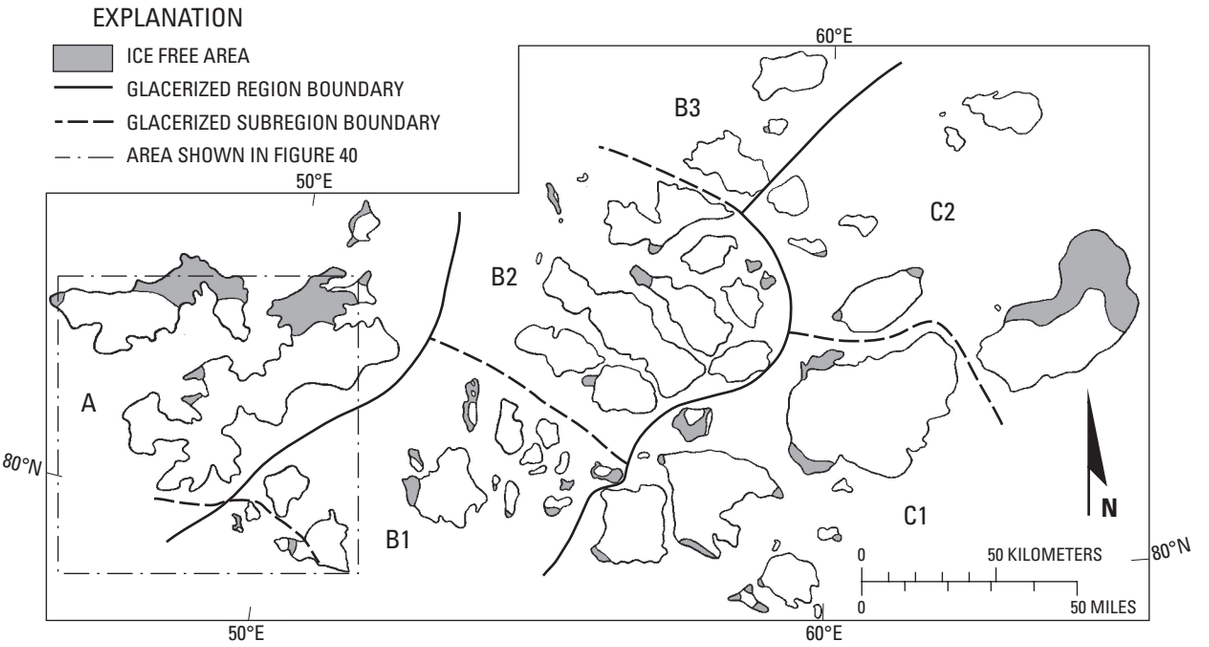


***Figure 39.**—Glacierized regions of Franz Josef Land:* **A**, *western region;* **B**, *central region (1, 2, 3 — southern, central and northern areas);* **C**, *eastern region (1, 2 — southern and northern areas). The non-glacierized areas are shown in grey. The coverage of the Landsat image used for figure 40 is shown. See table 13 for glacierized areas.*

TABLE 13.—*The area of glaciers in Franz Josef Land*
[Unit: km^2, square kilometer]

Areas and subareas	Ice-cap complexes (km^2)	Ice domes (km^2)	Other glaciers (km^2)	Total glacier area (km^2)
Western region	3,085.3	3.0	17.9	3,106.2
Central region				
Southern area	1,266.1	8.4	12.4	1,286.9
Central area	2,782.3	4.6	17.3	2,804.2
Northern area	640.9	0.6	2.9	644.4
Eastern region				
Southern area	3,739.9	—	14.4	3,754.3
Northern area	2,109.5	30.1	3.2	2,142.8
Total archipelago	13,624.0	46.7	68.1	13,738.8

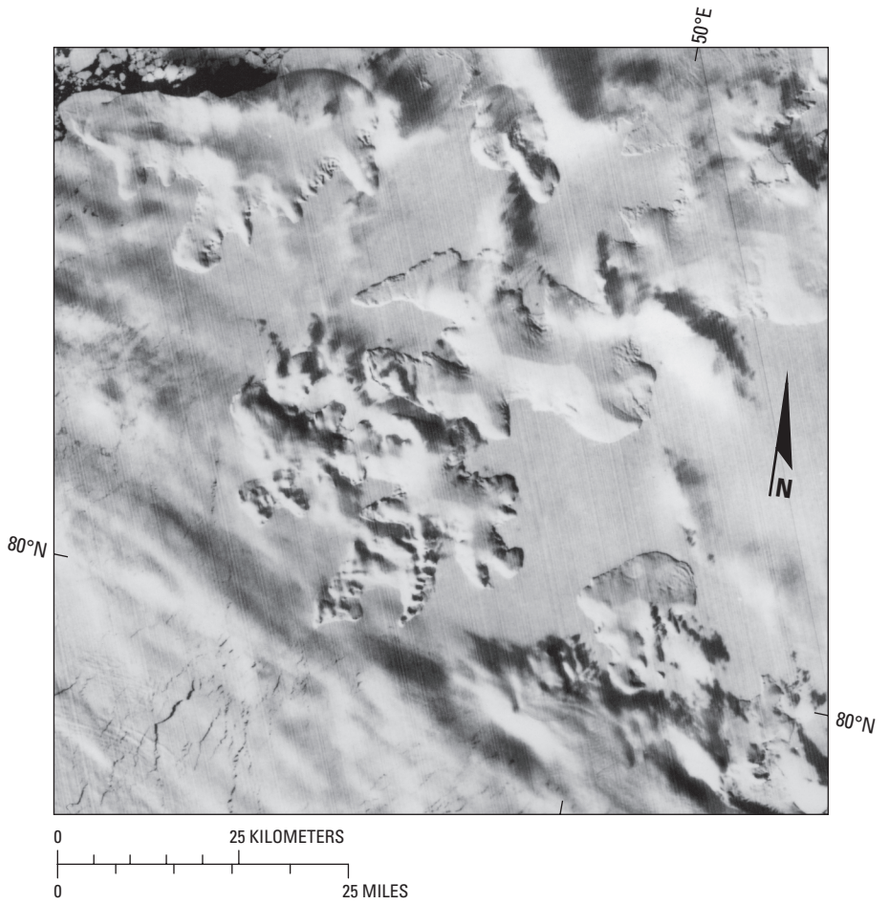


***Figure 40.**—Landsat 3 MSS image of the western part of Franz Josef Land acquired on 24 March 1978. The Landsat image 30019-10411 (3222001007808390), Path 222–Row 1, is from the U.S. Geological Survey, EROS Data Center, Sioux Falls, S. Dak. 57198.*

Ice caps on islands, valley outlet glaciers, and small glaciers are the main morphological types of glaciers in Franz Josef Land. They make up four morphogenetic glacier complexes: (a) ice-cap complexes (these prevail in the eastern area), (b) ice-cap-transition complexes, (c) transition-piedmont complexes (these two complexes prevail in the central area), (d) ice plateau complexes (prevail in the western area). The amount of glacierization in the eastern and southeastern parts of archipelago and on isolated islands is, as a rule, higher than in the western and northwestern areas.

The Landsat 3 MSS image shown in figure 40 includes only the smallest, most western part of the archipelago. Because the image was acquired in winter, it is impossible to determine the equilibrium line on the glaciers, although the margins of glaciers on the land and their contact with sea ice can be traced quite distinctly. Ice divides can be seen well, and, in the majority of cases, outlet glaciers that have rough topography and zones of crevasses are easily identified.

Severnaya Zemlya

Severnaya Zemlya was discovered by a Russian Expedition in 1913 (Starokadomskiy and Barr, 1977) that mapped the eastern coast of the archipelago. The first map of the islands was compiled in 1930–1932 by the expedition of G.A. Ushakov and N.N. Urvantsev (Anonymous, 1933), who determined the extent of glaciers on the archipelago by means of overland traverses. During the summer of 1931, an international expedition on board the Republic of Germany's LZ-127 airship *Graf Zeppelin* carried out aerial photography within the central part of the archipelago (Penck, 1931). A 1:400,000-scale map was compiled and published from these data, depicting some of the glaciers (Berson, 1933). For some areas, 1:25,000-scale maps

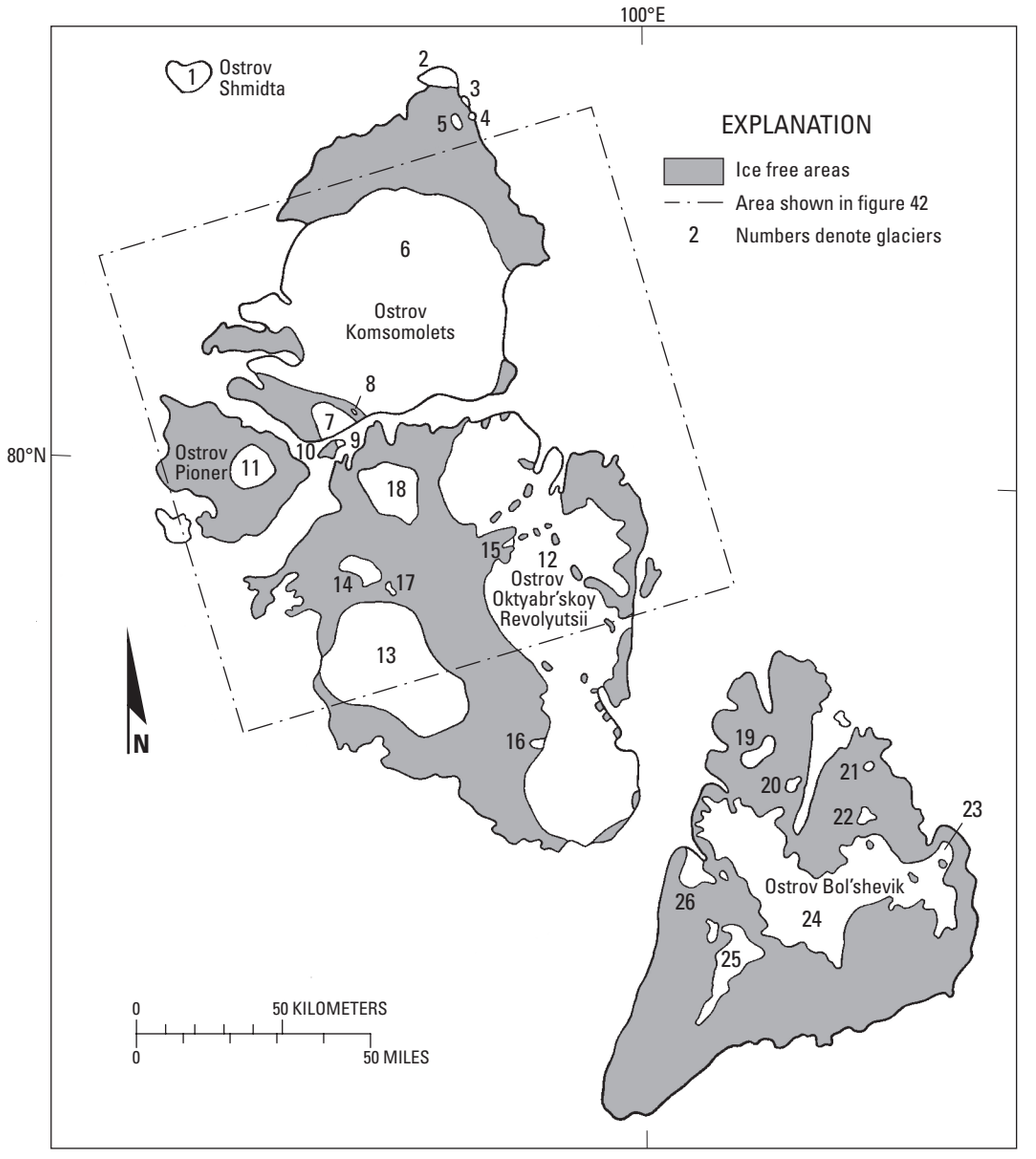


***Figure 41.**—Glacierization of Severnaya Zemlya. Location of the Landsat 3 MSS image used for figure 42 is shown.*

TABLE 14.—*The area of glaciers on Severnaya Zemlya*

[Unit: km^2, square kilometer]

Island	Glacier numbers on fig. 41	Area (km^2)
Shmidta	1	438.5
Komsomolets	2–8	6,171.6
Bol'shoy Isvestnyakoviy	9–10	6.1
Pioner	11	254.0
Oktyabr'skoy Revolyutsii	12–18	7,945.8
Bol'shevik	19–26	3,509.0
Total archipelago		18,325.0

were compiled. The map used for the compilation of glacier inventories (USSR, Academy of Sciences, 1981 [1965–1983], Katalog Lednikov SSSR, v. 10, iss. 1, pt. 1) was prepared from aerial photography acquired during the 1950s. Since 1962, glaciological expeditions from the Arctic and Antarctic Institute have been working on Severnaya Zemlya. A glaciological station was constructed on Lednik Vavilova in 1974 (Jania and Hagen, 1996).

Glaciers occupy 49.8 percent (18,325 km^2) (fig. 41, table 14) of the 36,788 km^2 total area of the archipelago. The average thickness of glaciers is 300 m, and the ice volume is about 5,500 km^3. Severnaya Zemlya contains 17 glacier complexes (occupying nearly 94 percent of the total glacierized area), 16 isolated ice domes, and 46 mountain glaciers. The extent of glacierization increases from south to north: on Ostrov Bol'shevik (island), glaciers cover 31 percent of the area; on Ostrov Oktyabr'skoy Revolutsii, glaciers occupy 58 percent of the area; and on Ostrov Komsomolets, glaciers occupy 68.5 percent

of the area. The length of glacierized coasts on these three islands makes up 1.6, 13.2 and 35.3 percent, respectively, and on Ostrov Shmidta, 96.1 percent of the total length of the coast line is glacierized.

The Landsat 1 MSS image used for figure 42 was taken in July — a favorable time; however, its interpretation was hampered by the spotty snow cover in the central part of Ostrov Bol'shevik. The newly fallen snow graphically emphasizes the hydrological network and geological structure, but at the same time obscures the margins of the glaciers. The sea ice in Proliv Shokal'skogo (strait), between Ostrova Bol'shevik and Oktyabr'skoy Revolutsii, is another source of difficulty, making it impossible to delineate the termini of small tidewater glaciers. The snow also makes it impossible to determine the equilibrium line of glaciers; ablation areas can only be seen on some of the outlet glaciers draining the ice cap on Ostrov Komsomolets.

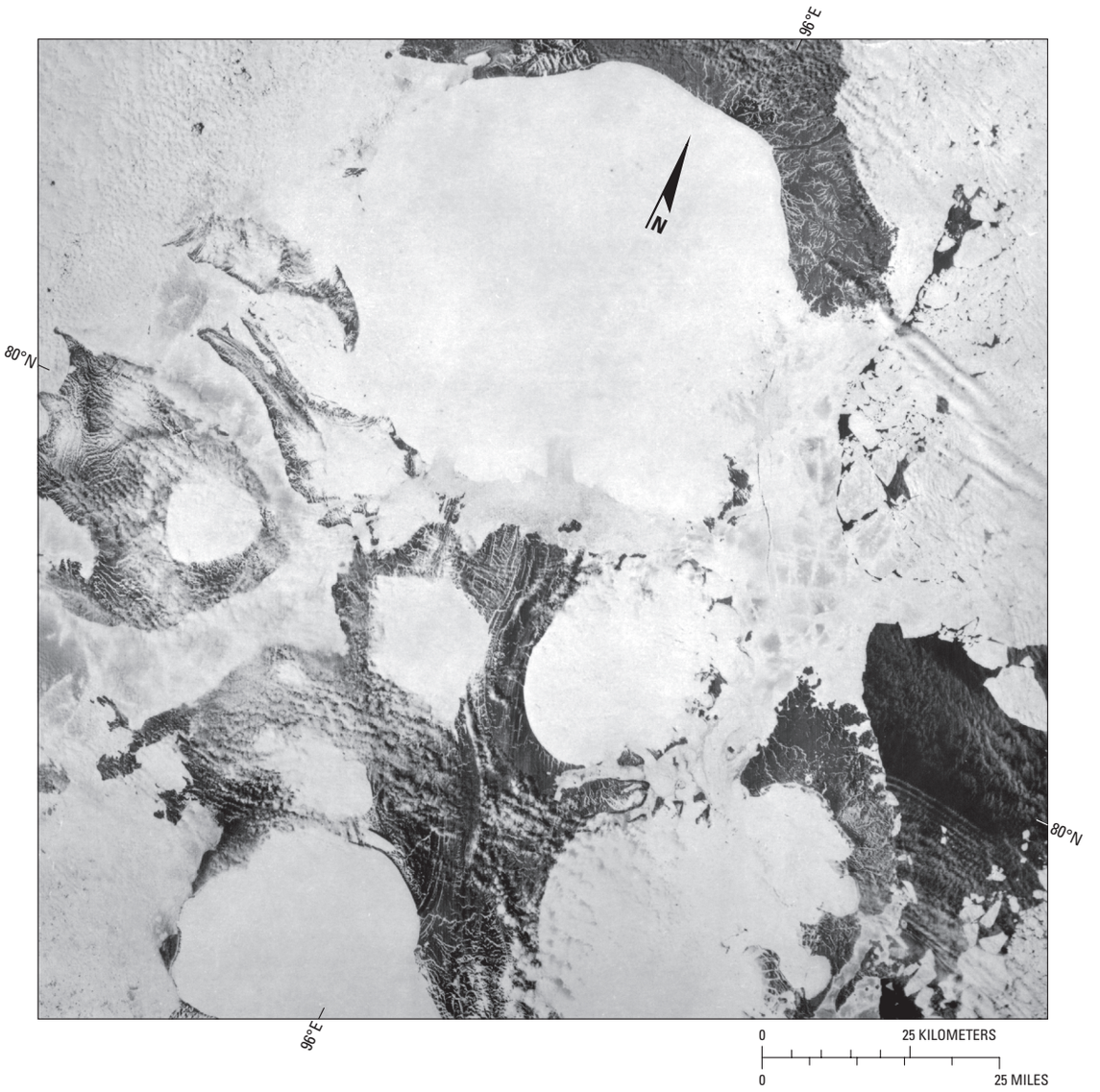


***Figure 42.**—Landsat 1 MSS image of the northern part of Severnaya Zemlya taken on 28 July 1973. The Landsat image 1362-07383 (1189001007320190), Path 189–Row 1, is from the U.S. Geological Survey, EROS Data Center, Sioux Falls, S. Dak. 57198.*

Novaya Zemlya

Although the mapping of the coastal area of Novaya Zemlya was accomplished as early as the 19th century, the first map with a schematic presentation of glaciers on *Ostrov Severniy*, the large northern island, was compiled by V.A. Rusanov in 1910. In 1913, the glaciers were mapped by an expedition led by G.Ya. Sedov (Chizhov and others, 1968). In the 1920s and 1930s, ground surveys were done by an Arctic Research Institute expedition. Some glaciers on western coasts were mapped by the Norwegian expedition to Novaya Zemlya in 1921 (Holtedahl, 1924, 1928, 1930). The glaciers of the eastern coasts were surveyed by means of aerial photography acquired in 1931, during the flight of the Republic of Germany's LZ-127 *Graf Zeppelin* airship (Penck, 1931). A map based on these aerial photographs was published in the proceedings of the expedition (Berson, 1933). A more recent map was compiled in the 1950s from subsequent aerial photography. This map served as the basis for the Glacier Inventory of the archipelago (USSR, Academy of Sciences, 1978 [1965–1983], Katalog Lednikov SSSR, v. 3, pt. 2). The inventory and a monograph, based on studies during the IGY-IGC (Chizhov and others, 1968), are the main sources of information on the glaciers of Novaya Zemlya.

The total area of glacierization on Novaya Zemlya is 24,413 km^2, the largest glacierized area in the Russian Arctic, and the ice volume is estimated to be about 6,800 km^3. All of the known types of glaciers exist here. The submeridional position of Novaya Zemlya produces a gradual increase in extent of glacierization from south to north and makes it possible to distinguish four areas based on the type of glacier located in each area: small glaciers, mountain glaciers, transitional glaciers, and ice caps (fig. 43, table 15).

The prevailing western transport of moisture-laden Atlantic air masses produces large areas of glacierization along the coast of the Barents Sea. Here, the amount of glacierization is 1.5 times greater, and the equilibrium line lies 200 m lower than on the coast of the Kara Sea. The ice divide is also shifted eastward in the direction of the Kara Sea.

The Landsat 1 MSS image shown in figure 44 characterizes the central part of the ice cap on *Ostrov Severniy* of Novaya Zemlya. The system of outlet glaciers reaching the sea can be seen well. The margin of the ice cap is very distinct. On the western coast, it is sometimes difficult to determine the position of glacier termini in the sea because of the presence of fast ice. The Landsat 1 MSS image spectacularly demonstrates the asymmetry of the ice-cap regime that has been induced climatically. The area of ablation in the Kara Sea basin is much larger than in the Barents Sea basin.

Conclusions

The preceding discussion has shown that Landsat 1, 2, and 3 MSS images have been used successfully in some areas to study the glaciers of the Former Soviet Union. In other areas, due to the small size of the glaciers, the spatial resolution of the satellite scanner, or the time of image acquistion, the images are less useful. Table 16 and figure 45 list the optimum Landsat images of the Former Soviet Union that were acquired during the decadal Landsat baseline period (1972–1981).

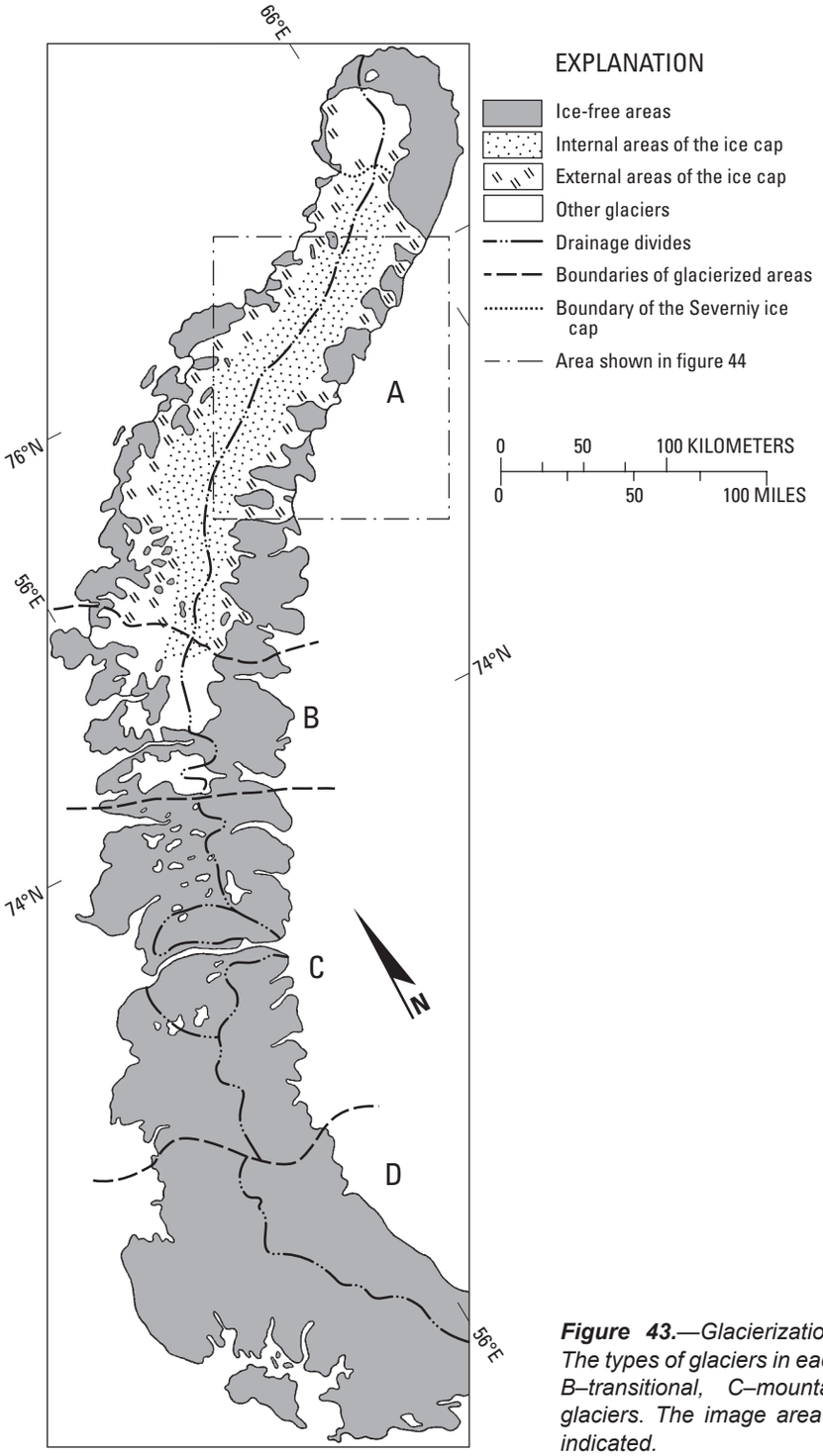


Figure 43.—*Glacierization of Novaya Zemlya. The types of glaciers in each area are: A–ice caps, B–transitional, C–mountain glaciers, D–small glaciers. The image area shown on figure 44 is indicated.*

Acknowledgments

We want to gratefully acknowledge the contributions of the following scientists to this part of the chapter, who assisted in the analysis of space images and/or photographs, aerial photographs, and in the preparation of scientific illustrations and maps of the glacierized regions indicated in parentheses after their names: V.G. Loseva (Caucasus and Altay), K.P. Rototayev and N.M. Zverkova (Caucasus), V.I. Kravtsova and N.F. Chaikina (Altay), and M.M. Koreisha (Siberia).

TABLE 15.—*The glaciers on Novaya Zemlya*

[Unit: km^2, square kilometer]

Glacier type	Number of glaciers	Total area (km^2)
AREA OF ICE CAPS		
Ice cap	1	18,911.3
Mountain	73	300.1
Small	611	398.9
Total	685	19,610.3
AREA OF TRANSITIONAL GLACIERIZATION		
Transitional forms	8	2,866.1
Mountain	94	296.1
Small	208	53.6
Total	310	3,215.8

Glacier type	Number of glaciers	Total area (km^2)
AREA OF MOUNTAIN GLACIERS		
Mountain	393	1,263.1
Small	417	119.4
Total	810	1,382.5
AREA OF SMALL GLACIERS		
Small	771	204.4
EXTENT OF GLACIERIZATION (A) AND LENGTH OF GLACIER FRONTS (B), IN PERCENT		
Glacierization zone	A	B
Ice cap	65.8	14.1
Transitional	41.5	2.0
Mountain	11.0	—
Small glaciers	2.0	—

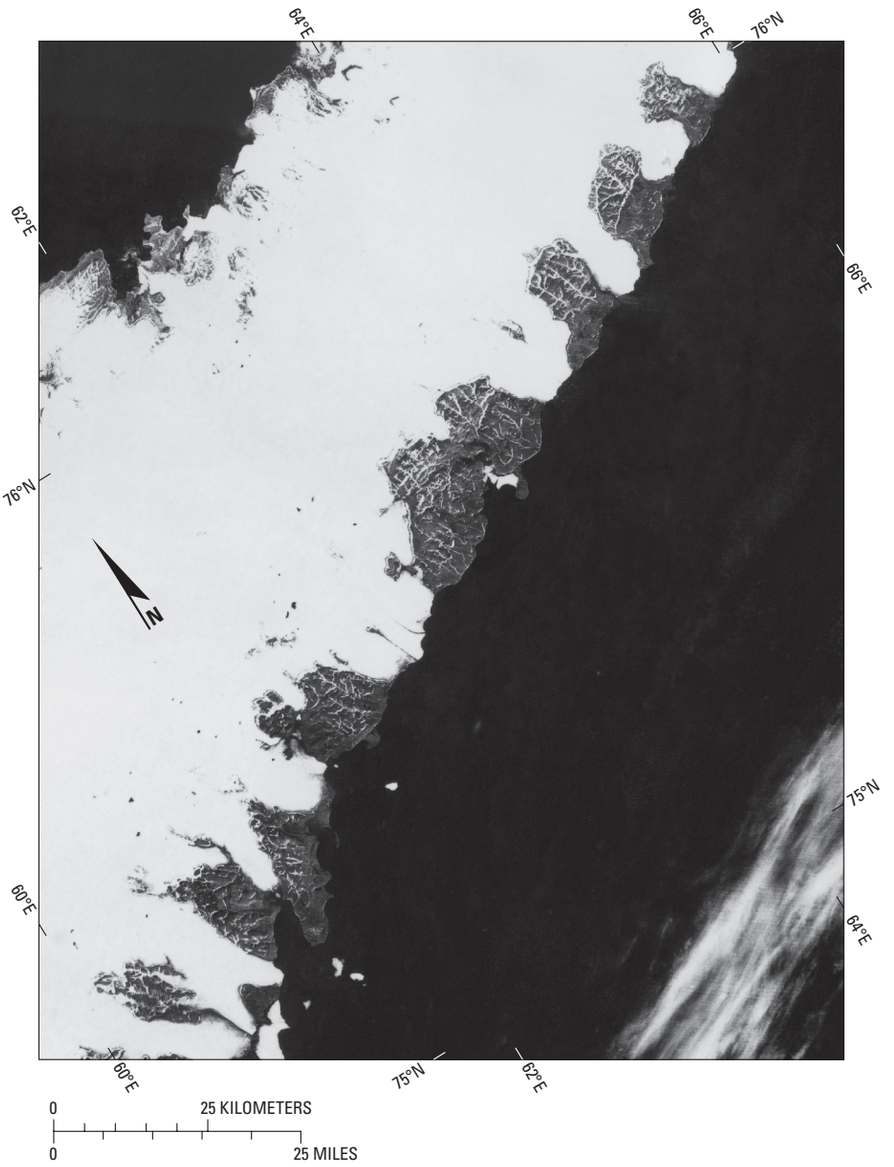


Figure 44.—*Landsat 1 MSS image of the central part of* Novozemel'skiy ice cap *taken on 23 July 1973. Landsat image 1365-07574 (1192006007320490), Path 192–Row 6, is from the U.S., Geological Survey, EROS Data Center, Sioux Falls, S. Dak. 57198.*

TABLE 16.—*Optimum Landsat 1, 2, and 3 MSS images of glaciers of the Former Soviet Union*

[Code column indicates usability for glacier studies; see figure 45 for explanation]

Path–row	Nominal scene-center latitude and longitude		Landsat identification number	Date	Code	Cloud cover (percent)	Remarks
CAUCASUS							
180–31	41°40′N.	48°56′E.	2180031007620490	22 Jul 76	◑	30	
180–32	40°14′N.	48°26′E.	2180032007620490	22 Jul 76	◑	30	
181–31	41°40′N.	47°30′E.	2181031007624190	28 Aug 76	●	0	
182–30	43°05′N.	46°36′E.	2182030007819580	14 Jul 78	◑	50	
182–31	41°40′N.	46°04′E.	2182031007819590	14 Jul 78	◑	20	
183–30	43°05′N.	45°10′E.	2183030007723790	25 Aug 77	●	0	Gora Kazbek
183–31	41°40′N.	44°38′E.	2183031007723790	25 Aug 77	●	0	
184–30	43°05′N.	43°44′E.	2184030007725690	13 Sep 77	◑	15	Gora Kazbek
185–30	43°05′N.	42°18′E.	2185030007619190	09 Jul 76	◑	15	Gora El'bruz
186–29	44°30′N.	41°24′E.	3186029008018090	28 Jun 80	◕	10	
186–30	41°40′N.	40°20′E.	2186030007718690	05 Jul 77	◑	70	
187–29	44°30′N.	39°58′E.	3187029008122090	08 Aug 81	◕	10	
PAMIRS AND ALAYSKIY KHREBET							
162–32	40°14′N.	74°15′E.	1162032007227090	26 Sep 72	●	0	Fresh snow
162–33	38°49′N.	73°46′E.	1162033007225290	08 Sep 72	◕	10	
162–34	37°24′N.	73°18′E.	2162034007622290	09 Aug 76	●	0	
163–32	40°14′N.	72°49′E.	2163032007526490	21 Sep 75	◑	35	Fresh snow
163–33	38°49′N.	72°20′E.	2163033007727190	28 Sep 77	●	0	Lednik Fedshenko
163–34	37°24′N.	71°52′E.	2163034007622390	10 Aug 76	●	5	
164–32	40°14′N.	71°23′E.	2164032007720090	19 Jul 77	◑	15	
164–33	38°49′N.	70°54′E.	2164033007225490	10 Sep 72	◑	20	
165–32	40°14′N.	69°57′E.	2165032007521290	31 Jul 75	●	0	
165–33	38°49′N.	69°28′E.	2165033007526690	23 Sep 75	●	5	
166–32	40°14′N.	68°31′E.	1166032007227490	30 Sep 72	●	0	
166–33	38°49′N.	68°02′E.	2166033007720290	21 Jul 77	●	5	
TIEN SHAN							
158–30	43°05′N.	81°01′E.	2158030007723090	18 Aug 77	●	0	
158–31	41°40′N.	80°30′E.	2158031007629090	16 Oct 76	●	0	
158–31	41°40′N.	80°30′E.	2158031007723090	18 Aug 77	●	0	
159–30	43°05′N.	79°35′E.	2159030007522490	12 Aug 75	●	0	
159–31	41°40′N.	79°04′E.	2159031007522490	12 Aug 75	●	0	
159–31	41°40′N.	79°04′E.	1159031007326190	18 Sep 73	●	0	
160–30	43°05′N.	78°09′E.	2160030007522590	13 Aug 75	●	0	
160–31	41°40′N.	77°37′E.	2160031007522590	13 Aug 75	●	0	
160–32	40°14′N.	77°07′E.	2160032007522590	13 Aug 75	●	0	
161–30	43°05′N.	76°43′E.	2161030007622190	08 Aug 76	●	0	
161–31	41°40′N.	76°11′E.	1161031007225190	07 Sep 72	◕	10	
161–32	40°14′N.	75°41′E.	2161032007529890	25 Oct 75	●	5	Snow
162–30	43°05′N.	75°17′E.	2162030007727090	27 Sep 77	●	0	

TABLE 16.—*Optimum Landsat 1, 2, and 3 MSS images of glaciers of the Former Soviet Union—Continued*

[Code column indicates usability for glacier studies; see figure 45 for explanation]

Path–row	Nominal scene-center latitude and longitude		Landsat identification number	Date	Code	Cloud cover (percent)	Remarks
162–31	41°40′N.	74°45′E.	2162031007727090	27 Sep 77	◑	15	
162–32	40°14′N.	74°15′E.	1162032007227090	26 Sep 72	●	0	Snow
163–30	43°05′N.	73°51′E.	2163030007723590	23 Aug 77	●	0	
163–31	41°40′N.	73°19′E.	2163031007522890	16 Aug 75	●	0	
164–30	43°05′N.	72°25′E.	2164030007723690	24 Aug 77	●	0	
164–31	41°40′N.	71°53′E.	2164031007720090	19 Jul 77	◑	20	
165–31	41°40′N.	70°27′E.	2165031007723790	25 Aug 77	●	0	
ZHONGGHAR ALATAŭ ZHOTASY							
158–29	44°30′N.	81°34′E.	2158029007723090	18 Aug 77	●	0	
159–29	44°30′N.	80°08′E.	2159029007723190	19 Aug 77	◕	10	
160–29	44°30′N.	78°42′E.	2160029007522590	13 Aug 75	●	0	
RUSSIAN ALTAY							
155–25	50°09′N.	88°17′E.	1155025007224590	01 Sep 72	●	0	
155–26	48°44′N.	87°38′E.	1155026007224590	01 Sep 72	●	0	
156–25	50°09′N.	86°50′E.	1156025007405590	24 Feb 74	◑	NA	Snow
157–25	50°09′N.	85°24′E.	3157025007922890	16 Aug 79	●	0	
157–26	48°44′N.	84°46′E.	3157026007922890	16 Aug 79	●	0	
SAŭYR ZHOTASY							
156–27	47°20′N.	85°35′E.	2156027007518590	04 Jul 75	●	0	
156–27	47°20′N.	85°35′E.	2156027007621690	03 Aug 76	◕	10	
KUZNETSKIY ALATAU							
156–21	55°45′N.	89°47′E.	No image		○		
156–22	54°22′N.	88°59′E.	2156022007619890	16 Jul 76	◑	35	
157–21	55°45′N.	88°21′E.	3157021007921090	29 Jul 79	●	0	
157–22	54°22′N.	87°33′E.	3157022007921090	29 Jul 79	●	0	
SAYAN MOUNTAINS							
148–23	52°58′N.	99°42′E.	1148023007330490	31 Oct 73	●	0	Snow
149–22	54°22′N.	99°01′E.	3149022007820790	26 Jul 78	◕	10	
150–22	54°22′N.	97°35′E.	215022007516190	10 Jun 75	◑	35	Cloudy and Snow
150–23	52°58′N.	96°50′E.	215023007516190	10 Jun 75	◑	50	Cloudy and Snow
KHREBET KODAR							
137–20	57°08′N.	117°53′E.	No usable image		◔		
138–20	57°08′N.	116°27′E.	No usable image		◔		
GORA KHIBINY							
202–12	67°59′N.	34°24′E.	No image		○		
203–12	67°59′N.	32°58′E.	No usable image		◔		
URAL MOUNTAINS							
179–12	67°59′N.	67°23′E.	1179012007306590	06 Mar 73	◕	10	
179–13	66°40′N.	65°45′E.	1179013007306590	06 Mar 73	◑	20	
179–14	65°20′N.	64°16′E.	1179014007306590	06 Mar 73	◑	20	
180–12	67°59′N.	65°57′E.	No image		○		

TABLE 16.—*Optimum Landsat 1, 2, and 3 MSS images of glaciers of the Former Soviet Union—Continued*

[Code column indicates usability for glacier studies; see figure 45 for explanation]

Path–row	Nominal scene-center latitude	Nominal scene-center longitude	Landsat identification number	Date	Code	Cloud cover (percent)	Remarks
180–13	66°40′N.	64°19′E.	1180013007317490	23 Jun 73	◑	60	
180–14	65°20′N.	62°50′E.	1180014007322890	16 Aug 73	●	0	
180–15	63°59′N.	61°29′E.	1180015007322890	16 Aug 73	●	0	
180–16	62°38′N.	60°16′E.	1180016007322890	16 Aug 73	●	0	
181–12	67°59′N.	64°31′E.	1181012007317590	24 Jun 73	◑	70	
181–13	66°40′N.	62°52′E.	1181013007317590	24 Jun 73	◑	60	
181–14	65°20′N.	61°24′E.	1181014007317590	24 Jun 73	◑	70	
181–15	63°59′N.	60°03′E.	1181015007317590	24 Jun 73	◑	90	
182–14	65°20′N.	59°58′E.	1182014007317690	25 Jun 73	●	0	
182–15	63°59′N.	58°37′E.	1182015007317690	25 Jun 73	◕	10	
PLATO PUTORANA							
157–12	67°59′N.	98°56′E.	1157012007324190	29 Aug 73	◑	50	
157–13	66°40′N.	97°18′E.	1157013007324190	29 Aug 73	◑	40	
158–11	69°17′N.	99°19′E.	1158011007324290	30 Aug 73	◕	10	
158–12	67°59′N.	97°30′E.	1158012007324290	30 Aug 73	◑	40	
158–13	66°40′N.	95°52′E.	1158013007324290	30 Aug 73	◑	40	
159–11	69°17′N.	93°53′E.	1159011007320790	26 Jul 73	◑	20	Snow
159–12	67°59′N.	96°04′E.	No usable image		◔		
159–13	66°40′N.	94°26′E.	No usable image		◔		
160–11	69°17′N.	96°27′E.	No usable image		◔		
160–12	67°59′N.	94°38′E.	1160012007322690	14 Aug 73	◑	40	Not seen
160–13	66°40′N.	93°00′E.	1160013007322690	14 Aug 73	◑	20	Not seen
161–11	69°17′N.	95°01′E.	No image		○		
161–12	67°59′N.	93°12′E.	1161012007322790	15 Aug 73	◑	30	
161–13	66°40′N.	91°34′E.	1161013007322790	15 Aug 73	◑	30	
162–11	69°17′N.	93°35′E.	No image		○		
162–12	67°59′N.	91°46′E.	No image		○		
163–11	69°17′N.	92°09′E.	No image		○		
164–11	69°17′N.	90°43′E.	No image		○		
GORY BYRRANGA							
158–6	75°25′N.	112°39′E.	1158006007320690	25 Jul 73	◕	10	
159–6	75°25′N.	111°13′E.	1159006007320790	26 Jul 73	◑	60	
160–6	75°25′N.	109°47′E.	No image		○		
161–6	75°25′N.	108°21′E.	No image		○		
162–6	75°25′N.	106°55′E.	No image		○		
163–6	75°25′N.	105°29′E.	No usable image		◔		
164–6	75°25′N.	104°03′E.	No usable image		◔		
KHREBET ORULGAN							
135–13	66°40′N.	128°51′E.	No image		○		
135–14	65°20′N.	127°22′E.	No image		○		

TABLE 16.—*Optimum Landsat 1, 2, and 3 MSS images of glaciers of the Former Soviet Union—Continued*

[Code column indicates usability for glacier studies; see figure 45 for explanation]

Path–row	Nominal scene-center latitude and longitude		Landsat identification number	Date	Code	Cloud cover (percent)	Remarks
136–12	67°59′N.	129°03′E.	1136012007323890	26 Aug 73	◑	70	
136–13	66°40′N.	127°25′E.	1136013007323890	26 Aug 73	◑	80	
136–14	65°20′N.	125°56′E.	1136014007323890	26 Aug 73	◑	20	
137–12	67°59′N.	127°37′E.	1137012007323990	26 Aug 73	◑	70	
137–13	66°40′N.	125°59′E.	1137013007314990	29 May 73	◑	20	Snow
KHREBET SUNTAR–KHAYATA							
122–16	62°38′N.	143°27′E.	1122016007230290	28 Oct 72	●	0	Snow
122–17	61°16′N.	142°19′E.	1122017007230290	28 Oct 72	●	0	Snow
123–16	62°38′N.	142°01′E.	1123016007220790	26 Jul 72	◑	50	Not seen
123–17	61°16′N.	140°53′E.	1123017007220790	26 Jul 72	◑	20	Not seen
124–16	62°38′N.	140°35′E.	1124016007228690	12 Oct 72	◑	20	Snow
124–17	61°16′N.	139°27′E.	1124017007228690	12 Oct 72	◑	20	Not seen
125–16	62°38′N.	139°09′E.	1125016007319190	10 Jul 73	◑	40	Not seen
125–17	61°16′N.	138°01′E.	1125017007324590	02 Sep 73	◑	20	Not seen
KHREBET CHERSKOGO							
122–14	65°20′N.	146°01′E.	1122014007230290	28 Oct 72	●	0	Snow
123–13	66°40′N.	146°04′E.	1123013007308190	22 Mar 73	●	0	Snow
123–14	65°20′N.	144°35′E.	1123014007308190	22 Mar 73	●	0	Snow
124–13	66°40′N.	144°38′E.	1124013007228690	12 Oct 72	◑	20	Snow
124–14	65°20′N.	143°09′E.	1124014007228690	12 Oct 72	◑	30	Snow
125–13	66°40′N.	143°12′E.	1125013007319190	10 Jul 73	◑	40	Not seen
125–14	65°20′N.	141°43′E.	1125014007319190	10 Jul 73	◑	30	Not seen
126–13	66°40′N.	141°46′E.	1126013007308490	25 Mar 73	●	0	Snow
126–14	65°20′N.	140°17′E.	1126014007308490	25 Mar 73	●	0	Snow
127–13	66°40′N.	140°20′E.	1127013007308590	26 Mar 73	●	0	Snow
127–14	65°20′N.	138°51′E.	1127014007308590	26 Mar 73	●	0	Snow
128–12	67°59′N.	140°32′E.	1128012007225490	10 Sep 72	◑	15	Snow
128–13	66°40′N.	138°54′E.	1128013007225490	10 Sep 72	◑	20	Snow
128–14	65°20′N.	137°25′E.	1128014007321290	31 Jul 73	◑	70	
129–12	67°59′N.	139°06′E.	1129012007227390	29 Sep 72	◑	60	Snow
129–13	66°40′N.	137°27′E.	1129013007227390	29 Sep 72	◑	20	Snow
130–12	67°59′N.	137°40′E.	1130012007307090	11 Mar 73	●	0	Snow
KORYAKSKOYE NAGOR'YE (UPLAND)							
101–16	62°38′N.	173°34′E.	1101016007426990	26 Sep 74	◑	30	Snow
101–17	61°16′N.	172°26′E.	1101017007322090	08 Aug 73	◑	70	
101–17	61°16′N.	172°26′E.	2101017007518390	02 Jul 75	◑	20	
102–16	62°38N.	172°08′E.	1102016007421690	04 Aug 74	◑	30	
102–17	61°16′N.	171°00′E.	1102017007421690	04 Aug 74	◑	30	
102–17	61°16′N.	171°00′E.	2102017007523890	26 Aug 75	◑	30	
103–17	61°16′N.	169°34′E.	1103017007409190	01 Apr 74	●	0	Snow

TABLE 16.—*Optimum Landsat 1, 2, and 3 MSS images of glaciers of the Former Soviet Union—Continued*

[Code column indicates usability for glacier studies; see figure 45 for explanation]

Path–row	Nominal scene-center latitude and longitude		Landsat identification number	Date	Code	Cloud cover (percent)	Remarks
KAMCHATKA							
106–20	57°08′N.	162°21′E.	2106020007524290	30 Aug 75	◑	50	
106–21	55°45′N.	161°30′E.	2106021007609390	02 Apr 76	◑	60	Snow
107–19	58°31′N.	161°49′E.	No usable image		◔		
107–20	57°08′N.	160°55′E.	No image		○		
107–21	55°45′N.	160°04′E.	1107021007331690	12 Nov 73	●	0	Snow
107–22	54°22′N.	159°16′E.	1107022007302890	28 Jan 73	◑	50	Snow
107–23	52°58′N.	158°31′E.	1107023007225090	06 Sep 72	◑	70	
107–24	51°34′N.	157°48′E.	1107024007232290	17 Nov 72	◑	20	Snow
108–19	58°31′N.	160°23′E.	No usable image		◔		
108–20	57°08′N.	159°29′E.	1108020007304890	17 Feb 73	●	0	Snow
108–21	55°45′N.	158°38′E.	1108021007225290	08 Sep 72	◑	80	
108–21	55°45′N.	158°38′E.	1108021007304890	17 Feb 73	●	0	Snow
108–22	54°22′N.	157°50′E.	1108022007225290	08 Sep 72	◑	80	
108–22	54°22′N.	157°50′E.	1108022007304890	17 Feb 73	◑	30	Snow
108–23	52°58′N.	157°05′E.	1108023007225290	08 Sep 72	◕	10	
108–24	51°34′N.	156°22′E.	1108024007225290	08 Sep 72	◕	10	
109–19	58°31′N.	158°57′E.	No image		○		
109–20	57°08′N.	158°03′E.	3109020007923390	21 Aug 79	◑	70	
109–21	55°45′N.	157°12′E.	3109021007923390	21 Aug 79	◑	80	
109–22	54°22′N.	156°24′E.	3109022007923390	21 Aug 79	◑	50	
FRANZ JOSEF LAND							
210–1	80°01′N.	65°28′E.	No image		○		
211–1	80°01′N.	64°02′E.	No image		○		
212–1	80°01′N.	62°35′E.	No image		○		
213–1	80°01′N.	61°09′E.	No image		○		
214–1	80°01′N.	59°43′E.	No image		○		
215–1	80°01′N.	58°17′E.	No image		○		
216–1	80°01′N.	56°51′E.	No image		○		
217–1	80°01′N.	55°25′E.	No image		○		
218–1	80°01′N.	53°59′E.	No image		○		
219–1	80°01′N.	52°33′E.	No image		○		
220–1	80°01′N.	51°07′E.	3220001197813790	17 May 78	◑	90	
221–1	80°01′N.	49°41′E.	No image.		○		
222–1	80°01′N.	48°15′E.	No image		○		
223–1	80°01′N.	46°49′E.	No image		○		
224–1	80°01′N.	45°23′E.	No image		○		
225–1	80°01′N.	43°57′E.	3225001197817690	25 Jun 78	◑	60	

TABLE 16.—*Optimum Landsat 1, 2, and 3 MSS images of glaciers of the Former Soviet Union—Continued*

[Code column indicates usability for glacier studies; see figure 45 for explanation]

Path–row	Nominal scene-center latitude and longitude		Landsat identification number	Date	Code	Cloud cover (percent)	Remarks
SEVERNAYA ZEMLYA							
171–3	78°29′N.	107°59′E.	1171003197412490	04 May 74	◑	80	
172–3	78°29′N.	106°33′E.	No image		○		
173–3	78°29′N.	105°07′E.	No image		○		
174–3	78°29′N.	103°40′E.	No image		○		
175–2	79°19′N.	108°29′E.	1175002197320690	25 Jul 73	◕	10	
175–3	78°29′N.	102°14′E.	1175003197320690	25 Jul 73	◕	10	Line drops
176–2	79°19′N.	107°03′E.	1176002197320690	25 Jul 73	◕	10	
176–3	78°29′N.	100°48′E.	1176003197320690	25 Jul 73	●	0	
177–2	79°19′N.	105°37′E.	No image		○		
177–3	78°29′N.	99°22′E.	1177003197322590	13 Aug 73	◑	70	
178–2	79°19′N.	104°11′E.	No image		○		
178–3	78°29′N.	97°56′E.	No image		○		
179–2	79°19′N.	102°45′E.	No image		○		
179–3	78°29′N.	96°30′E.	No image		○		
180–2	79°19′N.	101°19′E.	1180002197519290	11 Jul 75	◑	60	Line drops
180–3	78°29′N.	95°04′E.	No image		○		
181–2	79°19′N.	99°53′E.	No image		○		
182–2	79°19′N.	98°27′E.	No image		○		
183–2	79°19′N.	97°01′E.	No image		○		
184–2	79°19′N.	95°35′E.	2184002197610190	10 Apr 76	◕	10	Snowy
185–1	80°01′N.	101°19′E.	No image		○		
185–2	79°19′N.	94°09′E.	No image		○		
186–1	80°01′N.	99°53′E.	No image		○		
186–2	79°19′N.	92°43′E.	No image		○		
187–1	80°01′N.	98°27′E.	No image		○		
187–2	79°19′N.	91°17′E.	No image		○		
188–1	80°01′N.	97°01′E.	1188001197320190	20 Jul 73	◑	40	
189–1	80°01′N.	95°35′E.	1189001197320190	20 Jul 73	◑	40	
190–1	80°01′N.	94°09′E.	No image		○		
191–1	80°01′N.	92°43′E.	1191001197520390	22 Jul 75	◕	10	Line drops
192–1	80°01′N.	91°17′E.	No image		○		
193–1	80°01′N.	89°51′E.	No image		○		

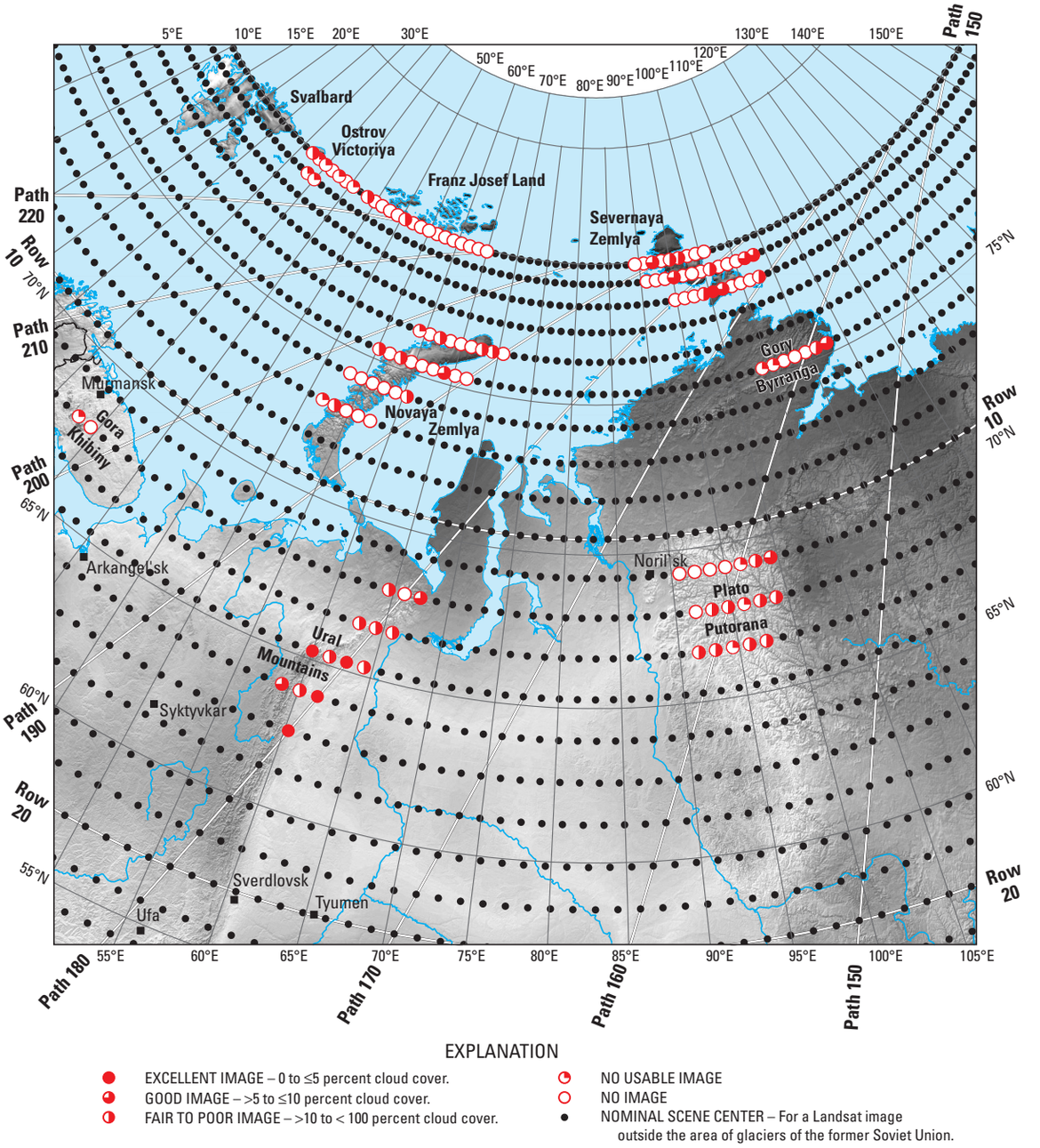


Figure 45.—*Index map of the optimum Landsat 1, 2, and 3 MSS images of the Former Soviet Union.*

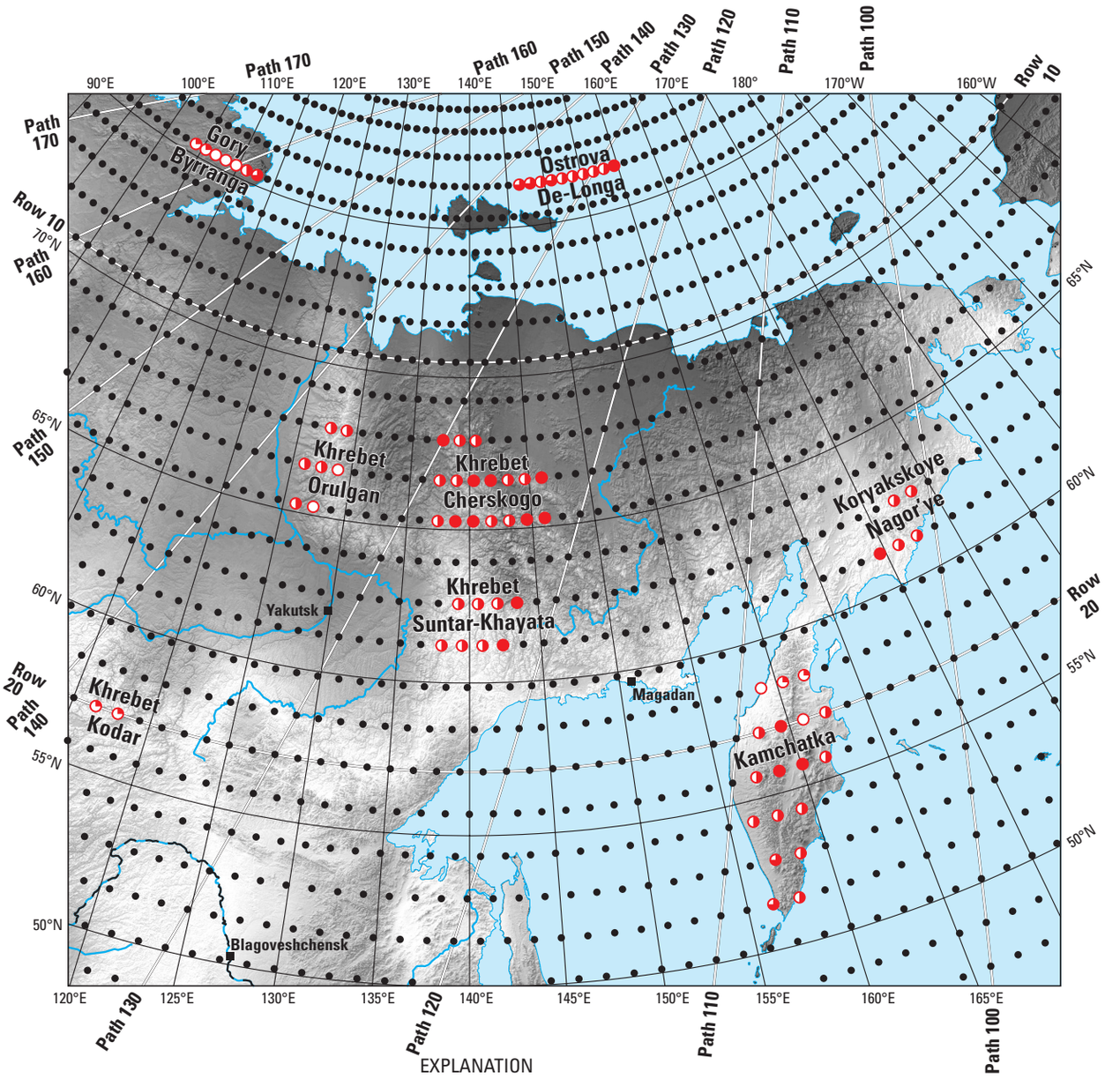
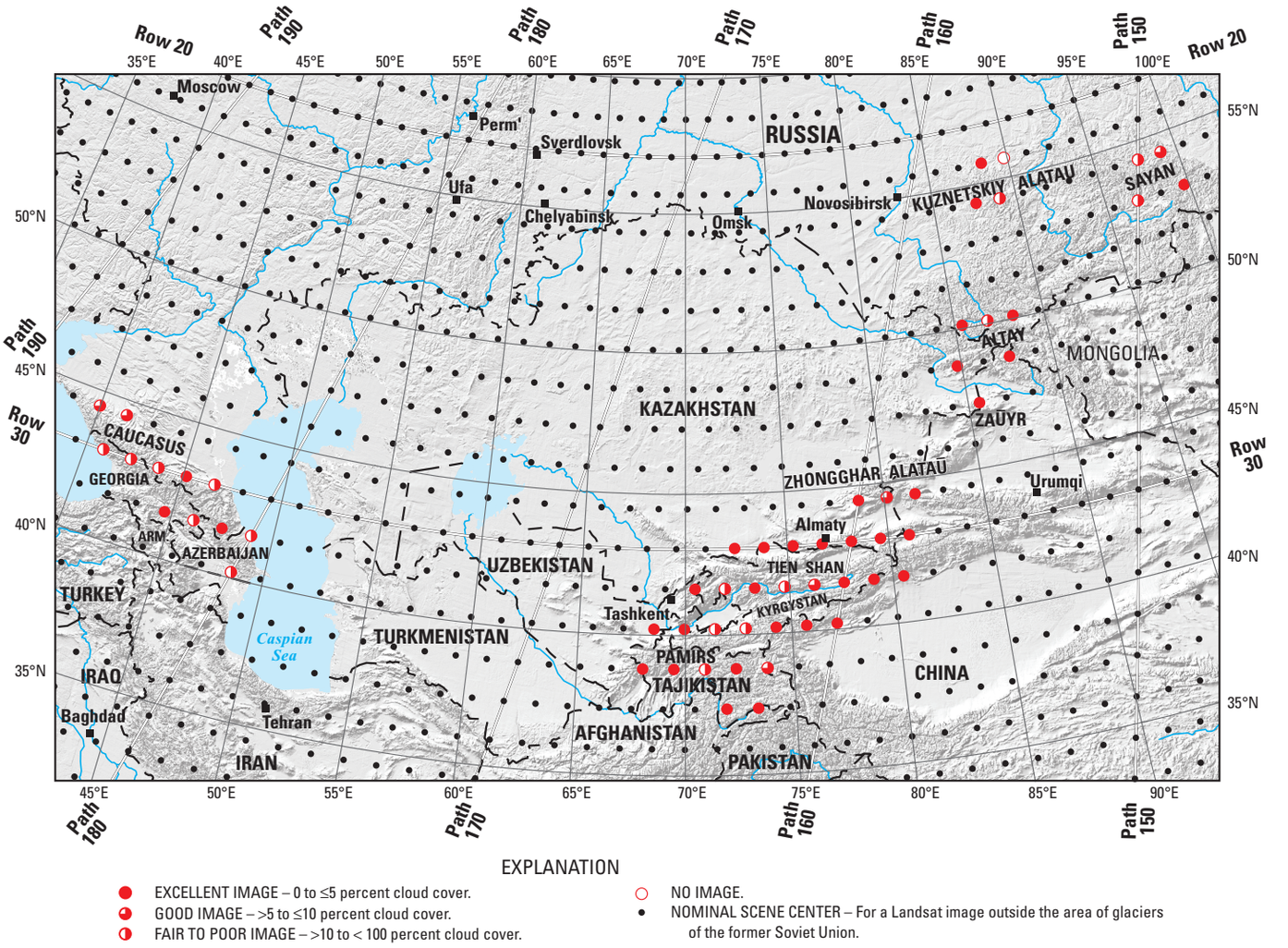


***Figure 45.**—Index map of the optimum Landsat 1, 2, and 3 MSS images of the Former Soviet Union. (Continued)*



EXPLANATION

- EXCELLENT IMAGE – 0 to ≤5 percent cloud cover.
- GOOD IMAGE – >5 to ≤10 percent cloud cover.
- FAIR TO POOR IMAGE – >10 to < 100 percent cloud cover.
- NO IMAGE.
- NOMINAL SCENE CENTER – For a Landsat image outside the area of glaciers of the former Soviet Union.

Figure 45.—*Index map of the optimum Landsat 1, 2, and 3 MSS images of the Former Soviet Union. (Continued)*

Fluctuations of Glaciers of the Central Caucasus and Gora El'brus, with a Section on the Glaciological Disaster in North Osetiya[1]

By V.M. Kotlyakov[2], O.V. Rototaeva[2], *and* G.A. Nosenko[2]

Introduction

The volcanic massif of Gora El'brus in the central Caucasus has 16 large glaciers and 9 smaller, peripheral ones (figs. 46, 47, 48). The largest glaciers are: *Lednik Bol'shoy Azau* (10.2 km long, 19.6 km^2 in area) on the southern slope and the vast *Dzhikiugankez Floe* on the northern slope formed by two glaciers, *Ledniki Birdzhalychiran* and *Chungurchatchiran*, that cover a total area of 27.8 km^2. At present, the total area of glaciers on Gora El'brus is 125.2 km^2 (Zolotarev and Khar'kovets, 2000).

Glacier observations began here in the middle of the 19th century. The first instrumental survey of glaciers was done by military topographers from 1887 to 1890; a map at a scale of 1:42,000 was compiled. During the International Geophysical Year, an expedition of the Department of Geography of Moscow University compiled a detailed map of the entire massif at a scale of 1:10,000; it was based on phototheodolite surveys and aerial photography. Repeated surveys were done in 1981, 1987, and 1997.

Glacier retreat has been a continuous general trend for the El'brus massif for more than 150 years, although the rate of retreat has not been constant (table 17). During the first century of observations (1850–1957), the average annual retreat of all glaciers, including area and length, was slightly greater during the first 37 years (1850–1887) than during the following 70 years. During the 70-year period (1887-1957), glaciers on the northern slope of El'brus retreated more than 600 m; those on the southern slope retreated more than 1,100 m, and glaciers in the western sector decreased in length by at least 300–400 m (Kravtsova and Loseva, 1968). Small advances of glacier termini were recorded during the period 1910 to 1914 and at the end of the 1920s.

During the subsequent 30-year period, 1957–1987, there was an increase in winter precipitation, and summer temperatures remained close to the norm; this caused the average annual retreat of El'brus glaciers to slow by 1.2 times. One exception, however, was the continued dramatic retreat of *Lednik Bol'shoy Azau* (see table 17). This was because a great mass of stagnant ice that was at the terminus of the glacier in 1959 melted and had completely disappeared by 1969. If one subtracts the melting of the stagnant ice, the retreat of the glacier terminus was only about 350 m. The tongues of *Dzhikiugankez Floe* exhibited the greatest rate of retreat during this time (see the measurements of the *Ledniki Birdzhalychiran* and *Chungurchatchiran* in table 17). In contrast to the general retreat of *Lednik Bol'shoy Azau* during this period, other glaciers, including Ledniki Kukurtli, *Bityuktyube*, Ullu-kam, Ulluchiran, and *Ullumalienderku*, were temporarily advancing.

During the following decade (1987 to 1997), aerial photography of Moscow State University (MSU) documented the advance of 8 glaciers out of the 16 (Zolotarev and Khar'kovets, 2000) and the other 8 showed much slower retreat. To determine the glacial fluctuation from 1997 to 2004, the locations of glacier termini on large-scale aerial photographs taken in 1987

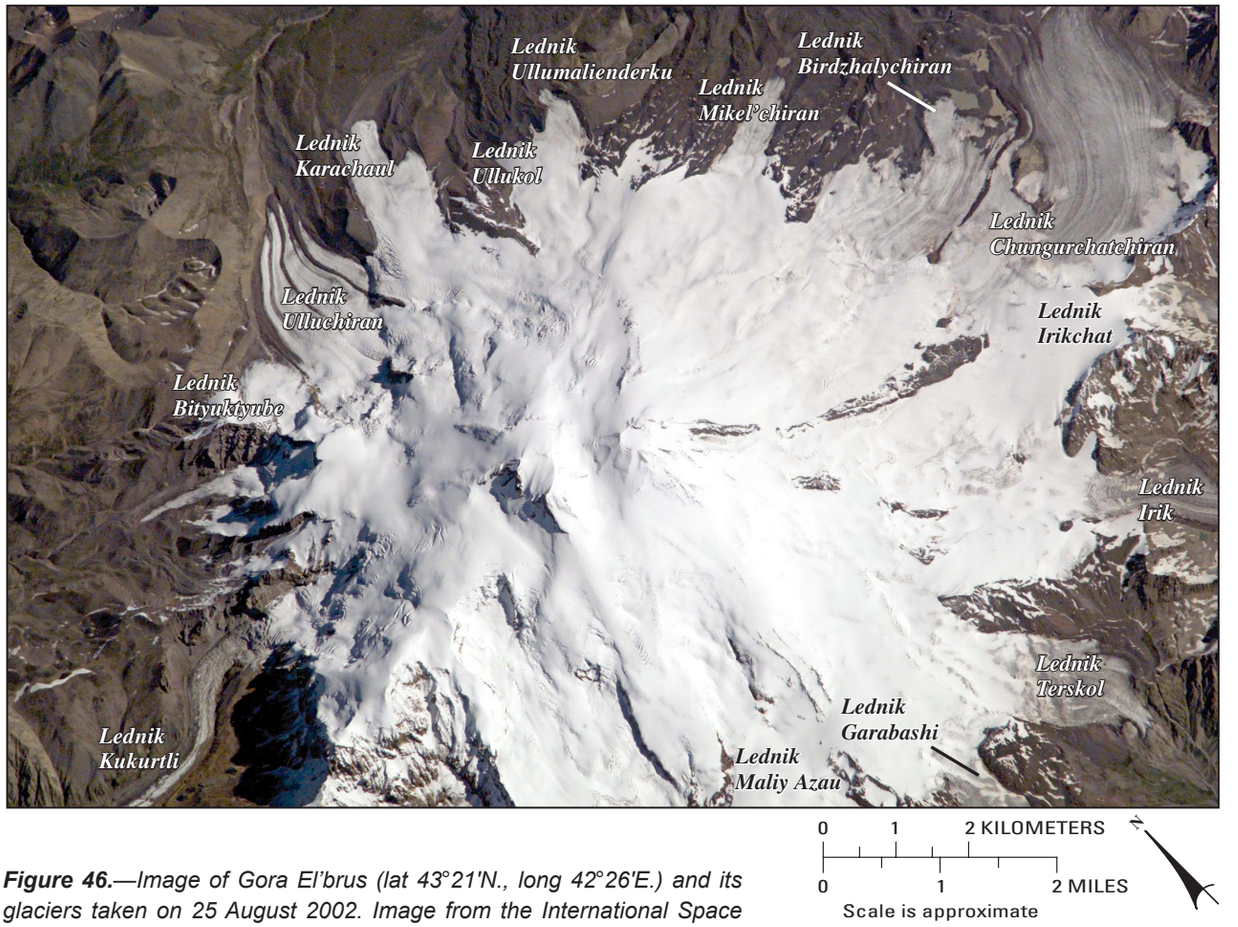


Figure 46.—*Image of Gora El'brus (lat 43°21'N., long 42°26'E.) and its glaciers taken on 25 August 2002. Image from the International Space Station. Mission ISS005, Roll E., Frame 11193.*

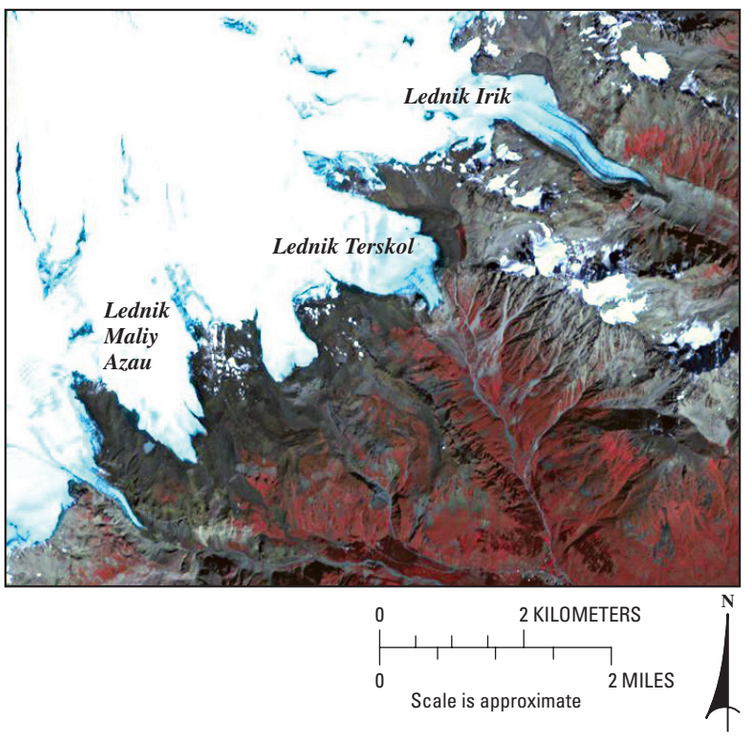


Figure 47.—*ASTER Image of the glaciers on the southern slope of Gora El'brus taken on 15 September 2001. Compare with Figures 46 and 48. ASTER image AST_LIB.003:2004260219.*

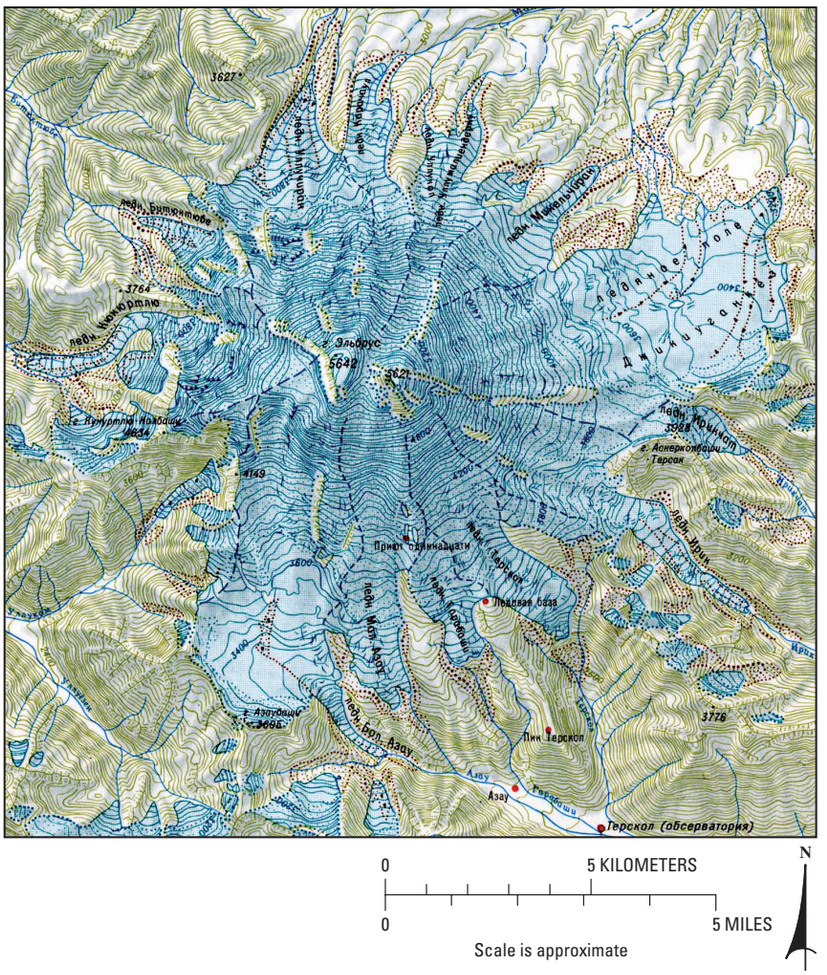


Figure 48.—*Map of the glaciers of Gora El'brus (lat 43°21'N., long 42°26'E.). From the World Atlas of Ice and Snow Resources (Kotlyakov, 1997).*

TABLE 17.—*Changes in the position of the termini of El'brus glaciers during different periods of observation*

[Unit: m a^{-1}, meters per year]

Name of glacier	1850–1887[1]	1887–1957[2]	1957–1987[2]	1987–1997[3]	1987–2001/04[4]
	37 years	70 years	30 years	10 years	15 years
Bol'shoy Azau	-550	-1,130	-1,150	-150	-300
Maliy Azau	-410	-637	-200	0	-70
Garabashi	-290	-1225	-70	0, -20	-50 right
Terskol	-430	-675	-60	0	-80 left
Irik	-270	-1,162	-355	-60	-75
Irikchat	-470	-750	-250	-170	-180, -200
Chungurchatchiran	-110	-925	-590	-200, +160	-165
Birdzhalychiran	-1,440	-850	-845	+90	-260
Mikel'chiran	-510	-525	-165	0	-130
Ullumalienderku	-460	-175	-120	+100	0
Ullukol	-380	-620	-205	-50	-50
Karachaul	-270	-275	-30	0, +3	-150
Ulluchiran	-240	-1,225	-220	+100	0
Bityuktyube	-80	-500	-20	+130	0
Kukurtli	-190	-275	+110	-90	-100
Ullu-Kam	-430	-320	+40	0	0
Average velocity of termini retreat (m a^{-1})	-11	-10.1	-8.6	-1.2	-6.5

[1]Kravtsova and Loseva (1968). [2]Zolotarev (1997). [3]Zolotarev and Khar'kovets (2000). [4]Nosenko and Rototaeva (this study).

were compared with those on space images from ASTER in 2001 and 2004, and with digital camera images from the International Space Station (ISS) in 2002. The ASTER images, having a picture element (pixel) resolution of 15 m in three spectral ranges (Band 1, 0.52–0.60 μm; Band 2, 0.63 –0.69 μm; and Band 3, 0.78–0.86 μm), were transformed to the WGS-84 projection. They are quite accurate for interpreting the boundaries of most large- and medium sized glaciers and for determining the conditions of the glacial surfaces based on differences in spectral reflectance in their accumulation and ablation areas. For more accurate identification of the position of the termini, very distinct perspective images from the ISS, with a pixel resolution of 5 m, as well as 2004 photographs taken from a helicopter supplied by the Moscow Institute of Electrical Engineering (MIEE), were used.

The difference between data obtained by MSU for the period 1987 to 1998 and our data for 1987 to 2001/2004 is very evident. From 1987 to 1997, conditions were very favorable for the existence of glaciers on Gora El'brus and in the whole Caucasus region. Lednik Garabashi had positive mass balances during 6 of the 10 years; and for 3 years there were slightly negative mass balances. The period from 1997 to 2001/2004 included the anomalous years of 1998 to 2001, in which rapid melting of glaciers occurred throughout the entire Caucasus and there was a great loss of ice on El'brus glaciers (Rototaeva and others, 2003). As a result, almost all of the El'brus glaciers retreated from 1987 to 2002, and the ones which had been advancing until 1997 had retreated approximately to their 1987 positions by 2002 (see table 17). Substantial melting occurred on *Dzhikiugankez Floe*. Part of the terminus of *Lednik Chungurchatchiran* lost an area of 100×60 m of ice, and the neighboring *Lednik Birdzhalychiran* changed its shape completely. The central part of the terminus preserved features of the former flow and retreated only slightly, but the right and the left parts of the tongue retreated 260–300 m. The marginal zone of the right side of the tongue melted most rapidly, and many lakes formed in the recessional moraines; some of the lakes were as long as 400 to 500 m (fig. 49).

Aerial photographs and space images have made it possible to identify surging glaciers and individual glacier surges on El'brus. Historically, many accounts exist of surge-like occurrences observed during field investigations. In 1849, G. Abikh discovered an intrusion of *Lednik Bol'shoy Azau* into a 100-years-old pine forest; broken pine trees and ice debris were piled together before a high glacier front. It was probably a glacier surge, a conclusion made more likely by later observations. In 1911, H. Burmester documented another surge of *Lednik Bol'shoy Azau*. The front of the tongue had a steep slope, there was strong fissuring of the lower icefall, and there was swelling of the glacier surface between 2,600 and 2,700 m. By 1920, the glacier had advanced by 50 m. In the 1970s, *Lednik Bol'shoy Azau* advanced again, this time by 120 m; the greatest rates of terminus advance were noted in 1975, 1977, and 1979 — up to 34 m a^{-1} (Panov, 1993). In addition, the height of the glacier surface increased by 8.5 m, and the tongue acquired the form of a drop (Martyshev, 1980). The interval between each of these three surges of *Lednik Bol'shoy Azau* was approximately 60 years.

Recently, *Lednik Bol'shoy Azau* has been continually retreating; however, one more surge has been noted. On aerial photographs taken in 1987, it can be seen that the glacier surface in the lower part of the icefall expanded, swelled, and acquired a convex form (fig. 50). A series of wide ogives shows that the ice is pushed through the narrowest gap in sections. A kinematic wave is traveling down the glacier, and a "new" tongue has started to advance on the surface of the tongue covered by a continuous mantle cover. Its frontal part is dissected by a dense network of oblique and arc-like fissures that illustrate the strong ice pressure.

In the following years, the advancing white tongue became more noticeable, and, during 1991, the "new" tongue advanced by 40 m; its surface in some places became higher by 10–12 m (Zolotarev, 1997). In addition, the new ice was separated from the old ice by a pressure ridge up to 5 m high. Similar ramparts on the tongue's surface had been noted during previous surges — in 1973, as well as 1956. Finally, on a 2002 image from the ISS, the white tongue extends even farther and has become narrower (see fig. 50).

This change in the longitudinal profile of the glacier is typical of surging ice; it is caused by the pulsation as well as the great decrease in the thickness and volume of the tongue in the first few years after advance begins — in this case, from 1987 until 1991. Later, the glacier became 4–5 times slower and a great volume of stagnant ice formed on the rapidly melting tongue (Seinova and Zolotarev, 2001).



***Figure 49.**—Part of the 25 August 2002 International Space Station image (fig. 46) enlarged to show the lake-moraine complex near the terminus of the retreating* Lednik Birdzhalytchiran, *Gora El'brus (in the center).* Lednick Chungurchatchiran *is to the right.*

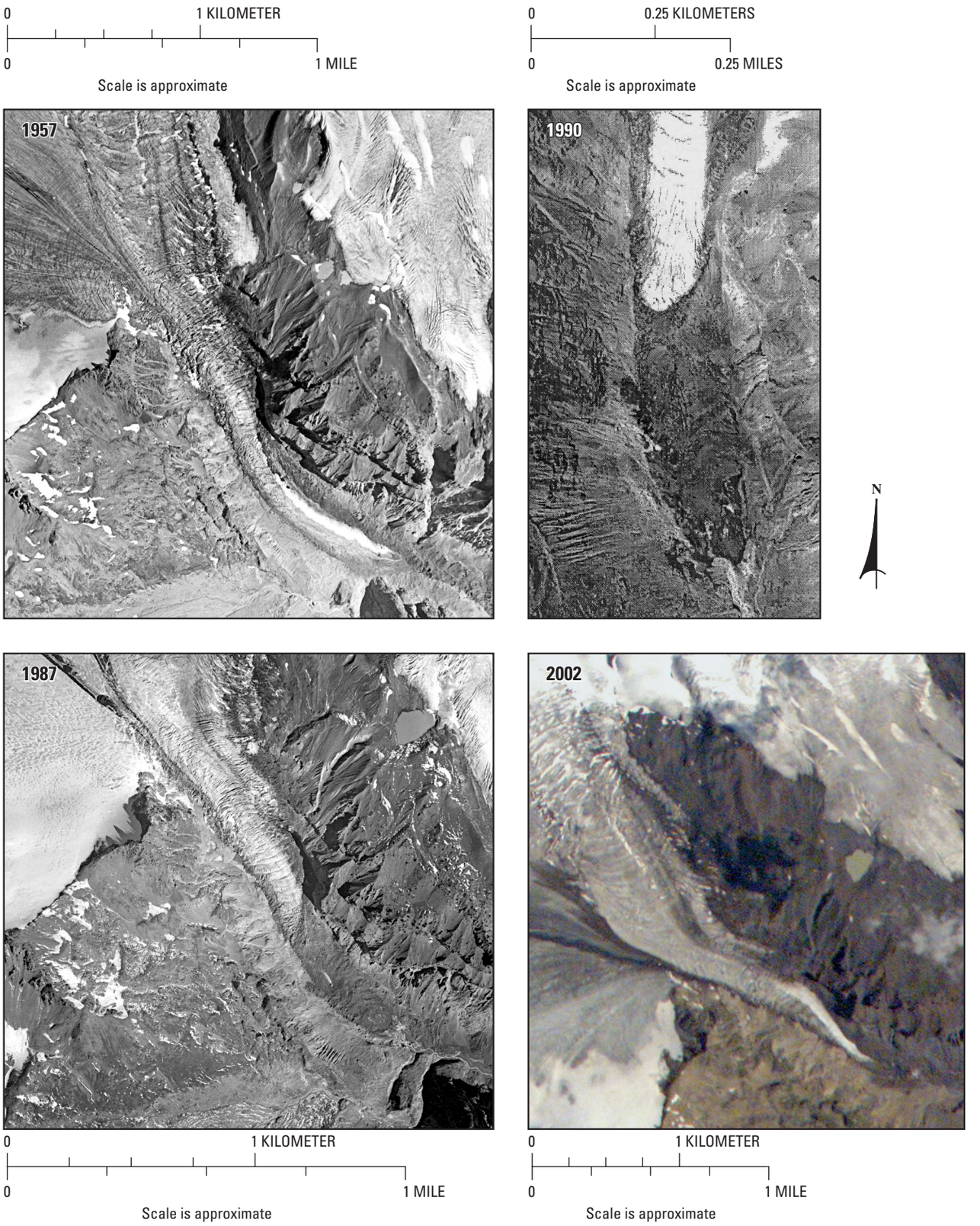


Figure 50.—*Aerial and space photographs of* Lednik Bol'shoy Azau, *Gora El'brus, showing changes in the terminus shape and position. 1957 and 1987 scenes are aerial photographs, the 1990 image was photographed from a helicopter on 20 August, and the 2002 image was taken from the International Space Station. See figure 48 for location.*

Obviously, such surges of ice occur on the glacier regularly and are caused by ice being constricted in the rock gap of *Bol'shoy Azau*. Huge amounts of ice from two glacier flow directions enter the narrowest part of the gap at an elevation of 3,200 m, and the release of stress results in pulsations.

Other glaciers of the El'brus complex are also notable for unstable dynamics. A 1987 survey noted a kinematic wave at the very end of *Lednik Ullumalienderku*; the terminus showed considerable cracking (fig. 51). The height of its front had increased by 40 m in comparison to its height in 1957, although during this period the glacier terminus retreated by 150 m. At the beginning of the 1970s, Lednik Terskol was advancing (Martyshev, 1983). In 1980, a surge of the right side of Lednik Ulluchiran took place. Its surface rose by 20–25 m and was dissected by fissures, and its terminus had a steep front that had advanced by 150–200 m. Its shape became like a "paw," a characteristic of other surge-type glaciers (Voloditcheva and others, 1983; Voitkovsky and others, 1989).

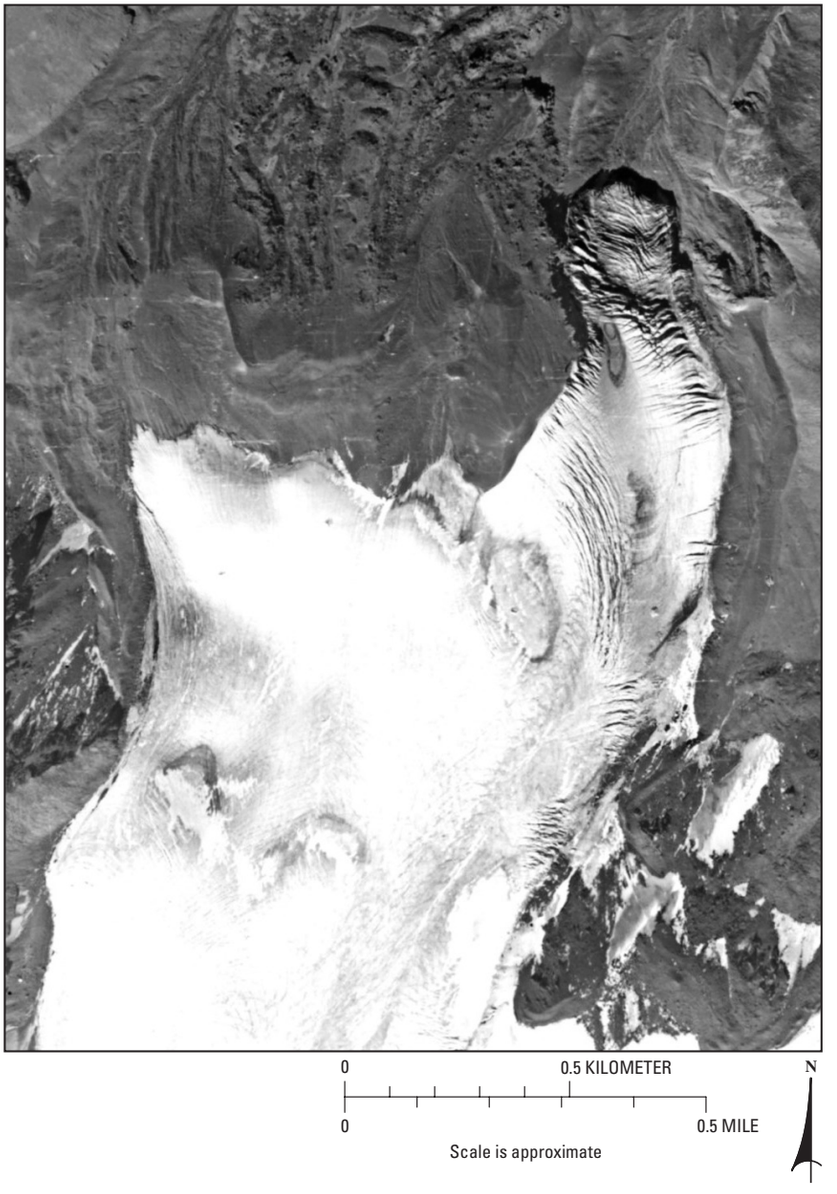


***Figure 51.**—Aerial photograph (1987) of the terminus of* Lednik Ullumalienderku, *Gora El'brus, during a surge event. See figure 46 for location.*

Pulsations are also characteristic of the Kukurtli glacier complex on the western slope of El'brus (fig. 52). *Lednik Maliy Kukurtli* (part of glacier No. 316) experienced a large surge in the 1960s. In 1981, a sheer high front of a small revived glacier (No. 317), dissected by large fissures, advanced and overhung the left moraine of the Kukurtli tongue, and, in the following 1 to 2 years, it reached the edge of the main glacier. In 2002, glacier No. 317 was completely backed by moraine and showed no signs of activity at all.

A surge of the main Lednik Kukurtli (no. 318) took place at the beginning of the 1980s. By 1983, the glacier had advanced 60 to 100 m. The surface near its terminus rose by 30–40 m; along a distance of 1.5 km, the ice volume increased by 7.2×10^6 m^3. Farther up the glacier, 2 km from the end of the tongue, the surface lowered by 5 to 10 m (Vinnikov and Labutina, 1987). Space images acquired from 2002 to 2004 show that the glacier terminus has retreated approximately 100 m since 1987, but this retreat cannot be accurately measured because the entire glacier terminus was buried under the moraine (see fig. 52).

The shape of Lednik Kukurtli favors its periodic pulsations. Its vast firn fields are positioned so that orographic uplift of moisture-laden air masses bring frequent periods of precipitation; as a result, great amounts of snow accumulate. The glacier tongue is separated from the firn area by a lava escarpment and a 500-m icefall. The large amounts of firn and ice that accumulate on the steep stepped slopes are periodically pushed through the icefall towards the long tongue.

Measurements made on space images of the El'brus glaciers and of 65 other glaciers of the Central Caucasus showed considerable retreat of almost all large glaciers from 1987 to 2001/2004 (fig. 53, table 18). The tongues of the following glaciers retreated the most: Karaugom (almost 600 m) (fig. 54); Shaurtu, *Rtsyvashki*, and Midagrabin (about 300 m); *Skhelda* and Bashil' (more than 200 m); and Tseya and Skazka (160 m). In addition, *Lednik Ailama* — the former tributary of *Lednik Dykh-Su* — became detached and isolated; it was separated from the tongue of the main glacier by large amounts of stagnant ice (figs. 53, 55).

Fluctuations of even adjacent glaciers are not always synchronous, however, and sometimes can have an opposite sign. It depends on characteristics of morphology, exposure, type of nourishment of a glacier, its internal dynamics, and so forth. Thus, for example, the largest glacier of the Caucasus — Bezengi — continues to retreat, whereas the adjacent *Lednik Mizhirgichiran* continues to advance, bulldozing a push moraine before it (figs. 53, 56).

Glaciological Disaster in North Osetiya

On 20 September 2002, a disaster took place in the Genaldon river valley of North Osetiya, north of Gora Kazbek (lat 42°42′N., long 44°31′E.). Huge masses of ice, water, and debris burst from the head of the valley, rushed swiftly 16 km down the valley, sweeping everything before it, shearing off forest, and scraping off unconsolidated deposits on slopes up to a height of 100 m. The ice and water-saturated debris avalanche (jökulhlaup) was stopped by a transverse ridge of Skalistyy Khrebet just before the river entered a narrow gap. The entire bottom of Karmadon basin was under glacial debris about 4 km long, 60 m thick on the average, and in some places up to 130 m (fig. 57, 58*A*, 58*B*). Downstream in the gap, a water-saturated mudflow, including ice debris, caused further destruction along 17 more kilometers. Several recreation sites were destroyed, a tunnel on a highway was blocked, and the *Nizhni Karmadon* settlement was completely demolished. More than 100 people died.

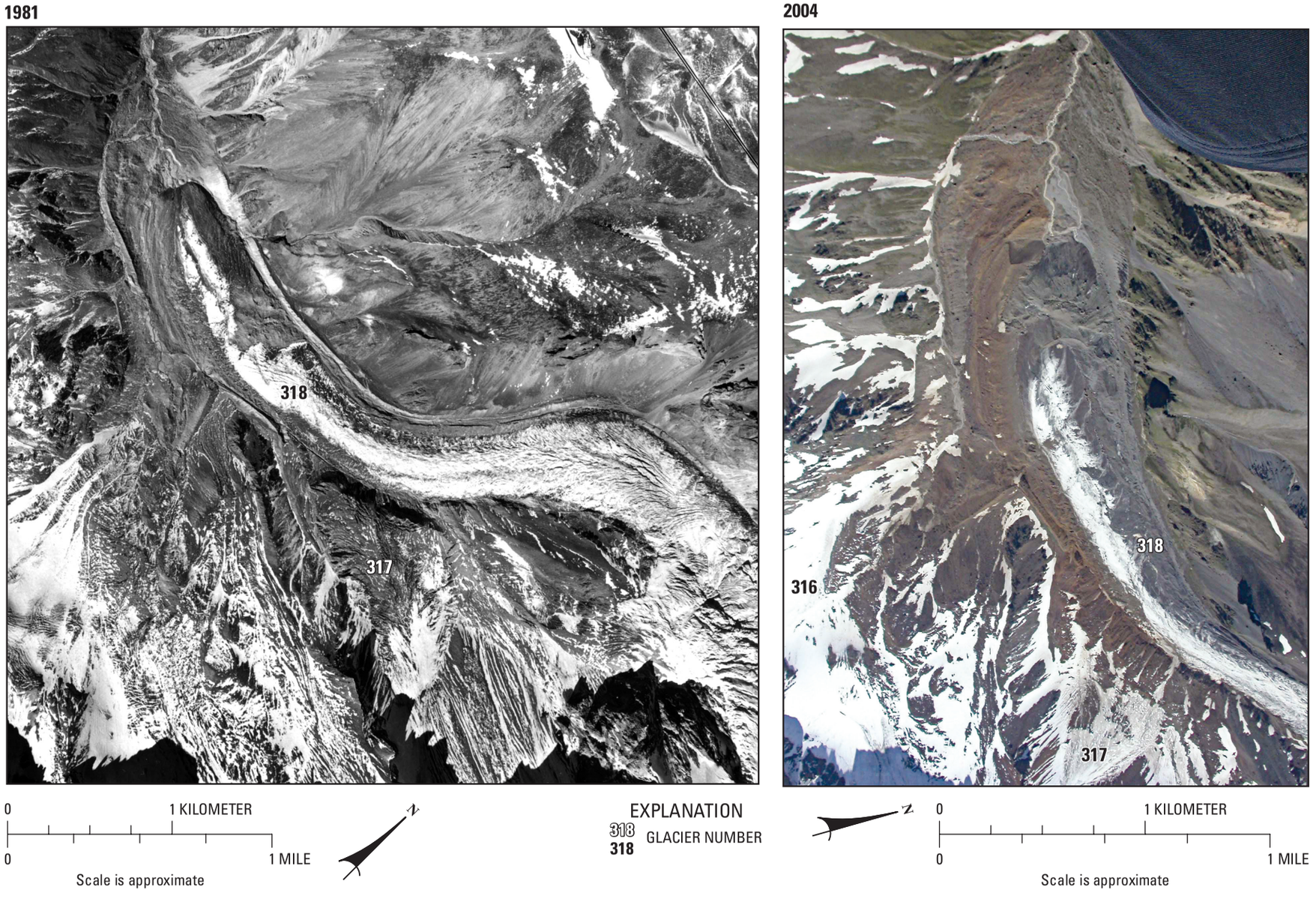


***Figure 52.**—Photographs (1981 and 2004) of the Lednik Kukurtli, Gora El'brus. The 1981 image is an aerial photograph; the July 2004 photograph was taken from a helicopter by I.V. Galushkin, Info Terra. Numbers refer to discussion in the text on p. F66. See figure 46 for location.*

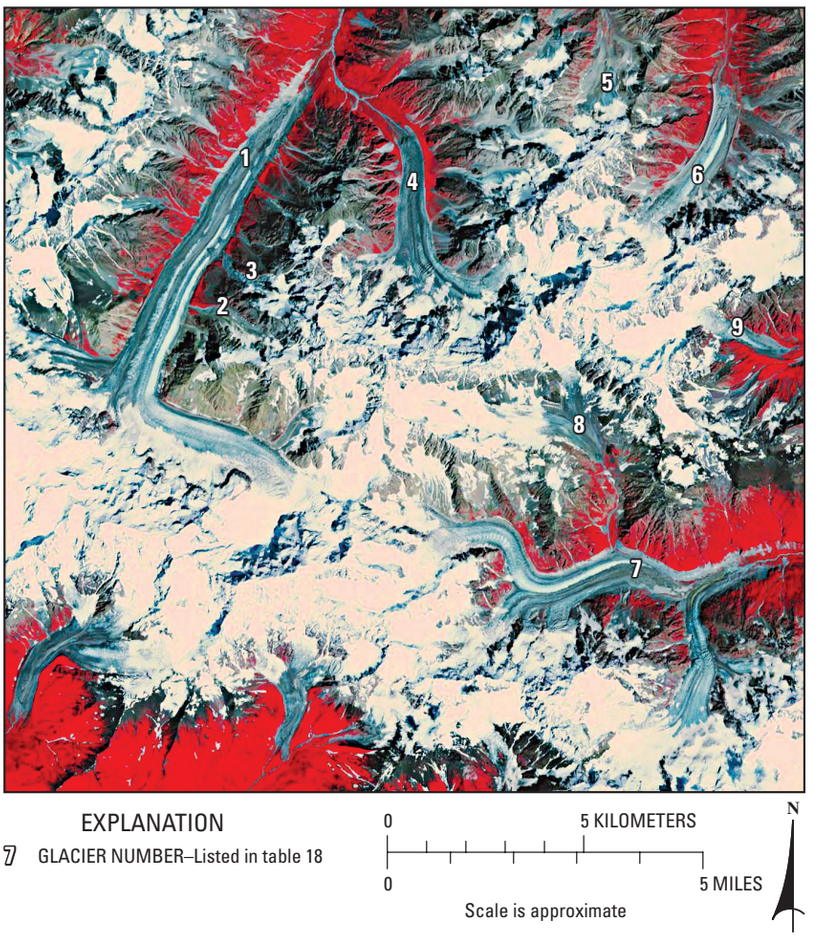


Figure 53.—*ASTER image taken on 15 September 2001, showing glaciers of the central Caucasus (approximate lat 43°N., long 43°E.). Numbers correlate with glaciers listed in table 18. ASTER image AST_LIB.003: 2004260219.*

TABLE 18.—*Changes in the position of glacier termini from 1987 to 2001/04 in the Tcherek River basin*

[Abbreviations: km, kilometer; masl, meters above sea level; m, meter]

	Name of glacier	Morphological type (of glacier)	Exposure	Length (km)	Area (km^2)	Height of terminus (masl)	The highest point (masl)	Change of length (m)
1	Bezengi	Compound-valley	NE	17.6	36.2	2,080	5,050	-190
2	*Misses*	Hanging corrie	NW	1.9	1.1	2,980	4,070	0
3	No. 32	Corrie-valley	NW	3.1	1.4	2,720	4,650	-90
4	*Mizhirgitchiran*	Compound-valley	N	8.8	9.9	2,380	4,670	150
5	Ukyu	Corrie-valley	NE	2.4	1.6	3,260	3,740	-80
6	*Ulluazna*	Compound-valley	NE	7.0	6.0	2,600	4,760	0
7	*Dykh-su*	Compound-valley	E, NE	13.3	34	2,070	5,150	-200
8	*Khrumkol*	Valley	SE	5.6	7.2	3,060	5,150	0
9	Tyutyun	Valley	SE	5.0	2.8	2,540	3,850	-180



***Figure 54.**—Image taken from the International Space Station in 2002, showing the retreating Lednik Karaugom (lat 42°48'N., long 43°44'E.). Note that cirques of tributary glaciers are becoming partially ice free.*



***Figure 55.**—Aerial photograph taken in July 2004 of the terminus of* Lednik Ailama *(top right) and the stagnant terminus of* Lednik Dykh-su *(approximate lat 43°N., long 43°E.) covered with debris. This area is also shown on figure 53.* Lednik Dykh-su *is number 7. Photograph was taken from a helicopter by I.V. Galushkin, Info Terra.*



***Figure 56.**—Photograph taken in August 2003 of the advancing front of* Lednik Mizhirgitchiran *(approximate lat 43°N., long 43°E.) taken by Yu.G. Iljitchev. See glacier number 4 on figure 53.*

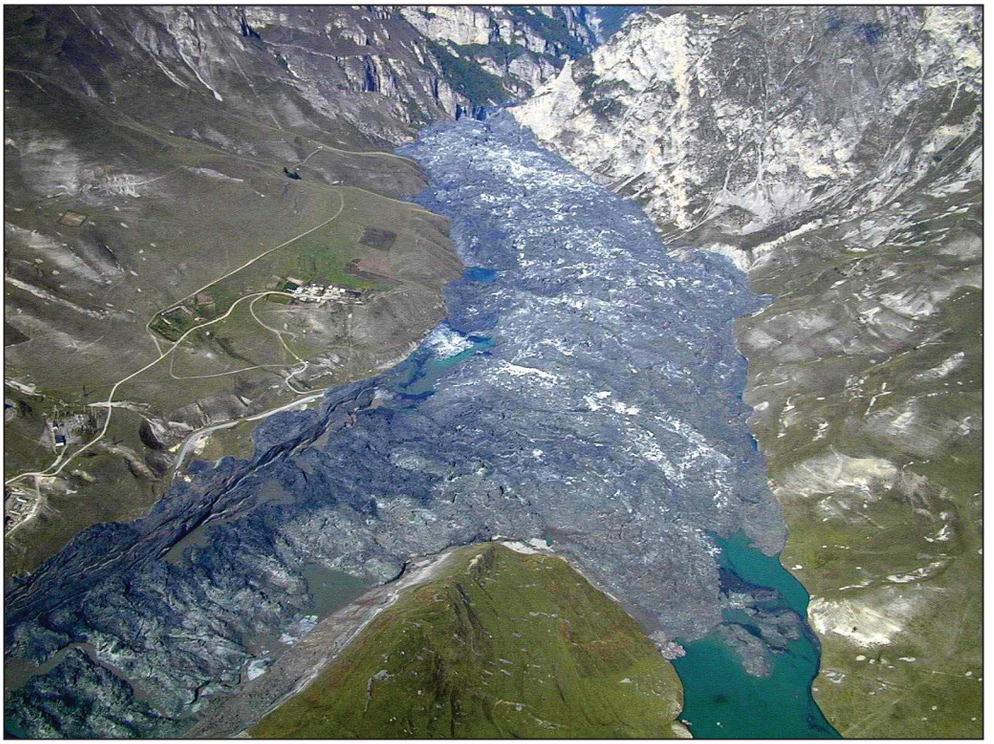


***Figure 57.**—Oblique aerial photograph of avalanche debris in the Karmadon basin caused by the 20 September 2002 catastrophic collapse of the* Lednik Kolka*. The view is looking north toward the narrow gorge in Skalistyy Khrebet that halted the avalanche. Photograph from the Geological Survey of North Osetiya.*

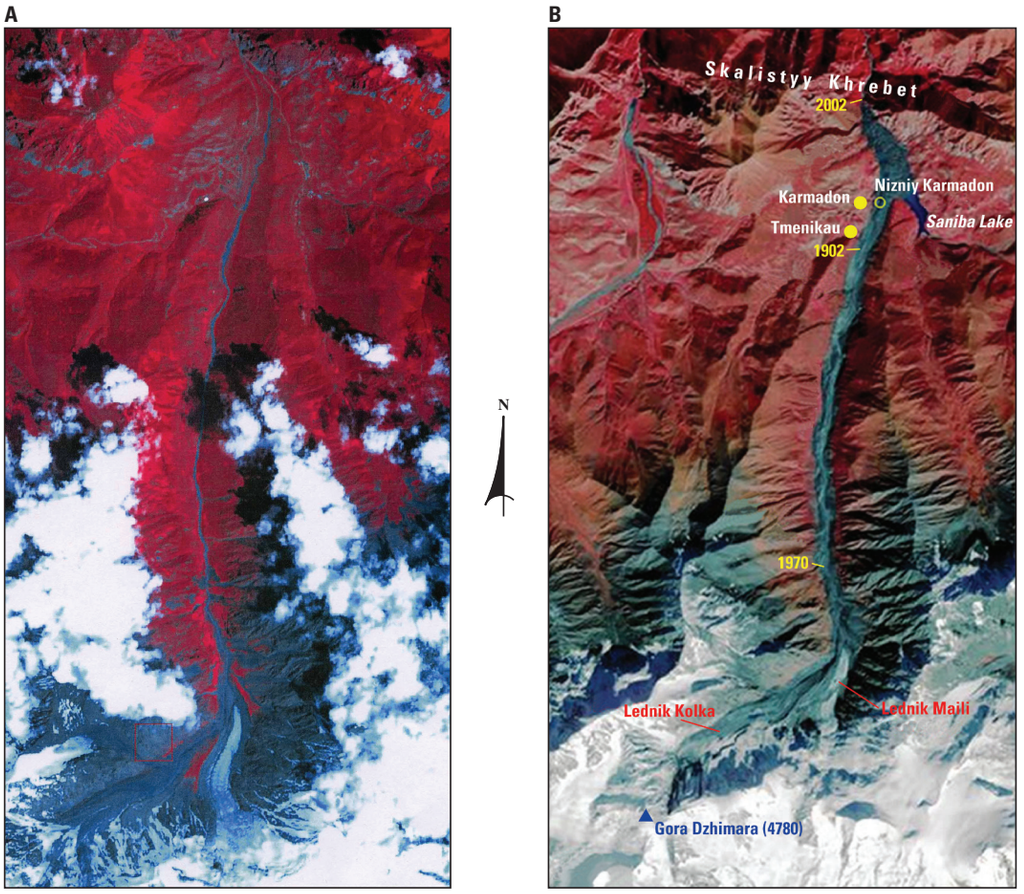


Figure 58.—*Two ASTER images of the Genaldon river valley, scene of the* Lednik Kolka *disaster. The distance from Gora Dzhimara to Skalistyy Khrebet is about 18 km.* **A**, *Section of the 22 July 2001 image taken before the disaster. ASTER image AST_LIB. 003: 2003583778.* **B**, *Annotated 27 September 2002 image taken after the 2002 disaster, showing locations of the* Lednik Kolka *terminus after earlier surges. ASTER image AST_LIA. 003:2008557907.*

In a tributary valley near the *Saniba* settlement, the glacier avalanche debris dammed the valley, forming a lake; its level continued to increase during the month after the glacial outburst flood (jökulhlaup) (fig. 59).

Lednik Kolka, a surge-type glacier noted for its historical record of repeated surges, had caused the disaster. Previous surges took place in 1835, 1902, and 1969 at intervals of about 70 years. The surge of 1902 ended in a similar glacial outburst flood that traveled 9 km, but it was not as destructive. In 1969/1970, a surge occurred that followed the "typical" scenario, the tongue advanced 4 km during a three month period without disastrous aftereffects. The glacier was studied in detail for many years by expeditions of the Institute of Geography, Russian Academy of Science (IGRAS) (Rototaev and others, 1983).

In contrast with earlier surges, only 32 years passed between the 1970 surge and the 2002 disaster. Interestingly, the glacier left its cirque completely, so that its bed became completely empty. In the empty glacial cirque (fig. 60) there was a cloud of vapor and gas with a strong smell of hydrogen sulphide for many days. An icy scarp was detected on the right margin of the glacier cirque — a steep rocky slope with hanging glaciers. In addition, a large part of the firn-ice fields under the ridge crest had disappeared. It was first thought that a great fall of ice, which struck the glacier and made it collapse, was the



Figure 59.—*Oblique aerial photograph taken on 21 September 2002, looking southwest at the avalanche debris saturated with water. The debris flowed into a tributary valley near the settlement of Saniba and a dammed lake is beginning to form. Photograph from the Geological Survey of North Osetiya.*

cause of the disaster. However, evidence and photographs of mountaineer witnesses showed that the unusually active destruction of ice and rock on the slope had already begun in summer, and by the beginning of September, this ice scarp had already been completely formed.

To investigate the causes, mechanism, and possible aftereffects of the September 2002 destructive process, many data sources were used, including multispectral Advanced Spaceborne Thermal Emission Radiometer (ASTER) images from the Terra spacecraft, images taken with a digital camera on the International Space Station (ISS), and observations from aerial and surface investigations of the glacier region, made by an expedition of IGRAS in the summer of 2003 (Kotlyakov, Kerimov, and others, 2004; Nosenko and others, 2004).

Structural features of a surge-type glacier preparing for a surge can be identified from space. These features include an increase in glacier thickness, a change in the glacier's surface structure, the appearance of new characteristic fissure fields, and changes in the position of the glacier terminus. *Lednik Kolka* is 3 km long and completely covered by moraine, so it was thought that the picture element (pixel) resolution of available ASTER images (15 m) taken a year before the disaster would not be sufficient to identify these pre-surge features (see fig. 58a). However, even on an ISS image with 5-m pixel resolution taken a month before the surge (13 August 2002), they are definitely absent (fig. 61). That means that the glacier had not yet accumulated critical mass and had not reached the threshold of a surge by the "classical" method.

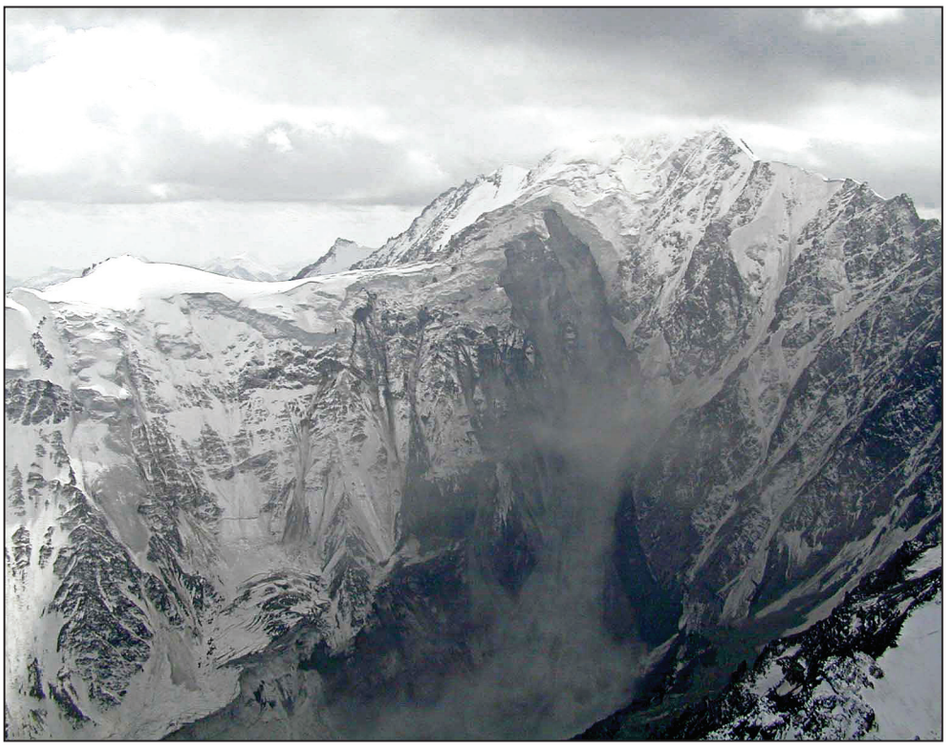


***Figure 60.**—Oblique aerial photograph taken on 24 September 2002, looking south at the mountain crest in the source region of* Lednik Kolka*. Rock outcrops are visible where the former snow and ice cover has slid onto the glacier below. Meltwater and fumeroles are present. Photograph from the Geological Survey of North Osetiya.*

Lednik Kolka is situated in a region where earthquakes occur often. It is in a fault zone of large fractures where movement of separate blocks is possible. Summer earthquakes which preceded the disaster were especially strong on 14 July and 22 August, and probably triggered the beginning of unusual ice, snow, and rock falls in the head wall of the glacier cirque. Both sporting groups and an ASTER image of 18 July 2002 confirmed that it was possible to see black patches of rock on snow-covered slopes where snowfall had occurred. The earthquakes caused not only the increase of falls, but probably the destruction of the internal structure of the glacier and its connection with the bed as well. Over time, these falls increased the mass of the glacier, considerably overloading its upper part, and increasing stress to the maximum throughout the whole body of ice.

From the very beginning, it was obvious that such a swift and extensive outburst of the glacier could occur only as the result of accumulation of a very great amount of water under the glacier, which "catastrophically separated" the glacier from its bed (Anonymous, 2002; Kotlyakov, Rototaeva, and others, 2004). Space images showed that there was a strong outburst of water, ice, and debris from the right margin of *Lednik Kolka* which moved over the moraine of Lednik Maili and down the right slope of the valley. This was confirmed by photography from a helicopter and surface observations. The surface structure of Lednik Maili itself did not change very much, but there are some well-defined traces of flooding on the upper edge of the flow, which had passed over ice (fig. 62). Talus on the slope under the tongue of Lednik Maili was not significantly disturbed.

Water accumulation in the glacier basin had increased in volume during preceding years not only due to anomalous melting (Lebedeva and Rototaeva, 2005), but probably by volcanic activity as well. Evidence of volcanic activity included gas emission, actively collapsing slope, and the appearance of fumaroles on the cirque wall (see fig. 60). The volcanic activity created special thermal conditions under the glacier that caused additional melting and accumulation of water. Analysis of the chemical composition of snow, ice, and water in the *Kolka* cirque proved that the hydrothermal factor played a role in the disaster. In Genaldon, the presence of a near-surface magma chamber was shown by two independent geophysical methods; its appearance in 2002 was also proven by analysis of thermal infrared space imagery from NOAA satellites (Gurbanov and others, 2004; Kornienko and others, 2004).

The large amount of water formed many lakes after the disaster. They even appeared in the floor of the cirque after the glacier surge (figs. 63, 64). The size of the main lake, identified on an ASTER image of 6 October 2002, was 300×80 m (Popovnin and others, 2003). Our surface observations in

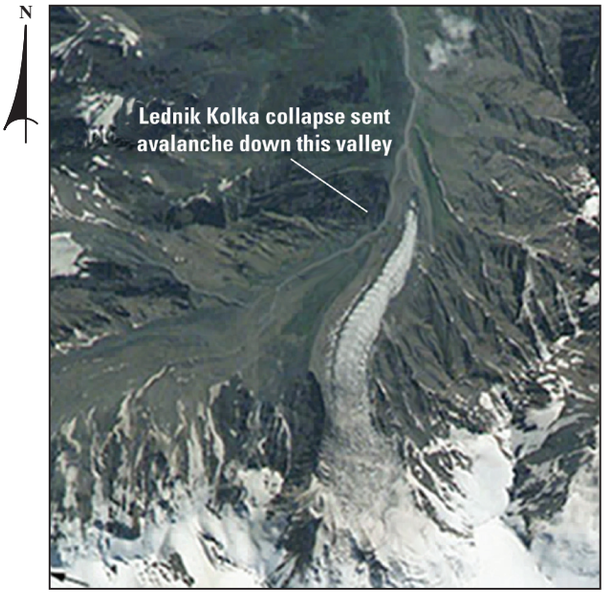


Figure 61.—*International Space Station image taken on 13 August 2002 of Lednik Maili (white tongue in center) and* Lednik Kolka *(dark, debris-covered tongue on left). Although it is a month before the disaster, there is no visible evidence of the coming event. Mission ISS005, Roll E, Frame 9691.*



Figure 62.—*Oblique aerial photograph taken September 2002, looking south at the empty cirque of* Lednik Kolka *(on right) after the disaster. Lednik Maili is on the left. Gora Dzhimara (4,780 m) is in the background on the right. Photograph from the Geological Survey of North Osetiya.*

2003 showed that the margins of the lake were composed of unconsolidated material; in June 2003, its size decreased to 150×50 m (fig. 65), and by the end of September 2003, the lake had disappeared completely.

The debris in Karmadon basin, deposited by the debris avalanche, was completely saturated with water, and chains of lakes appeared immediately along its margins (see fig. 59). The largest one — the dammed *Sanibanskoe Lake* — can be seen well on all space images. It began to fill immediately after the disaster, and in a month, more than 3 million cubic meters of water had accumulated in the lake, with a maximum depth of 40 m (Chernomorets, 2005). The avalanche debris gradually melted and was eroded by the river (fig. 66). The lake slowly drained, but at the beginning of September 2003, the appearance of the lake had changed very little. By late September 2003, however, only a small part of the lake remained.

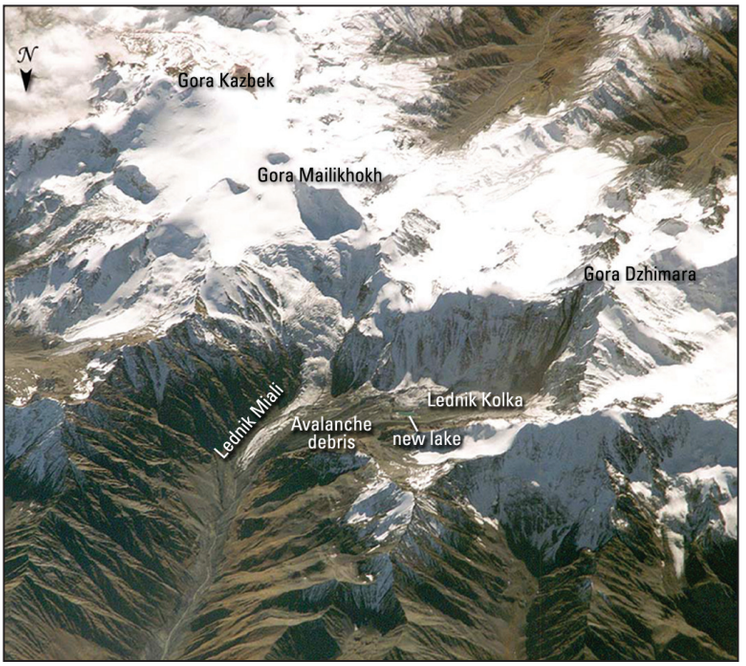


Figure 63.—*International Space Station image taken on 19 October 2002, looking south at Gora Kasbek volcanic massif and the cirques of Ledniki Maili and* Kolka. *Lakes are forming in the empty bed of* Lednik Kolka *and rock outcrops are visible on the valley wall. Mission ISS005, Roll E., Frame 17830.*

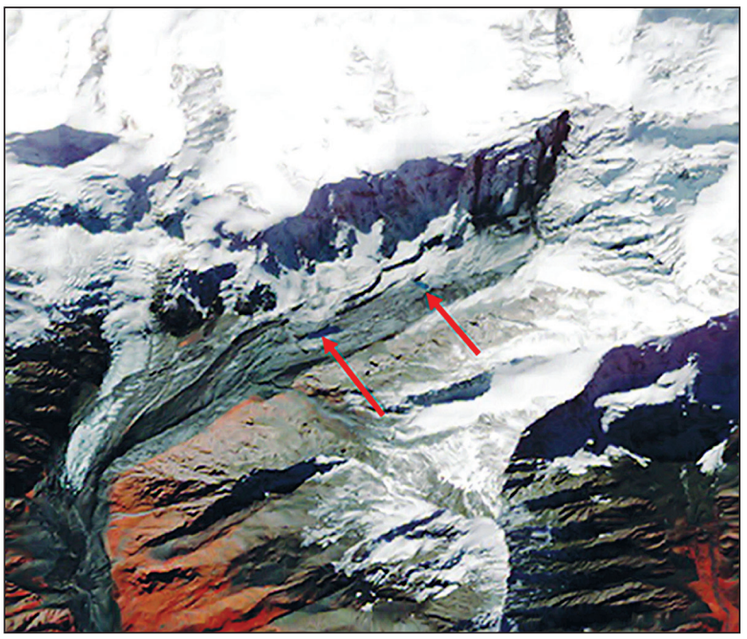


Figure 64.—*Enlarged and rotated section of 27 September 2002 ASTER image (fig. 58*B*). Arrows show the lakes in the empty bed of* Lednik Kolka. *It is also possible to see the traces of the mudflow on the surface of Lednik Maili. Compare with figure 63.*

In conclusion, the combined analysis of space, aerial, and surface photography made it possible to determine the causes and probable scenario of the September 2002 disaster (Rototaeva and others, 2005). The surge of *Lednik Kolka* was brought about prematurely and was much larger than previous surges because of a combination of factors. These were the unstable dynamic state of the surging glacier, significant accumulation of englacial and subglacial water, collapses of ice and rock which created an overload in the upper part of the glacier, and the growing activity of endogenous processes in the region of Gora Kazbek.



Figure 65.— *(at left) Terrestrial photograph taken on 28 June 2003 of one of the lakes in the* Kolka *bed dammed by a combination of ice and debris. Photograph by O.V. Rototaeva.*



Figure 66.— *(below) Oblique aerial photograph taken on September 2003, looking southeast at the collapsing avalanche debris in Karmadon basin and the dammed lake near Saniba settlement one year after the disaster. Compare with figure 59. Photograph by G.A. Nosenko.*

Investigations of the Fluctuations of Surge-Type Glaciers in the Pamirs based on Observations from Space

By V.M. Kotlyakov,[2] G.B. Osipova,[2] *and* D.G. Tsvetkov[2]

Introduction

Recently, investigations on glacier fluctuations in the Pamirs were carried out at the Institute of Geography of the Russian Academy of Sciences (IGRAS). A variety of space imagery was analyzed, including: (1) photographs from 1972 to 1991 (up to 13 repeated surveys) at a scale of 1:200,000–1:270,000 taken with the KFA-1000 camera from Russian Resurs-F1 satellites at a resolution of about 5 m, (2) Advanced Spaceborne Thermal Emission Radiometer (ASTER) images acquired from 2001 to 2004 from the Terra satellite, with a pixel resolution of 15 m, and (3) images taken from 2001 to 2004 by astronauts with a hand-operated digital camera from the International Space Station (ISS). Using this imagery, as well as historical data (aerial photographic surveys, topographic maps, surface observations, etc.), the following work was accomplished: (1) compilation of an inventory of surging glaciers of the Pamirs; (2) monitoring of the dynamics of large compound glaciers; (3) estimation of the present-day status of two surge-type glaciers, Ledniki Medvezhiy and Geograficheskogo Obshchestva; and (4) investigation of fluctuations of "normal" non-surging glaciers in the Eastern Pamirs. This paper summarizes the main results of these investigations.

Compilation of an Inventory of Surging Glaciers of the Pamirs

In 1997, compilation of the Inventory of Surging Glaciers of the Pamirs was finished (Osipova and others, 1998). It was the first complete catalogue of unstable glaciers of a large mountain region. The Inventory was based on stereoscopic interpretation of space photographs of 1972 to 1991. To identify surge-type glaciers and assign them to a group, a set of criteria was developed, including both direct (rapid changes of the form and structure of the glacier surface) and indirect criteria. Regular movement of surge-type glaciers and their interactions with the surrounding environment were considered. All glaciers that showed dynamic instability were subdivided into three groups. Glaciers with one or more observed surges were assigned to the first group. The second group consisted of glaciers with indications of periodic activity which could be rather confidently classified as "surging," Glaciers with some indication of recent unstable dynamics were assigned to the third group.

The analysis identified 630 glaciers in the Pamirs that showed indications of instability at the beginning of the 1990s (table 19). Results indicated that between 1960 and the middle of the 1990s, 17 large-scale surges occurred in the Pamirs. By comparing 1991 space photographs with a 2003 ASTER image, the surges of three more glaciers were detected after the Inventory of Surging Glaciers had been compiled (table 20).

TABLE 19.—*The number of surge-type glaciers in the large river basins of the Pamirs*

River basin	Group 1	Group 2	Group 3
Surkhob	1	2	—
Kyzylsu	5	23	21
Muksu	30	60	47
Obikhingob	5	26	22
Vanj	4	17	19
Yazgulem	2	20	22
Bartang	1	38	60
Murghob	—	4	54
Gunt	—	7	57
Panj (headwaters and eastern [right] confluents)	—	2	44
Qarokŭl	1	6	14
Markansu	1	7	4
Eastern Kyzylsu	1	3	—
Total	51	215	364

TABLE 20.—*The largest observed surges of the glaciers of the Pamirs from 1960 to 2003*

[Unit: km, kilometer]

No.	Glacier name	River basin	Latitude and longitude of center of the tongue		Area (km^2)	Length (km)	Years of the surges or intervals when recorded	Movement of tongue (km)
1	Gando- *Dorofeeva*	Obikhingob	38°54′N.	71°45′E.	22.0	44.6	1985–1991	[1](8.5)
2	*Vanchdara*	Obikhingob	38°45′N.	71°57′E.	11.5	9.5	1977–1980	2.5
3	No. 88 (*Vaizirek*, west)	Obikhingob	38°58′N.	71°18′E.	4.5	7.6	1975–1980	2.2
4	*Petra Pervogo*	Obikhingob	39°00′N.	71°25′E.	12.2	10.5	1976–1980	[1](?)
5	*Burs*	Obikhingob	38°42′N.	71°48′E.	6.9	5.3	1991–2003	3.6
6	*Sytargi*	Muksu	38°41′N.	71°46′E.	5.8	5.1	1991–2003	1.0
7	*Byrs*	Muksu	39°03′N.	71°45′E.	9.9	11.8	1981–1983	1.3
8	*Shini-Bini*	Muksu	38°59′N.	71°50′E.	16.4	10.3	1959–1961 about 1991	1.5
9	*Sugran*	Muksu	38°56′N.	71°44′E.	47.1	22.0	1976–1980	[1](5.0)
10	*Oshanina* (*Muzgazy*)	Muksu	39°03′N.	71°30′E.	15.6	10.7	1961 (1962) 1983–1984	7.5
11	*Valy*	Muksu	39°18′N.	72°45′E.	11.9	7.6	1975–1977	1.3
12	*Dzerzhinskogo*	Muksu	39°17′N.	72°49′E.	19.0	14.9	1972–1976	1.2
13	*Maliy Saukdara*	Muksu	39°16′N.	72°51′E.	23.5	14.3	1972–1975	2.8
14	*Shapak*	Muksu	39°02′N.	71°50′E.	13.7	8.0	1991–2003	1.0
15	*Bivachniy*	Muksu	38°56′N.	72°10′E.	61.2	29.6	1975–1978	[1](6.0)
16	Medvezhiy	Vanj	38°40′N.	72°12′E.	25.3	15.8	1963 1973 1988–1989	1.8 1.9 1.1
17	*Ravak*	Vanj	38°38′N.	72°04′E.	1.9	4.1	1967	0.2+ collapse
18	*Didal'*	Surkhob	38°59′N.	70°43′E.	1.5	4.9	1974	2.2+ collapse
19	Lenina (Eastern part)	Kyzylsu	38°25′N.	72°56′E.	12.4	9.6	1969–1970	1.1
20	*Oktyabr'skiy*	Qarokŭl (lake)	39°15′N.	73°00′E.	88.2	12.7	1985–1990	3.3

[1]Internal surges.

Surge-type glaciers are situated mainly in high mountain groups of the Central Pamirs near the junction of Akademii Nauk Khrebet (range) with Khrebet Petra Pervogo, *Darvozskiy Khrebet* (Qatorkŭhi Darvoz) and *Vanjskiy Khrebet* (Qatorkŭhi Vanj) (fig. 67), and in the central part of *Zaalayskiy Khrebet* (Qatorkŭhi Pasi Oloy in Tajikistan, Chong Alay Kyrka Toosu in Kyrgyzstan) (fig. 68). Surges on some of the glaciers are internal and occur only within the glacier itself; they do not cause the stagnant morphological tongue to advance. These so-called "internal" surges occurred on Ledniki Gando, Garmo, Bivachniy, *Petra Pervogo*, and other glaciers. However, in the Pamirs there are many surge-type glaciers whose tongues advance along ice-free valleys with velocities of up to 100 m d^{-1} during surge events; examples are the Ledniki Medvezhiy, *Byrs*, *Muzgazy*, *Vanchdara,* and other glaciers. Surges of the Lednik Medvezhiy in 1963 and 1973 caused disastrous aftereffects connected with outburst floods (jökulhlaups) from the lake dammed by the glacier. Also, surges of glaciers whose tongues break off and form a water-ice-debris surge can travel down valley with a high velocity and cause catastrophic damage. Such surges have occurred on the *Ledniki Ravak* and *Didal'*.

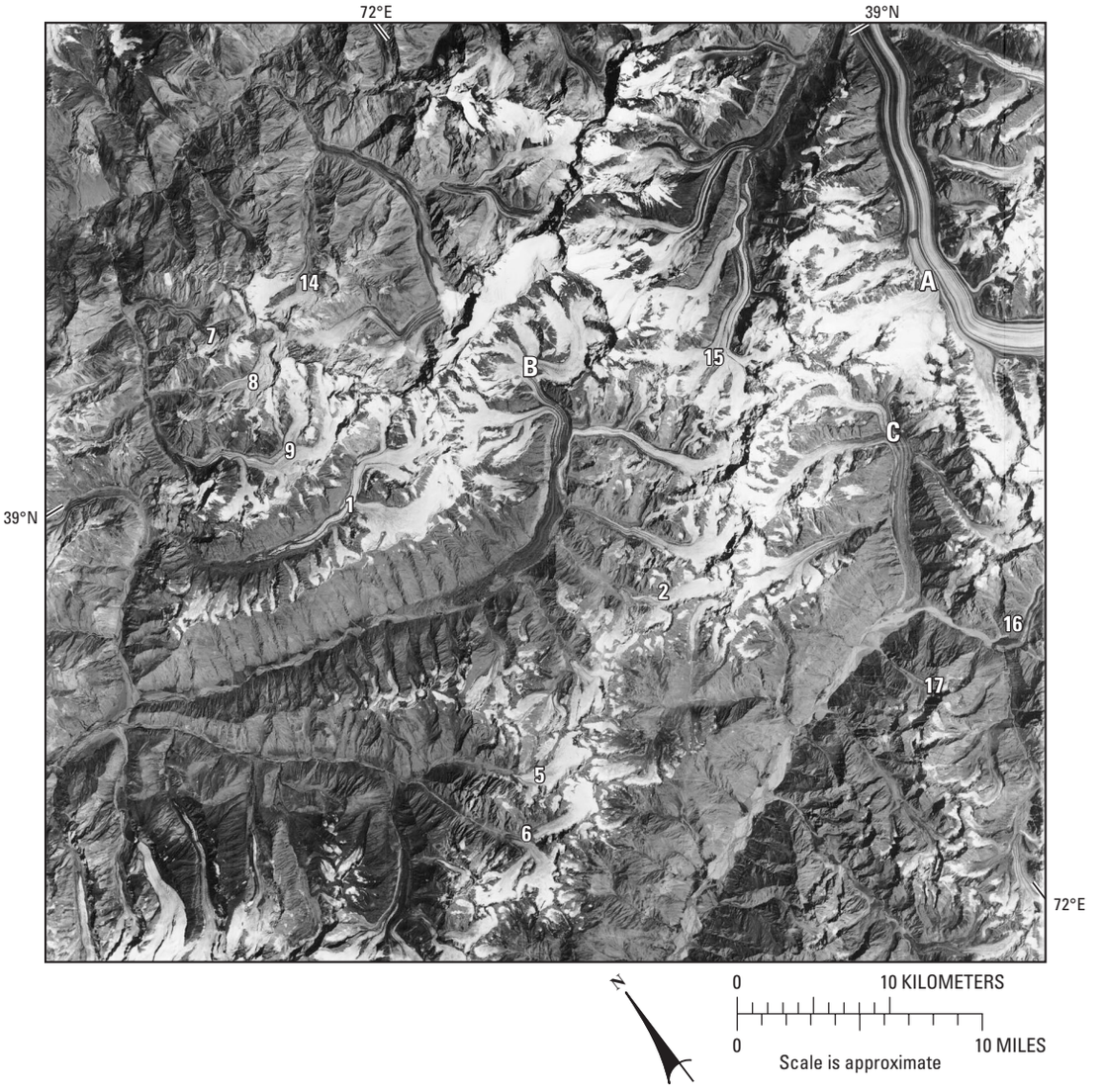


***Figure 67.**—KFA-1000 photograph taken in 1973 from a Resurs-F1 satellite showing surge-type glaciers in the Central Pamirs. The numbers of the glaciers correspond to the numbers in table 20. The largest glaciers of the Pamirs are:* **A**, *Lednik Fedchenko;* **B**, *Lednik Garmo; and* **C**, *Lednik Geograficheskogo Obshchestva.*

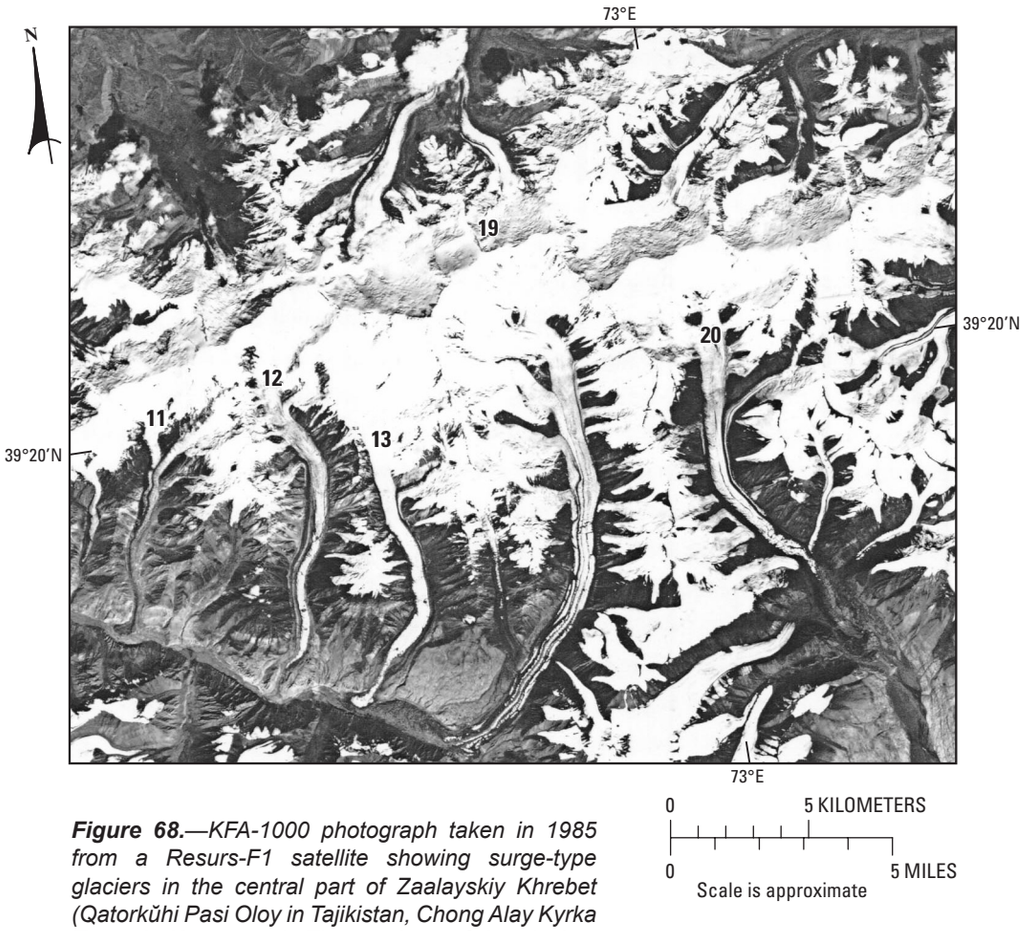


Figure 68.—*KFA-1000 photograph taken in 1985 from a Resurs-F1 satellite showing surge-type glaciers in the central part of Zaalayskiy Khrebet (Qatorkŭhi Pasi Oloy in Tajikistan, Chong Alay Kyrka Toosu in Kyrgyzstan). The numbers of the glaciers correspond to the numbers in table 20.*

Investigation of the Fluctuation Regime of Compound Glaciers

The Institute of Geography has developed methods of monitoring fluctuations of compound surge-type mountain glaciers from space (Osipova and Tsvetkov, 2000, 2002b). For many years, analysis of the dynamic regime of glaciers was done using data on the velocity of ice movement and changes in glacier morphology. The velocity of ice movement was measured by pseudo-parallax using space photography. The method has been improved so that it is now possible to determine the shift of identical contour points on photographs of different dates with an accuracy of 5–10 m. As a result of stereoscopic interpretation of space images, sketch maps reflecting the status of the glaciers and the morphology of their surfaces were compiled for the dates of each survey.

By performing joint analyses on a series of successive velocity profiles and morphological sketch maps, the main features of the glacial systems' dynamic regimes were identified. This, in turn, allowed for an assessment of the character of interaction of their main components. Remote investigations of the dynamics of several compound, surge-type glaciers were conducted over a long time interval. Results indicate that the role of mutual damming of tributary glaciers and the main trunk glacier at different stages of their evolution is a determining factor in dynamic instability of glaciers (Osipova and Tsvetko, 2002b). Several examples follow.

The most detailed investigations of change were carried out on Lednik Oktyabr'skiye for an extended period (Osipova and Tsvetkov, 2002a). The last strong surge of this glacier occurred in the mid-1930s, and its aftereffects are easily seen on 1946 aerial photography (fig. 69*A*). After 1946, activity gradually increased on the upper part of the tongue, the lower part of the tongue wasted away, and tributaries in the lower course of the glacier advanced into the valley of the main trunk (fig. 69*B*–69*C*). Toward the end of the recovery stage (1978), the cross section of the glacier tongue was approximately one third narrower (figs. 69*D* and 70). As a result, a region with considerable longitudinal compression formed a higher ice "dam." In the following years, the release of the accumulated stresses took place, and during 1988–1990, active ice advanced over this "dam," cut or stretched tongues of tributary glaciers on the lower course of the glacier, advanced 3 km down the valley, and reached within 0.3 km of the maximum tongue extent in the prior advance (figs. 69*F*, *G*, and 70) (1990). Average ice velocity from 1988 to 1990 was 1.6 km a^{-1} (fig. 71), but at the surge peak it was considerably higher.

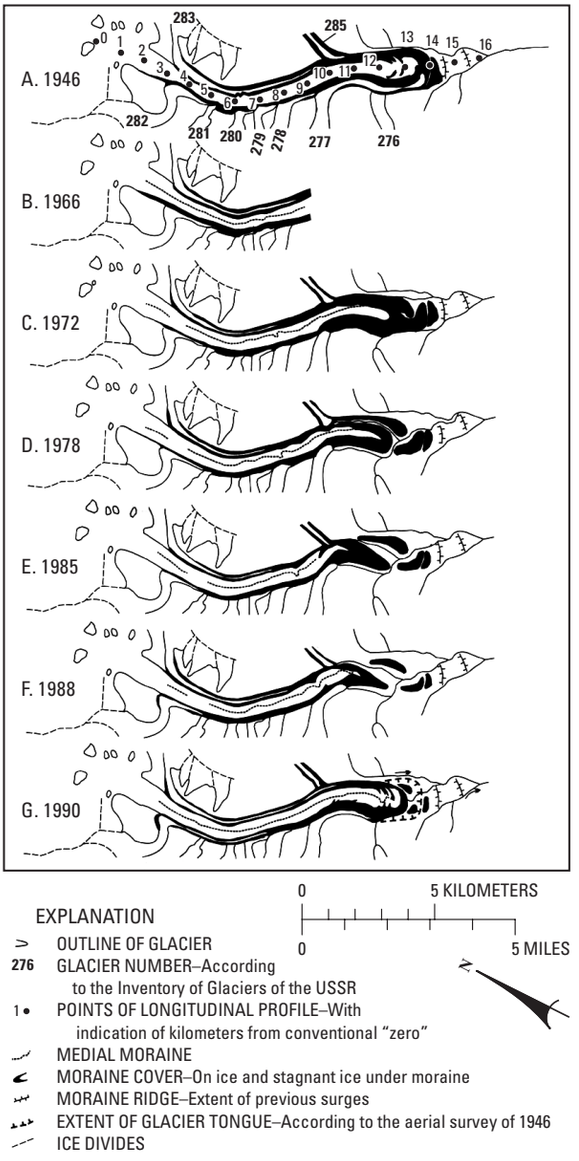


Figure 69.—*Morphology of the lower part of Lednik Oktyabr'skiye from 1946 to 1990.*



Figure 70.—*Photographs from space of Lednik Oktyabr'skiye. The photographs of 1978 (pre- surge) and 1990 (post-surge) were taken by the KFA-1000 camera (1000-mm lens) from the Resurs-F1 satellites.*

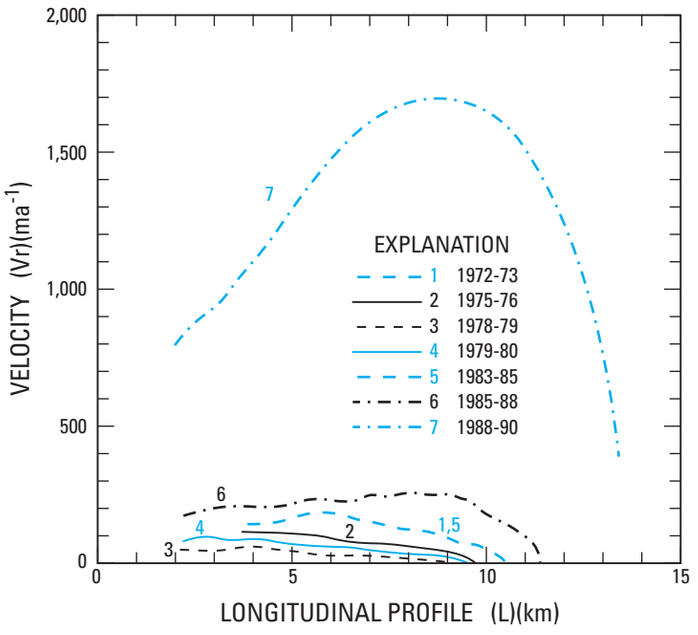


Figure 71.—*Graph of the velocity (V_r) of the ice movement along longitudinal profile L of Lednik Oktyabr'skiye, showing the stage of recovery (1972–1985) and the surge (1985–1990). The location of the longitudinal profile is shown on figure 69A.*

The impact of glacier tributaries and the main glacier trunk on each other during surges was investigated on *Lednik Bivachniy*, the largest, western tributary of Lednik Fedchenko. Figure 72 shows the change of the surface structure of *Lednik Bivachniy* from 1973 to 2001 in the region of the confluence of *Lednik Moskovskogo Gosudarstvennogo Universiteta* (abbreviated *MGU*) (Moscow State University), the large western (left) tributary. During this time period, two surges of *Lednik Bivachniy* occurred — one between 1975 and 1977 and the other probably in the late 1990s (Desinov and others, 2001).

Lednik MGU continuously advanced into the valley of *Lednik Bivachniy* with rather constant velocity. By 1973, the ice of *Lednik MGU* had formed a "bulge," displacing the ice of the main trunk of *Lednik Bivachniy* to the opposite side of the valley and acting as a dam to *Lednik Bivachniy* (fig. 72*A*). As a result, a compression zone formed behind the dam in *Lednik Bivachniy* and, in 1976–1977, the release of accumulated stresses caused a sharp increase in ice movement, increasing in velocity by almost an order of magnitude — a surge event. As a result of the rapid movement of ice in the main trunk of *Lednik Bivachniy*, the noticeable ice bulge of the *Lednik MGU* tongue was transported 3.5 km downstream from the place of its confluence (fig. 72*B*). After this surge, the tongue of *Lednik Bivachniy* became dormant and *Lednik MGU* started to advance into the main valley again. By 1990, a new "bulge" had formed in the region of the confluence of the two glaciers, and the situation was analogous to the one in 1973.

On figure 72*C*, it can be seen that *Lednik Bivachniy* experienced one more surge not long before 2001. It developed according to the same scenario, and the bulge formed by *Lednik MGU* in 1990 moved downstream, taking the place of the bulge of the previous surge. The bulge from the previous surge in turn moved considerably farther down-valley and became heavily covered with debris.

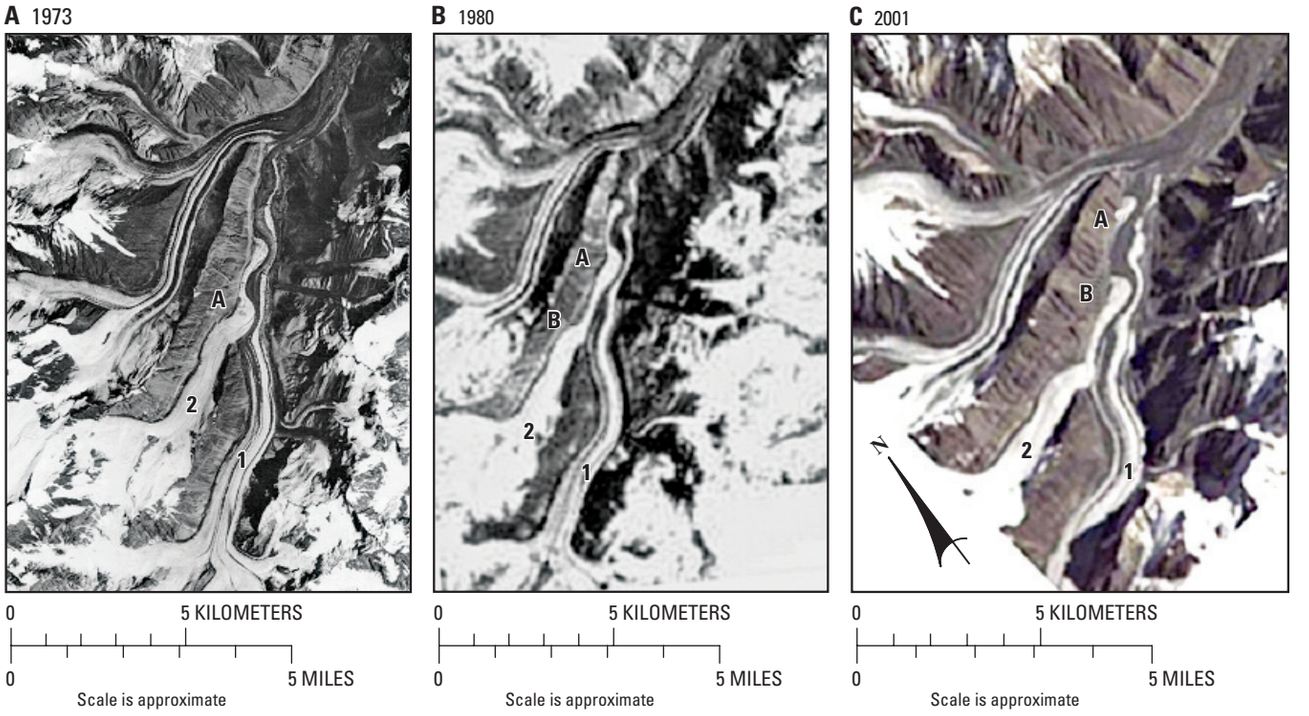


Figure 72.—*Photographs of* Lednik Bivachniy *(1) (approximate lat 39°N., long 72°E.) and Lednik Moscow State University (MGU) (2).* **A**, *1973, pre-surge;* **B**, *1980, post-surge; and* **C**, *2001 soon after the successive surge. On the photographs,* **A** *is the bulge formed before the 1976–1977 surge;* **B** *is the bulge formed before the late 1990s surge.* **A** *and* **B** *were taken by the KFA-1000 camera of a Resurs F-1 satellite.* **C** *was imaged from the International Space Station with an 80-cm lens.*

As a result of such periodicity, several bulges of *Lednik MGU* can be seen on the main trunk of *Lednik Bivachniy*, transported during successive surges. On figure 72, the bulges of *Lednik MGU* are identified by letters: A is the bulge formed before the surge of 1976–1977; B is the bulge formed before the surge of the late 1990s.

At present, the surges of *Lednik Bivachniy* are internal — despite high internal ice velocity (over 1,200 m a^{-1}), the surge events have taken place within the limits of the glacier. However, it has been reported that, at the beginning of the past century, the surges of *Lednik Bivachniy* activated the lower part of Lednik Fedchenko (Osipova and Tsvetkov, 1999).

On figure 73, three images from space show the condition of the complex system of Ledniki Gando-*Dorofeeva*: (A) before the 1989–1990 surge, (B) during the surge, and (C) after the surge. After a previous surge of this glacier at the end of the 1950s, there was degradation — the main trunk of the glacier was covered with debris, and the main tributary, *Lednik Dorofeeva,*

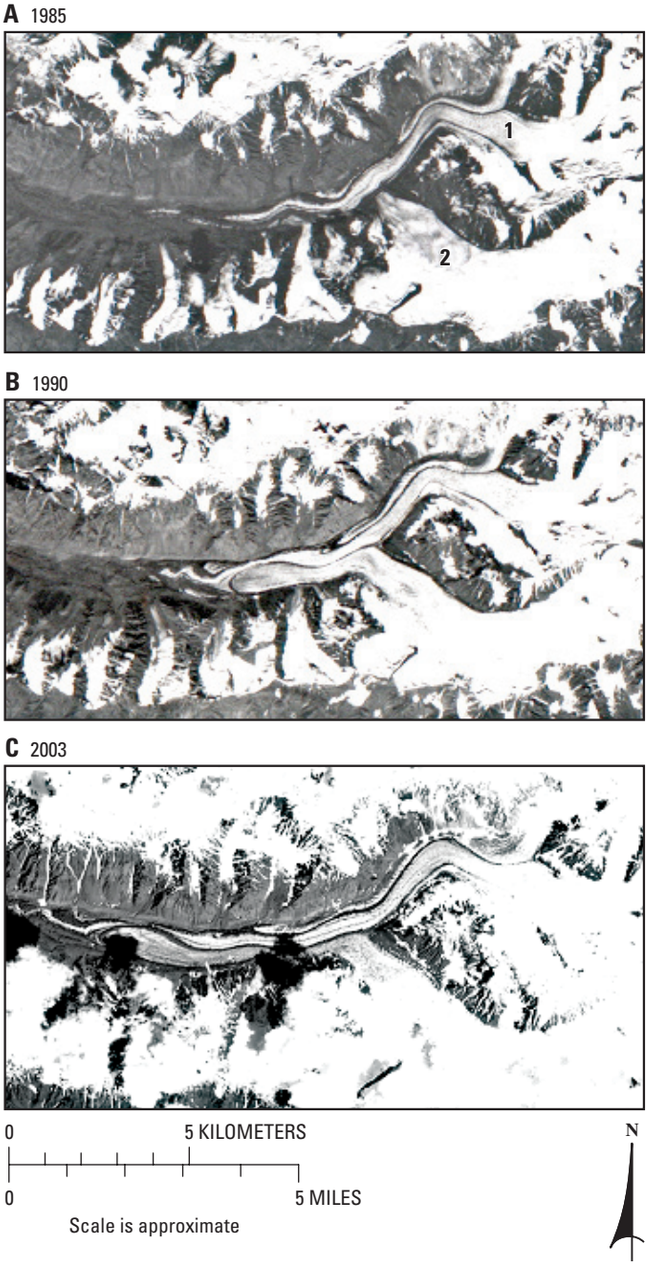


***Figure 73.**—Images from space of the Gando-*Dorofeeva *glacier system (approximate lat 38°55′N., long 71°45′E.) before, during, and after the 1989–1990 surge.* **A**, *August 1985 on the eve of the surge.* **B**, *September 1990 in the midst of the surge.* **C**, *23 August 2003 after the surge. 1, Lednik Gando, 2,* Lednik Dorofeeva. **A** *and* **B** *are photographs from the KFA-1000 camera on the Resurs-F1 satellite series.* **C** *is an Advanced Spaceborne Thermal Emission Radiometer (ASTER) image from the Terra satellite.*

separated. At the beginning of the 1980s, *Lednik Dorofeeva* became active again and its terminus advanced and became dammed by ice from the main trunk. As a result of strong longitudinal compression, the width and thickness of the lower part of the *Lednik Dorofeeva* tongue increased considerably, testifying to its critical state (fig. 73*A*).

On the space photograph of 1990 (fig. 73*B*), the Ledniki Gando-*Dorofeeva* system is in the midst of a large surge event. In 1989–1990, ice velocity was 1.4 km a^{-1} in the middle part of the tongue of Lednik Gando, and by 1991, the active ice front had advanced by 8 km. And, judging by velocity curves and the surface condition of the glacier, the surge was not over yet (Osipova and Tsvetkov, 2001).

A 2003 space survey (fig. 73*C*) documented the Ledniki Gando system after the surge. The total advance of the dynamic terminus was 9.5 km; however, the lower 1.5 km of the tongue was not affected. Therefore, the surge of this glacier, and that of some of the other compound glaciers observed by us (Ledniki Bivachnyy, *Sugran*, and others), is considered an internal surge.

This analysis shows the effectiveness of repeated space surveys (especially those acquired over a period of many years) for monitoring fluctuations of large compound glaciers. No other method makes it possible to observe the entire area, to repeat investigations with short time intervals, and to provide the opportunity for any investigator to make simple, accurate stereoscopic measurements, especially of ice velocity.

The State of Surging Glaciers — Ledniki Medvezhiy and Geograficheskogo Obshchestva

Data acquired by Earth-orbiting satellites make it possible to investigate potentially catastrophic natural hazards and associated phenomena that could not be studied otherwise. At present, several satellites are orbiting the Earth, carrying a variety of remote sensors which can provide solutions to various scientific problems and practical needs in conjunction with well-planned programs. One such program, "Uragan", was planned jointly by the Institute of Geography of the Russian Academy of Sciences and the Russian "Energiya" Space Rocket Corporation, and is being carried out on the International Space Station (ISS). Visual-instrumental observations are being made, and digital images are being acquired by astronauts to study changes in the geographical environment, including natural disasters. In particular, Ledniki Medvezhiy and Geograficheskogo Obshchestva, situated near each other in the upper course of the Vanj river, are objects of constant observation and photography from the ISS (see fig. 67).

Lednik Medvezhiy (approximate lat 38°40′N., long 72°12′E.) is a typical surge-type glacier. Scientists of the Institute of Geography carried out annual surface investigations on this glacier from 1963 to 1987. From 1988 to 1991, observations were made based on multiple repeat aerial photography surveys. These investigations made it possible to comprehensively study the evolution of the glacier during its three surges (1963, 1973, and 1989) and its two stages of recovery (Dolgoushin and Osipova, 1982; Osipova and Tsvetkov, 1991; Kotlyakov and others, 1997). As a result of these multi-year investigations, the method of forecasting glacier surges based on monitoring the changes in the surface altitude and ice movement was developed (Dolgoushin and Osipova, 1975).

Figure 74*A*, *B*, and *C* are parts of three of the eight aerial photographs taken of Lednik Medvezhiy during its surge in 1988–1989. At that time, investigations were based on photogrammetric analysis of aerial photographs and comparison of successive topographic maps of the glacier. At the beginning of

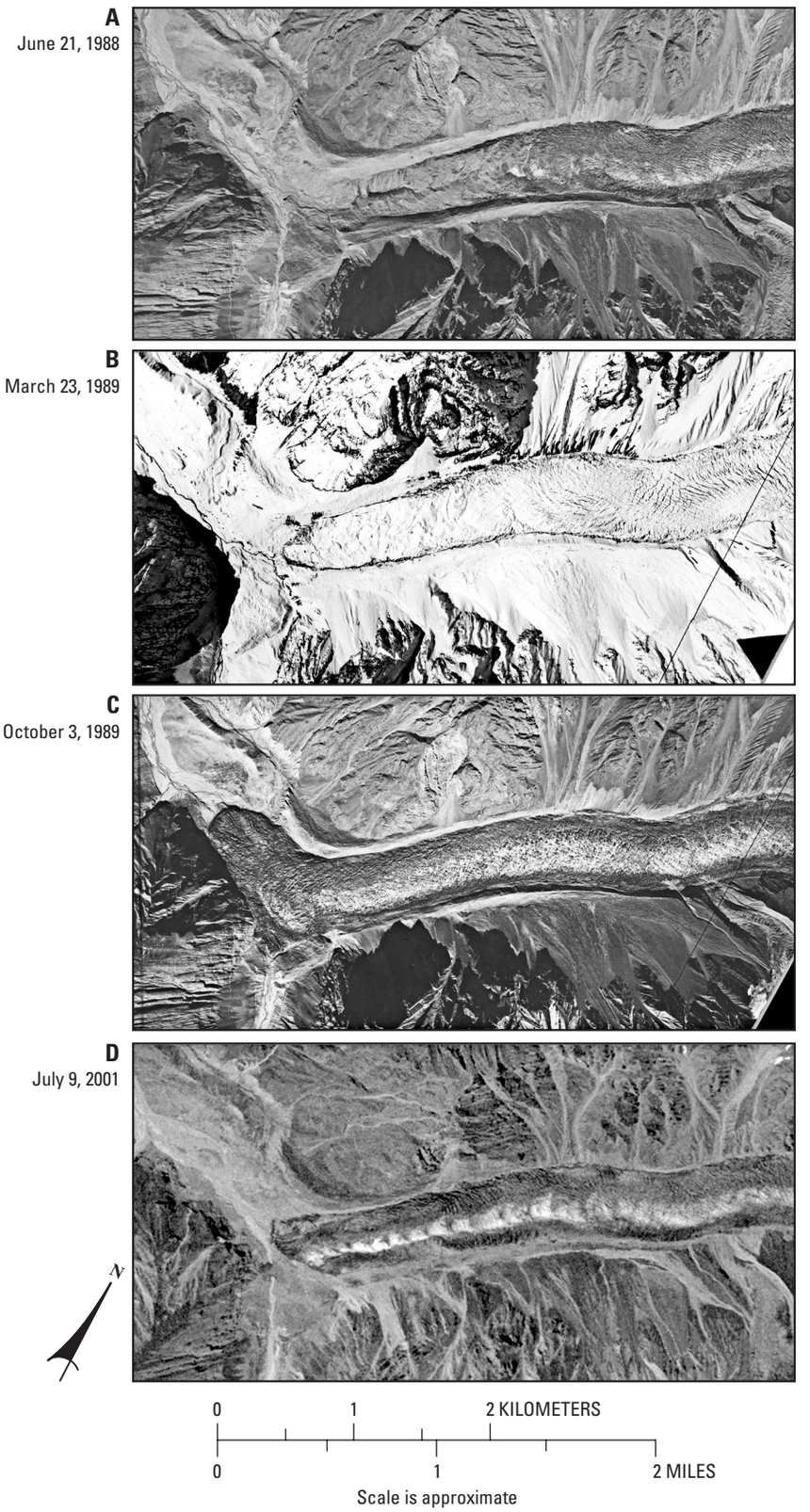


Figure 74.—*The tongue of Lednik Medvezhiy (approximate lat 38°40'N., long 72°12'E.) during the surge of 1988 to 1989, and in 2001. Aerial photographs:* **A**, *21 June 1988;* **B**, *23 March 1989;* **C**, *3 October 1989;* **D**, *an image from the International Space Station on 9 July 2001 with a digital camera with a 80-cm lens.*

the movement, the glacier terminus was situated at a distance of 1.2 km from the *Abdukagor* river (fig. 74*A*). Between the surveys of 21 June and 13 September 1988, it advanced 20–40 m. Figure 74*B* shows that the terminus of the tongue advanced 200 m more during winter, and the tongue assumed the shape typical of advance; it was fringed by a marginal fracture (a black line on the background of snow-covered slopes). The maximum rapid movement — up to 70 m d^{-1} — was measured by aerial pseudoparallax on surveys of 20 and 22 June 1989. The end of the surge occurred abruptly in July, and on an image of 3 October 1989 (fig. 74*C*), the surface structure of the tongue already had an "after-surge" appearance (Kotlyakov and others, 1997).

From 1996 to 2000, astronauts of the Russian Mir Orbital Space Station watched the dynamics of the glacier with the aid of binoculars. In February 2001, astronauts of the ISS transmitted information of renewed activity of the glacier — a distinct dark boundary fringing its snow-covered tongue. Such a boundary, as was seen on figure 74*B*, is a marginal fracture, and testifies to the fact that the glacier is in a state of rapid movement. Since that time, constant observations and images using hand-operated digital cameras were made from the ISS to track the condition of the glacier and to forecast a possible surge event.

Conclusions of the visual observations of the astronauts were passed to government officials of Tajikistan. Scientists from Glavtadjikgidromet, the Department of Hydrometeorology in Tajikistan, made surface observations on the glacier from 22 to 29 June 2001 and determined that, in comparison with 2000, the tongue had advanced by 450 to 500 m, but was still 200 to 250 m from the channel of the *Abdukagor* river. More than a week of observations determined velocity of the glacier — it was equal to 10–15 cm d^{-1}. Based on this, it was concluded that the glacier's advance was nearly complete, and the *Abdukagor* river would not be dammed.

By comparing these findings with previous investigations, we estimated that the peak of the glacier's activity occurred in May and early June. The first successful images (without cloud cover obscuring the tongue) were received from the ISS from a digital camera with 80-cm lens (pixel resolution of ~10 m) at the end of May and at the beginning of July (fig. 74*D*). By comparing ISS images taken from then (July 2001) until 2003, it was determined that during the two years, the glacier terminus advanced less than 100 m. However, during all this time, the structure of its surface, smooth alternating white and dark ramparts (ogives?), remained unchanged. But the most significant fact is that the tongue's movement from 2001 to 2003 was not as large or as destructive as during previous surges. For example, compare the structure of the surface and the overall morphology of the tongue on figs. 74*C* and *D*.

We concluded that a strong microsurge most likely took place on Lednik Medvezhiy in 2000–2001. As a result, the glacier front advanced down valley. It did not meet resistance from deposits of stagnant ice that were remnants of the former surge, because they had melted by this time. However, interpretations of ISS images indicated that the surface in the upper course of the surging part of the glacier (in the area below the icefall) did not lower. Therefore, it is likely that the glacier's state is critical, and in the near future, the next, and possibly major, surge of Lednik Medvezhiy will take place.

Lednik (Russkogo) Geograficheskogo Obshchestva, abbreviated RGO (lat 38°45′N., long 72°07′E.), is one of the six largest glaciers of the Pamirs. At the beginning of the 20th century, traces of its recent surge were detected — the tongue of the glacier had moved to the *Abdukagor* river valley and crossed it, and on the valley sides, the outline of a dammed lake was preserved (fig. 75). When the next surge of the glacier takes place, a dammed lake might reform, and its outburst flood may cause large-scale damage downstream in the Vanj river valley.

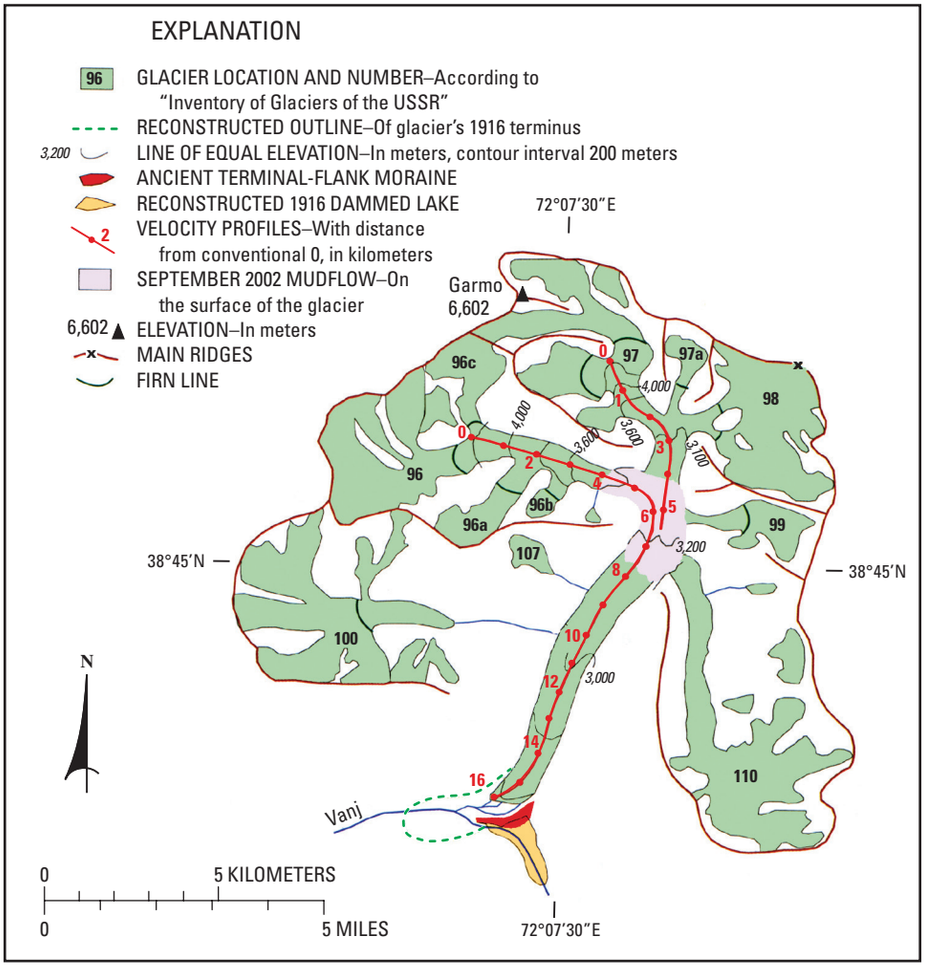


***Figure 75.**—Sketch map of the Lednik Geograficheskogo Obschestva (RGO Glacier) basin showing glaciers, the reconstructed outline of the glacier's terminus in 1916, a reconstructed dammed lake in 1916, locations of velocity profiles, and a mudflow on the surface of the glacier in September 2002.*

Therefore, the increasing activity of Lednik RGO tongue, detected in August–October 2002 with surface and helicopter surveys (fig. 76), drew the attention of scientists of the Institute of Geography (Kotlyakov and others, 2003). Analysis of ISS images and helicopter photographs detected a recent mudflow on Lednik RGO in the region of the confluence of the main flows of Numbers 96 and 97 glaciers (figs. 75, 77). Previously, such large-scale mudflows had not been observed on the glaciers of the Pamirs, although large-scale mudflows are common in other glacierized mountain regions.

Later, 2003 ASTER images and photographs taken from a helicopter with a hand-held camera were analyzed. It was determined that the glacier's terminus had started to degrade, and that the activity of the glacier had decreased. It was also found that the source of the mudflow was the slopes of the upper course of the left tributary — Number 96C glacier, 2.5-3 km southwest of Khrebet Garmo. The mudflow had traveled about 7-8 km, and it covered an area of about 10 km^2.

Whatever the cause of the mudflow, it could have had two major impacts on the glacier. On the one hand, it could have caused a dynamic impact that traveled down the glacier and increased activity at the Lednik RGO terminus. However, this probably did not happen, because no changes were found in the surface structure of the glacier either at the location of the mudflow or below it.

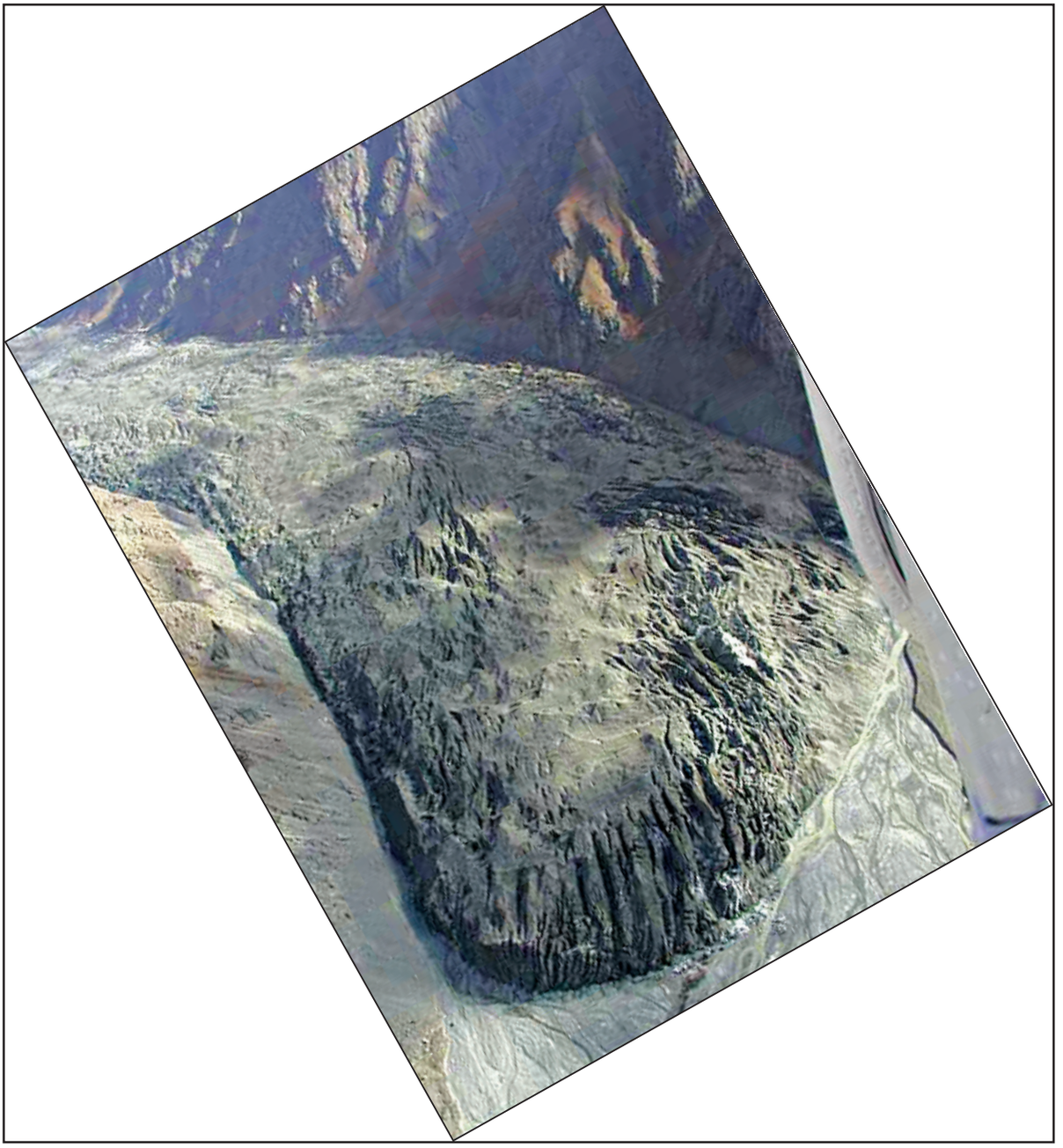
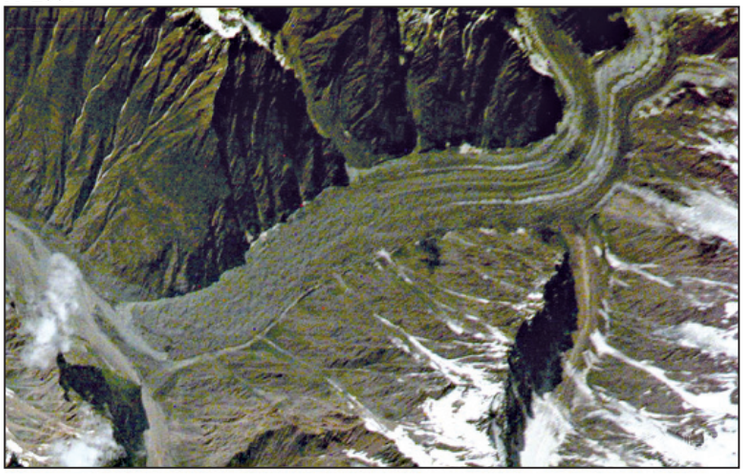


Figure 76.—*Aerial photograph taken on 13 October 2002 of the terminus of Lednik RGO, looking northeast. Longitudinal fissures and outcrops of ice are observed along the edges of the tongue and in other places. The transverse profile of the glacier is convex. Collapsed pieces of ice can be seen at the foot of the steep terminus of the tongue. Photo taken by Prof. Zh. F. Shneider.*

Most probably, the mudflow caused a change in ablation conditions. By covering the surface, the resulting decrease of ablation could have locally increased the thickness of the glacier, and eventually advanced its terminus.

In both of the examples cited here, data acquired from space images and photography provided invaluable help in scientifically observing and monitoring the evolution of surge-type glaciers and in forecasting catastrophic surge events. The space imagery periodicity, type, availability, and processing capabilities all affect the ability of scientists to perform regional- and global-scale glaciological monitoring.

A 2001



B 2002

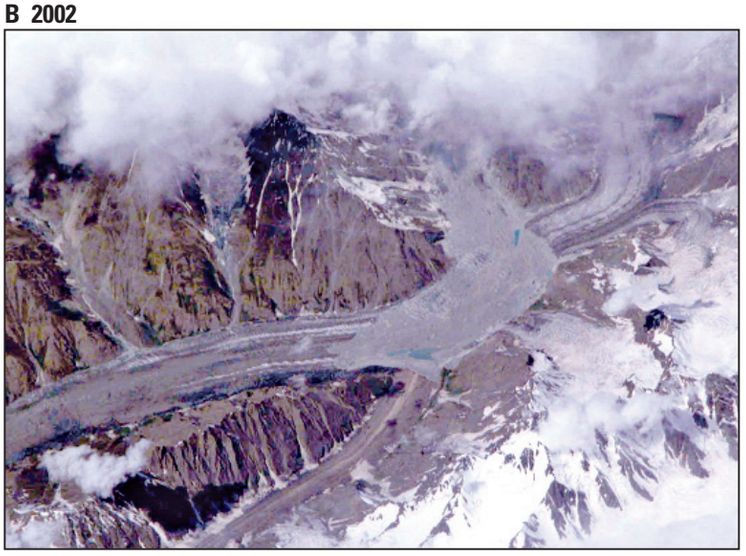


Figure 77.—*International Space Station images of Lednik RGO (lat 38°45'N., long 72°07'E.) taken on* **A**, *25 June 2001 and* **B**, *30 September 2002. On the second image, a mudflow is visible that post-dated the 2001 image. Compare with figure 75 for scale.*

Investigations of the Fluctuations of "Normal" Non-Surging Glaciers in the Eastern Pamirs

The Eastern Pamirs is the most continental part of the Pamirs. The area is characterized by high elevation, low dissection of relief, low values of accumulation and ablation, and few changes in the glaciers from year to year.

To estimate the contemporary evolution of the glacierization of the Eastern Pamirs, extensive data from remote monitoring of fluctuations of glaciers' termini were used (Osipova and Tsvetkov, 2000). The shifts of termini of more than 160 glaciers in different parts of the Eastern Pamirs were measured by stereocomparator and the pseudoparallax method on images and photographs from space acquired between 1972 and 2001 (fig. 78). In optimum circumstances, data for three time intervals were obtained and analyzed: 1972–1980, 1980–1990, and 1990–2001.

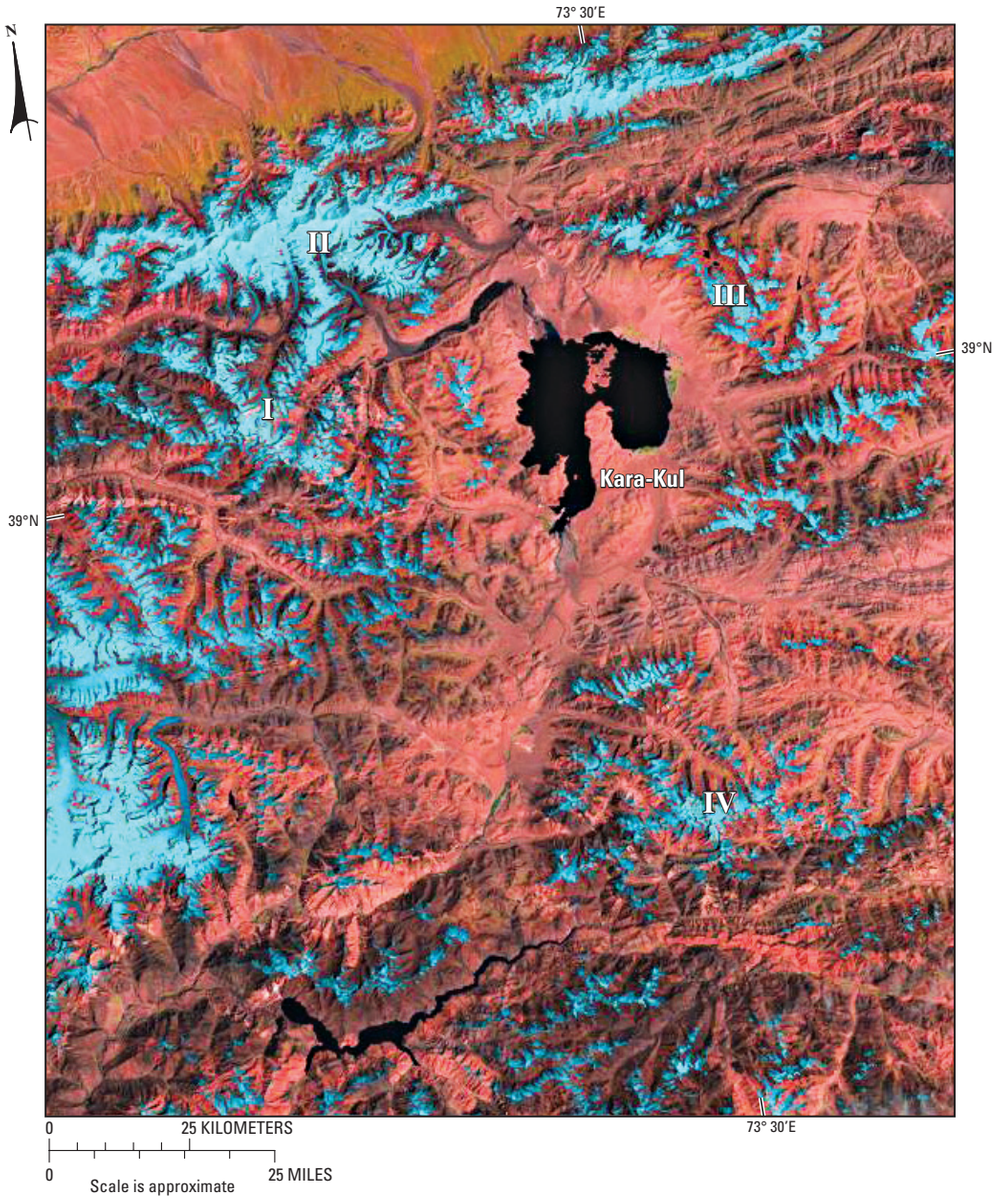


***Figure 78.**—Landsat image of the Eastern Pamirs where glacier-retreat measurements listed in table 21 were made.*

All investigated glaciers either retreated or were stationary. The greatest retreat velocities, up to or more than 20 m a^{-1}, were registered on tongues of large compound glaciers having termini that ended at low elevations. With a decrease in glacier size and an increase in the elevation of the glacier termini, ice retreat velocity decreased. Valley glaciers with areas from 2 to 5 km^2 correspond to the retreat value averaged by all investigated glaciers. An increase in the area of moraine cover on glacier tongues was documented everywhere.

The total results of the measurements are given in table 21. From this table we can see that the average retreat velocity (V_1) during the second time interval increased on an average of about 1.5 times. The minimum increase of 1.2 times was measured at *Zaalayskiy Khrebet* (Qatorkŭhi Pasi Oloy/Chong Alay Kyrka Toosu), the maximum — a two-fold increase — was measured on the western slope of Khrebet Sarykol'skiy. Average retreat velocity of 30 glaciers of Khrebet Zulumart from 1990 to 2001 was 14 percent less than on the same glaciers during the previous interval.

TABLE 21.—*Retreat velocity of the termini of glaciers of the Eastern Pamirs from 1972 to 2001*

[Retreat velocity (V_1) shown in meters per year ($m\ a^{-1}$)]

	Region	1972–1980		1980–1990		1990–2001	
		V_1 ($m\ a^{-1}$)	Number of glaciers	V_1 ($m\ a^{-1}$)	Number of glaciers	V_1 ($m\ a^{-1}$)	Number of glaciers
I	Khrebet Zulumart	-4.4	49	-6.5	51	-6.0	30
	Western slope	—	—	—	—	—	—
	Eastern slope	-3.0	11	-5.8	12	—	—
II	Zaalayskiy Khrebet	-5.5	8	-6.8	8	—	—
III	Khrebet Sarykol'skiy, western slope	-1.3	5	-2.6	19	—	—
IV	Khrebet Muzkol	—	—	-5.0	9	—	—
V	Severo-Alichursky Khrebet, northern slope	-1.3	7	-2.5	7	—	—
	Eastern Pamirs as a whole	—	80	—	106	-6.0	30

On *Lednik Severniy Zulumart* (lat 39°06′N., long 72°50′E., length 11.6 km, area 29.1 km^2, according to data for 1966) investigations of fluctuations of its area and terminus location were carried out for several years on the basis of comparison of an aerial photographic survey of 1946, imagery and photography of 1972, 1978, 1990 (KFA-1000 camera on the Resurs-F1 satellite) and ASTER imagery of 2001. Results are presented on figure 79 and in table 22.

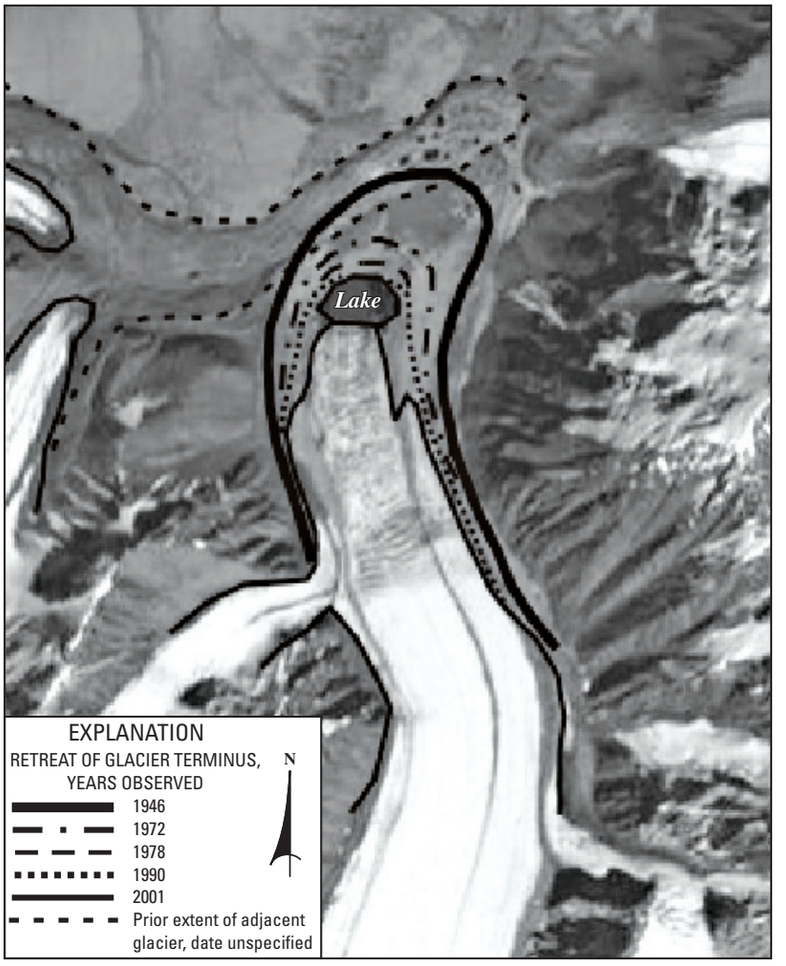


Figure 79.—*Sketch map showing the retreat of the terminus of* Lednik Severniy Zulumart *(Eastern Pamirs) (lat 39°06′N., long 72°50′E.) based on interpretation of a 1946 aerial photograph and 1972, 1978, 1990, and 2001 space images and photographs.*

TABLE 22.—*Retreat of the terminus and decrease in the area of the tongue of* Lednik Severniy Zulumart *from 1946 to 2001*

[Abbreviations: m, meter; m a^{-1}, meters per year; km^2, square kilometer]

Intervals between surveys	1946–1972	1972–1978	1978–1990	1990–2001	1946–2001
Retreat of terminus (m)	-500	-100	-200	-200	-1,000
Retreat velocity (m a^{-1})	-19	-17	-18	-18	-18
Change of area (km^2)	-0.5	-0.1	-0.2	-0.2	-1.0

From 1946 until 2001, the glacier retreated with approximately the same average velocity — 18 m a^{-1} — and shortened by 1.0 km (10 percent). During the same time period, the area of the tongue decreased by 1.0 km^2, 3 percent of the initial area of the entire glacier. By 2001, a proglacial lake had formed in front of its terminus. Detailed stereoscopic interpretation of the structure and morphology of the surface of the firn area of *Lednik Severniy Zulumart* did not reveal any substantial change of boundaries in its upper area during the entire 55 years of remote observations. Later studies compared the changes in glacier extent using historical data and ASTER imagery (Khromova and others, 2006).

Investigations of glacier fluctuations carried out in several areas have shown that there is a real possibility of replacing labor-intensive field measurements with remote observations based on simple stereomeasurements of large-scale images obtained at intervals of 5–10 years, as well as using other remote sensing tools and methods.

The Glaciology of the Russian High Arctic from Landsat Imagery

By J.A. Dowdeswell,[5] E.K. Dowdeswell,[5] M. Williams,[6]
and A.F. Glazovskii[2]

Abstract

The Russian High Arctic archipelagos of Franz Josef Land (Zemlya Frantsa-Iosifa), Severnaya Zemlya, and Novaya Zemlya, fringing the Barents and Kara (Karaskoye) Seas, contain more than 56,000 km^2 of glaciers and ice caps, or about 10 percent of the Earth's ice outside Antarctica and Greenland. In the Russian Far East, ice covering an area of less than 100 km^2 occurs in the DeLong[7] archipelago (Ostrova De-Longa), east of the ice-free New Siberian Islands (Novosibirskiye Ostrova). Relatively little is known about the glaciology of some of these islands. However, Landsat satellite imagery has provided a valuable descriptive and interpretative tool for acquiring baseline glaciological data, despite problems of cloud cover which restrict the number of high-quality images available. Drainage basins are a basic unit for glaciological measurements, and for modeling ice dynamics and responses to climate change. Ice divides throughout the Russian High Arctic have been mapped from Landsat imagery to define catchment basin geometry. Major ice-cap outlet glaciers have been identified from Landsat data, and sources and magnitudes of iceberg production have been investigated. The largest icebergs observed were more than 2 km long at the Znamenity Glacier (Lednik Znamenityy), located on Vilchek Land (Zemlya Vil'cheka) in the Franz Josef Land archipelago, and more than 4 km long off the Matusevich Ice Shelf (Lednik Matusevicha) in Severnaya Zemlya. Fringing ice shelves were also identified from Landsat imagery of Franz Josef Land. Relatively few surge-type glaciers are present in the Russian High Arctic, but looped medial moraines indicate that a number of ice-cap outlets in Novaya Zemlya, and possibly Severnaya Zemlya, are of surge-type. Summer Landsat imagery displays marked zones of different brightness which are interpreted to represent, with increasing altitude, bare ice, slush, and snow. Some low-elevation ice caps in Franz Josef Land in particular may be undergoing rapid decay, with little or no net accumulation even at their crests. This decay is probably related to the termination of the cold "Little Ice Age" in the Eurasian Arctic about 100 years ago, combined with recent warming.

[5]Scott Polar Research Institute, University of Cambridge, Cambridge CB2 1ER, U.K.

[6]School of Civil Engineering and Geosciences, University of Newcastle, Newcastle NE1 7RU, U.K.

[7]U.S. Government publications require that official geographic place-names for foreign countries be used to the greatest extent possible. In the Glaciology of the Russian High Arctic section, the use of geographic place-names is based on the U.S. Board on Geographic Names (BGN) website: *http://earth-info.nga.mil/gns/html/index.html*. The website lists some conventional names for the areas such as Franz Josef Land, Barents and Kara Seas, and Wrangel Island. All other names will be introduced in the text by the common English equivalent with the Russian name in parenthesis. The Russian placename will then be used throughout the text. Names not listed in the BGN website will be shown in italics.

Introduction

Glaciers and ice caps are present on the islands of the Russian High Arctic between latitudes 73° and 82°N., and longitudes 36° and 158°E., providing a high latitude west-east transect of about 2,000 km across Eurasia (fig. 80) (Sharp, 1956). These ice masses have a total glacierized area of more than 56,000 km^2 (Kotlyakov and others, this volume), which represents about 10 percent of the Earth's ice cover other than Greenland and Antarctica (Meier, 1984; Dyurgerov and Meier, 1997; Dowdeswell and Hagen, 2004). The three large archipelagos — Franz Josef Land, Novaya Zemlya and Severnaya Zemlya — account for more than 99 percent of this ice. Small isolated islands, for example Victoria Island (Ostrov Viktoriya) in the west and Ostrova De-Longa in the far east of the Eurasian High Arctic, contain ice caps up to only a few tens of square kilometers in areal extent (Govorukha, 1964; Verkulich and others, 1992).

In a companion paper, Kotlyakov and others (this chapter) describe the distribution and dimensions of the ice masses within the Russian High Arctic. This paper describes briefly what is known about the glaciology of the archipelagos and islands in the Russian Arctic sector, and demonstrates the utility of Landsat satellite imagery for studying the glaciers and ice caps in this remote and little-known region of the Arctic. The topics discussed here have been investigated in other glacierized regions using Landsat imagery (for example, Bindschadler and others, 2001); they include: (1) ice-surface topography, and in particular the definition of ice divides and drainage basins; (2) ice dynamics; and (3) snow-and-ice facies, with their implications for glacier mass balance.

The Russian High Arctic is cloud-covered for many days each year, which substantially impacts the acquisition of usable visible-band satellite imagery. Marshall and others (1994) analyzed cloud-cover statistics for a number of Landsat path-rows over each of the main ice-covered areas of the Eurasian Arctic sector, including Franz Josef Land, Novaya Zemlya and Severnaya Zemlya (fig. 81). They showed that, in general, very few high-quality images with low cloud cover are available for the Russian High Arctic. The probability of obtaining relatively cloud-free scenes is greatest for Novaya Zemlya (fig. 81*A*). Cloud-free images of Franz Josef Land are most likely to be obtained in May (fig. 81*B*), whereas July is the optimum month for Novaya Zemlya (fig. 81*C*), and September imagery is of uniformly poor quality, except for some opportunities in Severnaya Zemlya (fig. 81*D*).

Glaciological Background

The following section describes general glacier characterisitics, including meteorological conditions, for each of the three primary archipelagos in the Russian High Arctic — Franz Joseph Land, Severnaya Zemlya, and Novaya Zemlya. Only one percent of the glacierized Russian High Arctic lies outside these archipelagos; however, these small glacierized islands are also discussed here.

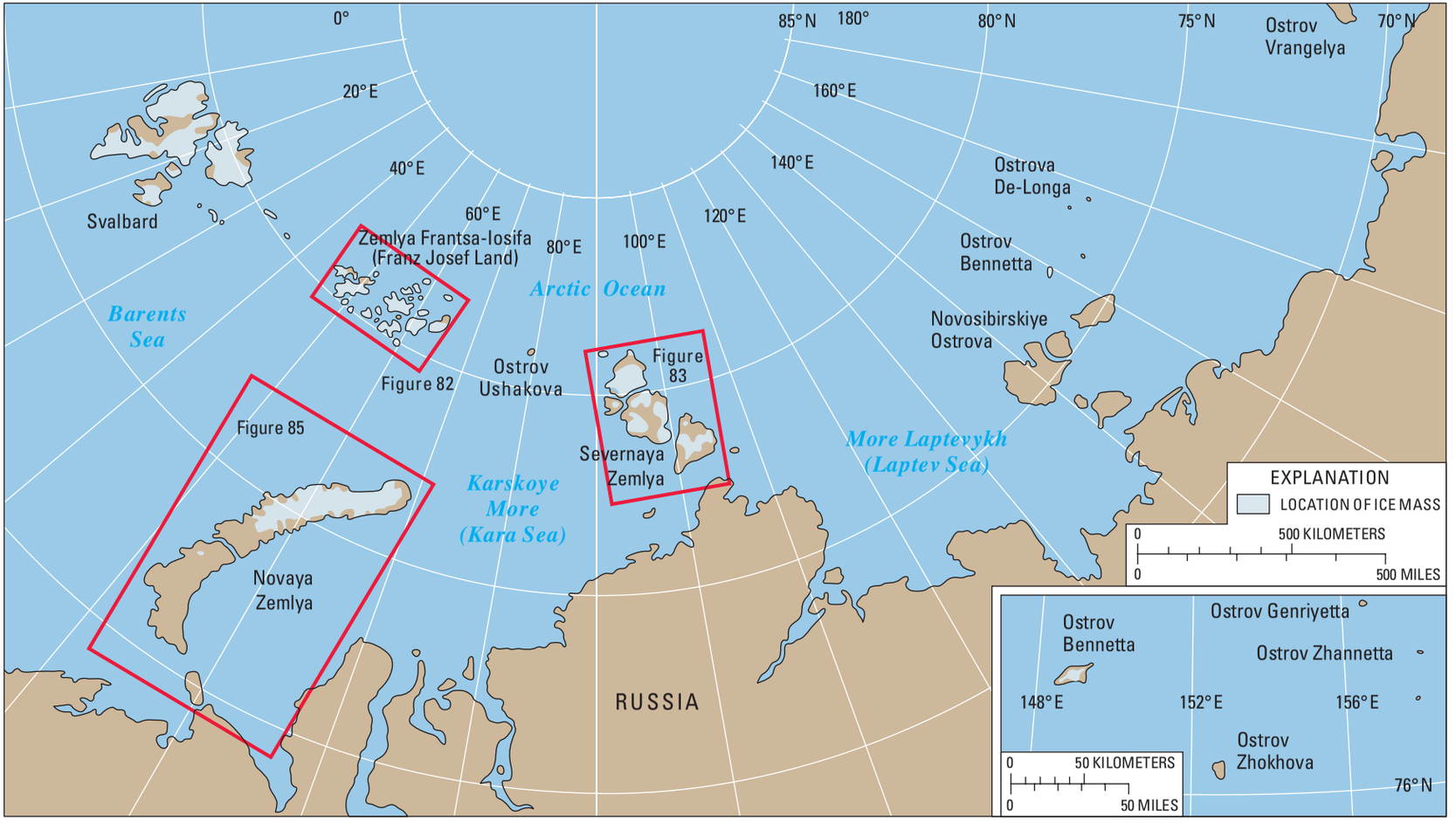


Figure 80.—*Map of the Russian High Arctic showing the major ice-covered archipelagos of Franz Josef Land, Novaya Zemlya, and Severnaya Zemlya, together with the smaller glacierized islands further east (inset).*

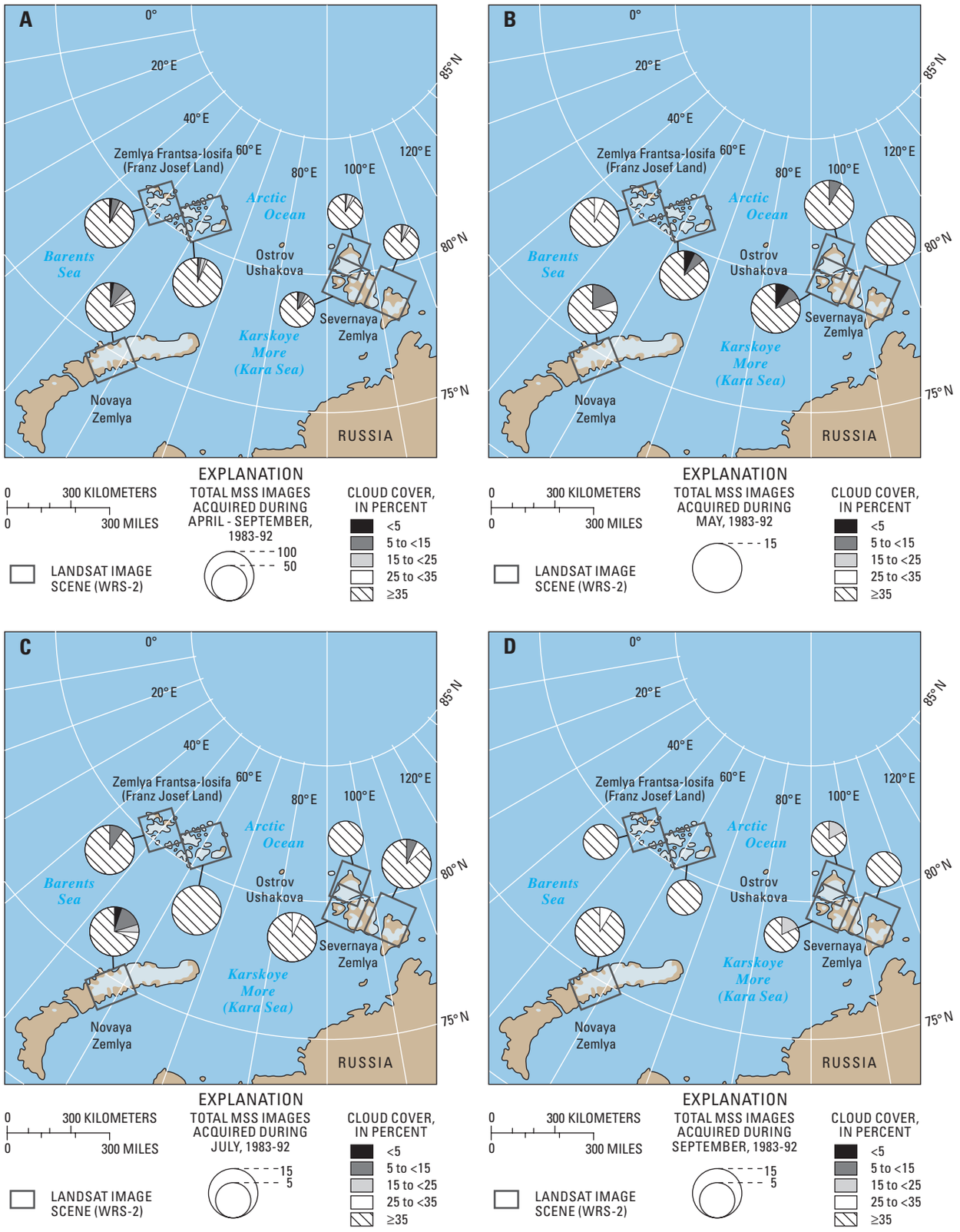


***Figure 81.**—Diagrams showing the effects of cloud cover on Landsat image quality for selected Path–Rows in the Russian High Arctic, including Franz Josef Land (Path 203–Row 001, Path 197–Row 001), Novaya Zemlya (Path 178–Row 007) and Severnaya Zemlya (Path 174–Row 001, Path 170–Row 002, Path 161–Row 003):* **A**, *April to September;* **B**, *May;* **C**, *July; and* **D**, *September. Modified from Marshall and others (1994).*

Franz Josef Land

Glacier ice covers about 13,700 km^2 or 85 percent of the Franz Josef Land archipelago, and glaciers reach tidewater along approximately 60 percent of the coast (fig. 82). Relatively little is known about these ice masses (cf. Grosswald and Krenke, 1962; Grosswald and others, 1973; Sin'kevich and others, 1991; Dowdeswell, Gorman, and others, 1994; Dowdeswell, Glazovskii, and Macheret, 1995; Dowdeswell, Gorman, Glazovskii, and others, 1996). Mean annual temperature in Franz Josef Land is about −12 to −13 °C and mean July temperature is approximately 0 to 1 °C (Dowdeswell, 1995). Precipitation is about 0.3–0.5 m a^{-1} (ice equivalent), and is greatest in the southeast part of the archipelago, because of the direction of the prevailing moisture-bearing winds. The highest point in Franz Josef Land is 670 m, but many glaciers and ice caps have extensive areas at relatively low elevations (Dowdeswell, Gorman, and others, 1994).

Glacier mass balance is generally negative (mean of −0.26 m a^{-1}), according to field measurements linked to meteorological data for the period 1930–59 (Grosswald and Krenke, 1962). The modern equilibrium line altitude (ELA) is at about 300 m above sea level, based on an analysis of aerial photographs of the archipelago acquired in the 1950s. According to these studies, the ELA varies relatively little across Franz Josef Land (Grosswald and others, 1973). The summits of a number of smaller ice caps lie below 300 m, and these ice masses appear to be downwasting rapidly (Grosswald and Krenke, 1962; Dowdeswell, 1995). Many glaciers also show evidence of retreat during the present century from a "Little Ice Age" maximum position (Miller and others, 1992). This retreat applies particularly to tidewater glaciers, where mass is lost by significant iceberg calving as well as by melting (Grosswald and Krenke, 1962; Dowdeswell, Gorman, and others, 1994).

Severnaya Zemlya

The archipelago of Severnaya Zemlya is made up of four main islands: Komsomolets, Pioneer (Pioner), October Revolution (Oktyabr'skoy Revolyutsii), and Bol'shevik Islands, together with several smaller islands (fig. 83). Approximately 50 percent of the 36,800 km^2 archipelago is glacierized (Kotlyakov and others, this chapter). The largest ice mass is the Academy of Sciences Ice Cap (Lednik Akademii Nauk) on Ostrov Komsomolets, which has an area of 5,575 km^2 (Dowdeswell and others, 2002) (fig. 84). Floating ice shelves are fed from several of the ice caps on Severnaya Zemlya; the best-documented example is the *Matusevich Ice Shelf* on Ostrov Oktyabr'skoy Revolyutsii, which has an area of about 200 km^2 and a surface slope of less than 0.2° near its margin (Govorukha, 1988a; Dowdeswell, Gorman, and others, 1994; Williams and Dowdeswell, 2001).

Mean annual temperature recorded at Fëdorova at the northern tip of the Taymyr Peninsula (Poluostrov Taymyr), about 40 km south of Severnaya Zemlya, is approximately −15 °C, and mean July temperature is about 1.5 °C (Dowdeswell, 1995). Precipitation is about 0.25–0.3 m a^{-1} (ice equivalent). Mass-balance data for the Vavilov Ice Cap (Lednik Vavilova) (Barkov and others, 1992), a 1,820 km^2 ice cap on Ostrov Oktyabr'skoy Revolyutsii, show that the mean net balance was slightly negative between 1974 and 1988 (−0.03 m a^{-1} water equivalent), but that there was significant interannual variability about this value (standard deviation ±0.36 m a^{-1}). The equilibrium line altitude (ELA) varies from more than 600 m in southeastern Severnaya Zemlya, to about 300 m on Ostrov Komsomolets, to 200 m or less on Schmidt Island (Ostrov Shmidta) in the northwest (Govorukha, 1970), suggesting a moisture source and precipitation gradient from the southeast.

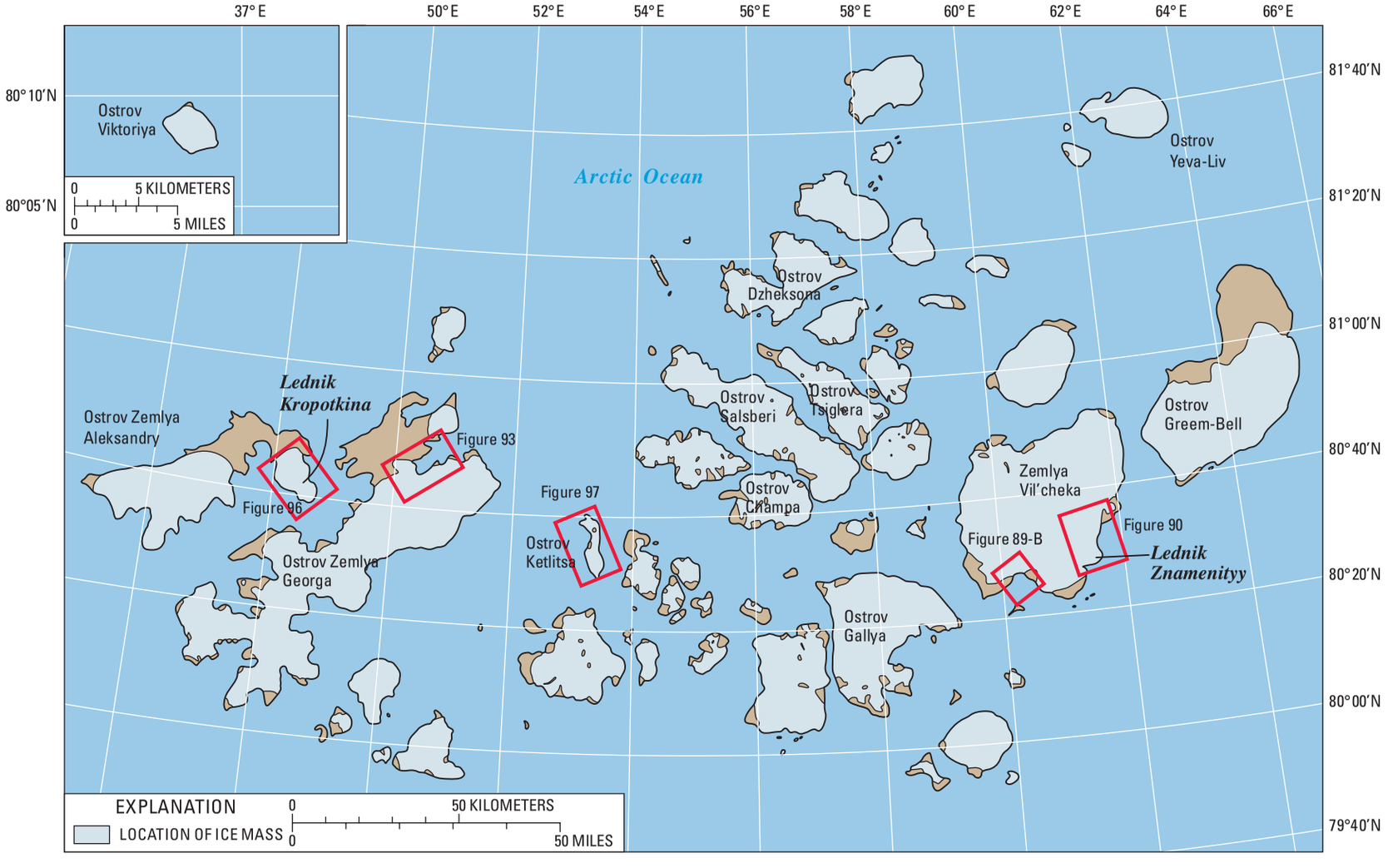


***Figure 82.**—Map of the Franz Josef Land archipelago showing the distribution of ice masses. The locations of Landsat images in subsequent figures are shown as boxes.*



Figure 83.—*Map of the islands of Severnaya Zemlya showing the distribution of ice masses. The locations of Landsat images in subsequent figures are shown as boxes.*

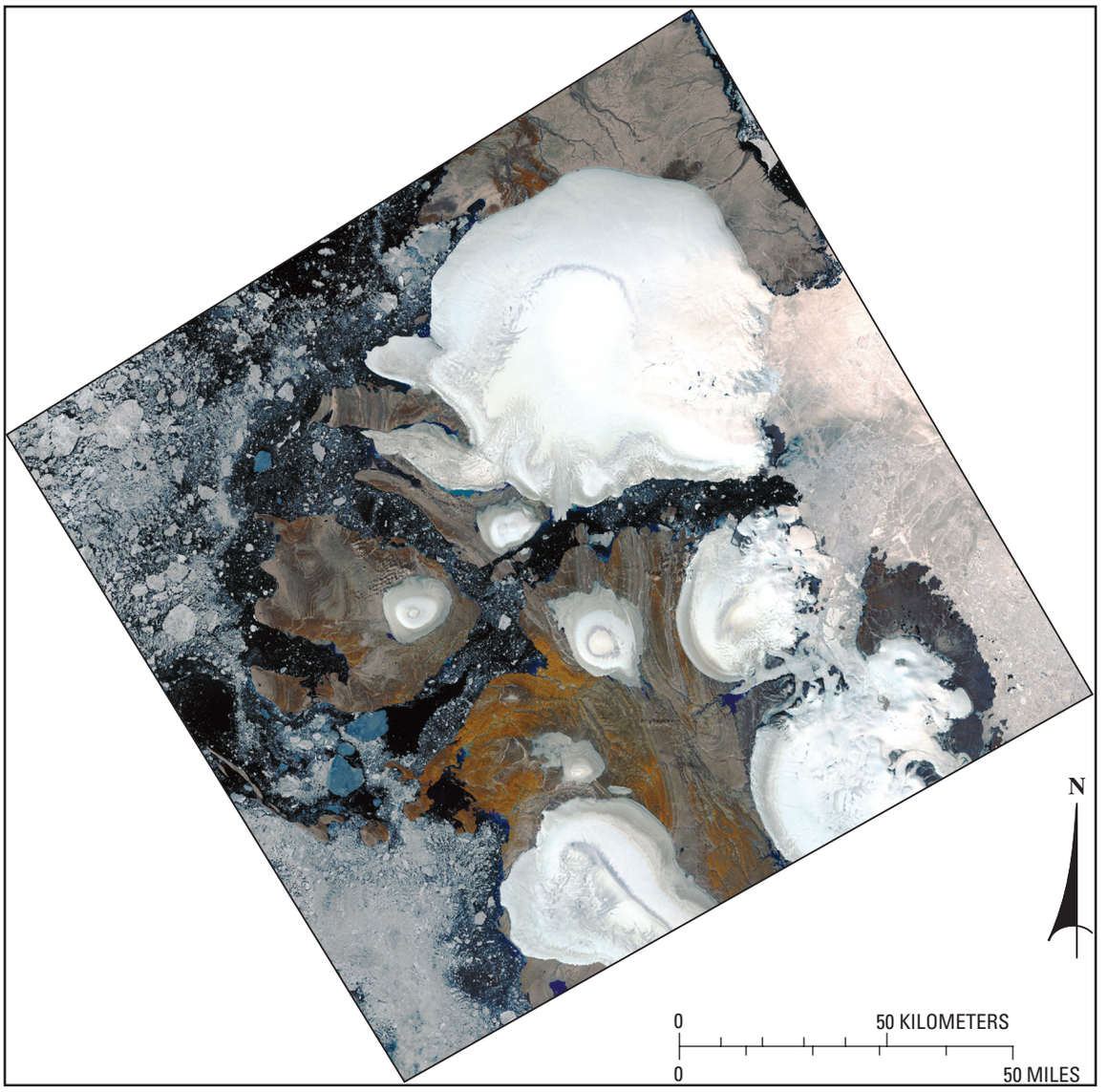


***Figure 84.**—Landsat false-color Multispectral Scanner (MSS) image of the ice caps in northern Severnaya Zemlya (located in fig. 83). The 185 x 185 km full scene was acquired on 22 July 1975. It shows the zones of melting on several ice caps. The 5,575 km^2 Lednik Akademii Nauk is the largest in the archipelago. The grayish zones closest to the ice-cap margins are interpreted to represent bare glacier ice. The upper, white regions are snow-covered ice, and the thin blue/gray zone separating them is interpreted as a slush zone. A summer cover of shorefast sea ice is present around the islands.*

The oxygen-isotope and melt-layer records in deep ice cores (550–760 m deep) from the Ledniki Vavilova and Akademii Nauk indicate that temperatures have risen markedly in the last 120–140 years (Vaikmyae and Punning, 1984; Kotlyakov and others, 1989, 1990), but interpretation of the older parts of each core is hampered by poor chronological control associated with strong surface melting (Tarussov, 1992). Analysis of aerial photographs of the archipelago, acquired since the 1930s, shows a general retreat of glacier margins, interpreted to be linked to the termination of the "Little Ice Age," as indicated in the ice-core record. A loss of about 500 km^2 of ice-covered area in Severnaya Zemlya between 1931- 84 was reported by Govorukha and others (1987), although Koryakin (1986) suggests that this may be an over-estimate resulting from errors in interpretation of aerial photographs.

Novaya Zemlya

About 24,400 km^2 or 30 percent of the two major islands making up Novaya Zemlya is ice covered (fig. 85), with the larger proportion on the northern island (Kotlyakov and others, this volume). There appears to be little recent glaciological information available on Novaya Zemlya, perhaps reflecting its role as a major site for nuclear weapons testing (Lamb, 1991). Mean annual temperature on the northern tip of Novaya Zemlya is -9 °C, with a July mean of 2 °C; on the milder west coast, the July mean is 6.5 °C. Precipitation is also higher on the west coast, reflecting the influence of relatively moist westerly air masses derived from the Norwegian Sea. The late summer snowline elevation decreases toward the north; the elevation is about 600 m near Matochkin Shar, the strait separating the main islands (fig. 85), it falls to 450 m at about lat 75°N., and is at 325 m in the northernmost part of Novaya Zemlya (McCauley, 1958). The equilibrium line is about 200 m lower on the western Barents Sea margin than on the eastern Kara Sea side of the islands. Calculations of net mass balance for the ice cover on Novaya Zemlya, based on empirical relationships between temperature, accumulation, and ablation, suggest that the net balance has been negative, by a mean of about 0.16 m a^{-1}, for most years since the 1920s (Chizhov and Koryakin, 1962). Measurements on a number of glaciers, some of which drain the central ice field on the north island, indicate that ice masses shrank by about 2–3 percent between the 1930s and the 1950s, and some tidewater glaciers retreated by up to 7 km (Chizhov and Koryakin, 1962; Chizhov and others, 1968). Zeeberg (2001) and Zeeberg and Forman (2001) also report that most of the 20th century glacier retreat in northern Novaya Zemlya was complete by the 1950s, with slower retreat since that time.

Other Glacierized Islands in the Russian High Arctic

Less than 1 percent of the glacierized area in the Russian High Arctic occurs outside Franz Josef Land, Severnaya Zemlya, and Novaya Zemlya (fig. 80). Ostrov Viktoriya, between Svalbard and Franz Josef Land at 80°N., 37°E., is the westernmost island in the Russian Arctic and lies only about 60 km east of the 99 percent ice covered Norwegian island of Kvitøya (Bamber and Dowdeswell, 1990). The 11 km^2 ice cap on Ostrov Viktoriya has a maximum elevation of 110 m. It has a consistently negative mass balance; its entire surface exhibits summer melting, and old glacier ice is exposed at the surface (Govorukha, 1964, 1988b).

Ushakov Island (Ostrov Ushakova), with a completely glacierized surface of 325 km^2, is located between Franz Josef Land and Severnaya Zemlya at lat 81°N., long 79.5°E. (fig. 80). The ice cap has a negative mass balance, but retains a zone of net accumulation above an equilibrium line at 200–250 m in altitude (Govorukha, 1988b). It has a maximum ice thickness of almost 300 m, measured from radio-echo sounding (Bogorodskii and Federov, 1971).

In the Asian Far East sector of the Russian High Arctic, ice masses totaling about 60 km^2 occur on Ostrova De-Longa, located northeast of the ice-free Novosibirskiye Ostrova between lat 76–77°N. and long 149–158°E. (fig. 80). On Ostrova De-Longa, the largest ice mass is the *Tollya Ice Cap* on Bennett Island (Ostrov Bennetta), with an area of about 55 km^2, a maximum elevation of 380 m, and a firn line at about 180 m. Smaller ice masses occur on Henrietta Island (Ostrov Genriyetta) and Jeanette Island (Ostrov Zhannetta), with areas of 6 and 0.4 km^2, respectively (Bazheva, 1981; Verkulich and others, 1992). Mass balance investigations on Ostrov Bennetta in 1986–87 showed net losses on each of the four ice masses and, combined with meteorological data for the previous 30 years, suggested negative balances for about 70 percent of this period (Verkulich and others, 1992). Wrangel Island (Ostrov Vrangelya), at 71°N., 180°E., contains a few semi-permanent snow patches but no glaciers.



Figure 85.—*Map of Novaya Zemlya showing the distribution of ice masses. The locations of Landsat images in subsequent figures are shown as boxes.*

Glaciological Investigation of Russian High Arctic Ice Masses from Landsat Imagery

Landsat imagery has been used effectively to better define the Russian High Arctic ice masses. It has been used to determine ice-surface topography, delineating ice divides and drainage basins. Secondly, it has been effective in identifying the ice dynamics of the outlet glaciers, icebergs, and floating ice shelves, and in locating surge-type glaciers. Thirdly, snow and ice facies visible on glacier surfaces have provided information on snow- and equilibrium-line positions, and have been used as proxy indicators of mass balance.

Ice-Surface Topography

Drainage basin geometry is a basic unit for glaciological studies of large ice masses. Neighboring drainage basins within ice caps can display varying dynamic behavior (for example, Dowdeswell, 1986a). Glaciological measurement programs and modeling studies need to take into account this morphological and dynamic variability. The identification and mapping of ice divides and drainage basins therefore represents an important prerequisite to the planning and execution of detailed glaciological investigations on the relatively little known ice caps of the Russian High Arctic.

Drainage basins on large ice masses, and the ice divides that define their boundaries, can be identified using evidence derived from satellite remote sensing. By contrast, field-survey methods cannot usually provide sufficient spatial coverage for such investigations. On the large ice sheets of Antarctica and Greenland, satellite radar altimetry can yield topographic data of high absolute accuracy in order to identify drainage basins. For ice caps of less than a few thousand square kilometers in area, such as those in the Russian High Arctic, the 18-km diameter footprint of the radar altimeter of the ERS series is large relative to the size of the ice mass; therefore, data from this source are of limited use for topographic mapping of these smaller ice caps. However, satellite imagery from both the visible and near-infrared instruments aboard Landsat, along with high-resolution data from Russian satellite photographic cameras (for example, KFA-1000, KATE-200), SPOT, ASTER, and from the ERS synthetic aperture radar (SAR), can be used to define ice divides and drainage basins on smaller ice caps (Martin and Sanderson, 1980; Dowdeswell and McIntyre, 1987; Williams and others, 1991; Dowdeswell, Rees, and Diament, 1994).

The results of satellite image identification of ice divides for the Franz Josef Land archipelago are shown in figure 86. About 915 km of ice divides are mapped from the available imagery (Dowdeswell, Glazovskii, and Macheret, 1995). The map does not necessarily show all of the major ice divides in the archipelago, but only those that could be identified from the available Landsat, Russian, and ERS-1 SAR satellite imagery. It was possible to map drainage basins in greater detail on some of the Franz Josef Land ice caps which were more heavily dissected by bedrock outcrops, especially where nunataks (isolated bedrock outcrops exposed above the general ice cover) acted as basin margins.

There is, in general, an inverse relationship between ice-cap size and the ability to plot basin boundaries from rock outcrops. The largest ice masses in the Franz Josef Land archipelago, on Vilchek (Vil'cheka) and Graham Bell (Greem-Bell) islands (figs. 82, 86), have very few nunataks; therefore, basin extent can, for the most part, be mapped only from the identification of ice divides on satellite imagery, as illustrated on the satellite image of the Hall

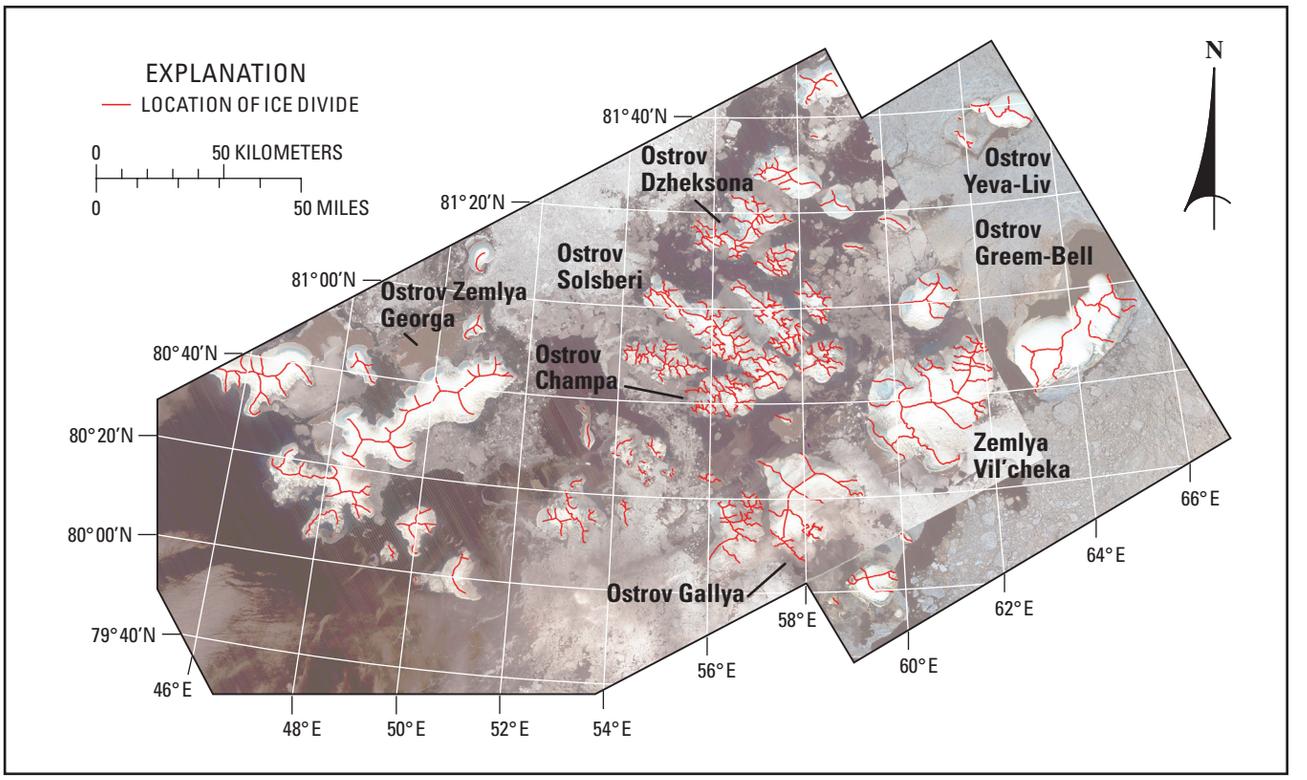


***Figure 86.**—Map of the ice divides on the ice caps of Franz Josef Land, shown on a georeferenced mosaic of Landsat TM images from Path 199–Rows 001 and 002, acquired on 25 July 1986. From Williams (2003).*

Island (Ostrov Gallya) ice cap in figure 87. By contrast, the ice caps on islands such as Salisbury (Solsberi), Champ (Champa), and Jackson (Dzheksona) can be subdivided extensively on the basis of large numbers of nunataks. On a few ice caps, particularly those on Ostrova Greem-Bell and Eva-Liv (Yeva-Liv) (fig. 86), few ice divides were identified, probably because these ice masses have a particularly well-defined shape with a single summit, rather than having elongate crests with similar summit elevations extending for a number of kilometers, such as George Land (Ostrov Zemlya Georga), where the crest extends for tens of kilometers (fig. 86).

Similar analyses of the locations of ice-cap divides and drainage basins have been conducted for the archipelagos of Severnaya Zemlya and Novaya Zemlya (for example, Williams and Dowdeswell, 2001). On the northern island of Novaya Zemlya (fig. 85), the position of the major ice divide separating ice flowing west to the Barents Sea and east to the Kara Sea is shown in figure 88. The ice ridges between the drainage basins of individual outlet glaciers ending in tidewater can also be seen. The outlet glaciers generally have less smooth surfaces than the intervening ridges.

Ice Dynamics

Landsat imagery has been used to determine the ice dynamics of Russian High Arctic outlet glaciers, icebergs, and floating ice shelves, or ice tongues. It has also been valuable in identifying surge-type glaciers in the region.

Outlet Glaciers and Icebergs

Examination of Landsat imagery of many of the larger ice caps in the Russian High Arctic archipelagos shows that they are composed of a number of clearly identifiable drainage basins which are likely to behave as dynamically distinct entities (for example, Dowdeswell and others, 2002). Marked

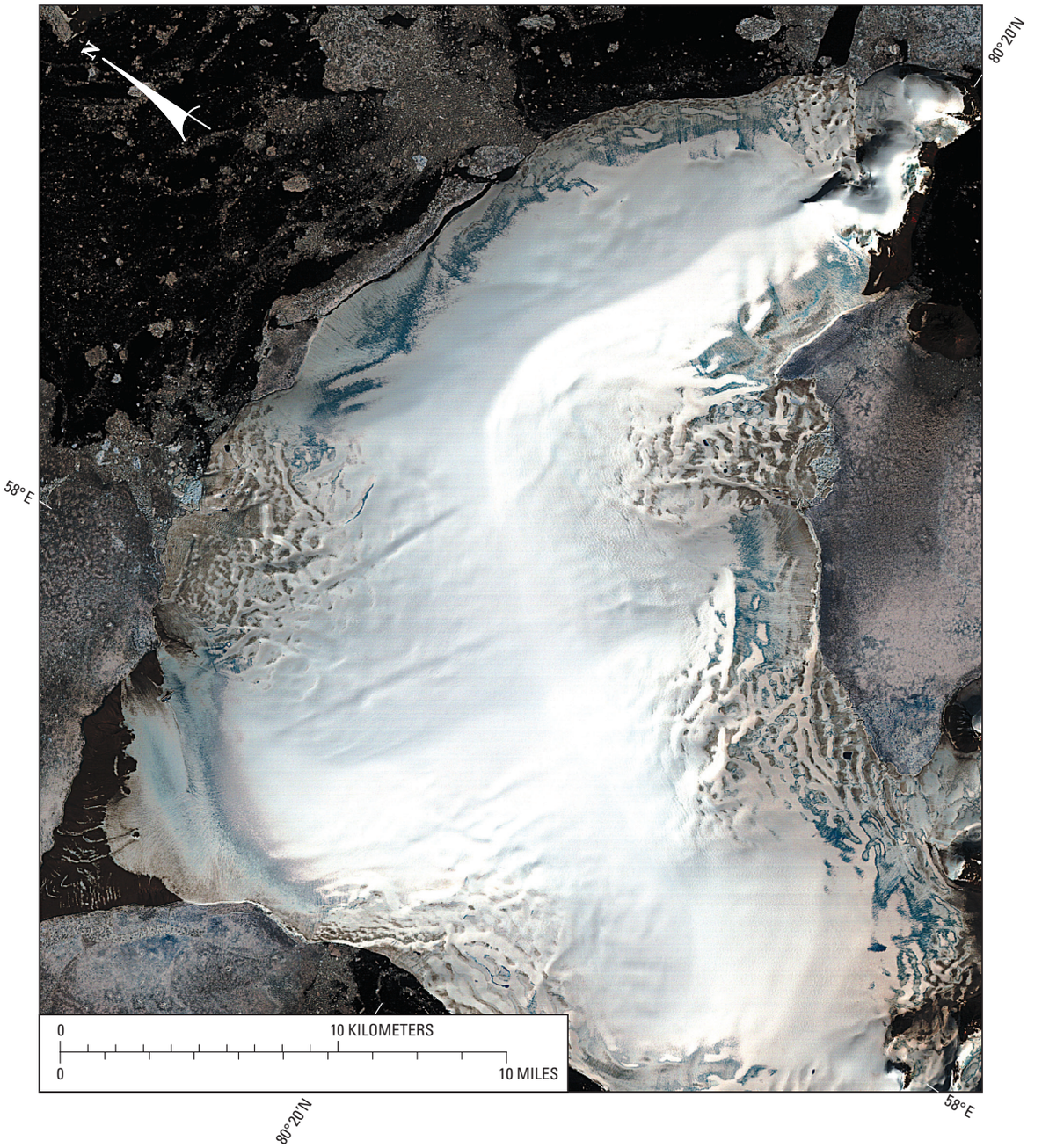


***Figure 87.**—An example of the major ice divides on the Ostrov Gallya ice cap in Franz Josef Land. The digitally enhanced Landsat TM sub-scene is from Path 197–Row 001, acquired on 1 August 1988. Ostrov Gallya is located in figure 82.*

differences in the behavior of individual drainage basins within Arctic ice caps have been demonstrated previously for the two largest ice caps on Nordaustlandet in the Norwegian archipelago of Svalbard, west of Franz Josef Land (Dowdeswell, 1986a; Dowdeswell and Collin, 1990; Dowdeswell and others, 1999, 2008), and for the Devon Island Ice Cap in Arctic Canada (Dowdeswell and others, 2004; Burgess and others, 2005).

A number of the ice caps and drainage basins on Franz Josef Land, Severnaya Zemlya, and Novaya Zemlya have outlet glaciers which appear to have relatively rapid flow speeds and significant production of large tabular icebergs. Landsat images of the seaward margins of several outlet glaciers are shown

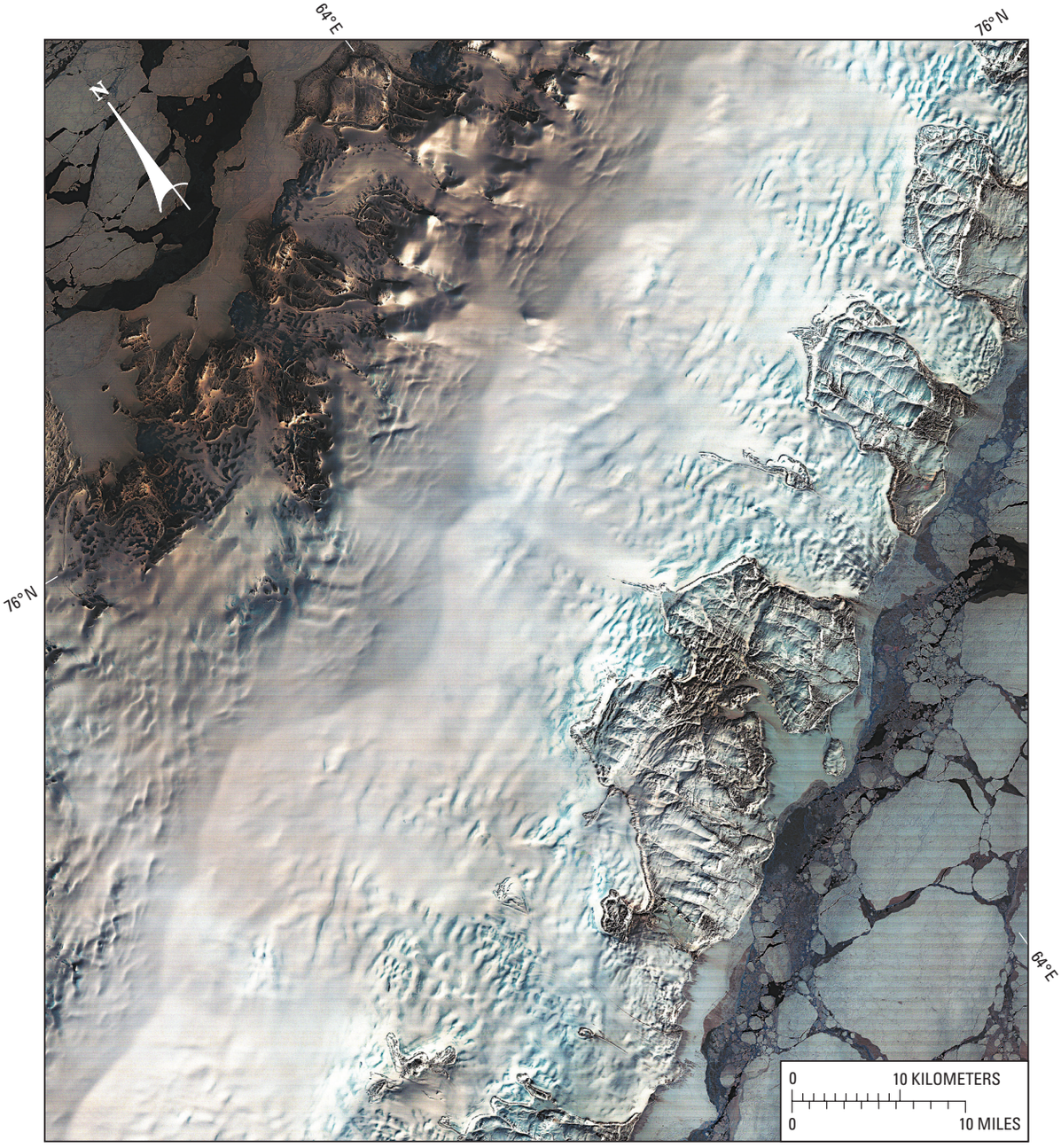
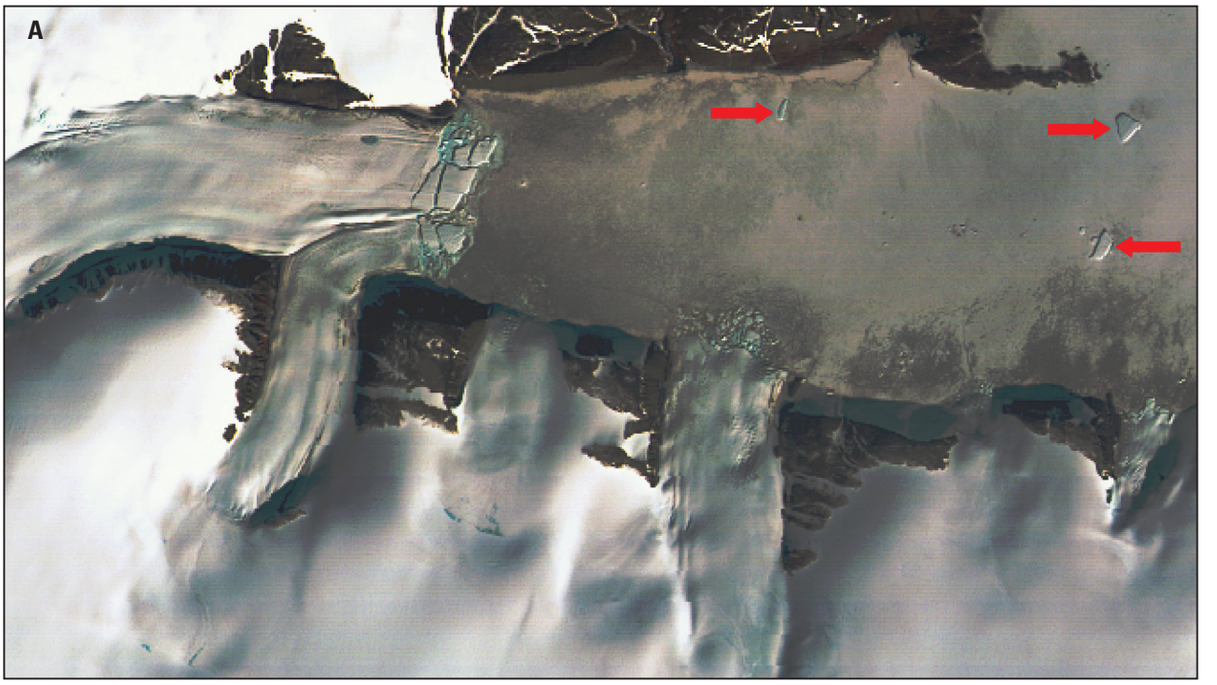
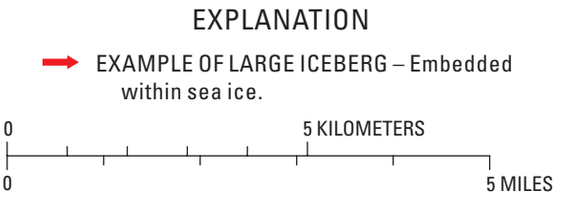


***Figure 88.**—Digitally-enhanced Landsat TM sub-scene of the major ice divide running along the northeast-southwest trending spine of Novaya Zemlya. Outlet glaciers descending from the central divide to end in tidewater are shown on both sides of the island. The TM image is from Path 178–Row 006, acquired on 6 July 1986. It is located in figure 85.*

in figure 89. Each image shows linear boundaries, delineating ice-flow units from different parts of the upper drainage basin. In each case, the outlet glacier or ice stream appears on Landsat imagery to be the site of iceberg production (Dowdeswell and others, 2002). Close to several of the tidewater ice margins, transverse and sometimes chaotic crevassing is observed on the satellite imagery. The transverse crevasses indicate longitudinal tension at the unconfined ice cliffs at the glacier terminus (Hodgkins and Dowdeswell, 1994), and provide fractures along which iceberg calving takes place. The fast-flowing ice streams within the Lednik Akademii Nauk on Severnaya Zemlya can be clearly identified using both Landsat imagery and synthetic aperture radar interferometry (Dowdeswell and





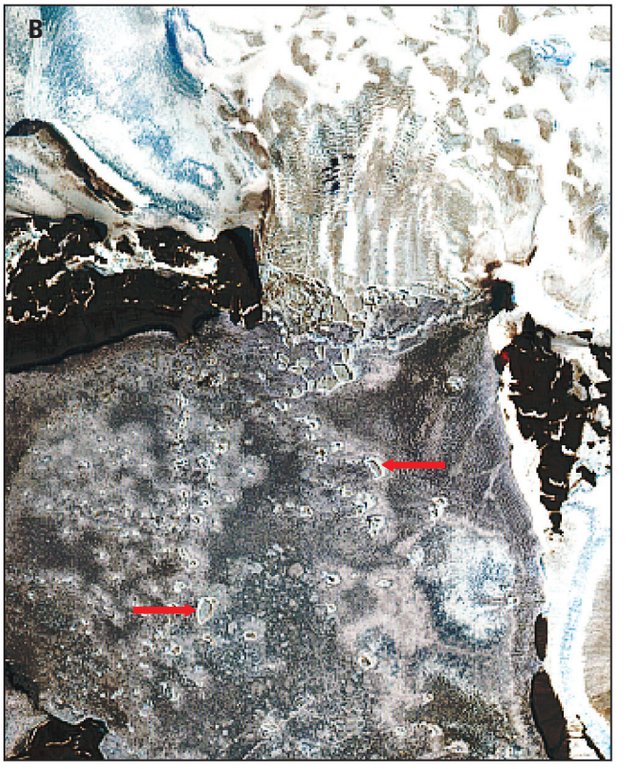


***Figure 89.**—Landsat TM images of iceberg-producing outlet glaciers draining ice caps in the Russian High Arctic. The sea is usually covered by sea ice a meter or two thick in these images, and many icebergs (some larger bergs arrowed) can be seen embedded within this ice, which is often shorefast.* **A**, *Outlet glaciers and tabular icebergs from Severnaya Zemlya (located in figure 83). The scene is from Path 164–Row 003, acquired on 26 August 1988.* **B**, *Outlet glacier of the Zemlya Vil'cheka ice cap in Franz Josef Land (located in figure 82). The scene is from Path 197–Row 001, acquired on 1 August 1988.*

others, 1999); these ice streams produce large numbers of tabular icebergs (up to 1.7 km in length and about 2 km^2 in area) and a total flux of about 0.5 $km^3\ a^{-1}$ (Dowdeswell and others, 2002).

Several authors, including Sandford (1955), Voevodin (1972), and Abramov (1992), have reported the occurrence of tabular icebergs in Franz Josef Land waters, and icebergs in the Barents Sea which are inferred to be derived from the ice caps of Franz Josef Land. The calving of tabular icebergs from several low-gradient margins of ice caps on Franz

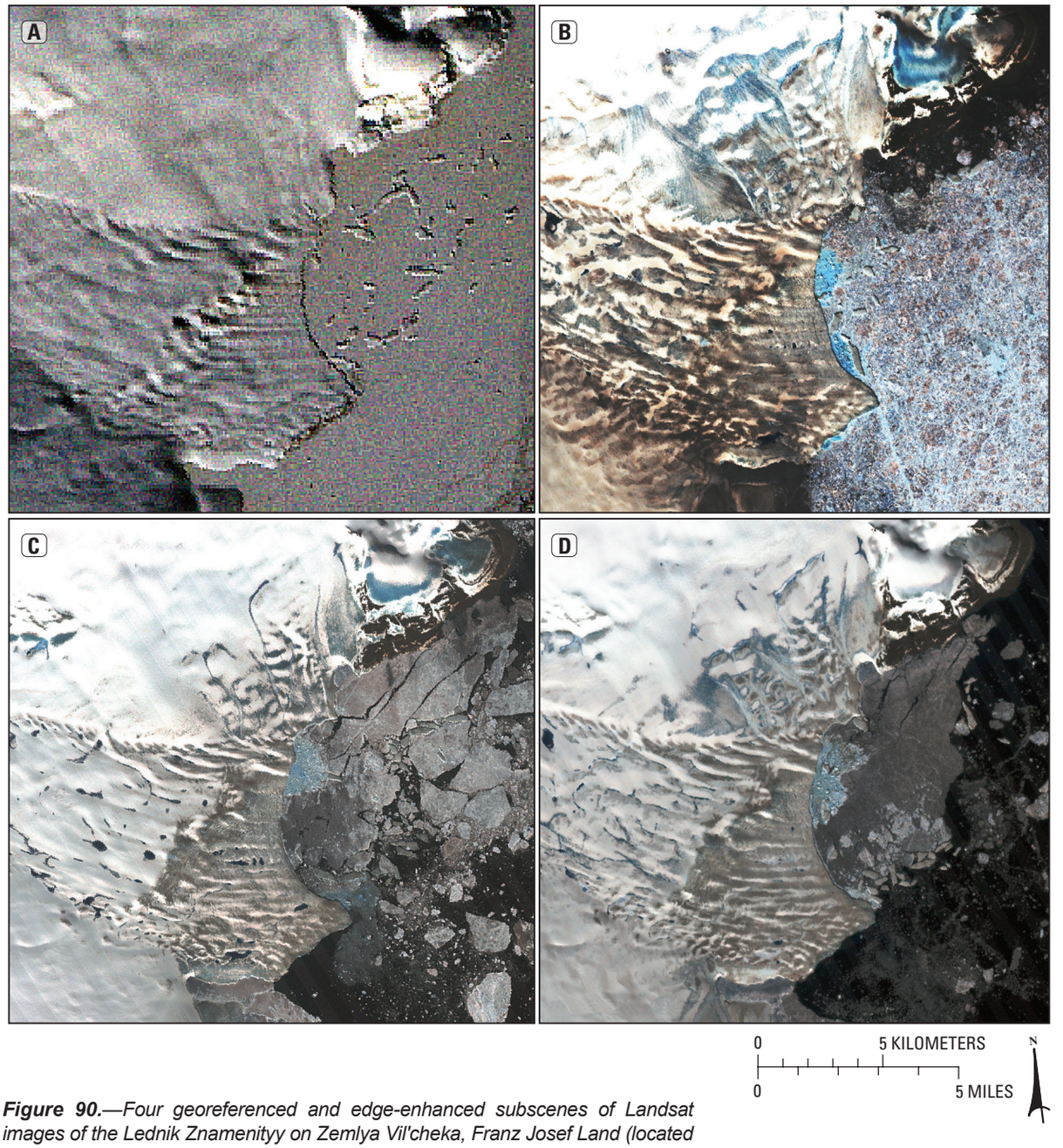


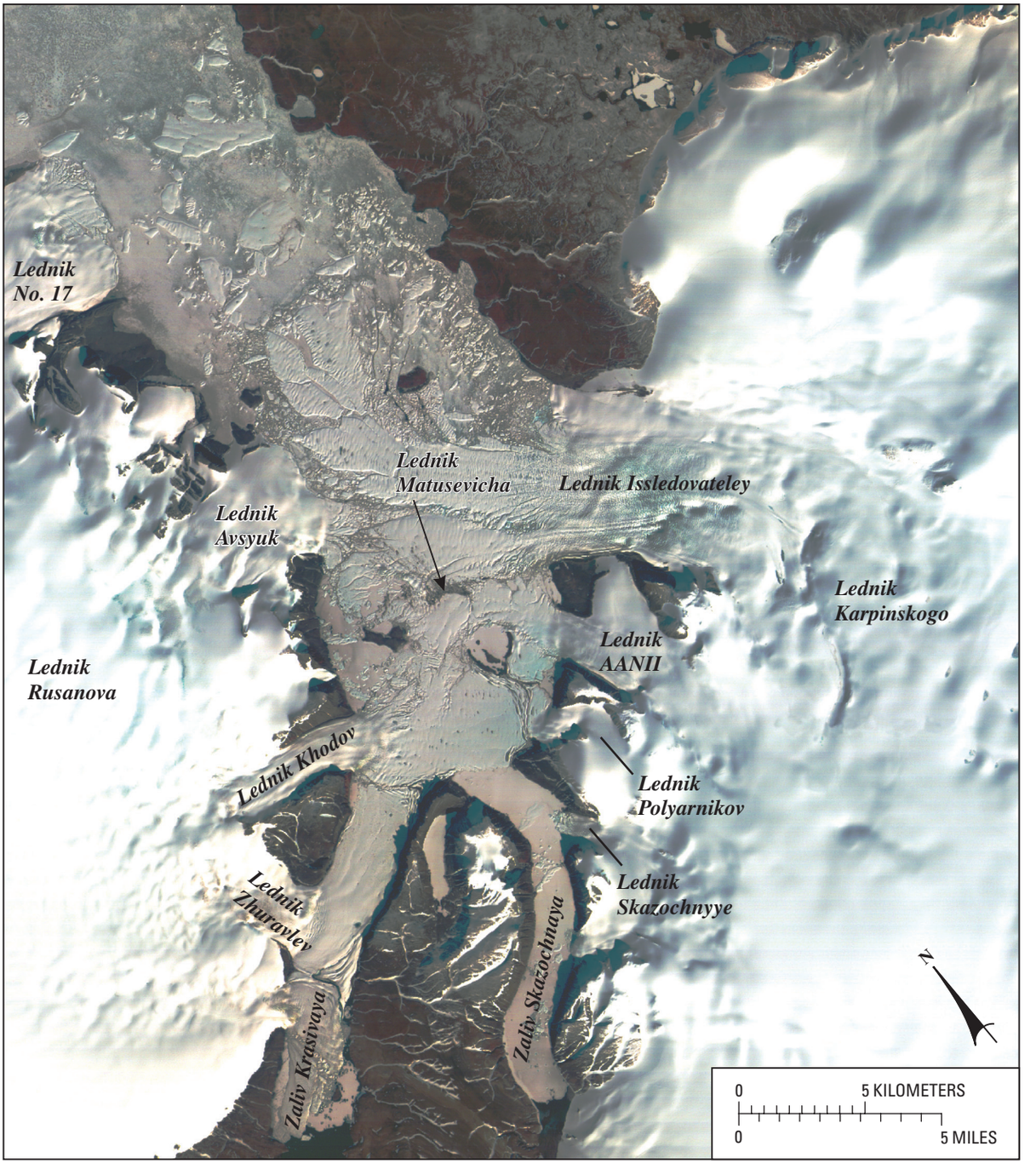
***Figure 90.**—Four georeferenced and edge-enhanced subscenes of Landsat images of the Lednik Znamenityy on Zemlya Vil'cheka, Franz Josef Land (located in figure 82) showing large numbers of tabular icebergs. The tabular icebergs calved from this outlet glacier are among the largest produced in Franz Josef Land. The large iceberg in image **B** is >1.9 km in length. **A**, MSS image, of 8 May 1983 (Path 197–Row 001). **B**, TM scene of 25 July 1986 (Path 199–Row 001). **C**, TM scene of 8 August 1987 (Path 196–Row 001) and **D**, TM scene of 1 August 1988 (Path 197–Row 001) (From Williams, 2003).*

Josef Land has also been observed on Landsat imagery. The largest tabular icebergs observed on available satellite scenes are found offshore of Lednik Znamenityy, on Zemlya Vil'cheka (fig. 90). The icebergs appear to have smooth upper surfaces and are up to about 2 km in length and about 3 km^2 in area. Tabular icebergs longer than 200 m have also been observed on Landsat TM imagery, offshore of other drainage basins of Zemlya Vil'cheka, and offshore of Ostrova Zemlya Georga, Ziegler (Tsiglera), Solsberi, and Gallya in Franz Josef Land (fig. 82). Upon examination of photographic

products from the Russian KATE-200 satellite camera system, the largest tabular iceberg observed in Franz Josef Land was 2.3 km in length (Dowdeswell, Gorman, Macheret and others, 1996).

Floating Ice Shelves or Ice Tongues

Ice shelves have been noted only infrequently in the little-known Eurasian Arctic sector, and the largest northern hemisphere ice shelf is the Ward Hunt off Ellesmere Island, Canada (Jeffries, 1987, 2002). Three ice shelves have, nonetheless, been reported from the Severnaya Zemlya archipelago (Dibner, 1955; Zinger and Koryakin, 1965; Govorukha, 1988a). These occur on Ostrova Komsomolets and Oktyabr'skoy Revolyutsii (fig. 83). The largest, the *Lednik Matusevicha*, is illustrated on the Landsat image in figure 91.



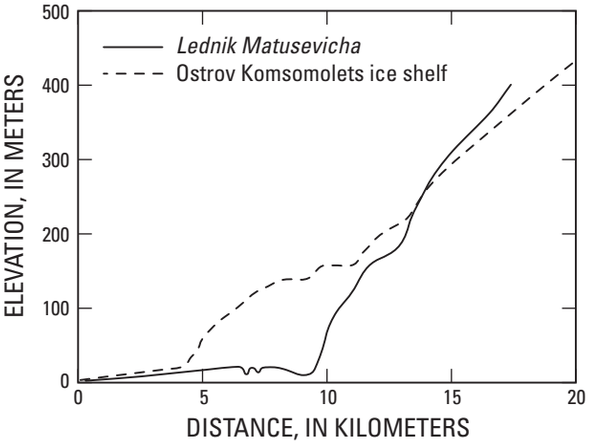


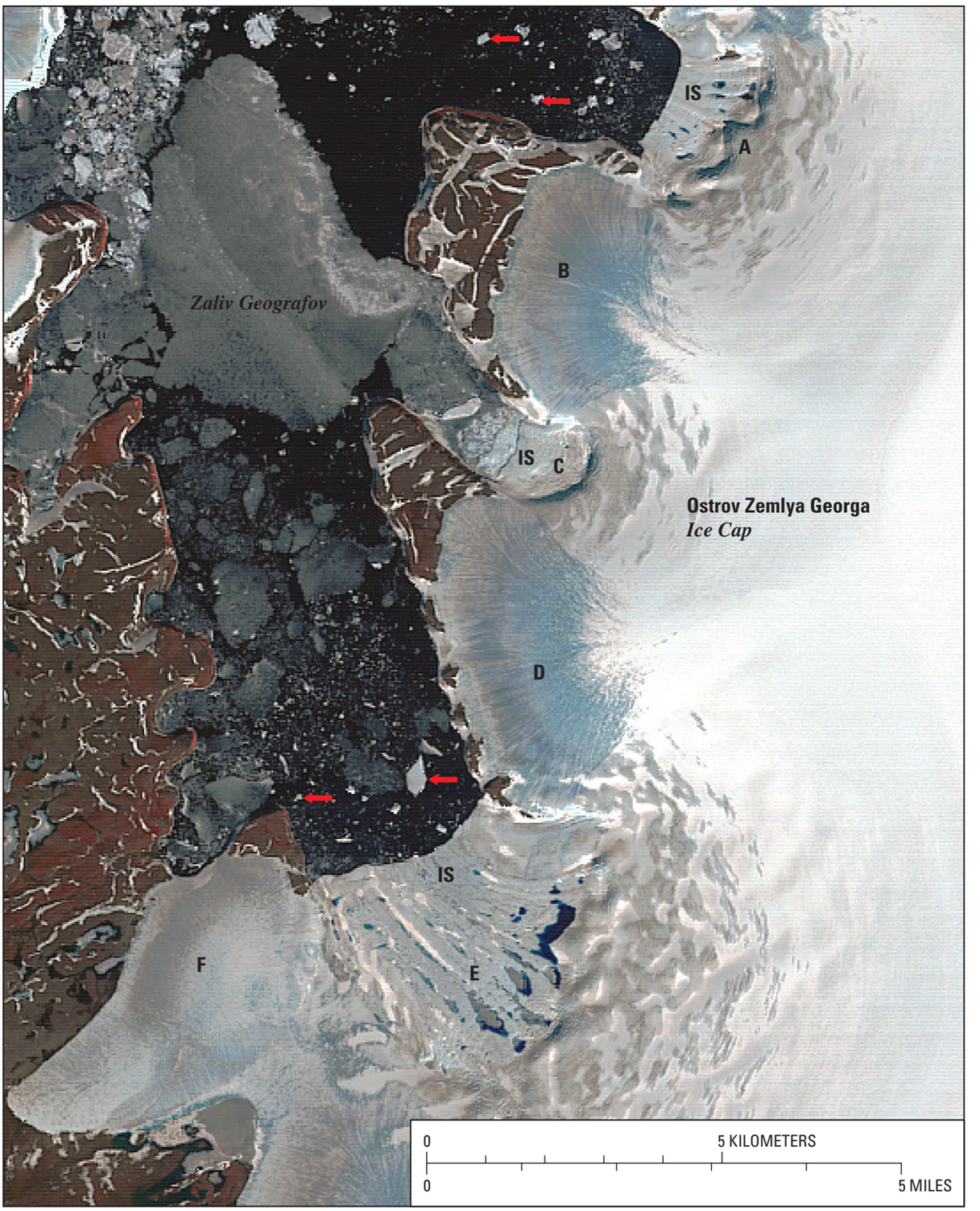
***Figure 92.**—Ice-surface profiles from two ice shelves and their parent drainage basins on Severnaya Zemlya, derived from analysis of Russian aerial photographs from the 1950s. The* Lednik Matusevicha *is imaged in figure 91, and the smaller ice shelf on Ostrov Komsomolets is fed by an eastern outlet of the Lednik Akademii Nauk. Modified from Dowdeswell, Gorman, and others (1994)*

This ice shelf is about 200 km^2 in area, with a surface slope of less than 0.2° near its margin (Govorukha, 1988a). Although this feature is referred to as an ice shelf, according to the definition of Armstrong and others (1966), it is similar to a floating ice tongue. Ice-surface profiles of (1) the *Lednik Matusevicha* and its drainage basin, and (2) an outlet glacier of the Lednik Akademii Nauk, on Ostrov Komsomolets, are given in figure 92. The marginal 9- and 4-km elevations of these profiles, respectively, represent floating ice shelves. Williams and Dowdeswell (2001) measured terminus fluctuations and the drift of icebergs calved from *Lednik Matusevicha* using Landsat and earlier imagery. Between 1931 and 1994, the floating margin of the ice shelf underwent at least 2 cycles of retreat followed by advance. Most icebergs calved from the ice shelf remain trapped within the adjacent fjord for 10 to 20 years.

There is some controversy in the early Russian literature as to the occurrence of ice shelves in Franz Josef Land. Spizharskiy (1936), Shumskiy (1949), and Govorukha (1968) each suggest that some small ice shelves may be present, whereas Grosswald and others (1973) argue that none exist. Evidence in support of either case is ambiguous, although Govorukha (1968) states specifically that an ice shelf is present in the northeast of Ostrov Zemlya Georga (fig. 82).

A number of ice caps with smooth and apparently very low surface gradients at their seaward margins were observed on Landsat Thematic Mapper (TM) and Multispectral Scanner (MSS) satellite imagery of Franz Josef Land (fig. 93) (Dowdeswell, Gorman, and others, 1994). These areas are often associated with the production of relatively large tabular icebergs. The areas are dynamically part of the parent ice mass and have a marked break of slope at their inner margins. Most, although not all, of the low gradient margins are located in relatively protected embayments, rather than along sections of open coastline, and there is often relatively deep water offshore. These flat features account for 315 km^2 or 2.3 percent of the total area of the ice caps in the archipelago and the largest of these low gradient areas is 45 km^2 (fig. 94).

***Figure 91.**— (at left) Annotated Landsat TM band 3 subscene of the* Lednik Matusevicha *on Ostrov Oktyabr'skoy Revolyutsii, Severnaya Zemlya (located in figure 83). The ice shelf is composed of units derived from outlet glaciers of the Rusanova (west) and Karpinskogo (east) ice caps. Tabular icebergs up to about 4 km long are being calved from the ice-shelf margin. The Landsat TM subscene was acquired on 26 August 1988 from Path 164–Row 003. From Williams (2003).*



EXPLANATION

IS at A, C, and E INTERPRETED AS POSSIBLE ICE SHELVES
B, D, and F ICE RIDGES OR CAPS – Separating flat marginal areas
INDICATES EXAMPLE OF TABULAR ICEBERG

***Figure 93**.—Landsat TM image of three flat ice-marginal glacier termini on the ice cap on Ostrov Zemlya Georga, western Franz Josef Land (located in figure 82). IS denotes ice shelves. Ice ridges or caps separate the flat marginal areas. Tabular icebergs (examples arrowed) can be seen in the sea beyond the ice shelf margins among sea-ice floes. The scene is from Path 199–Row 002, acquired on 25 July 1986.*

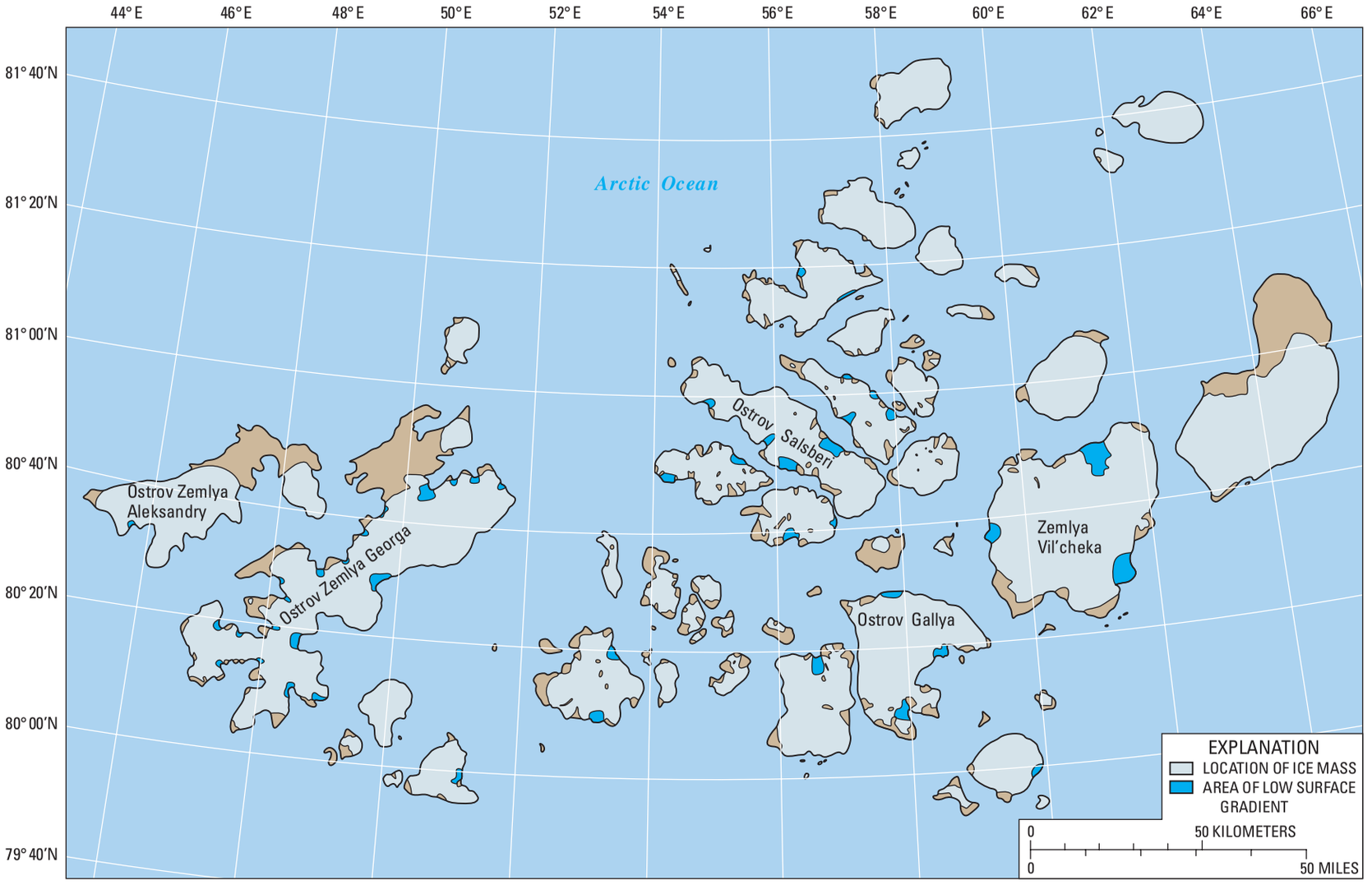


Figure 94.—*Map of the ice caps on Franz Josef Land, with marginal areas of low surface gradient shaded dark blue. Some of these ice-cap margins may be floating or near to full buoyancy. (Modified from Dowdeswell, Gorman, and others, 1994.)*

They make up a total of 175 km or 6 percent of the ice-ocean interface from which iceberg calving takes place. Ice-surface profiles, derived from analysis of vertical aerial photographs, show slopes of 0.5° on these features, as compared with 3.5–5° slopes on other ice caps in Franz Josef Land.

At least some of these smooth, low-gradient features at the margins of Franz Josef Land ice caps are likely to be floating ice shelves (Dowdeswell, Gorman, and others, 1994). They have ice surface gradients similar to gradients on the known ice shelves on Severnaya Zemlya (fig. 92). There is no requirement for deep water to occur beneath these features, but they must be buoyant over a significant part of their base. They provide one of the modern sources of tabular icebergs to both the eastern Barents Sea and to the Eurasian Basin of the Arctic Ocean (Dowdeswell, Gorman, and others, 1994).

Surge-Type Glaciers

Landsat imagery of the Russian High Arctic archipelagos has been examined for the presence of surge-type glaciers within the 56,000 km^2 of glacierized land. Ice-surface features and rapid changes in ice extent, sometimes easily identified on Landsat imagery, have been used to identify a large number of surge-type glaciers in the Svalbard archipelago to the west of Franz Josef Land (fig. 80). These features include looped medial moraines and highly crevassed ice surfaces, together with the rapid advance of the glacier terminus in a time series of images (for example, Meier and Post, 1969; Dowdeswell, 1986b; Liestøl, 1993; Kotlyakov and others, this chapter).

Landsat imagery covering more than 95 percent of the ice masses in the Russian High Arctic contains only very limited evidence of glacier surging (Dowdeswell and Williams, 1997). On Novaya Zemlya, three surge-type glaciers were identified using ice-surface characteristics. Two of these glaciers are located in the Nordenskiöld Bay (Zaliv Nordenshel'da) area on the west side of Novaya Zemlya (fig. 85), and are illustrated in the Landsat subscene in figure 95. The more northerly of these surge-type glaciers is heavily crevassed, as well as having a diagnostic looped medial moraine; it is inferred to be in the active phase of the surge cycle. A recent comprehensive analysis of Landsat and ASTER images of Novaya Zemlya has shown the presence of more than 30 glaciers of likely surge-type (Grant and others, 2009). On Severnaya Zemlya, two outlet glaciers of the Karpinsky Ice Cap (Lednik Karpinskogo) (fig. 83) also have looped medial moraines, suggesting past surge activity. On Franz Josef Land, no ice-surface features indicative of surging have been identified from Landsat imagery. It is concluded from these observations that there are only very small numbers of surge-type glaciers in this region (Dowdeswell and Williams, 1997). However, having incomplete coverage of the Russian High Arctic ice masses during times of the year most suitable for the identification of specific ice-surface features, and having time series of images for only a few Landsat Path–Rows, there may be more yet unidentified surge-type glaciers in this region.

The relative scarcity of identified surge-type glaciers in the Russian High Arctic provides a significant contrast with neighboring Svalbard (Liestøl, 1993), where more than 35 percent of ice masses are considered to be of surge-type (Hamilton and Dowdeswell, 1996). It is possible that the generally negative mass balances reported for Russian High Arctic ice masses since the end of the cold "Little Ice Age," about 100 years ago, have resulted in some glaciers switching from surge-type to non-surge type behavior. In Svalbard, it has been shown that some glaciers no longer surge; their consistently negative mass balance means they are thinning, their vertical temperature gradients are increasing, and basal melting is being replaced by a cold bed without the active hydrological system necessary for fast flow (Dowdeswell, Hodgkins, and others, 1995).

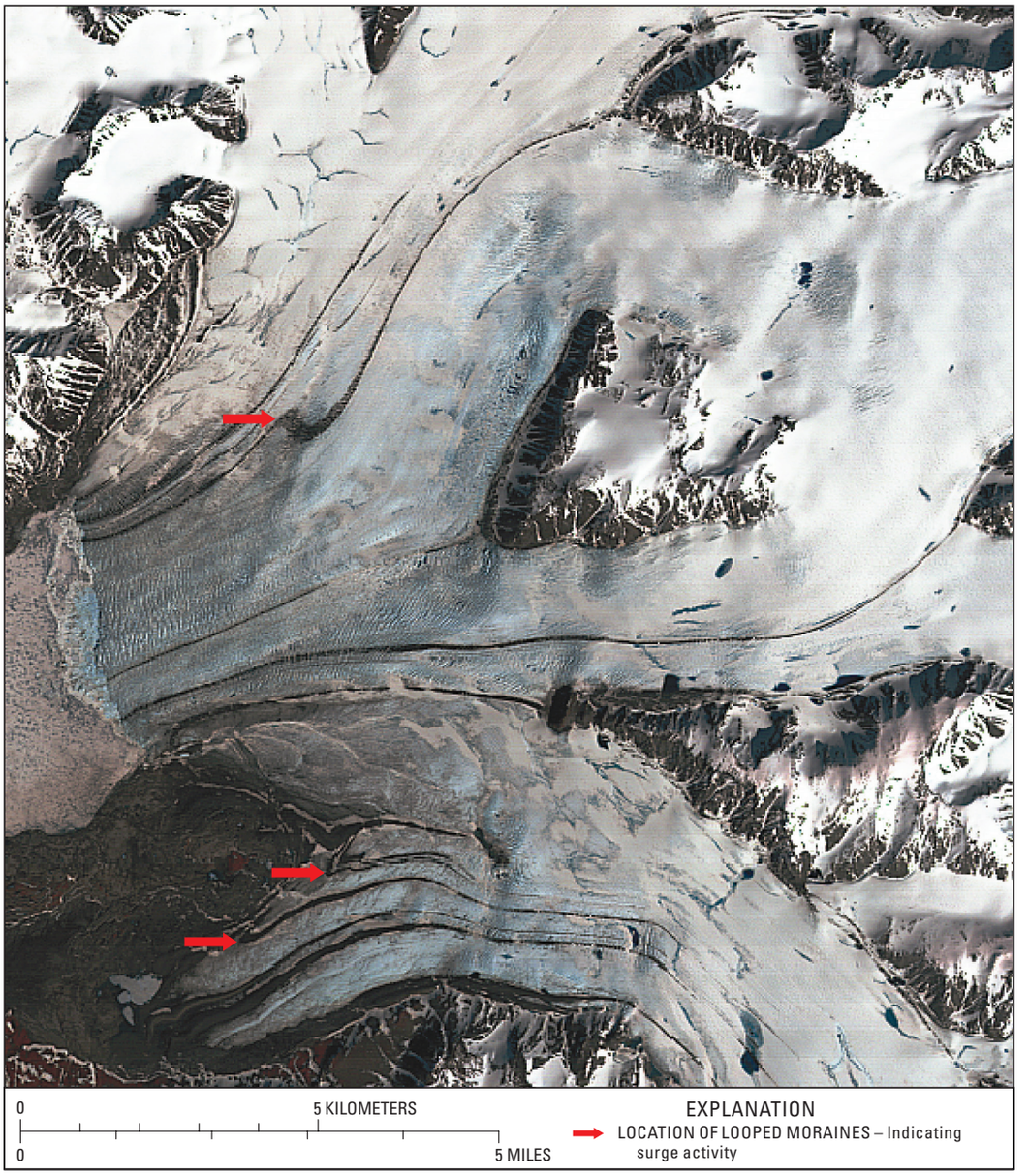


***Figure 95.**—Digitally enhanced Landsat TM image of the outlet glaciers entering Zaliv Nordenshel'da, Novaya Zemlya (located in figure 85). Note the looped moraines (arrowed) indicating surge activity. The image is from Path 178–Row 007, acquired on 6 July 1986.*

Snow-and-Ice Facies and Glacier Mass Balance

The patterns of snow-and-ice facies on the surfaces of glaciers (Benson, 1962) have been used in a number of satellite studies (1) to provide information on snow- and equilibrium-line positions, and (2) as proxy indicators of mass balance (for example, Williams and others, 1991). Late summer satellite images are required, and time series of observations can be constructed either within a given year, to monitor the up-glacier retreat of the transient snow-line, or for successive years, at the end of each melt season (for example, Dowdeswell and Drewry, 1989).

Three examples of the complexity of the spectral response associated with summer Landsat TM images of the Russian High Arctic are illustrated in figures 84, 96, and 97. A full 185-by-185 km Landsat TM image of the

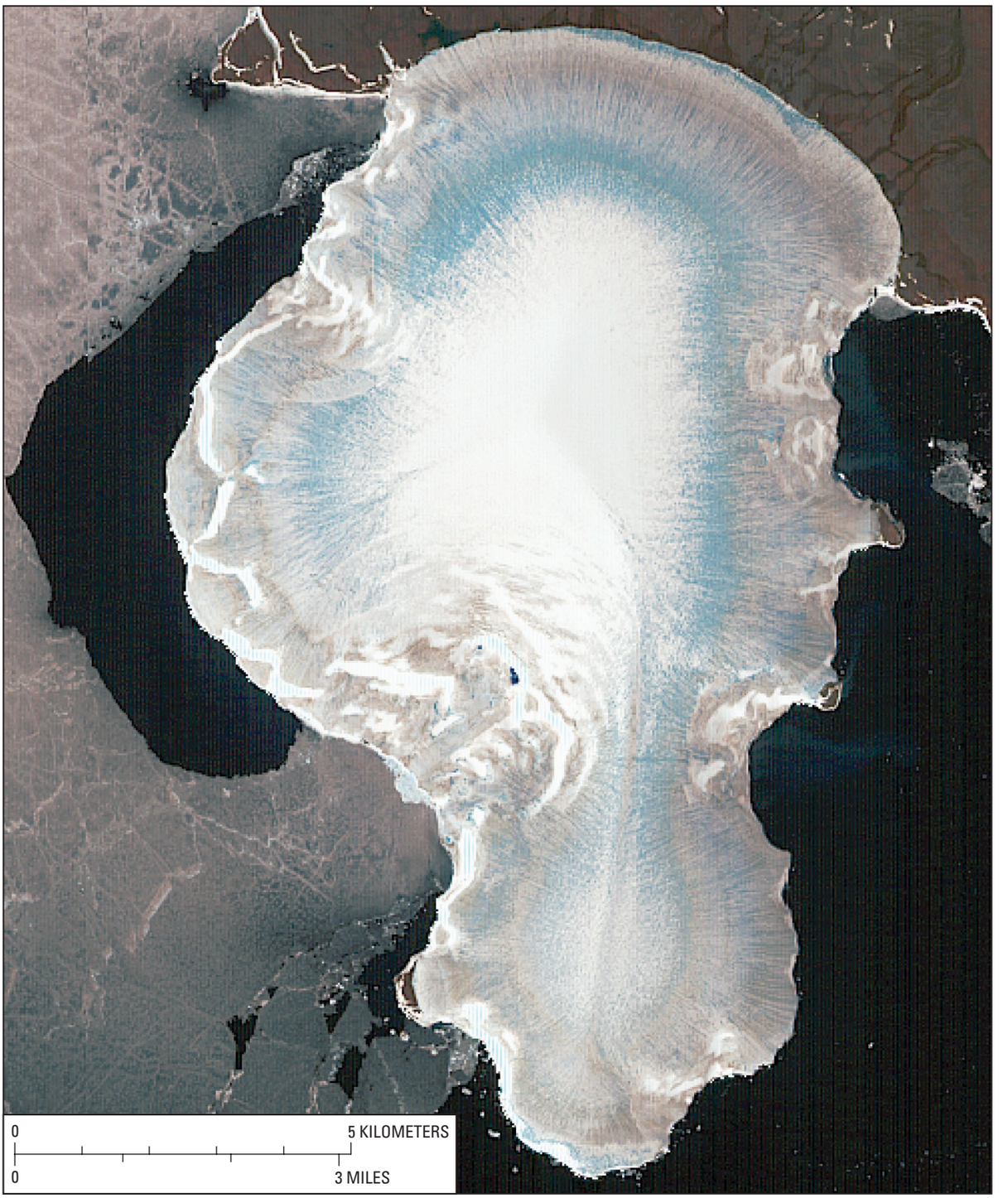


Figure 96.—*Digitally enhanced Landsat TM sub-scene showing the snow-and-ice facies on a summer image of the Lednik Kropotkina on Ostrov Zemlya Aleksandry, Franz Josef Land (Path 199–Row 001, acquired on 25 July 1986). The image is located in figure 82.*

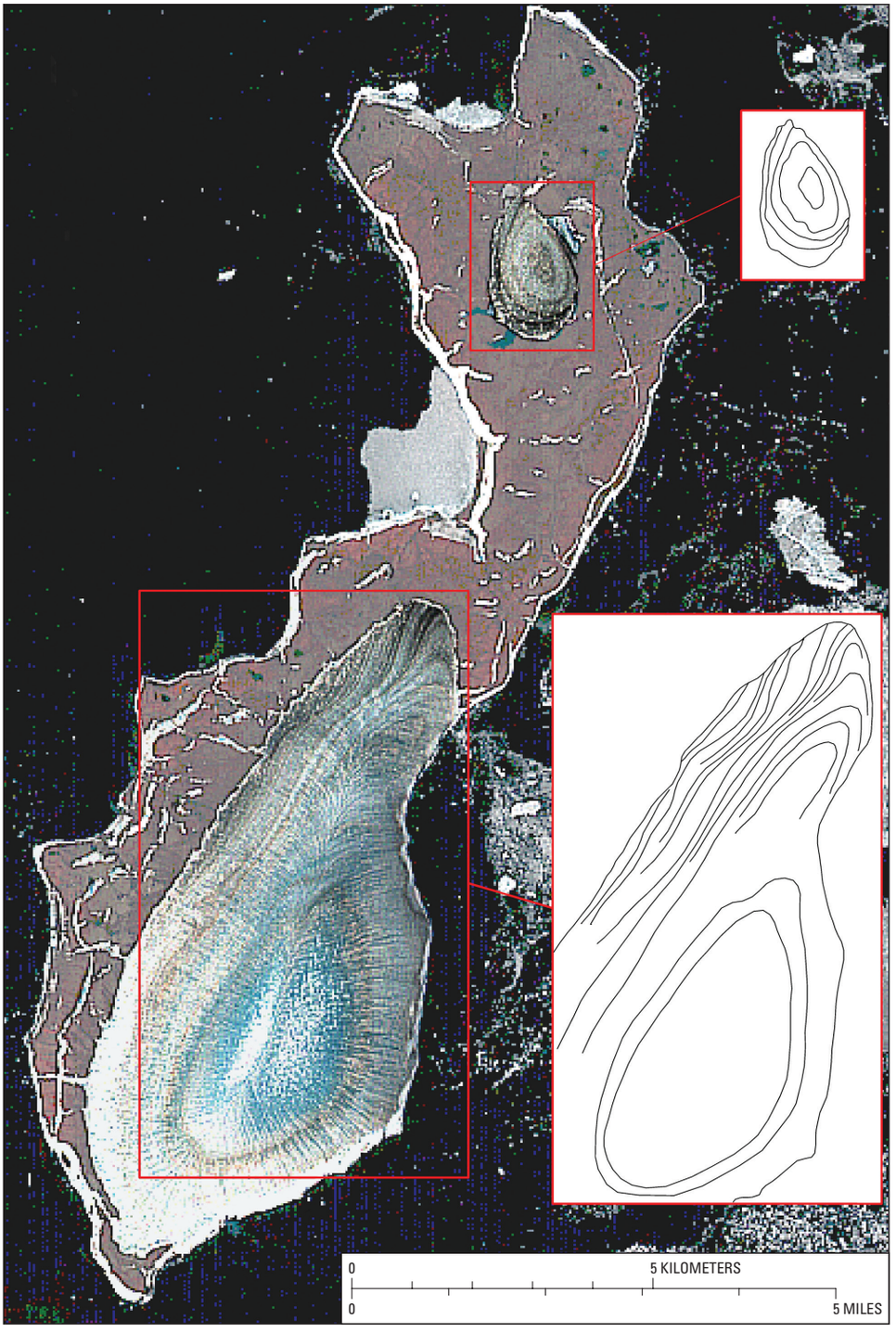


Figure 97.—*Landsat TM sub-scene of Ostrov Ketlitsa, Franz Josef Land (Path 199–Row 001, 25 July 1986) (located in figure 82). The two ice caps have bare ice exposed over most of their surface. The two insets are interpretations of the primary stratification exposed at the surface of each ice cap.*

northern part of Severnaya Zemlya, acquired during summer, shows a series of several spectral zones ranging from bare ice at the margin, through a thin slush zone, to snow on the crest of the main ice caps (fig. 84).

A second image (fig. 96) shows a TM sub-scene of the 120 km^2 Kropotkin Ice Cap (Lednik Kropotkina) on Alexandra Land (Ostrov Zemlya Aleksandry) in the Franz Josef Land archipelago. The detail in this image shows a large spectral variability within zones and the generally transitional nature of the boundaries between them. The surface of the ice cap is clearly not smooth, and snow remains in hollows close to sea level even in summer. The blue-colored slush zone, above the bare ice zone, appears to have a series of lineaments within it which extend in some cases down into the bare ice facies. These are interpreted as supraglacial drainage channels, which have been observed on glaciers in Franz Josef Land and eastern Svalbard (Rees and others, 1995). Two small supraglacial ponds are also observed. The ice cap appears to have two domes. The larger one has a continuous covering of snow at this stage of the summer melt season, but the lower one, to the south, appears to be composed largely of bare ice (fig. 96). This pattern may indicate that either accumulation is by superimposed ice only, or that net mass loss is taking place even at the crest of this smaller ice cap.

The image of the two small ice caps on Koettlitz Island (Ostrov Ketlitsa) (fig. 97), in western Franz Josef Land, illustrates an application of Landsat data to the problem of glacier response to climate change. The south and north ice caps cover a total of about 40 km^2 and have crests at 160 m and 50 m above sea level, respectively. The TM image was acquired on 25 July 1986, relatively early in the melt season, and yet the winter snow has almost completely disappeared from both ice caps to reveal ice. In the smaller (north) ice cap, ice structures assumed to represent primary depositional stratification are exposed right up to the summit, indicating that there is net mass loss over the entire ice cap (fig. 97). The northern margin of the larger (south) ice cap also contains primary structures or foliation which are clearly truncated (cf. Hambrey, 1975; Hambrey and Müller, 1978). This pattern suggests that thinning and retreat of this larger ice cap is also taking place. It is likely that most ice caps with summit elevations below about 150–200 m in the archipelago are in a state of strong negative balance, probably as a result of the warming experienced in the Eurasian High Arctic at the termination of the "Little Ice Age" and through modern warming.

Conclusions

Landsat digital and photographic products have provided important insights into several aspects of the morphology and dynamics of the relatively little-known glaciers and ice caps in the Russian High Arctic. This is so, despite the fact that this part of the Eurasian Arctic sector is most severely affected by cloud-cover problems (Marshall and others, 1994). Landsat imagery has been used at both a synoptic scale and at a more detailed level, through the selective digital enhancement of sub-scenes, to further our understanding of the surface topography, ice dynamics, and mass balance of the more than 56,000 km^2 of ice masses in the Russian Arctic archipelagos. Analysis of the imagery has demonstrated, for example, that these ice masses produce the largest icebergs in the Eurasian Arctic and that small ice caps are likely to be in negative net balance in response to recent climate change (ACIA, 2004). Information derived from these investigations has been incorporated in numerical models testing the sensitivity of Russian High Arctic ice masses to both future and past climate change (Glazovskii and others, 1996; Siegert and Dowdeswell, 1995).

Acknowledgments

Funding was provided through U.K. NERC Grants GR3/8507 and GR3/9958, INTASGrant 1010-CT93-0006, the John Ellerman Foundation, Conoco Phillips, and the Newton Trust. The Royal Society provided financial support for satellite image purchase and for collaborative meetings in Cambridge and Moscow with Russian colleagues. This is a contribution to the European Science Foundation program on the Quaternary Environment of the Eurasian North (QUEEN).

References Cited

Abramov, V.A., 1992, Russian iceberg observations in the Barents Sea, 1933–1990: Polar Research, v. 11, no. 2, p. 93–97.

ACIA, 2004, Impacts of a warming Arctic: Arctic climate impact assessment: Cambridge, U.K., Cambridge University Press, 139 p. [*http://www.acia.uaf.edu*]

Ahlmann, H.W., 1933, Scientific results of the Swedish-Norwegian Arctic expedition in the summer of 1931: Geografiska Annaler, v. 15, nos. 1–4, 348 p.

Aizen, V.B., Aizen, E.M., and Kuzmichenok, V.A., 2007, Glaciers and hydrological changes in the Tien Shan – Simulation and prediction: Environmental Research Letters, v.2, 045019, 10 p., doi:10.1088/1748-9326/2/4/045019.

Aizen, V.B., and Kuzmichenok, V.A., 2007, Glacier changes in the Tien Shan as determined from topographic and remotely sensed data: Global and Planetary Change, v. 56, no. 3, p. 328-340.

Aizen, V.B., Kuzmichenok, V.A., Surazakov, A.B., and Aizen, E.M., 2006, Glacier changes in central and northern Tien Shan during the last 150 years based on surface and remote sensing data: Annals of Glaciology, v. 43, p. 202–213.

Anonymous, 1933, Soviet work in the Arctic: Geographical Journal, v. 81, no. 6, p. 532–535.

Anonymous, 2002, Lednik Kolka: snova katastrofa [Kolka Glacier: disaster again]: Materialy Glyatsiologicheskikh Issledovanii, Pub. 93, p. 221–228. (In Russian)

Armstrong, T., Roberts, B., and Swithinbank, C., 1966, Illustrated glossary of snow and ice, (2d ed.): Cambridge, U.K., Scott Polar Research Institute Special Publication No. 4, 60 p.

Avsiuk, G.A., 1952, Nekotoriye dannye ob oledenenii i orografii gornogo massiva Ak-Shyyrak [Some data on the glaciers and orography of the Ak-Shyyrak Mountain Massif]: Moscow, Trudy Instituta Geografii AN SSSR, v. 49, p. 5–32. (In Russian)

Bagrationes, Vakhushti, 1997, Atlas of Georgia: Tibilsi, 95 p. (In Georgian) [Originally published in the 1740s.]

Bamber, J.L., and Dowdeswell, J.A., 1990. Remote-sensing studies of Kvitøyjøkulen, an ice cap on Kvitøya, north-east Svalbard: Journal of Glaciology, v. 36, no. 122, p. 75–81.

Barkov, N.I., Bol'shiyanov, D.Yu., Gvozdik, O.A., Klement'yev, O.L., Makeev, V.M., Moskalenko, I.G., Potapenko, V.Yu., and Yunak, R.I., 1992, Novye dannye o stroenii i razvitii lednika Vavilova na Severnoi Zemle [New data on the structure and development of the Vavilov Ice Dome, Severnaya Zemlya]: Materialy Glyatsiologicheskikh Issledovanii, Pub. 75, p. 35–41. (In Russian)

Bazheva, V.Ya., 1981, Katalog Lednikov SSSR [Catalogue of Glaciers of the USSR], Ostrova De-Longa [DeLong Islands]: Gidrometeoizdat (Leningrad), v. 17, p. 15–25. (In Russian)

Benson, C.S., 1962, Stratigraphic studies in the snow and firn of the Greenland Ice Sheet: [Hanover, New Hampshire,] Snow, Ice and Permafrost Research Establishment (SIPRE), U.S. Army Cold Regions Research and Engineering Laboratory (CRREL) Research Report No. 70, 93 p. [Published version of C.S. Benson's Ph.D. dissertation (1960), Division of Geological Sciences, California Institute of Technology, Pasadena, CA, 213 p.]

Berman, L.L., 1947, Sovremennoe oledenenie verkhov'ev reki Indigirki [Present day glaciers of the Indigirka upper reaches]: Moscow, Voprosy geographii, iss. 4. (In Russian)

Berson, Arthur, 1933, Die Arktisfahrt des Luftschiffes "Graf Zeppelin" im Juli 1931 [The Arctic expedition of the airship "Graf Zeppelin" in July 1931] Wissenschaftliche Ergebnisse: Petermanns Mitteilungen Ergänzungsheft No. 216, Gotha, 112 p. (In German)

Bindschadler, R.A., Dowdeswell, J.A., Hall, D.K., and Winther, J.-G., 2001, Glaciological applications with Landsat-7: early assessments: Remote Sensing of Environment, v. 78, nos. 1–2, p. 163–179.

Bogdanovich, K.I., 1899, Ocherk deyatel'nosti Okhotsko-Kamchatskoi gornoi ekspeditsii 1895–1898 gg [Notes on the Okhotsk-Kamchatka Mountain Expedition, 1895-1898]: Izvestiya Imperatorskogo Geograficheskogo Obshchestva, v. 35, no. 6, p. 549–600. (In Russian)

Bogorodskii, V.V., and Fedorov, B.A., 1971. Radar probing of Severnaya Zemlya glaciers, *in* Bogorodskii, V.V., ed., The Physics of Ice: Springfield, Virginia, National Technical Information Service, p. 1–16.

Bolch, T., 2007, Climate change and glacier retreat in northern Tien Shan (Kazakhstan/ Kyrgyzstan) using remote sensing data: Global and Planetary Change, v. 56, iss. 1–2, p. 1–12.

Bondarev, L.G., 1963, Ocherki po oledeneniyu massiva Ak-Shyyrak [Notes on the glaciers of the Ak-Shyyrak Massif]: Frunze, AN Kirgizskoy SSR, 202 p. (In Russian)

Burgess, D.O., Sharp, M., Mair, D.W.F., Dowdeswell, J.A., and Benham, T.J., 2005, Flow dynamics and iceberg calving rates of the Devon Ice Cap, Nunavut, Canada: Journal of Glaciology, v. 51, p. 219-230.

Burmester, H., 1913, Rezente glaziale Untersuchungen und photogrammetrische Aufnahmen im Baksanquellgebiete (Kaukasus) [Recent glaciological investigations and photogrammetric surveys in Baksan upper reaches [Quellgebiet] (Caucasus)]: Zeitschrift für Gletscherkunde, v. 8, no. 1, p. 1–41. (In German)

Chernomorets, S.S., 2005, Selevye ochagi do i posle katastrof [Mudflow foci before and after disasters]: Moscow, Nauchnyi Mir, 182 p. (In Russian)

Chizhov, O.P., and Koryakin, V.S., 1962, Recent changes in the regimen of the Novaya Zemlya ice sheet: International Association of Scientific Hydrology, Publication No. 58, p. 187–193.

Chizhov, O.P., Koryakin, V.S., Davidovich, N.V., Kanevskii, Z.M., Zinger, E.M., Bazheva, V.Ya., Bazhev, A.B., and Khmelevskoi, I.F., 1968, Oledenenie Novoi Zemli [Glaciers of Novaya Zemlya]: Rezul'taty Issledovanii po Programme Mezhdunarodnogo Geofizicheskogo Goda. IX Razdel Programmy MGG, v. 18,

Moscow, Nauka, 338 p. (In Russian) [Also released in translation as Glaciation of the Novaya Zemlya, 1974, Springfield, VA, NTIS TT-70-59126, 2 parts, 727 p.]

Desinov, L.V., Kotlyakov, V.M., Osipova, G.B., Tsvetkov, D.G., 2001, Snova dal o sebe znat' lednik Medvezhiy [Medvezhiy Glacier in retrospect]: Materialy Glyatsiologicheskikh Issledovanii, Pub. 91, p. 249–253. (In Russian)

Desinov, L.V., Zakharov, V.G., Kotlyakov, V.M., and Suslov, V.F., 1978, Itogy pervogo podsputnikovogo experimenta po indikatsii pul'siruyushchikh lednikov Pamira [Results of the first satellite experiment of the indication of surging glaciers of the Pamirs]: Izvestiya Vsesoyuznogo Geograficheskogo obshchestva, v. 110, no. 6, p. 505–511. (In Russian)

Dibner, V.D., 1955, O proiskhozhdenii plovuchikh ledianykh ostrovov [The origin of floating ice-islands]: Priroda, v. 3, p. 89–92. (In Russian)

Dolgoushin, L.D., and Osipova, G.B., 1975, Glacier surges and the problem of their forecasting: International Association of Hydrological Sciences, IAHS Publication No. 104, p. 292–304.

Dolgushin, L.D., and Osipova, G.B., 1979, Novye ledniki na khrebte Telpoz-Iz [New glaciers on the Telpoziz Range]: Materialy Glyatsiologicheskikh Issledovanii, Pub. 36, p. 214–218. (In Russian)

Dolgushin, L.D., and Osipova, G.B., 1982, Pul'siruiushchie ledniki [Surging glaciers]: Leningrad, Gidrometeoizdat, 192 p. (In Russian)

Dolgushin, L.D., and Osipova, G.B., 1989, Ledniki [Glaciers]: Moscow, 444 p. (In Russian)

Dowdeswell, J.A., 1986a, Drainage-basin characteristics of Nordaustlandet ice caps, Svalbard: Journal of Glaciology, v. 32, no. 110, p. 31–38.

Dowdeswell, J.A., 1986b, Remote sensing of ice cap outlet glacier fluctuations on Nordaustlandet, Svalbard: Polar Research, v. 4, no. 1, p. 25–32.

Dowdeswell, J.A., 1995, Glaciers in the High Arctic and recent environmental change: Philosophical Transactions of the Royal Society, London, Series A, v. 352, no. 1699, p. 321–334.

Dowdeswell, J.A., Bassford, R.P., Gorman, M.R., Williams, M., Glazovskii, A.F., and others, 2002, Form and flow of the Academy of Sciences Ice Cap, Severnaya Zemlya, Russian High Arctic: Journal of Geophysical Research, v. 107, No. B4, EPM5, doi: 10.1029/2000 JB000129, 17 p.

Dowdeswell, J.A., Benham, T.J., Gorman, M.R., Burgess, D., and Sharp, M.J., 2004, Form and flow of the Devon Island Ice Cap, Canadian Arctic: Journal of Geophysical Research, v. 109, no. F2, F02002, doi: 10.1029/2003 JF000095, 14 p.

Dowdeswell, J.A., Benham, T.J., Strozzi, T., and Hagen, J.O., 2008, Iceberg calving flux and mass balance of the Austfonna ice cap on Nordaustlandet, Svalbard: Journal of Geophysical Research, v. 113, F03022, doi:10.1029/2007JF000905.

Dowdeswell, J.A., and Collin, R.L., 1990, Fast-flowing outlet glaciers on Svalbard ice caps: Geology, v. 18, no. 8, p. 778–781.

Dowdeswell, J.A., and Drewry, D.J., 1989, The dynamics of Austfonna, Nordaustlandet, Svalbard: surface velocities, mass balance and subglacial meltwater: Annals of Glaciology, v. 12, p. 37–45.

Dowdeswell, J.A., Glazovskii, A.F., and Macheret, Yu.Ya., 1995, Ice divides and drainage basins on the ice caps of Franz Josef Land, Russian High Arctic, defined from Landsat, Russian KFA-1000 and ERS-1 SAR satellite imagery: Arctic and Alpine Research, v. 27, no. 3, p. 264–270.

Dowdeswell, J.A., Gorman, M.R., Glazovskii, A.F., and Macheret, Yu.Ya., 1994, Evidence for floating ice shelves on Franz Josef Land, Russian High Arctic: Arctic and Alpine Research, v. 26, no. 1, p. 86–92.

Dowdeswell, J.A., Gorman, M.R., Glazovskii, A.F., and Macheret, Yu.Ya., 1996, Airborne radio-echo sounding of the ice caps on Franz Josef Land in 1994: Materialy Glyatsiologicheskikh Issledovanii, Pub. 80, p. 248–254.

Dowdeswell, J.A., Gorman, M.R., Macheret, Yu.Ya., Glazovskii, A.F., and Moskalevski, M.Y., 1996, High resolution imagery from the Russian KATE-200 satellite camera: morphology and dynamics of ice masses in the European High Arctic: International Journal of Remote Sensing, v. 17, no. 17, p. 3343–3356.

Dowdeswell, J.A, and Hagen, J.O., 2004, Arctic ice caps and glaciers, *in* Bamber, J.L., and Payne, A.J., eds., Mass balance of the cryosphere: Cambridge, U.K., Cambridge University Press, p. 527–557.

Dowdeswell, J.A., Hodgkins, R., Nuttall, A-M., Hagen, J.O., and Hamilton, G.S., 1995, Mass balance change as a control on the frequency and occurrence of glacier surges in Svalbard, Norwegian High Arctic: Geophysical Research Letters, v. 22, no. 21, p. 2909–2912.

Dowdeswell, J.A., and McIntyre, N.F., 1987, The surface topography of large ice masses from Landsat imagery: Journal of Glaciology, v. 33, no. 113, p. 16–23.

Dowdeswell, J.A., Rees, W.G., and Diament, A.D., 1994, ERS-1 SAR investigations of snow and ice facies on ice caps in the European High Arctic, *in* Kaldeick-Schumann, B., ed., Space at the service of our environment, proceedings of the Second ERS-1 Symposium, Hamburg, Germany, 11–14 October 1993: European Space Agency Special Publication 361, p. 1171–1176.

Dowdeswell, J.A., Unwin, B., Nuttall, A.-M., and Wingham, D.J., 1999, Velocity structure, flow instability and mass flux on a large Arctic ice cap from satellite radar interferometry: Earth and Planetary Science Letters, v. 167, nos. 3–4, p. 131–140.

Dowdeswell, J.A., and Williams, M., 1997, Surge-type glaciers in the Russian High Arctic identified from digital satellite imagery: Journal of Glaciology, v. 43, no. 145, p. 489–494.

Dyurgerov, M.B., Chaohai, L., and Zichu, X., eds., 1995, Oledenenie Tian' Shanya [Glaciation of the Tien Shan]: Moscow, VINITI Publishing House, 237 p. (In Russian)

Dyurgerov, M.B., and Meier, M.F., 1997, Mass balance of mountain and subpolar glaciers: a new global assessment for 1961–1990: Arctic and Alpine Research, v. 29, no. 4, p. 379–391.

Galakhov, V.P., Narozhniy, Yu.K., Nikitin, S.A., Okishev, P.A., Sevastyanov, V.V., Sevastyanova, L.N., Shurov, V.I., 1987, Ledniki Aktru, Altai — vodnyi, ledovoi i teplovoi balansy gorno-lednikovykh basseynov [Aktru glaciers, Altai — water, ice and energy balances of glacier-mountain basins]: Leningrad, Gidrometeoizdat, 118 p. (In Russian)

Glazovskii, A.F., Ignat'eva, I.Yu., and Macheret, Yu.Ya., 1996, Modelirovanie evolyutsii lednikovogo kupola Greem-Bell, Zemlya Frantsa-Iosifa: Chustvitel'nost'modeli k zadaniyu vnutrennikh parametrov i izmeneniyam vneshnikh uslovii [Modelling the evolution of an ice cap on Graham Bell

Island, Franz Josef Land: sensitivity of the model to internal parameters and changes in external conditions]: Materialy Glyatsiologicheskikh Issledovanii, Pub. 80, p. 18–30. (In Russian)

Golubev, G.N., Dyurgerov, M.B., Markin, V.A., and others, 1978, Lednik Dzhankuat (Tsentralnyi Kavkas) [Dzhankuat Glacier (Central Caucasus)]: Leningrad, Gidrometeoizdat, 184 p. (In Russian)

Govorukha, L.S., 1964, Novye dannye o sovremennom i drevnem oledenenii ostrova Viktorii [New data on the current and former glaciations of Victoria Island]: Izvestiya Vsesoyuznogo Geograficheskogo Obshchestva, v. 96, p. 352–354. (In Russian)

Govorukha, L.S., 1968, Glyatsiologicheskie issledovaniya Arkticheskogo i Antarkticheskogo nauchno-issledovatel'skogo instituta na Zemle Frantsa-Iosifa v 1960 godu [Glaciological studies of the Arctic and Antarctic Research Institute on Franz Joseph Land in 1960]: Materialy Glyatsiologicheskikh Issledovanii, Pub. 8, p. 79–87. (In Russian)

Govorukha, L.S., 1970, Raschet srednego mnogoletnego byudzheta l'da v sisteme vneshnego massoobmena lednikovogo pokrova Severnoi Zemli [Calculation of the average multi-year budget of ice in the system of external mass exchange of the Severnaya Zemlya ice cover]: Arkticheskii i Antarkticheskii Nauchno-Issledovatel'skii Institut, Trudy, v. 294, p. 12–27. (In Russian)

Govorukha, L.S., 1988a, Sovremennoe nazemnoe oledenenie Sovetskoi Arktiki [The modern land glacierization of the Soviet Arctic]: Leningrad, Hydrometeorological Publishing House, 256 p. (In Russian)

Govorukha, L.S., 1988b, The present state of ice cap islands in the Soviet Arctic: Polar Geography and Geology, v. 12, no. 4, p. 312–316. [Translated from Materialy Glyatsiologicheskikh Issledovanii, Pub. 63, p. 114–117, 1988.]

Govorukha, L.S., Bol'shiyanov, D.Yu., Zarkhidze, V.S., Pinchuk, L.Ya., and Yunak, R.I., 1987, Changes in the glacier cover of Severnaya Zemlya in the twentieth century: Polar Geography and Geology, v. 11, no. 4, p. 300–305. [Translated from Materialy Glyatsiologicheskikh Issledovanii, Pub. 60, p. 155–158, 1987.]

Grant, K.L., Stokes, C.R., and Evans, I.S., 2009, Identification and characteristics of surge-type glaciers on Novaya Zemlya, Russian Arctic: Journal of Glaciology, v. 55, no. 124, p. 960–972.

Grosswald, M.G., and Krenke, A.N., 1962, Recent changes and the mass balance of glaciers on Franz Josef Land: International Association of Scientific Hydrology, Publication No. 58, p. 194–200.

Grosswald, M.G., Krenke, A.N., Vinogradov, O.N., Markin, V.A., Psariova, T.V., Rasumeiko, N.G., and Sukhodrovskii, V.L., 1973, Oledenenie Zemli Frantsa-Iosifa Resul'taty issledovanii po programme Mezhdunarodnogo Geofizicheskogo Goda [Glaciers of Franz Josef Land: Results of research under the programme of the International Geophysical Year]: Moscow, Nauka, 351 p. (In Russian)

Gurbanov, A.G., Kusraev, A.G., and Tchel'diev, A.Kh., 2004, First results of investigation of endogene processes in Genaldonskoe and adjoining gaps: Vestnik of Vladikavkaz Research Center, Vladikavkaz, v. 4, iss. 3, p. 2–8. (In Russian)

Hambrey, M.J., 1975, The origin of foliation in glaciers: Evidence from some Norwegian examples: Journal of Glaciology, v. 14, no. 70, p. 181–185.

Hambrey, M.J., and Müller, F., 1978, Structures and ice deformation in the White Glacier, Axel Heiberg Island, Northwest Territories, Canada: Journal of Glaciology, v. 20, no. 82, p. 41–66.

Hamilton, G.S., and Dowdeswell, J.A., 1996, Controls on glacier surging in Svalbard: Journal of Glaciology, v. 42, no. 140, p. 157–168.

Hodgkins, R., and Dowdeswell, J.A., 1994, Tectonic processes in Svalbard tidewater glacier surges: evidence from structural glaciology: Journal of Glaciology, v. 40, no. 136, p. 553–560.

Holtedahl, O., 1924, 1928, 1930, Report of the scientific results of the Norwegian expedition to Novaya Zemlya, 1921: Oslo, Det Norske Videnskaps-Akademi, 3 v., 1600 p., v.1 (1924), v. 2 (1928), v. 3 (1930).

Ivan'kov, P.A., 1958, Oledenenie Kamchatki [Glaciers of Kamchatka]: AN SSSR, Seriya geograficheskaya, no. 2, p. 42–53. (In Russian)

Jania, Jacek, and Hagen, J.O., 1996, Mass balance of Arctic glaciers: International Arctic Science Committee, IASC Report No. 5, 54 p.

Jeffries, M.O., 1987, The growth, structure and disintegration of Arctic ice shelves: Polar Record, v. 23, no. 147, p. 631–649.

Jeffries, M.O., 2002, Ellesmere Island ice shelves and ice islands, *in* Williams, R.S., Jr., and Ferrigno, J.G., eds., Satellite image atlas of glaciers of the world: U.S. Geological Survey Professional Paper 1386–J (Glaciers of North America), p. J147–J164. [*http://pubs.usgs.gov/prof/p1386j*]

Kalesnik, S.V., 1937, Gornye lednikovye rayony SSSR [Mountain glaciers of the USSR]: Leningrad-Moscow, 182 p. (In Russian)

Kaulbars, A.V., 1874, Materialy po geografii Tian'-Shanya, sobrannye vo vremya puteshestviya 1869 goda [Information on the geography of Tien Shan collected during travel in 1869]: St. Petersburg, Tipografia M. Stasyulevicha, 286 p. (In Russian)

Kharkov University, 1960–61, Materialy Kavkazskoi Ekspeditsii (po programme MGG) [Data of the Caucasus expedition (under the IGY program)]: Kharkov, Kharkov State University, v. 1, 363 p.; v. 2, 257 p.; and v. 3, 439 p. (In Russian)

Khromova, T.E., Dyurgerov, M.B., and Barry, R.G., 2003, Late twentieth century changes in glacier extent in the Ak-shirak Range, Central Asia, determined from historical data and ASTER imagery: Geophysical Research Letters, v. 30, no. 16, 1863. (doi 10.1029/2003GLO17233)

Khromova, T.E., Osipova, G.B., Tsvetkov, D.G., and Barry, R.G., 2006, Changes in glacier extent in the eastern Pamir, Central Asia, determined from historical data and ASTER imagery: Remote Sensing of Environment, v. 102, nos. 1–2, p. 24–32.

Koreisha, M.M., 1963, Sovremennoe oledenenie khrebta Suntar-Khyata [Present day glaciers of the Suntar-Khyata Range]: Moscow, AN SSSR, 167 p. (In Russian)

Kornienko, S.G., Lyashenko, O.V., Gurbanov, A.G., 2004, Identification of indications of focus magmatism within the limits of the Kazbek volcanic center from data of thermal space photography: Vestnik of Vladikavkaz Research Center, Vladikavkaz, v. 4, iss. 3, p. 25–32. (In Russian)

Koryakin, V.S., 1986, Decrease in glacier cover on the islands of the Eurasian Arctic during the twentieth century: Polar Geography and Geology, v. 10, no. 2, p. 157–165. [Translated from Materialy Glyatsiologicheskikh Issledovanii, Pub. 54, p. 103–108, 1985.]

Korzhenevskii, N. L., 1930, Katalog lednikov srednei Asii [Glacier inventory of central Asia]: Tashkent, 200 p. (In Russian)

Kotlyakov, V.M., 1997, Atlas snezhno-ledovykh resursov mira [World atlas of ice and snow resources]: Moscow, Rossiiskaya Akademiya Nauk, v. 3, 392 p. (In Russian)

Kotlyakov, V.M., ed., 2006, Oledenenie severnoi i tsentral'noi Evrazii v sovremennuyu epokhu [Glaciation in north central Eurasia at the present time]: Moscow, Nauka, 482 p. (In Russian)

Kotlyakov, V.M., Desinov, L.V., Osipova, G.B., Hauser, M., Tsvetkov, D.G., Schneider, J.F., 2003, Sobytiya 2002 goda na lednike Geograficheskogo Obshchestva (RGO), Pamir [Events in 2002 on Geographical Society Glacier (RGO), Pamirs]: Materialy Glyatsiologicheskikh Issledovanii, Pub. 95, p. 221–230. (In Russian)

Kotlyakov, V.M., Kerimov, A.M., Nosenko, G.A., Nosenko, O.A., Rototaeva, O.V., Khmelevskoi, I.F., 2004, Estimation of the state of Kolka and Maili glaciers according to surface investigation in June–September 2003. Problems of forecast of extreme situations: Third Scientific Practical Conference, October, 2003, Moscow, p. 136–143. (In Russian)

Kotlyakov, V.M., Korotkov, I.M., Nikolaev, V.I., Petrov, V.N., Barkov, N.I., and Klement'ev, O.L., 1989, Rekonstruktsiya klimata golotsena po resul'tatam issledovaniya ledyanogo kerna lednika Vavilova na Severnoi Zemle [Reconstruction of the Holocene climate from the results of ice-core studies on the Vavilov Dome, Severnaya Zemlya]: Materialy Glyatsiologicheskikh Issledovanii, Pub. 67, p. 103–108. (In Russian)

Kotlyakov, V.M., Osipova, G.B., Tsvetkov, D.G., 1997, Fluctuations of unstable glaciers: scale and character: Annals of Glaciology, v. 24, p. 338–343.

Kotlyakov, V.M., Rototaeva, O.V., Desinov, L.V., Zotikov, I.A., Osokin, N.I., 2004, Causes and effects of a catastrophic surge of Kolka Glacier in the central Caucasus: Zeitschrift für Gletscherkunde und Glazialgeologie, v. 38, no. 2, p. 117–128.

Kotlyakov, V.M., Zagorodnov, V.S., and Nikolaev, V.I., 1990, Drilling on ice caps in the Soviet Arctic and on Svalbard and prospects of ice core treatment, *in* Kotlyakov, V. M., and Sokolov, V.Y., eds., Arctic research: Advances and prospects, Moscow, Nauka, v. 2, p. 5–18.

Kravtsova, V.I., and Chaikina, N.F., 1980, Primenenie snimkov s kosmicheskogo korablya "Sojuz-22" dlya kartigrafirovania oledenenia Alaiskogo khrebta [Application of images taken from the Soyuz-22 for the mapping of Alai Range glaciers]: Materialy Glyatsiologicheskikh Issledovanii, Pub. 37, p. 56–62. (In Russian)

Kravtsova, V.I., and Loseva, V.G., 1968, Izmeneniya lednikov Elbrusa za sto let, *in* Uspekhi Sovetskoi gliatsiologii [Change of El'brus glaciation over 100 years, *in* Advances in Soviet glaciology]: Vsesoiuznyi gliatsiologicheskii simpozium III [Third All-Union Glaciological Symposium], Proceedings, Frunze, Kyrgyzstan, p. 262–270. (In Russian)

Krenke, A.N., Menshutin, V.M., Voloshina, A.P., and others, 1988, Lednik Marukh (Zapadniy Kavkaz) [Marukh Glacier (Western Caucasus)]: Leningrad, Gidrometeoizdat, 254 p. (In Russian)

Krimmel, R.M., 1978, Detection of surging glaciers using aerial photography and LANDSAT images: Materialy Glyatsiologicheskikh Issledovanii, Pub. 33, p. 43–46, (In Russian), p. 131–133. (In English)

Krimmel, R.M., Post, A., and Meier, M.F., 1976, Surging and nonsurging glaciers in the Pamir Mountains, U.S.S.R., *in* Williams, R.S., Jr., and Carter, W.D., eds., ERTS-1. A new window on our planet: U.S. Geological Survey Professional Paper 929, p. 178–179.

Kuzmichenok, V.A., and Chaohai, L., 1995, The distribution of glaciers and their morphology over Tien Shan, *in* Dyurgerov, M.B., Chaohai, L., and Zichu, X., eds., Oledenenie Tian' Shanya [Tien Shan glaciers]: Moscow, VINITI Publishing House. (In Russian)

Lamb, J.M., 1991, The battle of Novaya Zemlya: Arctic Circle, v. 1, p. 46–47.

Lebedeva, I.M., and Rototaeva, O.V., 2005, Klimaticheskii faktor katastroficheskoi podvizhki lednika Kolka v 2002 godu [Climatic factor of the disastrous surge of Kolka Glacier in 2002]: Materialy Glyatsiologicheskikh Issledovanii, Pub. 98, p. 155–161. (In Russian)

Liestøl, O., 1993, Glaciers of Svalbard, Norway, *in* Williams, R.S., Jr., and Ferrigno, J.G., eds., Satellite Image Atlas of Glaciers of the World: U.S. Geological Survey Professional Paper 1386-E (Europe), p. E127–E151. [*http://pubs.usgs.gov/prof/p1386e*]

Marshall, G.J., Dowdeswell, J.A., and Rees, W.G., 1994, The spatial and temporal effect of cloud cover on the acquisition of high quality Landsat imagery in the European Arctic sector: Remote Sensing of Environment, v. 50, no. 2, p. 149–160.

Martin, P.J., and Sanderson, T.J.O., 1980, Morphology and dynamics of ice rises: Journal of Glaciology, v. 25, no. 91, p. 33–45.

Martyshev, A.P., 1980, Kolebaniya yazyka lednika Bol'shoy Azau na Elbruse [Fluctuations of the tongue of Bol'shoy Azau Glacier on El'brus]: Materialy Glyatsiologicheskikh Issledovanii, Pub. 39, p. 207–209. (In Russian)

Martyshev, A.P., 1983, Sovremennye izmeneniya lednikov v verkhoviakh r. Baksan v Prielbruse [Present-day changes of glaciers in the headwaters of the Baksan River in the El'brus region]: Materialy Glyatsiologicheskikh Issledovanii, Pub. 47, p. 209–210. (In Russian)

McCauley, C., 1958, Glaciers of the Arctic islands of the Soviet Union, *in* Geographic Study of Mountain Glaciation in the Northern Hemisphere, pt. 6, ch. 5: New York, American Geographical Society.

Meier, M.F., 1984, Contribution of small glaciers to global sea level: Science, v. 226, no. 4681, p. 1418–1421.

Meier, M.F., and Post, A.S., 1969, What are glacier surges?: Canadian Journal of Earth Sciences, v. 6, no. 4, pt. 2, p. 807–817.

Merzbacher, Gottfried, 1905, The central Tian Shan Mountains, 1902-1903: New York, E.P. Dalton, v. 8.

Miller, G.H., Forman, S.L., Synder, J.A., Lubinski, D.J., Matishov, G.G., and Korsun, S., 1992, Neoglaciation of Franz Josef Land, Russia [abs.]: Geological Society of America, Abstracts with Programs, 1992, p. 346.

Nansen, Fridtjof, 1897, Farthest north: Westminster, Archibald Constable and Co., v. 1, 510 p.; and v. 2, 671 p.

Narama, C., Shimamura, Y., Nakayama, D., and Abdrakhmatov, K., 2006, Recent changes of glacier coverage in the western Terskey-Alatoo range (sic), Kyrgyz Republic, using Corona and Landsat: Annals of Glaciology, v. 43, p. 223–229.

Nosenko, G.A., Rototaeva, O.V., Nosenko, O.A., 2004, Possibilities of monitoring from space the dangerous glacial processes in mountain regions that are difficult to access (from the example of the Karmadon disaster of 2002): Issledovanie Zemli iz Kosmosa: no. 6, p. 24–31. (In Russian)

Osipova, G.B.,and Tsvetkov, D.G., 1991, Kinematics of the surface of a surging glacier (comparison of the Medvezhiy and Variegated Glaciers): International Association of Hydrological Sciences, IAHS Pub. 208, p. 345–357.

Osipova, G.B., and Tsvetkov, D.G., 1999, Rol' podpruzhivaniya v dinamike slozhnykh gornykh lednikov. Ledniki Bivachniy i Sugran, Tsentralinyi Pamir [Role of damming in the dynamics of compound mountain glaciers. Bivachniy and Sugran Glaciers, Central Pamirs]: Materialy Glyatsiologicheskikh Issledovanii, Pub. 86, p. 133–141. (In Russian)

Osipova, G.B., and Tsvetkov, D.G., 2000, Kosmicheskii monitoring oledeneniya Vostochnogo Pamira [Satellite monitoring of glaciation in the Eastern Pamirs]: Materialy Glyatsiologicheskikh Issledovanii, Pub. 89, p. 163–174. (In Russian)

Osipova, G.B., and Tsvetkov, D.G., 2001, Dinamika pul'siruyushchikh lednikov Gando i Dorofeeva v 1972–1991gg [Dynamics of the surging glaciers Gando and Dorofeev from 1972 to 1991]: Materialy Glyatsiologicheskikh Issledovanii, Pub. 90, p. 193–198. (In Russian)

Osipova, G.B., and Tsvetkov, D.G., 2002a, Lednik Oktyabr'skii, vostochnyi Pamir, v 1945–1990 gg; osobennasti evolyutsii v stadii vosstanovleniya i podvizhki [Oktyabr'skiy Glacier, Eastern Pamirs, from 1945 to 1990. Development trends in recovery and surge stages]: Materialy Glyatsiologicheskikh Issledovanii, Pub. 93, p. 25–34. (In Russian)

Osipova, G.B., and Tsvetkov, D.G., 2002b, Issledovanie dinamiki slozhnykh lednikov po kosmicheskim snimkam [Investigations of the dynamics of compound glaciers on the basis of space images]: Izvestiya Akademii Nauk, Seriya Geograficheskaya, No. 3, p. 29–38. (In Russian)

Osipova, G.B., Tsvetkov, D.G., Schetinnikov, A.S., Rudak, M.S., 1998, Katalog pul'siruyushchikh lednikov Pamira [Inventory of surging glaciers of the Pamirs]: Materialy Glyiatsiologicheskikh Issledovanii, Pub. 85, p. 1–136. (In Russian)

Panov, V.D., 1993, Evolutsiia sovremennogo oledeneniia na Kavkaze [Evolution of the recent glaciation of the Caucasus]: Saint Petersburg, Gidrometeoizdat, 432 p. (In Russian)

Payer, Julius, 1876, Die Osterreichisch-Ungarische Nordpol-Expedition in den Jahren 1872–1874 [The Austro-Hungarian Expedition to the North Pole in the years 1872–74]: Vienna, Alfred Hölder, 696 p. (In German)

Penck, Albrecht, 1931, Geographical and photogrammetric results from the Arctic cruise of the Graf Zeppelin: Geographical Journal, v. 78, no. 6, p. 569–570.

Podozerskii, K.I., 1911, Ledniki Kavkazskogo Khrebta [Glaciers of the Caucasus Range]: Zapiski Kavkazskogo otdela Russkogo Geograficheskogo Obshchestva, v. 29, iss. 1, Tiflis, 200 p. (In Russian)

Popovnin, V.V., Petrakov, D.A., Tutubalina, O.V., Chernomorets, S.S., 2003, The glacial disaster of 2002 in North-Ossetia: Kriosfera Zemli, v. 7, no. 1, p. 1–10. (In Russian)

Post, Austin, 1969, Distribution of surging glaciers in western North America: Journal of Glaciology, v. 8, no. 53, p. 229–240.

Post, A., and Mayo, L.R., 1971, Glacier dammed lakes and outburst floods in Alaska: U.S. Geological Survey Hydrological Investigations Atlas HA-455, 10 p., and 3 maps.

Rees, W.G., Dowdeswell, J.A., and Diament, A.D., 1995, Analysis of ERS-1 synthetic aperture radar data from Nordaustlandet, Svalbard: International Journal of Remote Sensing, v. 16, no. 5, p. 905–924.

Rototaev, K.P., Khodakov, V.G., and Krenke, A.N., 1983, Issledovanie pul'siruyushchego lednika Kolka [Investigation of the surging Kolka Glacier]: Moscow, Nauka, 169 p. (In Russian)

Rototaeva, O.V., Kotlyakov, V.M., Nosenko, G.A., Khmelevskoi, I.F., Chernov, R.A., 2005, Istoricheskie dannye o podvizhkakh lednikov na severnom Kavkaze i Karmadonskaya katastrofa 2002 g. [Historical data on glacier surges in the Northern Caucasus and Karmadon disaster of 2002]: Materialy Glyatsiologicheskikh Issledovanii, Pub. 98, p. 136–145. (In Russian)

Rototaeva, O.V., Nosenko, G.A., Khmelevskoi, I.F., Tarasova, L.N., 2003, Balansovoe sostoyanie lednika Garabashi (Elbrus) v 80-kh i 90-kh godakh stoletiya [Mass balance of Garabashi Glacier (El'brus) in the 1980s and 1990s]: Materialy Glyatsiologicheskikh Issledovanii, Pub. 95, p. 111–121. (In Russian)

Russia, Committee of the Second International Polar Year, 1936a, Trudy lednikovykh ekspeditsii [Transactions of glaciological expeditions], iss. 1: Leningrad, 485 p. (In Russian)

Russia, Committee of the Second International Polar Year, 1936b, Trudy lednikovykh ekspeditsii [Transactions of glaciological expeditions], iss. 5, Kavkas. Lednikovye rayony [Caucasus. Glacier regions] 488 p. (In Russian)

Sandford, K.S., 1955, Tabular icebergs between Spitsbergen and Franz Josef Land: Geographical Journal, v. 121, pt. 2, p. 164–170.

Sapozhnikov, V.V., 1901, Katun' i ee istoki [Katun and its headwaters]: Tomsk, 271 p. (In Russian)

Sapozhnikov, V.V., 1911, Mongol'skii Altai v istokakh Irtysha i Kobdo [Mongolian Altay in the headwaters of the Irtysh and Kobdo rivers]: Tomsk, 408 p. (In Russian)

Schilling, Nikolai, 1865, Soobrazheniya o novom puti dlya otkryti v Severnom Polyarnom okeane [The conceptualization of a new route for opening the northern polar ocean]: Moskow Sbornik, v. 78, no. 5, p. 213–224. (In Russian)

Sedov, R.V., 1997a, Glaciers of the Chukotka: Materialy Glyatsiologicheskikh Issledovanii, Pub. 82, p. 213–217. (In Russian)

Sedov, R.V., 1997b, Glaciers of the Taigonos peninsula: Materialy Glyatsiologicheskikh Issledovanii, Pub. 82, p. 218–221. (In Russian)

Seinova, I.B., and Zolotarev, E.A., 2001, Ledniki i seli Priel'brusya (Evolutsiya oledeneniya i selevoi aktivnosti) [Glaciers and mudflows of the El'brus region (Evolution of glaciation and mudflow activity)]: Moscow, Nauchnyi mir, 204 p. (In Russian)

Semenov, P.P., 1858, Pervaya poezdka na Tien'Shan' ili Nebesny khrebet [The first trip to Tien Shan or Sky Range]: Vestnik RGO [Proceedings of the Russian Geographical Society], v. 1, no. 24. (In Russian)

Sharp, R.P., 1956, Glaciers in the Arctic: Arctic, v. 9, nos. 1–2, p. 78–117.

Shumskii, P.A., 1949, Sovremennoe oledenenie Sovetskoi Arktiki [Modern glaciation of the Soviet Arctic]: Trudy Arkticheskogo Instituta: v. 111, p. 11–39. (In Russian)

Siegert, M.J., and Dowdeswell, J.A., 1995, Late Weichselian ice-sheet sensitivity over Franz Josef Land, Russian High Arctic, from numerical modelling experiments: Boreas, v. 24, no. 3, p. 207–224.

Sin'kevich, S.A., Korolev, P.A., and Smirnov, K.E., 1991, Glaciological reconnaissance on the Loonney ice cap, Alexandra Land, Franz Josef Land: Journal of Glaciology, v. 37, no. 125, p. 183–185.

Solomina, O.N., Barry, R.G., Bodnya, V., 2004, The retreat of Tien Shan glaciers (Kyrgyzstan) since the Little Ice Age estimated from aerial photographs, lichenometric, and historical data: Geografiska Annaler, v. 46A, no. 2, p. 205–216.

Spizharskiy, T.N., 1936, Oledenenie Zemli Frantsa-Iosifa [Glaciation of Franz Josef Land]: Trudy Arkticheskogo Instituta, v. 41, p. 5–37. (In Russian)

Starokadomskiy, L.M., and Barr, William (translator), 1977, Charting the Russian northern sea route — The Arctic Ocean hydrographic expedition, 1910–1915: Montreal, McGill-Queens University Press, 332 p.

Tarussov, A., 1992, The Arctic from Svalbard to Severnaya Zemlya: climatic reconstructions from ice cores, *in* Bradley, R.S., and Jones, P.D., eds., Climate since A.D. 1500: London, Routledge, p. 505–516.

Troitskii, L.S., Khodakov, V.G., Mikhalev, V.I., Gus'kov, A.S., Lebedeva, I.M., Adamenko, V.N., and Zhivkovich, L.A., 1966, Oledenenie Urala [Glaciers of the Urals]: Moscow, Nauka, 307 p. (In Russian)

Tronov, M.V., 1949, Ocherki oledenenia Altaya [Notes on the glaciers of Altay]: Moscow, Geografizdat, 375 p. (In Russian)

Tronov, M.V., 1954, Voprosy gornoi glyatsiologii [Problems of mountain glaciation]: Moscow, Geografizdat, 276 p. (In Russian)

Tushinskii, G.K., 1968, Oledenenie Elbrusa [Glaciers of the Elbrus]: Izdatel'stvo Moskovskogo Universiteta, 344 p. (In Russian)

USSR Academy of Sciences, 1965–1983, Katalog lednikov SSSR [Glacier inventory of the USSR]: Leningrad, Gidrometeoizdat, 20 v. [Also available in digital form as part of the World Glacier Inventory at *http://nsidc.org/data/glacier_inventory*

USSR Academy of Sciences, 1966, Rukovodstvo po sostavleniyu Kataloga lednikov SSSR [Instructions for the compilation of the glacier inventory of the USSR]: Leningrad, Gidrometeoizdat, 154 p. (In Russian)

Vaikmyae, R.A., and Punning, Ya.M.K., 1984, Isotope and geochemical investigations on the Vavilov Glacier Dome, Severnaya Zemlya: Polar Geography and Geology, v. 8, no. 1, p. 73–79. [Translated from Materialy Glyatsiologicheskikh Issledovanii, Pub. 44, p. 145–149, 1982.]

Various authors, 1964, Nekotorye itogi issledovanii Instituta Geografii AN SSSR na Elbruse [Some results of the investigations of the Institute of Geography, Academy of Sciences, USSR, on Elbrus]: Materialy Glyatsiologicheskikh Issledovanii, Pub. 10, p. 55–103. (In Russian)

Various authors, 1967, Atlas lednikov Elbrusa [Atlas of the Elbrus glaciers]: Materialy Glyatsiologicheskikh Issledovanii, Pub. 13, p. 125–186. (in Russian)

Verkulich, S.R., Krasanov, A.G., and Anisimov, M.A., 1992, The present state of, and trends displayed by, the glaciers of Bennett Island in the past 40 years: Polar Geography and Geology, v. 16, no.1, p. 51–57. [Translated from Materialy Glyatsiologicheskikh Issledovanii, Pub. 70, p. 111–115, 1990.]

Vilesov, E.N., and Uvarov, V.N., 2001, Evolutsiya sovremennogo oledeneniya Zailiiskogo Alatau v XX veke [The evolution of modern glaciation of the Zailiyskiy Alatau in the 20th century]: Almaty, Kazakh State University, 252 p. (In Russian)

Vinnikov, L.P., and Labutina, I.A., 1987, Izmeneniya lednika Kiukiurtliu na Elbruse za chetvert' veka [Changes of Kukurtli Glacier on El'brus for more than a quarter of a century]: Materialy Glyatsiologicheskikh Issledovanii, Pub. 60, p. 147–152. (In Russian)

Vinogradov, V.N., 1968, Katalog lednikov SSSR, Kamchatka [Inventory of glaciers of the USSR, Kamchatka], v. 20: Leningrad, Gidrometeoizdat, 2–4. (In Russian)

Vinogradov, V.N., 1975, Sovremennoe oledenenie rayonov aktivnogo vulkanizma [Present day glaciers in the areas of the active volcanism]: Moscow, Nauka, 103 p. (In Russian)

Vinogradov, V.N., and Glazyrin, G.E., 1979, Statisticheskii podkhod k izucheniyu morfologii lednikov Kamchatki [Statistical approach to the studies of the morphology of Kamchatka glaciers]: Isvestiya Vsesoyuznogo Geograficheskogo Obshchestva, v. 111, iss. 4, p. 325–329. (In Russian)

Vinogradov, O.N., Konovalova, G.I., and Psareva, T.V., 1976, Novye dannye o glaziogeomorfologii sovremennykh lednikov Kavkasa i ikh evolyutsii v. xx veke [New data on glaciogeomorphology of modern glaciers of the Caucasus and their evolution in the twentieth century]: Materialy Glyatsiologicheskikh Issledovanii, Pub. 27, p. 44–50. (In Russian)

Vinogradov, O.N., Konovalova, G.I., and Psareva, T.V., 1980, Morfologicheskie kharakteristiki lednikovoi sistemy Tien'-shanya na kartakh masshtaba 1:1500000 v Atlase snezhno-ledovykh resursov mira [Morphological characteristics of the Tien Shan glacier system on the 1:1,500,000-scale maps in the World Atlas of Snow and Ice Resources: Materialy Glyatsiologicheskikh Issledovanii, Pub. 37, p. 56–62. (In Russian)

Voevodin, V.A., 1972, O razmerakh aisbergov v rayone Zemli Frantsa-Iosifa i Shpitsbergena [Dimensions of icebergs in the region of Franz-Josef Land and Spitsbergen]: Problemy Arktiki i Antarktiki, v. 39, p. 138–140. (In Russian)

Voitkovsky, K.F., Benkevich, V.V., Volodicheva, N.A., 1989, Sovremennye tendentsii razvitiya lednikovoi sistemy Elbrusa [Present-day trends of development of the El'brus glacial system]: Materialy Glyatsiologicheskikh Issledovanii, Pub. 67, p. 73–80. (In Russian)

Volodicheva, N.A., Evteev, O.A., Kirpichenkov, S.Ya., Knizhnikov, Yu.F., Kravtsova, V.I., Martyshev, A.P., and Myagkov, S.M., 1983, Izuchenie izmenenii oledeneniya Elbrusa za poslednie 25 let [Study of changes of El'brus glaciation over the past 25 years]: Materialy Glyatsiologicheskikh Issledovanii, Pub. 47, p. 130–137. (In Russian)

Williams, M., 2003, Remote sensing of glacierized area ice dynamics in the Russian High Arctic: Aberystwyth, University of Wales Aberystwyth, Ph.D. thesis, 428 p.

Williams, M., and Dowdeswell, J.A., 2001, Historical fluctuations of the Matusevich Ice Shelf, Severnaya Zemlya, Russian High Arctic: Arctic, Antarctic, and Alpine Research, v. 33, no. 2, p. 211–222.

Williams, R.S., Jr., 1986, Glaciers and glacial landforms; Chapter 9, *in* Short, N.M., and Blair, R.W., Jr., editors, Geomorphology from space. A global overview of regional landforms: NASA Special Publication, SP-486, p. 521–596. [*http://disc.gsfc.nasa.gov/geomorphology/index.shtml*]

Williams, R.S., Jr., Hall, D.K., and Benson, C.S., 1991, Analysis of glacier facies using satellite techniques: Journal of Glaciology, v. 37, no. 125, p. 120–128.

Zabirov, R.D., 1955, Oledenenie Pamira [Glaciers of the Pamirs]: Moscow, Geografizdat, 372 p. (In Russian)

Zabirov, R.D., and Bakov, E.K., 1981, Ozero Mertsbakhera. Glyatsiologicheskie issledovaniya v Kirgizii [Lake Mertsbakhera. Glaciological studies in Kyrgyzstan]: Frunze, p. 82–92. (In Russian)

Zabirov, R.D., and Knizhnikov, Yu. F., 1962, Fototeodolitnaya s'emka lednikov Tian Shania v period MGG [Photogrammetric survey of the Tien Shan glaciers during the International Geophysical Year]: Frunze, Izd-vo Akademii nauk Kirgizskoi SSR, 99 p. (In Russian)

Zeeberg, J.J., 2001, Climate and glacial history of the Novaya Zemlya Archipelago, Russian Arctic: Amsterdam, Rozenberg, 174 p.

Zeeberg, J.J., and Forman, S.L., 2001, Changes in glacier extent on northern Novaya Zemlya in the twentieth century: The Holocene, v. 11, p. 161–175.

Zinger, E.M., and Koryakin, V.S., 1965, Yest' li shel'fovye ledniki na Severnoi Zemle? [Are there ice shelves on Severnaya Zemlya?]: Materialy Glyatsiologicheskikh Issledovanii, Pub. 11, p. 250–253. (In Russian)

Zolotarev, E.A., 1997, Izmeneniya lednikov Elbrusa v poslednem stoletii [Changes of El'brus glaciers in the past century]: Materialy Glyatsiologicheskikh Issledovanii, Pub. 83, p. 146–153. (In Russian)

Zolotarev, E.A., and Khar'kovets, E.G., 2000, Oledenenie Elbrusa v kontse XX v. (tsifrovaya ortofotokarta Elbrusa na 1997 g.)[Glaciation of El'brus at the end of the 20th century (digital orthophotomap of El'brus for 1997)]: Materialy Glyatsiologicheskikh Issledovanii, Pub. 89, p. 175–181. (In Russian)